Université de Montréal

Faculté des études supérieures

An Investigation of the Beam-Induced Dehalogenation Process in Liquid Secondary Ion Mass Spectrometry

par

Roger Théberge

Département de Chimie

Faculté des arts et des sciences

Thèse présentée à la Faculté des études supérieures

en vue de l'obtention du grade de

Philosophiæ Doctor (Ph.D.)

en chimie

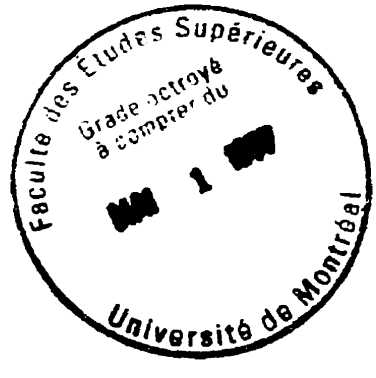

octobre, 1996

Université de Montréal

Faculté des études supérieures

Cette thèse intitulée

An Investigation of the Beam-Induced Dehalogenation Process in Liquid Secondary Ion Mass Spectrometry

Présentée par:

Roger Théberge

a été évaluée par un jury composé des personnes suivantes:

M. D'Amboise.....président rapporteur
M.J. Bertrand.....directeur de recherche
M. Zador.....membre du jury
K.L. Busch.....examinateur externe

accepté le 18.03.97

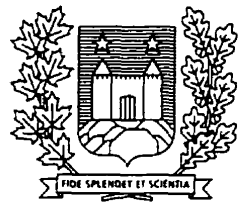

Summary

Summary

The ultimate goal of this work is to improve the understanding of beam-induced reduction processes ocurring in the FAB/LSIMS technique. This goal was pursued through the study of the reductive dehalogenation of halogenated aromatic compounds. The thrust of the investigation was mainly threefold:

1-Characterization of the experimental parameters influencing the dehalogenation process, primarily liquid matrix selection.

2-Identification of the structural characteristics of the analyte affecting the process.

3-Application of radiation chemistry concepts and data to rationalize beam-induced dehalogenation, based on the analogous nature of the processes triggered by non-discriminate energy deposition arising from bombardment by energetic particles in radiolysis and FAB/LSIMS.

The effect of experimental parameters such as time of irradiation, analyte concentration, primary beam density, matrix selection, and matrix additives on the beam-induced dehalogenation of the model compound chlorpromazine in LSIMS was investigated. It was found that dehalogenation of chlorpromazine in glycerol increased with time of irradiation, analyte concentration, and primary beam density. It was recognised that matrix selection is the key experimental parameter affecting the extent of beam-induced dehalogenation in LSIMS.

The dehalogenation inhibiting efficiency of the matrices was rationalised in terms of matrix electron scavenging capacity. The matrix electron scavenging capacity was initially related only to the electron affinity of the intact molecule. Subsequently, the nature of the matrix radical cascade generated under bombardment conditions was postulated to affect the observed extent of dehalogenation. For example, the lower extent of dehalogenation

observed in sulfur containing matrices may be explained by the beam induced generation of oxidizing thiyl radicals ($RS^{\bullet}$). The highly reducing character of the glycerol radical cascade was described and rationalised using the known radiation chemistry of alcohols.

The effect of the analyte electron affinity on dehalogenation of simple bromoaromatic compounds in a glycerol matrix was investigated. The results show a definite trend of decreasing dehalogenation with increasing analyte electron affinity. These results are consistent with electrochemical and pulse radiolysis studies where one electron reduction was shown to be responsible for dehalogenation. The observation that dehalogenation decreases with analyte electron affinity is mechanistically consistent with the proposition that secondary electron production is an intrinsic part of the bombardment process.

The effect of analyte surface concentration on the observed extent of beam-induced dehalogenation in LSIMS was investigated using a three-pronged approach. The thrust of the experiments was to vary the analyte surface concentration through various means and monitor the observed extent of dehalogenation. These experimental approaches consisted of the use of an anionic surfactant as a doping agent, synthetically modifying the hydrophobicity of a model analyte, and changing matrix surface tension through suitable matrix liquid selection. The results obtained show that increased analyte surface concentration leads to an increased extent of dehalogenation. These results are in agreement with the postulate that beam-induced reactions occur mainly at/or very near the surface, where the concentration of reactive species generated by the interaction of the bombarding particles and the sample is highest. It is proposed that this relationship is applicable to other beam-induced phenomena in FAB/LSIMS.

The core of the work presented here stems from a series of four papers concerning the beam-induced dehalogenation of haloaromatic compounds and published during the course of the author's doctoral studies. The arguments presented in the thesis are not necessarily grouped in the chronological order of the publications. This state of affairs is due to the fact that each publication was a discreet, distinct work on a specific aspects of the topic. Whereas the thesis is mainly concerned with a coherent discourse constructed for the purpose of explaining the general aspects of beam-induced dehalogenation and its possible ramification for the bulk of beam-induced redox processes in FAB/LSIMS. The transition from the former to the latter has required a certain rearrangement of the order in which the results were presented in the literature.

Résumé

Résumé

Des artefacts ont été observés lors de l'analyse par FAB/LSIMS dès les premières applications de cette technique d'ionisation. On trouve que des réactions d'oxydo-réduction sont responsables de ces artefacts. Le faisceau primaire est présumé être la cause de ces réactions. L'interaction du faisceau primaire avec l'échantillon peut donc induire la formation d'artéfacts pouvant compromettre l'intégrité analytique de la technique. Malgré une pléthore d'observations concernant ces réactions, il existe peu d'études ayant tenté de fournir un cadre mécaniste à ces phénomènes. La déshalogénation de composés haloaromatiques fait partie de ces réactions d'oxydo-réductions induites par le faisceau primaire. Dans ce cas-ci, l'artéfact résulte de la substitution de l'halogène par un hydrogène.

Le but ultime de cette étude est de tenter d'élucider plus en profondeur les mécanismes qui sous-tendent la déshalogénation de composés haloaromatiques et, par le truchement de ce processus, d'engendrer une compréhension plus étendue de la chimie oxydoréductrice des matrices soumises à l'effet du bombardement. Les idées maîtresses de la thèse peuvent être résumées de la manière suivante:

1-Caractérisation des facteurs expérimentaux affectant le processus de déshalogénation.

2-Identification des aspects structuraux de l'analyte affectant le processus de déshalogénation.

3-Application de concepts et de données appartenant à la chimie des radiations dans le but de rationaliser la déshalogénation induite par le faisceau primaire. Cette approche est basée sur la similitude des événements physico-chimiques engendrés par la radiolyse et le bombardement par des ions possédant des énergies de l'ordre de 5-20 kiloelectron volts caractérisant LSIMS.

Les effets des paramètres expérimentaux tels que le temps d'irradiation, la concentration de l'analyte, la densité du faisceau primaire, la sélection des matrices, ainsi que la présence d'additifs sur la déshalogénation d'un composé modèle ont été étudiés. La chlorpromazine a été utilisée comme composé modèle. On a observé que la déshalogénation de la chlorpromazine augmente avec le temps d'irradiation et la densité du faisceau primaire. Il a été reconnu que la sélection de la matrice est le facteur expérimental le plus déterminant quant à l'induction de la déshalogénation par le faisceau primaire en LSIMS. Une échelle de capacité d'inhibition de la déshalogénation a été établie et confirmée avec des composés différents de la chlorpromazine. La tendance des matrices à inhiber la déshalogénation a été reliée à certaines caractéristiques structurelles. Cette tendance peut être représentée par la séquence suivante:

NBA, HBSA, DEP > HEDS > HPEA, DMBA, BOP > TDG, THIOGLY > AET, GLY

Aromatiques	**>**	**Aliphatiques**	**>**	**Aromatiques**	**>**	**Aliphatiques**	**>**	**Aliphatiques**
Avec groupes électroattracteur		RSSR		Avec groupes donneur d'électrons		RSH		Groupe alcool

Nous avons aussi observé la tendance de certaines matrices à induire la formation du cation radical, $M^{+\cdot}$, avec la chlorpromazine. En fait, une étude plus poussée a démontré l'existence d'un lien entre la capacité de la matrice à inhiber la déshalogénation et sa tendance à favoriser la formation des ions $M^{+\cdot}$. Ce lien a été établi en tentant de définir le potentiel de réduction des matrices dans les conditions de bombardement. Des composés ayant des potentiels d'oxydation connus ont été utilisés à cette fin. La tendance des matrices à favoriser la formation des ions $M^{+\cdot}$ a été liée à la propension à la capture d'électrons.

La sélection de la matrice ayant été reconnue comme étant le facteur déterminant, nous avons donc porté une grande partie de nos efforts sur cette facette de la déshalogénation en LSIMS. L'obstacle principal à une rationalisation systématique de la capacité des matrices à inhiber la déshalogénation (ainsi que d'autres processus de réduction) consiste surtout en un manque d'information endémique concernant l'identité de l'agent initiateur des processus de réduction. Cet état de chose exclut d'office l'établissement d'une corrélation entre l'affinité des matrices pour l'agent initiateur et l'inhibition du processus de réduction. En effet, l'inhibition du processus ne peut trouver son origine que dans la désactivation des agents initiateurs. Dans le but d'identifier l'agent initiateur de la déshalogénation, l'effet de l'affinité électronique des composés halo-aromatiques sur le taux de leur déshalogénation fut étudié. L'observation d'un effet de l'affinité électronique sur la déshalogénation peut indiquer la contribution des électrons secondaires à ce processus de réduction. La déshalogénation décroît avec une augmentation de l'affinité électronique du composé haloaromatique. Cette observation est compatible avec le postulat que les électrons secondaires générés par le faisceau primaire sont les agents initiateurs de la déshalogénation. Cette interprétation est appuyée par l'existence d'une tendance similaire en radiolyse et en électrochimie où la déshalogénation est induite par l'électron. Les résultats d'études en radiolyse ont aussi démontré que les composés halo-aromatiques dans l'isopropanol sont dehalogénés exclusivement par les électrons solvatés.

Les résultats de nos travaux présentent donc de fortes évidences que les électrons secondaires produits par l'interaction du faisceau primaire avec l'échantillon sont responsables de la déshalogénation. La tendance de la matrice à inhiber la déshalogénation peut donc être expliquée en terme de sa capacité à capter des électrons. Initialement, la capacité de la matrice à capter un électron a été limitée à son affinité électronique. Cependant, cette approche simpliste s'est révélée être fort limitée puisque la grande majorité des matrices ne possèdent aucune affinité électronique. Il apparaît donc

ardu d'expliquer les tendances à la déshalogénation observées strictement en terme d'affinité électronique. En conséquence, une analogie a été établie entre les propriétés oxydoréductrices des matrices et le comportement de composés organiques similaires sous conditions radiolytiques. Cette analogie semble appropriée étant donné que sous condition de radiolyse et de bombardement par FAB/LSIMS, l'énergie est distribuée à l'échantillon de façon non-discriminatoire. Il en résulte en la formation d'ions, d'électrons, d'espèces excitées, ainsi qu'une multitude de radicaux. Donc, à l'instar de l'approche radiolytique, l'emphase a été placée sur les propriétés oxydoréductrices des espèces transitoires produites sous l'influence du bombardement particulaire. En fait, il s'agit de décrire qualitativement le milieu créé par la matrice sous condition de bombardement.

Par exemple, dans le cas des alcools, des électrons ainsi qu'un certain nombre de radicaux sont produits par bombardement particulaire. La plupart de ces radicaux réagissent rapidement avec des molécules intactes d'alcools pour générer un radical α-hydroxyalkyl par abstraction d'un hydrogène de l'alcool. En d'autres termes, il y a convergence de la cascade radicalaire des alcools aliphatiques vers le radical α-hydroxyalkyl. Ces radicaux peuvent aussi être produits par l'action directe des particules de bombardement. Plusieurs études FAB/LSIMS du glycérol ont également établie de façon indiscutable la formation de ces radicaux par l'effet du bombardement particulaire. De plus, les électrons issus du bombardement sont relativement stables lorsque solvatés dans les alcools. Par conséquent, on peut résumer la cascade radicalaire des alcools aliphatiques par le schéma suivant:

Les radicaux α-hydroxyalkyls sont de puissants réducteurs capables de transférer un électron à une grande variété de composés organiques. Le comportement des alcools sous conditions de bombardement particulaire est caractérisé par (a) la production d'une cascade radicalaire réductive et (b) l'absence d'un mécanisme de désactivation des électrons fruit du processus de bombardement. Le comportement des alcools aliphatiques sous conditions de radiolyse offre donc une excellente rationalisation qualitative de la propension du glycérol à favoriser les processus de réduction sous conditions FAB/LSIMS. Dans ce cas, on peut résumer la cascade radicalaire du glycérol dans les condition de bombardement FAB/LSIMS par le schéma suivant.

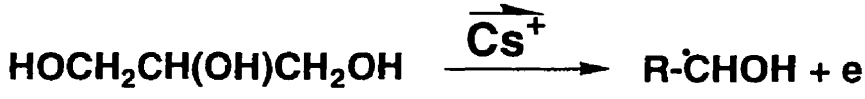

La contribution possible des radicaux α-hydroxyalkyls au processus de réduction en FAB/LSIMS n'a jamais été reconnue, bien que leur existence soit clairement démontrée et largement documentée. Les composés tels que les porphyrines, quinones, cétones aromatiques, cations métalliques, composés pyridinium et teintures organiques sont sujets à la réduction induite par le faisceau en FAB/LSIMS. Des expériences de radiolyse ont démontré que ces composés sont réduits par les radicaux α-hydroxyalkyls.

Des arguments attenant à la nature de la cascade radicalaire ont été avancés pour expliquer le comportement de matrices aliphatiques contenant groupement thiol ou disulfide. Ces arguments se sont avérés aussi utiles que dans le cas des alcools. Dans ce cas-ci, la cascade radicalaire des molécules contenant du soufre (thiol et disulfide) 'converge' vers le radical thiyle (RS$^{\cdot}$) dont les propriétés sont oxydantes. De même, les molécules intactes ont une bonne aptitude à capter les électrons. Ces deux aspects différentient de façon claire et nette le comportement différent des matrices contenant du soufre (thiol et

disulfide) et de celles contenant des groupements fonctionnels alcools sous conditions de bombardement particulaire. Cette démarcation n'avait vraiment jamais été effectuée auparavant de façon systématique.

La situation est plus simple pour les matrices aromatiques étant donné leur capacité à capter des électrons, tel que démontré par des résultats obtenus par des techniques de radiolyse et par l'affinité électronique positive affichée par les matrices aromatiques ayant des groupements fonctionnels électroattracteurs. Nos travaux ont aussi montré l'effet important de la concentration de l'analyte à la surface de la gouttelette sur la déshalogénation. L'hypothèse émise ici suggère qu'une haute concentration de l'analyte à la surface de la gouttelette résulterait en une plus grande tendance à déhalogéner. Ceci serait dû à la concentration accrue des espèces réactives (électrons) à la surface de la matrice. Dans le but d'appuyer cette hypothèse, on a tenté de comparer la déshalogénation dans plusieurs situations où la concentration de l'analyte à la surface de la gouttelette varie: (a) pour des composés analogues ayant une activité de surface différente a été comparée (b) par l'utilisation d'une matrice analogue au glycérol mais possédant une tension superficielle inférieure, et (c) par l'utilisation d'un surfactant anionique comme additif. Les résultats les plus probants dans ce domaine se présentent par l'observation d'un taux de déshalogénation nettement plus haut pour un composé doté d'une activité de surface plus grande que celle d'un analogue non-surfactant. Les résultats attenant à l'effet de la tension de surface de la matrice sur la déshalogénation semblent indiquer que cette variable pourrait jouer un rôle dans ce processus.

Même si les hypothèses présentées ici ne pourvoient pas une rationalisation complète des processus induits par le faisceau primaire, elles présentent somme toute une des premières approches systématiques à un problème extrêmement complexe. On ne peut suffisamment accentuer le fait que le but de ces travaux consiste surtout à l'identification

des caractéristiques saillantes de la chimie des matrices induites par le faisceau, et non pas une explication complète et détaillée des réactions oxydoréductrices rencontrées dans la pratiques des techniques de FAB/LSIMS. On peut cependant affirmer que l'utilisation de concepts et de données émanant de la chimie des radiations a été fructueuse dans la mesure où cette approche a permis une rationalisation qualitative de la capacité des matrices d'inhiber la déshalogénation. La chimie oxydoréductive du glycérol est particulièrement bien décrite au moyen de cette approche. La rationalisation qualitative de la capacité des matrices à inhiber la déshalogénation est basée sur les résultats probants qui ont été assemblés et qui impliquent les électrons secondaires en tant qu'agent initiateur de la déshalogénation.

TABLE OF CONTENTS

List of Figures

List of Tables

Glossary

AET	1,4-anhydroethrytol
BOP	2-benzyloxy-1,3-propanediol
CRF	Charge remote fragmentation
DEP	Diethyl Phthalate
DMBA	3,4-dimethoxybenzyl alcohol
$E_{1/2}$	Half-wave reduction potentials
EA	Electron affinity
FAB	Fast atom bombardment
Gly	Glycerol
HBSA	4-hydroxybenzene sulfonic acid
HEDS	2-hydroxyethyl disulfide
HPEA	2-hydroxyphenethyl alcohol
LUMO	Lowest unoccupied molecular orbital
LSIMS	Liquid secondary ion mass spectrometry
MES	2-mercaptoethyl sulfide
NBA	3-nitrobenzyl alcohol
TDG	Thiodiglycol
Thiogly	Thioglycerol

To my parents,

For their love, trust
and unrelenting support.

"There's a light and a shadow on every man
who at last attains his lifted mark,
nursing the spark through ethereal night."

Herman Melville
from 'Commemorative of naval victory'

Acknowledgements

Je désire exprimer ma gratitude au Professeur Michel Bertrand, mon directeur de thèse, pour ses conseils et ses encouragements tout au long de mon parcours académique à l'université de Montréal. De fertiles discussions m'ont permis de bénéficier de sa grande expérience d'un champs de recherche en pleine effervescence. Je ne peux me permettre d'oublier de mentionner la confiance qu'il m'a témoignée en me donnant une place dans son laboratoire.

I cannot forget my very good friend Dr Gary Paul who showed me relentlessness in science as well as in the criticism of my writing style. I daresay his friendship and unmatched sense of humour were highlights of my stay at U de M. Mike Evans deserves a special place here which goes well beyond the willingness to initiate the many to the knowledge of the few. However, I will still greet his claim that he is not british with a fair amount of skepticism. I am indebted to Dr R.E. March for sparking and encouraging my initial interest in the wonders of mass spectrometry. Je désire aussi remercier Pierre-Nicholas Roy pour son aide avec le programme MOPAC ainsi que pour avoir partagé mes anxiétés d'origine bureaucratique. Son enthousiasme pour des idées fort éloignées du domaine théorique a toujours été des plus rafraichissant. J'ai eu le plaisir de bénificer de l'aide inestimable de Lyne Laurin et Carolle Billette. Je leur dois un grand merci. Merci aussi aux membres du C.R.S.M. pour avoir partagé avec moi leurs expertises et leurs tribulations.

À Nancy Leymarie, qui m'a toujours donné son support et son amour sans lesquels mes jours auraient été autrement plus gris et certainement moins gais, je ne puis que lui dire qu'elle a rendu tout plus facile. "So thrive my soul"...

Chapter 1

1. Introduction

In the preface of his 1913 book "Rays of positive electricity and their application to chemical analysis", J.J. Thomson, the man widely recognized as the father of mass spectrometry assessed with astonishing prescience the future role of mass spectrometry:

> "I have described at length the application of positive rays to chemical analysis. One of the main reasons for writing this book was the hope that it might induce others, especially chemists, to try this method of analysis. I feel sure that there are many problems which could be solved with far greater ease by this than any other method."[1]

In its infancy, the technique was primarily used for the precise measurement of isotope abundances and accurate atomic masses, making valuable contributions to those areas. It is ironic that Thomson's disciple Aston stated in the late 30's that the iminent completion of elemental isotopic composition studies would doom mass spectrometry as a field of research[2]. The introduction of an electron impact source and the extensive use of mass spectrometry in vital wartime research such as the Manhattan project led to the production of the first commercial machines. These instruments were devoted to use by the petroleum industry and inaugurated the beginnings of organic mass spectrometry. A further important development was the birth of high

resolution mass spectrometry brought about by the introduction of double focussing instruments[3].

However, the achievement of optimal results in mass spectrometry is highly dependent on the method of ionization. Hence, the development of new ionization techniques has been essential to the growth of mass spectrometry as a method of organic analysis. Unfortunately, the 'classical' ionization techniques such as electron impact and chemical ionization were severely hampered by the requirement that the analyte be volatilized prior to ionization. This requirement greatly curtailed the analytical applications of mass spectrometry. The field desorption technique somewhat alleviated this lack but an arcane sample preparation method and transient ion currents seriously limited any widespread use of this technique.

The use of energetic particles bombarding a sample to produce ions provided an essential step in attempting to circumvent the volatilization requirement. This approach characterized plasma desorption[4] which utilised MeV fission products from ^{252}Cf as bombarding particles and allowed the generation of mass spectra from thermally labile, polar, and involatile molecules. The extension of secondary ion mass spectrometry (SIMS), normally a method of inorganic analysis, to the organic realm was attempted by Benninghoven[5]. The main problem associated with this endeavour resided in the short sample lifetime due to 'radiation damage' by the high flux primary beam. The magnitude of this problem was attenuated by diminishing the flux of the primary beam and its angle of incidence to the target. However,

diminishing the primary beam flux required longer acquisition times as the weaker signal had to be integrated over a significant period.

The inception of Fast Atom Bombardment (FAB) in 1981 considerably broadened the scope of mass spectrometry into the hitherto inacessible heartland of thermally labile, polar and high molecular weight molecules common to the biochemical and biomedical fields[6]. The problem of sample lifetime due to radiation damage was resolved by the use of a low vapour pressure liquid to dissolve the sample. This innovation allowed the uses of high primary beam fluxes to obtain long lasting sample ion currents ($\geq$ 5 minutes) compatible with the generation of high resolution and tandem mass spectrometry data. The liquid matrix, not the neutral primary beam, is the heart of fast atom bombardment. A neutral beam had already been used in organic analysis[7]. Its sister technique, liquid secondary ion mass spectrometry (LSIMS), produces virtually identical results whilst using ions as the bombarding species.

The success of FAB has been ascribed to its ease of use, simplicity, adaptability to older instruments, and low cost. However, the main reason for the success of the technique stems from its ability to produce analytically relevant gaseous ionic species from a given sample. The ions commonly observed in FAB/LSIMS analysis are protonated or cationized analytes and fragments. These gaseous ionic species arise from the interaction of a beam of primary particles of kiloelectronvolt energy with a liquid sample.

The effect of the interaction of the primary beam with the sample has turned out to be both a blessing and a curse. For whilst it is the *raison d'être* of the technique, primary beam-sample interactions are now widely recognized as the potential source of many undesirable artefacts. The propensity of the technique to produce artefacts fostered by the interaction of the primary beam with the sample was recognized at an early stage. The year following the first FAB publication, Field[8] published a landmark paper focussing excusively on the FAB behaviour of the most common liquid matrix, glycerol. The findings of the author prompted him to comment thus:

> ''However, one immediately wonders whether radiation damage such as that found for glycerol will also occur for solutes dissolved in glycerol, which could lead to erroneous spectra.''[8]

This statement foretold of the opening of a new area of research within FAB concerning the generation of artefacts through what is now commonly called beam-induced processes. There now exists a sizable literature concerned with the study of such phenomena[9]. The question can be asked whether such efforts are justifiable. The answer is emphatically affirmative considering the following reasons.

For the analyst, artefacts are at best a nuisance which he must constantly strive to eliminate. Where the study of the fundamental processes of a technique are concerned, however, investigating the formation of artefacts can yield potentially useful information related

to the physico-chemical events characteristic of the technique. Conversely, elucidating the genesis of artefacts can provide the analyst with precious information leading to steps enabling the suppression of artefacts. Mass spectrometrists have been particularly concerned by the artefact generating potential of ionization techniques since physical alteration of the analyte through ionization is required for analysis to be carried out.

The occurrence of beam-induced reactions can lead to alkylations[10], formation of covalent analyte-matrix adducts[11-14] and a multiplicity of redox processes[15-33]. The largest group of beam-induced reactions commanding the most attention concerns reductive processes. In many cases, the ionic species generated under FAB/LSIMS conditions are the result of reductive processes involving the analyte. These processes can cause the intensities of A+n peaks ($A=[M+H]^+$, $n \geq 1$) to be higher than the theoretical values calculated using natural abundances. These observations prompted the investigation of this phenomenon, particularly for peptides[15-16]. Cationic organic dyes can undergo beam-induced reduction which is typified by the addition of one or more hydrogen atoms to the molecular ion and gives rise to ions one or two mass units heavier than the molecular ion. These dyes are the most extensively studied systems[17-22]. In certain instances, a specific functional group of the analyte is known to be involved in the reductive process. Examples include the reduction of nitro[23] and azide[24] groups to the amine, reduction of aromatic oximes to imines [25], dehydroxylation[26] (substitution of a hydroxy function by a hydrogen), deamination[27] (substitution of a primary amine by a hydrogen),

reductions of disulfides to thiols[28] and dehalogenation[29-36] (substitution of a halogen by a hydrogen).

This thesis concerns the investigation of the beam-induced dehalogenation of haloaromatic compounds. This process is characterized by the appearance in the FAB/LSIMS mass spectrum of a haloaromatic compound of an ion resulting from the substitution of the halogen by a hydrogen. The importance of beam-induced dehalogenation resides in the fact that its occurrence can lead one to falsely conclude that a dehalogenated species is present in a sample of a pure haloaromatic compound. This can have serious consequences in metabolic studies[32] or compound identification[29].

The motivation behind the investigation of the LSIMS beam-induced dehalogenation of haloaromatic compounds can be summarised as follows; (i) alleviate the lack of systematic studies on the experimental parameters affecting the reaction, (ii) search for means of inhibiting the reaction, (iii) attain a deeper understanding of matrix chemistry, and (iv) strive to elucidate the mechanism of beam-induced reductions through the particulars of dehalogenation that could possibly be applicable to other systems.

Haloaromatic compounds confer certain advantages to the investigation of reduction processes in LSIMS as outlined below. In contrast to other extensively studied systems such as organic dyes, haloaromatics offer several advantages: (i) a wide variety of compounds are available in a high state of purity; (ii) structurally analogous compounds of the

same family can be studied, i.e. where the halogen is varied for a single organic moiety; (iii) relatively simple compounds can be used as model compounds and their physicochemical properties modified using known synthethic procedures; and (iv) there exists an important body of research where the reductive dehalogenation of haloaromatics has been extensively investigated using a variety of techniques such as pulse radiolysis[37-38] and electrochemistry[39-40]. This last point is important since one may then seek analogies, however indirect, with known radiation chemistry and/or electrochemistry.

An important aspect of the study of the beam-induced dehalogenation of haloaromatics consists of probing the aspects of matrix chemistry which could possibly affect redox processes. A major effort will be deployed to identify the matrix structural features influencing redox processes. For this purpose, a maximum number of liquid matrix compounds were utilised in the hope of achieving a meaningful classification of such structural features. These structural features could then be associated with the extent of the redox processes observed in the FAB/LSIMS spectrum which could in turn be rationalized in terms of the known or assumed properties of matrix structural features.

A distinctive facet of the investigation will be to draw extensively on the radiation chemistry literature in order to explain the behaviour of the systems under FAB/LSIMS conditions. The potential similarities between FAB/LSIMS conditions and radiolysis has been mentioned before[41-45] but there has been no attempt to systematically use radiation chemistry data and concepts to rationalize FAB/LSIMS beam-

induced redox processes. This is somewhat surprising since in both cases an energetic particle generates a 'track' in the medium it penetrates, along which energy is deposited and transient reactive species are formed. In essence, energy is imparted to the sample in a non-discriminate way, generating a 'radical cascade'. In both cases a rich and diverse chemistry results from the subsequent reaction of the radiation-induced transients. The fact is that the *awareness* of the existence and consequences of beam-induced 'radical cascades' in FAB/LSIMS is well documented. It is indeed ironic that one of the conceptors of the fast atom bombardment technique, R.D. Sedgwick, carried out research concerning the behaviour of organic liquids (including alcohols) under radiolytic conditions prior to his involvement with the FAB project[46]. Hence, the line of investigation consisting of using radiation chemistry data and concepts to rationalize FAB/LSIMS data will be extensively explored.

The radiation chemistry literature can provide useful information concerning beam-induced processes in FAB/LSIMS since the field is essentially about the chemical behaviour of irradiated material. Of paramount importance is the ability of pulse radiolysis to provide information about the redox properties[47] (reduction potentials) of radiation-induced transient species originating from organic molecules as well as the kinetics[48] of such transients with particular solutes. For example, the known rates of reactions of the hydrogen atom and solvated electron with organic and inorganic solutes have been tabulated[48]. The hydrogen atom and solvated electron are the beam-generated species most often associated with the reduction processes

characteristic of FAB/LSIMS. A comparison of the data pertaining to those transient species might yield useful information.

The radiation chemistry of many organic liquids have been investigated and the characteristics of their radiation-induced transients elucidated. It is fortunate that alcohols have been particularly well studied[49-50], perhaps allowing insight into the beam-induced radical cascade of glycerol. This point is particularly important since glycerol is widely recognized as being the matrix where beam-induced reduction processes have the greatest tendency to occur.

It is not the aim of this work to comprehensively elucidate FAB/LSIMS beam-induced reduction mechanisms. This is not a feasible goal given the complexity of the problem and the dearth of tools to obtain conclusive data. Rather, the goal is to expand our current knowledge of these phenomena through the detailed study of a particular process in parallel with a systematic study of the aspects of radiation chemistry which could broadly apply to FAB/LSIMS beam-induced processes.

Chapter 2

2.1 The FAB/LSIMS source

The various designs[51] of FAB and LSIMS sources share the same basic principle: the production of an energetic beam of particles having keV energy which is used to generate ions from a liquid sample. These ions can subsequently be mass analysed to yield information pertaining to the structure of the analyte or the nature of the sample.

In FAB sources, the source of energetic particles overwhelmingly consists of rare gases such as argon and xenon. The fast atom beam is produced by ionizing the atoms, accelerating them through a potential (typically 2-8 keV), and finally allowing the fast ions to be neutralized through resonant gas phase charge exchange. The widespread use of a fast atom beam stems from the initial beliefs of the conceptors of this ionization method.

In the first publication describing FAB[52], the authors reported that a neutral primary beam was preferable to a charged primary beam given the tendency of the latter to generate surface charging and subsequent loss of the secondary ion beam. The difficulty of steering a charged primary beam into the high voltage ion source of a magnetic sector instrument was also cited as a reason for using a neutral atom primary beam. These objections to charged primary beams were not substantive since earlier sputtering and SIMS research had demonstrated that surface charging was not a problem and fast ions performed equally well as fast atoms.

The introduction of LSIMS sources occurred shortly after the inception of FAB[53]. The most typical LSIMS component is the caesium ion gun. This design consists of thermionically emitting caesium ions from a heated alkali aluminosilicate solid where the alkali species have relatively free movement. Upon desorption from the surface, the ions are accelerated by electric fields. The schematic of the caesium ion gun is shown in Figure 1. This configuration actually present several advantages over the FAB design.

(1) Charged beams are more easily focussed than neutral beams.
(2) The caesium ion gun does not contribute to background source pressure. This can be a significant advantage when using volatile liquid matrices.

It is now widely recognised that bombardment of a nonvolatile organic analyte in a low vapour pressure solvent gives virtually identical results whether bombarded with ions or atoms provided the bombarding particles are of similar mass[53]. This is the case when the primary FAB and LSIMS beams are comprised of xenon atoms (m/z 132) and caesium ions (m/z 133), respectively.

Whatever the nature of the bombarding keV particle, the principles of FAB and LSIMS are the same. A sample, usually a few micrograms, is dissolved in 1-3 μL of a low vapour pressure solvent. The resulting solution is deposited on a metal target attached to a direct insertion probe. The probe is then inserted into the ion source where the probe tip (metal target) intercepts the primary beam. The position of the

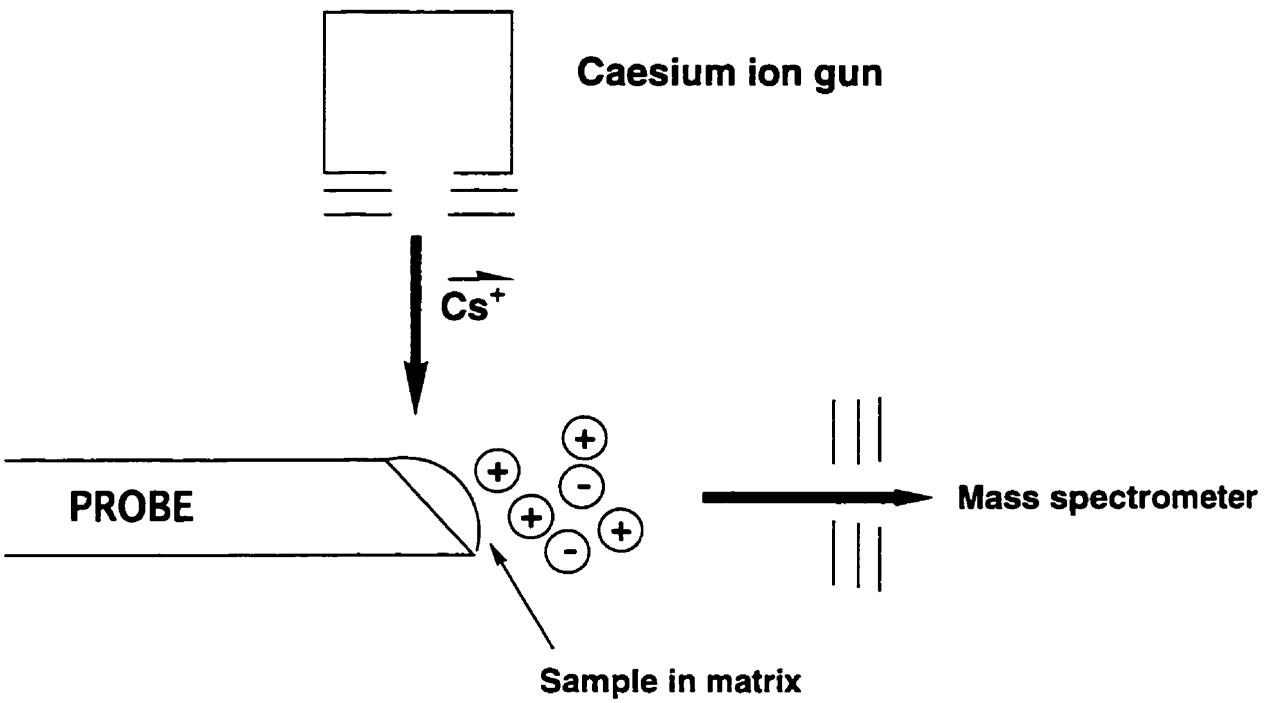

Figure 1. Schematic diagram of the caesium ion gun.

probe tip is such that the primary beam produces a 60 degree angle with respect to the normal of the probe tip surface and/or maximizes sputtering into the mass spectrometer.

The positive ions resulting from the interaction of the primary beam with the sample are of the following general types if the sample is an organic analyte.

- The protonated molecule, $(M+H)^+$.
- Fragments from the analyte that are informative as to its structure.
- Ions emanating from the matrix as fragments, protonated molecule and proton bound oligomers.
- Analyte-matrix adducts, mostly proton bound, having the general formula $(M_nG_mH)^+$ where M is the analyte and G the matrix.
- Cation-analyte adducts of the type $(M+C)^+$ where C is a metal cation. These ions arise from the presence of alkali metal cation such as sodium or potassium in the sample solution as contaminants or by design.

2.2 The Matrix Liquid in FAB/LSIMS

Notwithstanding the polemics surrounding the original appelation of the FAB technique, the crucial innovating component is the use of a liquid matrix. The problems associated with the rapid decay of the secondary ion yield due to radiation damage imparted to a 'dry' organic sample by keV particle bombardment can be circumvented by the use of a liquid

matrix. The resulting solution allows the production of intense secondary ion signals for prolonged time periods useful for scanning sector instruments. The overwhelming importance of this component of the technique is underlined by the number of reviews[54-57] on the subject as well as numerous publications exploring the effect of the matrix on the appearance of the mass spectra. The fact that sensitivity can be immensely improved by proper matrix selection shows how crucial this component is to the FAB/LSIMS technique.

Notwithstanding the chemical effects of analyte/matrix permutations, the main role of the matrix is to dissipate the energy of the impacting primary beam thus allowing the desorption of intact analyte ion through diminishment of the internal energy acquired the analyte molecules[57]. A recent study[58] suggested that matrix selection can influence the extent of fragmentation and types of ions observed in the FAB mass spectra of peptides. The differences were rationalized in terms of the internal energy of the molecular ions of the analyte which is controlled by the desolvation of the FAB desorbed analyte-molecule clusters. Another essential feature of the matrix concerns its ability to act as a "reservoir" where the sample can be replenished at the sites where sputtering and/or radiation damage occurs.

As with any other technique where a solvent is necessary, no 'universal' liquid matrix can be expected to furnish optimal analytical conditions for any analyte or sample. The inventory of liquid matrices is long, given the many permutations possible with co-solvents and additives. In order to be used as a matrix liquid, a compound must

demonstrate the following features related to its physico-chemical properties.

(1) Ability to dissolve the sample

The lack of solubility of an analyte in a particular matrix generally spells complete failure to obtain relevant FAB/LSIMS data. At best, a very low intensity spectrum may be obtained. The use of co-solvents and additives can substantially broaden the scope of a particular matrix. The ability of the matrix to dissolve the analyte allows the matrix to perform one of its main functions, replenishing the analyte molecules that have been sputtered or destroyed by primary beam irradiation. The mechanism(s) involved are still poorly understood. Recent experiments appear to indicate that diffusion by itself is too slow to ensure the desired surface replenishment of the analyte. Auxilliary processes such as mixing, Marangoni effects and electric field migration (for pre-formed ions) may contribute[57,59].

(2) Relative involatility under the analysis conditions

This requirement is essential given the necessity to provide a timescale where a mass spectrum must be recorded. The ion source of a mass spectrometer is generally imcompatible with high vapour pressure compounds. Furthermore, a low matrix vapour pressure will allow the sustainment of steady secondary ions beam necessary for the performance of experiments such as exact mass measurement and collisionally activated dissociation.

(3) Chemical inertness

The matrix should be chemically unreactive towards the sample unless the reaction is one which is known or desired as in the case where simple ionization is promoted. The deleterious effect of matrix-analyte reactions prior to analysis has been noted[60].

(4) Spectral transparence and weak signal

The ions due to the matrix should be as unobtrusive as possible in the analysis process. Therefore, features such as low molecular weight and a relatively low ionization efficiency are desirable for a matrix compound. The cases arising when a matrix ion is isobaric with an analyte ion can be problematic.

Cook et al[61] have advocated the tabulation of matrix physical properties in an effort to promote more systematic matrix selection. However, the relative obscurity of some important matrix compounds has left important gaps in the tabulation. Some matrix physical properties which can affect FAB/LSIMS mass spectra quality are viscosity, surface tension, dielectric constant, redox chemistry, pKa, and proton affinities.

Viscosity can affect the mass transport of analyte molecules to the surface. The dielectric constant affects ion pairing and solvation in solution which can affect the abundance of free ions in solution and thus the sensitivity of the technique for preformed ions. The matrix surface tension is known to influence the analyte surface concentration through preferential migration of molecules with significant surface

activity. A high analyte surface concentration increases the propensity of the molecules to be preferentially desorbed and detected[62]. The pKa and proton affinity are the matrix chemical properties which relate to protonation. These properties affect the relative thermodynamic stability of analyte ions with respect to proton transfer in the condensed and gas phases. For example, triethanol amine[63] is not used as a liquid matrix for positive ion work since this compound will protonate preferentially both in the gas and condensed phases due to its high basicity and proton affinity.

The matrix reduction potentials can be helpful to evaluate the stability of the analyte with respect to oxidation or reduction induced by the matrix *prior* to bombardment. It is well known that some coordination compounds are reduced by glycerol[60]. The matrix reduction potentials are less useful in gauging their ability to quench the radiation chemistry induced by the primary particle beam. The rich and diverse (as well as poorly understood) chemistry resulting from the interaction of keV particles with the sample has been recognized as a potential source of misleading artefacts. The redox chemistry of these beam-generated transient species may play an important role in analyte reduction/oxidation. The role of the nature of the radical cascade generated under FAB/LSIMS conditions has never been addressed in a systematic fashion and remains a relatively unexplored area.

Glycerol was the first matrix liquid used as well as being the most versatile. However, this compound has a low capacity to inhibit the artefact-generating processes mentioned above. Matrices possessing

'radical scavenging' properties can be used to diminish or avoid the deleterious effects of beam-induced reactions. These matrix compounds, such as thioglycerol, 3-nitrobenzyl alcohol (NBA), 2-hydroxyethyldisulfide (HEDS) and 4-hydroxybenzenesulfonic acid (4-HBSA) can be used as an alternative to glycerol. There exists a plethora of other matrix compounds although their use has been scant.

The effectiveness of glycerol can be enhanced by the use of additives. The most common and well documented use of additives in FAB/LSIMS concerns the use of acids to increase the sensitivity for positive ion mass spectra through analyte protonation in solution. The 'acid effect' has been thoroughly discussed and evaluated by Ligon[64] and Sunner[65]. Conversely, the FAB/LSIMS negative ion signal of analytes having acidic functional groups can be enhanced by the addition of base.

Another strategy involving additives with the aim of improving FAB/LSIMS sensitivity consists of using surfactants having a charge opposite to the mode of analysis[66-68]. The charged surfactant molecules can 'bind' the analyte ions to a position near the matrix surface where they can be efficiently desorbed. One of the more baffling developments in the area of additives consists of the use of carbon powder(!) to improve the ionization efficiency of apolar compounds[69]. The reduction processes common to glycerol can be completly or partly quenched by the judicious use of additives scavenging the beam-induced reactive species responsible. Such additives range from TFA (trifluoroacetic acid)[70], camphorsulphonic

acid[71] and Copper(II)[72]. The electron/radical scavenging capacity of the additives was invoked to rationalize their effectiveness in inhibiting reduction processes.

The fact remains that despite the efforts invested in understanding the crucial role of the matrix in obtaining optimal FAB/LSIMS results, matrix selection for a particular analysis remains very much an empirical exercise.

2.3 Ionization Mechanisms

The mechanism(s) by which analyte molecules are ionized under FAB/LSIMS conditions has generated much attention and speculation since the inception of FAB in 1981. The development of a coherent ionization mechanism accounting for the genesis of ions in FAB/LSIMS has been actively pursued from the outset. The fact that the debate remains unresolved after more than ten years can probably be attributed to a simple truth[73]. *The technique works* and hence the specific mechanism or mechanisms of ion formation are of secondary interest to those who utilize FAB/LSIMS techniques as a means of introducing thermally labile, polar and high molecular weight molecules into the gas phase for subsequent mass analysis.

Given the number of reactions which can take place under FAB/LSIMS conditions, it is not surprising that elucidating in a clear fashion the ion formation process remains a challenge. Nevertheless, a considerable amount of experimental data has been accumulated on the

subject using various chemical systems. On the basis of this data, several models have been proposed to rationalize the ionic species observed in the FAB/LSIMS spectra. Of particular interest is the mechanistic pathway(s) by which protonated molecules, $(M+H)^+$, are formed.

The FAB/LSIMS ionization models proposed generally fall into two distinct categories which are related to where ionization processes are believed to occur. Hence, the models are referred to as pertaining to the condensed or gas phase. One of the problems associated with these ionization models is the nebulous definition of the phase boundaries that the terms 'gas' phase and 'condensed' phase convey. Nevertheless, the approach of rationalizing the formation of FAB/LSIMS ionic species through condensed phase ionization or by gas phase ion/molecule reactions of analyte molecules has been reasonably successful.

It is of paramount importance to remember that the use of different chemical systems implies different chemical properties which can in turn significantly affect the contribution of gas- and condensed-phase mechanism to the FAB/LSIMS ionization process. For example, condensed phase mechanism(s) are much less likely to be important for volatile analytes.

2.3.1 Condensed Phase Models

The condensed phase models can essentially be broken down into two more or less distinct categories: the simplest involves ion formation as a

result of chemical equilibrium in the liquid matrix and a more complicated mechanism implicating beam-induced ionization that produces similar or different ionic species in solution. The model depicting the simplest scenario, the direct ejection of preformed ions from the matrix without an ionization step, is referred to as the 'precursor' model. The precursor model is applicable to ionic analytes in solution and highly basic (positive ion mode) or acidic (negative ion mode) molecules.

In the precursor model, the desorption of ions is essentially analogous to the scheme proposed by Benninghoven[74] for molecular SIMS and which comprises the following features: (1) surface impact, (2) very fast energy transfer ($<10^{-12}$ s) over a certain volume and (3) ejection of secondary ions from the surface. The extremely short period of time in which the energy transfer occurs is believed to be responsible for the fact that vibrational excitation of the emitted molecules and their subsequent fragmentation is dampened. For the area very close to the the point of impact, it appears likely that the amount of energy transferred to the solution is high enough to cause the dissociation of chemical bonds in the matrix and analyte molecules and thus lead to the emission of fragments. Conversely, in the vicinity of the point of impact, the energy transferred to the target is not sufficient to break bonds but enough is furnished to result in the desorption of the preformed ions as well as cluster of ions and matrix. The fragments can also be formed through unimolecular decomposition of excited preformed ions following the desorption process.

Another proposed mechanism involves ion formation through the ejection of charged micro-droplets[75]. In this case, particle bombardment causes a rapid succession of collisions in solution which in turn results in rapid vaporization of neighbouring molecules. The abrupt increase in local pressure results in the ejection of molecular clusters of different dimensions. These clusters are ionic or neutral in nature. The charged droplet then sheds solvent molecules through successive evaporation of solvent molecules[76].

Where non-ionic analytes are concerned, however, the situation is much more complex and the models proposed for preformed ions ions are often inadequate to explain the FAB/LSIMS spectra generated from neutral molecules. In his investigation of the secondary ion emission arising from the bombardment of pure glycerol solutions with a pulsed and continuous primary ion beam, Todd[77] speculated that species generated by the primary ion beam could diffuse into the glycerol samples to react with glycerol or some other solute dissolved in the matrix to promote secondary ion emission. In other words, $(M+H)^+$ ions could arise through beam-induced solution processes.

Todd[78] attempted to substantiate this proposal through thought provoking experiments which resulted in one of the most comprehensive studies of the condensed phase beam-induced ionization hypothesis. In these experiments, the LSIMS spectra of primary n-alkylamines were obtained. The amines were introduced via the gas phase onto the surface of the glycerol matrix. The ion intensities observed for the protonated amines were found to be much higher than the concentration

calculated for the protonated amines using Henry's law. This observation led the author to suggest that the precursors to the protonated amine observed in the mass spectra were not free-base amines but protonated amines in solution resulting from beam-induced processes. The protonating agent was thought to be protonated glycerol formed by beam-induced chemistry, and protonating amines between impact events. It is interesting to note that a gas phase model was presented by Sunner[79] where it was postulated that the ionic precursors to the protonated matrix ions were formed in solution through beam-induced processes.

In his FAB study of deuterated and nondeuterated cyclic acetals, Paul and co-workers[80] found that these compounds yielded dominant $(M-D)^+$ and $(M-H)^+$ ions, respectively. Using chemical ionization, dominant $(M+H)^+$ ions were observed with all acetals. The comparison of FAB and chemical ionization data led to the conclusion that the predominant $(M-H)^+$ ions observed in FAB for the non-deuterated compounds could not be rationalised using thermodynamic terms of known gas phase ion-molecule reactions. A condensed phase model featuring beam-induced generation of ionizing precursors in the matrix was proposed and rationalized along a kinetic basis[81]. Also, the condensed phase model offered better solvation for the multicharged transition state featured for hydride abstraction compared to the transition state for protonation. However, this rationale was not entirely satisfactory to explain the data obtained for the deuterated acetals where a dramatic time dependence was observed. This time dependence suggested that the beam-induced reactive species responsible for hydride abstraction were

generated in the condensed phase and that the time dependence observed resulted from the gradual buildup of such species over time. The comparison of the results obtained with deuterated acetals having different surface activities substanstiated the hypothesis underlying the condensed phase model proposed by the authors.

The hydrogen/deuterium exchange reactions of a variety of protonated aromatic amines with ND_3 in the collision cell of a hybrid BEqQ tandem instrument were studied by Dookeran and Harrison[82]. The protonated amines were generated using FAB and chemical ionization with a variety of reagent gases (NH_3, isobutane, methane). The $(M+H)^+$ ion of 1,3-phenylene diamine produced by chemical ionzation exchanged only slightly with ND_3 whereas a significant fraction of $(M+H)^+$ formed by FAB exchanged protons for deuterium extensively. These results were rationalized in terms of the dominant formation of ring protonated and N-protonated species in chemmical ionization and FAB, respectively. The hydrogen/deuterium exchange being more efficient with N-protonated species. The observation of reactive (and hence N-protonated) $(M+H)^+$ ions in the FAB ionization of 1,3-phenylene diamine was interpreted in terms of significant $(M+H)^+$ formation in solution reactions with direct transfer of these ions to the gas phase.

The FAB/LSIMS ionization processes were thouroughly reviewed in a recent account by Sunner[83]. In his assessment of the evidence presented in the literature, the author contended that gas phase ionization is, in most cases, not important in the FAB ionization process. The parallel between FAB/LSIMS and radiation chemistry was

extensively drawn upon to model the initial collision cascade ionization processes in FAB/LSIMS. It was proposed that glycerol molecular ions ($G^{+\cdot}$) are formed in the collision cascade. The glycerol molecular ions rapidly proton transfer to form protonated matrix ions [1]. The resulting secondary electrons form $[G-H]^-$ presumably through a dissociative electron capture process [2] to produce the $(M-H)^-$ ions typical of FAB/LSIMS spectra.

$$(G^{+\cdot}) + G \longrightarrow [G+H]^+ + [G-H]^{\cdot} \qquad [1]$$

$$ROH + e \longrightarrow RO^- + H^{\cdot} \qquad [2]$$

2.3.2 Gas Phase Models

The contention that FAB/LSIMS ionization processes are akin to those taking place in a chemical ionization plasma has been fuelled by the apparent similarity of the mass spectra obtained with both techniques for a number of compounds[90]. This holds true both in the observation of the protonated molecule $(M+H)^+$ and similar fragmentation patterns. On the basis of these observations, it has been proposed that FAB/LSIMS ionization is essentially governed by gas phase ion-molecule reactions which are known to dominate chemical ionization processes.

Essentially, the gas phase model implies the formation of a high density region above the surface of the liquid surface where ionic and neutral species are present. In this plasma like region, often referred to as the selvedge, ionization may occur through reactions

between highly reactive ionic species and neutral molecules. The term selvedge has also been the subject of much vivid controversy[83]. It is interesting to note that the nature of the selvedge varies considerably throughout the literature and this probably reflects the great flexibility associated with the gas phase model as well as the fact that the term was coined by the SIMS community[84]. In fact, the concept of the selvedge was extensively developed in molecular SIMS by Cooks and co-workers[85,86]. There was early evidence of cationization and electron transfer reactions in organic SIMS. In FAB/LSIMS, however, it soon became evident that proton transfer is the dominant reaction[87-89].

The impetus behind the gas phase model was provided by the work of Schroeder et al[90] who proposed a CI-like mechanism to account for FAB/LSIMS ionization. The use of simple vapour pressure calculations showed that a pressure regime similar to that commonly used in chemical ionization existed above the surface of the matrix. This led to the suggestion that FAB/LSIMS ionization occurs through transport of the analyte to the surface of the matrix, followed by desorption of the neutral analyte and matrix into the gas phase and subsequent ionization of the matrix through interaction with the primary beam. The ionization of the analyte results from CI-type reactions with the ionized matrix molecules.

Inspired by the ideas of Michl[91], who proposed an important role for net ionization (ejection of secondary electrons) in SIMS and FAB/LSIMS, Sunner et al[92,93] elaborated the gas collision model (GCM). According

to this model, the chemistry in FAB/LSIMS is expected to be similar to what is found in high energy radiation chemistry. The initiating step involves the formation of ions from neutral molecules due to the inpinging energetic primary particles. The energy is released to the surroundings by the primary (bombarding) particle and a 'cavity' is formed where hot gas like molecules and fragments are found. A portion of the 'gas' in the cavity is expelled into the vacuum. Subsequently, the positive and negative ions in the gas undergo recombination which leads to the formation of ion pairs or neutral molecules and fragments. The last steps involve proton transfer and ion-molecule reactions.

The popularity of this model was largely fostered by the result of experiments showing a correlation between gas phase basicity of the analyte and matrix to the relative intensities of positive ions observed in the FAB spectra. It should be noted that all the molecules used in these studies were volatile. This leads one to question whether this model is applicable to larger, thermally labile and involatile molecules whose proton affinity is not known and which are the analytes of choice for FAB/LSIMS analysis. Although the GCM adequately explains the formation of protonated analyte and matrix molecules as well as fragments and dimers, it does not take into account the extensive formation of proton bound molecular clusters typically encountered in FAB/LSIMS. For example, glycerol clusters extend up to $(G_{10}+H)^+$ and beyond. In high pressure mass spectrometry, where the partial pressure of the matrix is below that of the equilibrium vapour pressure, such large clusters are not observed.

This is due to the fact that the free energy of nucleation is too large[83].

The observation of metastable peaks in FAB spectra provides evidence of unimolecular fragmentation in the vacuum of both the $(M+H)^+$ and of cluster ions[94]. A fair portion of fragment ions may originate from this process[95]. The close similarity of FAB MS/MS spectra of $(M+H)^+$ and the FAB spectra themselves appear to support this hypothesis.

As stated earlier, Cooks and co-workers[85] comtemplated the question of ionization mechanism in SIMS and proposed a unified theory broadly applicable to SIMS and other desorption methods such as laser desorption and FAB. Initially, the energy is transferred to the target by momentum transfer, ionization, as well as vibrational and rotational excitation. In short, energy isomerization occurs shortly after impact. This leads to the production of electrons, photons, radicals, ions and neutral molecules which are ejected from the surface into the selvedge region. The formation of molecular ions is explained in terms that are comprised in both the precursor model as well as the GCM. Hence, direct desorption of preformed ions and desorption of neutrals followed by gas phase ion-molecule reaction in the selvedge can contribute to the formation of molecular ions. The formation of fragments can take place through the impact of bombarding particles or the unimolecular dissociation of molecular species desorbed from the surface. In essence, the unified theory allows a broad latitude by encompassing aspects of the GCM and precursor model though it is too

general to indicate the relative contributions of each to the FAB/LSIMS mass spectra.

It is evident that there exists an intrinsic difficulty in evaluating the merits of the gas and condensed phase models: the unavoidable fact that a multiplicity of ionization mechanisms exist in FAB/LSIMS, as they do in other techniques such as field desorption, and that their relative contribution will inevitably vary with different chemical systems[96].

2.4 An Overview of Beam-induced Chemistry in FAB/LSIMS

Despite the success of FAB/LSIMS in significantly broadening the scope of mass spectrometry through the generation of analytically relevant gaseous ionic species from hitherto inacessible analytes, the chemistry induced by the primary beam remains an area shrouded in a veil of complexity, woven from the interaction of many interdependant physico-chemical parameters on which the experimentalist's control is all too tenuous. The chemistry induced by the primary beam affects two very important aspects of FAB/LSIMS which are directly related to its effectiveness as an anlytical technique: (1) the ionization process and (2) the fostering of artefact formation. Although the nature of the FAB/LSIMS ionization process(es) has generated considerable attention, speculation and study, the elucidation of such processes remains elusive. In fact, the main contention of the most recent condensed phase ionization models[78, 81] is that the ionization of non-ionic analytes essentially occurs through beam-induced processes in solution.

When any new mass spectrometry technique is introduced, the factors affecting its inherent sensitivity inevitably become the focal point of numerous investigations. Of similar concern to mass spectrometrists is the propensity of a technique to generate artefacts. Such concern is justified by the possibility of complicating spectrum interpretation and/or drawing erroneous conclusions as to the nature of the sample. The potential of the technique to produce artefacts fostered by the interaction of the primary beam with the sample was also recognized at an early stage of the technique[8,9]. The ubiquity of such reactions clearly requires an awareness from mass spectrometrists which was hitherto acquired empirically. Because beam-induced chemistry is quintessentially the *raison d'être* of FAB/LSIMS, it is only logical that the processes derived from it should be thouroughly studied.

Quite apart from honing the analytical capabilities of FAB/LSIMS, a knowledge of the chemistry induced by the beam can be of interest to chemists [8,9,56]. The difficulty of classifying beam-induced reactions is apparent when one considers that dehalogenation is described by some reviewers as a substitution[9] and by others as a reduction[97]. In the following section, beam-induced reactions will be discussed as the following separate categories: Bronsted and Lewis acid-base reactions, matrix-sample adduct formation, and finally reduction-oxidation reactions.

2.4.1 Acid-Base Reactions (Bronsted and Lewis)

2.4.1.1 Bronsted

The use of Bronsted acid-base chemistry has been widely practised in FAB/LSIMS to foster an improvement in sensitivity through ion formation in solution[54-55]. However, the effect on the FAB/LSIMS spectra behind this conventional wisdom has been challenged by the work of Ligon[64] and Shiea[65].

A study on the effect of the addition of bases and acid on the secondary ion signal intensity showed that the effect is not uniform[64]. Polybasic and polyacidic compounds invariably showed a decrease in secondary ion signal after treatment with acid and base, respectively. The effect of adding acid to surface active amines was to actually diminish the ion signal due to $(M+H)^+$. These observations were explained in terms of decreased analyte surface activity for the charged analyte. Hence, the effect of acid addition does not invariably result in an increase in the ion intensity of the analyte.

A critical investigation[65] of the acid effect confirmed that the effect is not uniform and actually demonstrated the deleterious effect of acid addition on $(M+H)^+$ ion intensity. However, the role of preformed ion formation in the uppermost layers of the matrix was acknowledged. In the cases where $(M+H)^+$ ion intensity increased, the effect could be explained using a variety of different rationalizations, e.g. changes in solubility, surface activity, volatility, radiation-induced chemistry and desorption energetics.

Nevertheless, there remains clear evidence that preformed ion formation actually occurs in FAB/LSIMS[98].

2.4.1.2 Lewis Acid-Base Reactions

Lewis acid base chemistry plays an important role in FAB/LSIMS as cationization of analytes with low basicity or proton affinity allows the observation of high intensity analyte-cation ions, $(M+C)^+$. A case in point are the carbohydrates where the cationization process can be used for molecular weight and structure determination since these compounds which do not always give abundant $(M+H)^+$ ions[99]. The presence of a multiplicity of molecular ion signals, $(M+H)^+$, $(M+Na)^+$, and $(M+K)^+$ offer the advantage of confirming the mass measurement of the molecular ion. Conversely, doping the sample with alkali metal ions such as sodium or potassium can lead to the extensive formation of matrix-metal ion adducts which can complicate spectrum interpretation as well as reduce the sensitivity of the analysis. The uncontrolled presence of alkali metal salts in biological samples can lead to considerable difficulties and clean-up methods have been proposed[100]. Anionization has also been observed in FAB/LSIMS. In this case, the organic molecule acts as a Lewis acid to form $[M+X]^-$. This reaction is much less common.

2.4.2 Matrix-Analyte Reactions

The interaction of the primary beam with the sample often leads to the formation of molecular species originating from beam-induced matrix-

analyte reactions of non-redox type. Lehman et al[12] observed an $(M+H+12)^+$ ion in the FAB spectrum of peptides. The use of deuterated glycerol yielded a $(M+H+14)^+$ ion, confirming that the product arises from beam-induced matrix-sample interaction. A mechanism involving beam-induced formaldehyde generation followed by addition to the amino group of the peptide N-terminus and subsequent Schiff base formation through dehydration was proposed. A similar study by Dass[13] and Desiderio suggested that the mechanism of $(M+H+12)^+$ formation consisted of electrophilic attack of ionized glycerol and its oligomers onto the N atom of the N-terminus amino group and subsequent fragmentation of the resulting adducts. A time dependence was observed in both studies. The use of thiol-containing matrices diminished the extent of $(M+H+12)^+$ formation. It should be noted that formaldehyde is an important product of the radiolysis of polyhydric alcohols[101].

The matrix-analyte adducts of quaternary ammonium surfactants and glycerol generated under FAB/LSIMS conditions have been extensively studied. Keough[102] observed formation of covalent adducts formed by condensation reactions (with H elimination) between the glycerol solvent and cetyl pyridinium compounds. The adducts were not observed when thioglycerol was the matrix. Tuinman and Cook[103] investigated similar adducts with trimethylalkyl ammonium surfactants and found a series of peaks corresponding to $(M+30)^+$, $(M+60)^+$ and $(M+90)^+$ ions. These ions represent strong evidence supporting the beam-induced formation of C-centered radicals upon keV particle bombardment of glycerol as suggested by others [8,104,105]. A further study presented

evidence that the mechanism of formation of these adducts was inconsistent with a gas phase process[106].

Molecules containing the aldehyde or ketone group undergo beam-induced condensation reactions with matrices such as glycerol and thioglycerol to form cyclic acetals [11,14]. The reaction was found to be catalyzed by an acid such as p-toluenesulfonic acid. The beam-induced formation of a $(M+133+H)^+$ ion in the FAB mass spectrum of amines and peptides obtained in 3-nitrobenzyl alcohol was studied by Barber et al[107]. This adduct was thought to arise from the condensation of the analyte amine group with nitrobenzaldehyde which was proposed to form as a consequence of atom bombardment.

2.4.3 Beam-Induced Redox Reactions

2.4.3.1 Reductions

Of all the types of reactions induced by keV particle bombardment, reductions are the most reported and thouroughly investigated. These reactions can be classified phenomenologically as two distinct cases:

(1) reduction involving an unidentified site in the molecule, yielding $(M+nH)^+$ ions.

(2) reduction targeting a specific functional group, X, usually yielding $(M-X+2H)^+$ ions.

An example of the former, the observation of $(M+2H)^+$ and $(M+3H)^+$ ions in the FAB/LSIMS spectrum attracted much attention early on. This is due to the fact that these ions can distort the isotopic pattern of the

molecular ion region. The discrepancy between measured and expected values in the isotopic pattern can prevent reliable empirical formulae determination. Reduction processes consisting of simple hydrogen additions have been observed in FAB/LSIMS for several classes of compounds including nucleosides[108], dyes[17-22], porphyrins[109] and peptides[15,16].

In the second general reduction case, a specific functional group of the analyte is known to be involved in the reductive process. Examples include the reduction of nitro[23] and azide[24] groups to the amine, reduction of aromatic oximes to imines[25], dehydroxylation[26] (substitution of a hydroxy function by a hydrogen), deamination[27] (substitution of a primary amine by a hydrogen), reductions of disulfides to thiols[28] and dehalogenation[29-36] (substitution of a halogen by a hydrogen). These reactions can significantly complicate spectrum interpretation or, conversely, lead to erroneous conclusions as to the nature of the analyte.

Reduction processes consisting of simple hydrogen additions resulting in the formation of $(M+nH)^+$ ions were originally thought to occur through hydrogen atom reactions with the analyte[17]. Alternatively, the $(M+2H)^+$ and $(M+3H)^+$ ions could originate from one- and two-electron reductions of multiply protonated species as suggested by Gross and co-workers[108].

$$M_{(Soln)} + 2H^+ \longrightarrow (M+2H)^{2+} + 1e^- \longrightarrow (M+2H)^{+\bullet}_{(g)} \quad [3]$$

$$M_{(Soln)} + 3H^+ \longrightarrow (M+3H)^{3+} + 2e^- \longrightarrow (M+3H)^{+}_{(g)} \quad [4]$$

Another possibility involves electron capture by the analyte followed by protonation[36,108]. It has been suggested that reductions in FAB/LSIMS depend on the availability of low-lying unoccupied molecular orbitals[108]. The lowest unoccupied molecular orbitals (LUMOs) could capture thermalized electrons and initiate further reactions leading to reduction. Indeed, Williams et al[110] suggested that many reduction processes in FAB/LSIMS can be explained by one-electron reductions where solvated electrons act as reducing agents. The relative contribution of secondary electrons in these reductions as not been delineated[96]. Other purported sources of reduction suggested include UV photons and X-rays generated from the FAB gun discharge[111].

That some of these reactions involve the matrix and occur at least partly in solution is well illustrated by the FAB spectrum of the dicationic compound methyl viologen. The spectrum is dominated by the $M^{+\cdot}$ ion, and the production of the radical cation is confirmed by its characteristic purple colour observed in the solution after the experiment[112]. This contention is well supported by the detection of the reduction product in the matrix using post-bombardment HPLC analysis of a FAB irradiated glycerol solution of a halonucleoside[24,31]. The crucial role of the matrix in reduction processes has been well established given the fact that some matrix compounds will foster reduction whilst other completely inhibit the process[21,22,25,31,34-36]. The parameters influencing FAB/LSIMS reduction processes will be further discussed in a subsequent section.

Reduction in FAB has been used to provide information on the structures of peptides. The FAB/LSIMS induced reduction of disulfides has been used to locate disulfides bonds in peptides[28]. Determination of the location of disulfide bonds is crucial for the characterization of the three-dimensional structures of peptides. In another practical use of reduction processes, Bogess and Cook[113] have studied the possibility of using the reduction of methylene blue in glycerol as a dosimetric system for the flux calibration of primary atom from FAB guns.

It is important to note that reduction of the analyte can occur chemically in the matrix *prior* to irradiation by the primary beam. The reduction of some coordination compounds in glycerol[60] is one such case. The reduction of disulfide bonds in peptides by thiol-containing matrices such as thioglycerol and magic bullet is a reaction well known to biochemists. This reaction has become a structure elucidation tool for mass spectrometrists. The 'bleaching' (reduction) of methylene blue by thioglycerol prior to FAB/LSIMS analysis was observed by Kazakoff[114] and is a complex though known solution reaction.

2.4.3.2 Beam-Induced Oxidations

The beam-induced oxidations observed in FAB/LSIMS are generally associated with the radical molecular cation, $M^{+\cdot}$. The formation of radical cations can result from one-electron oxidation processes though this is certainly not the only possible pathway available for the formation of $M^{+\cdot}$ ions[115].

For example, the abundance of $M^{+\cdot}$ ions in FAB/LSIMS can be enhanced by charge transfer reaction using an electron acceptor. When benzoquinone is added to a solution consisting of N,N,N',N'-tetramethyl phenylenediamine and glycerol, the $M^{+\cdot}$ ion becomes dominant instead of $(M+H)^+$[116]. In some cases the matrix itself can act as an electron acceptor. The LSIMS spectrum of phenothiazine in NBA showed almost exclusively the $M^{+\cdot}$ ion and very little $(M+H)^+$. The possible formation of a charge transfer complex was indicated by an abrupt change in solution colour upon addition of phenothiazine to the matrix[35]. The formation of oxidizing radicals in some matrices under FAB/LSIMS conditions has been discussed[35]. The chemical bleaching of methylene blue by thioglycerol was found to be reversed by exposure of the solution to the primary beam[117]. It was suggested that these observations were consistent with the beam-induced generation of oxidizing sulfur-centered radicals from the matrix[35].

One electron oxidation processes have been observed in the FAB/LSIMS spectra of flavonoids and low molecular weight alcohols[118,119]. The oxidation of peptides can also be discerned in the molecular ion region and distort the isotopic pattern of the molecular ion region[15]. The negative ion FAB spectra of some nitroaromatic compounds exhibited ions characteristic of oxygen addition to the molecule, $(M+O-H)^-$ [120].

2.5 Experimental Parameters Affecting the Extent of Reduction in FAB/LSIMS.

The initial observation[17] of reduction processes sparked a marked interest in this area of FAB/LSIMS. The emerging ubiquity of these

beam-induced reactions, touching the organic and inorganic realms, fueled a more systematic effort to understand the physico-chemical parameters underlying reduction phenomena. The thrust of the investigations were generally two-pronged. One concerned the importance of inhibiting this potential source of artefacts to safegard the analytical integrity of the technique, whilst the other sought to elucidate the basic processes to gain a deeper understanding of beam-induced phenomena including ionization mechanism.

Essentially, the FAB/LSIMS experimental parameters affecting reduction processes can be separated into two distinct categories: chemical and physical. The physical parameters generally pertain to the characteristics of the primary beam and are as follows:

(a) Primary beam energy.

(b) Primary beam flux or density.

(c) Time of sample irradiation.

A sizable problem in evaluating the effect of physical parameters on reduction processes is the lack of reliable dosimetric methods to evaluate the primary beam characteristics. The chemical parameters are those which describe the characteristics of the solution being irradiated, namely:

(a) Analyte concentration.

(b) Matrix composition.

(c) Analyte structure (reduction potential, electron affinity, surface activity)

The following section will endeavour to give a brief overview of the salient features of the effects of experimental parameters on FAB/LSIMS reduction processes.

2.5.1 Physical Parameters

2.5.1.1 Beam Density

Beam density is defined as the number of bombarding particles hitting the target area per unit time. The effect of this parameter on the secondary ion current has been shown to be a linear one[77]. Where reduction processes are concerned, a similar effect has been reported[22,34,121-3]. This is logical since an increase in the number of particle impacting on the sample should lead to the increased production of reactive species thought to be responsible for reduction.

Busch et al[121] showed that the reduction of oxazine dyes increased with a concomitant increase in Cs^+ beam current from 1μA to 10μA. The observation that the extent of reduction decreased instantaneously upon a decrease in beam flux led the authors to suggest that the reduction process took place at the surface of the matrix. The reduction products would be removed as part of the bombardment process through sputtering and evaporation. In their study on the experimental parameters in FAB, Reynolds et al[22] reported that the intensity of the reduction products of methylene blue increased with an increase in beam flux.

The efforts to gain an understanding of the dependence of beam-induced artifacts on primary beam characteristics have been greatly hampered by the difficulty in characterizing the neutral primary beam used in FAB. The recent work of Boguess and Cook[113] has shown that the performance of the FAB gun is heavily dependent on the age of its electrodes. Such behavior can adversely affect spectral reproducibility even when nominal FAB gun voltage and emission current are used. The authors suggested a chemical-based flux calibrant based on a methylene blue-glycerol solution which could allow comparison of operating conditions. The flux calibration was performed by comparing the extent of reduction measured with a FAB and LSIMS gun. The flux of the Cs^+ beam of the LSIMS gun was previously measured using a shielded Faraday cup. It should be noted that this type of approach is typical of radiation chemistry, where dosimetric measurements are crucial to the relevance of any experiment. Chemical dosimetry is probably the only way to attempt to secure a means of ensuring meaningful interlaboratory comparisons. Visentini et al[122-3] have investigated the effects of primary beam flux on the reduction of peptides and found a significant effect originating from the variation of this experimental parameter.

2.5.1.2 Beam energy

The earliest report of primary beam effect on reduction belongs to Nakaruma et al[33] who observed a linear increase in the reduction of bromo-phenylalanine with increasing beam energy. The reduction of pyridinium salts was found to exhibit a concentration dependence at a beam energy of 9keV[20]. This trend was eliminated when the energy was

decreased to 5keV. It should be pointed out that the analyte concentrations used were high (up to 1 molar). If one considers the data obtained at 5 and 9keV with concentrations below 0.1 molar, then an increase in reduction is observed with a concomitant increase in beam energy.

The above trends are contradicted by the thorough study of Reynolds and Cook[22] who observed a slight though significant decrease in the extent of reduction of methylene blue in glycerol with increasing beam energy. The authors speculated that this decrease in reduction could be attributed to the change in sampling volume with increasing particle energy though this issue is not resolved[124]. Alternatively, it was suggested that the decrease in reduction could have been caused by a change in beam focussing and hence beam flux. The interdependance of the parameters prevents any clear cut distinction as to the effect of beam energy. A quantitative study of the reduction processes occurring in the FAB/LSIMS of peptides showed that beam energy had a negligible effect[123].

2.5.1.3 Time of irradiation (time dependence of reduction phenomena)

The time of irradiation of a sample can be an important factor on the extent of reduction observed and lead to a gradual increase in the abundance of the beam-induced products[24,25,28,32,34]. Wirth et al[125] observed a gradual increase in the $(M+3H)^+/(M+H)^+$ intensity ratio of azo-containing peptides. This led the authors to suggest that

the concentration of the reactive species responsible for reduction builds up in the matrix with time. The build up of reactive species in the bulk of the solution would be expected to result in an increase in reduction with increased time of irradiation. The reduction of the analyte was confirmed by the gradual fading of the original yellow colour of the sample as the time of irradiation increased. Such a time dependence was also observed for the deuteride abstraction (to form $M-H^+$) from deuterated cyclic acetals. The time dependence was interpreted as the build up (or delayed sampling) of radiation damage products in the bulk of the matrix. The lack of time dependence in the LSIMS spectra of more surface active acetals was interpreted as further support for the above hypothesis[81].

Gross et al[25] investigated the time dependence of the reduction of aromatic oximes. The results obtained with and without the anionic surfactant lithium dodecyl sulfate indicated that the rate determining step of the reduction process is the migration of the analyte to the surface of the matrix. The role of the surfactant is to increase the analyte surface concentration by 'bringing' the analyte to the surface. The addition of the surfactant caused the disappearance of the time dependence hence supporting the hypothesis formulated by the authors. A similar experiment with halogenated analytes yielded similar results[126].

An interesting experiment contrasted the reduction of chlorpromazine using 'static' FAB and continuous flow FAB. In the static mode, a gradual increase in dehalogenation products with time of irradiation

was evident whereas the continuous flow mode yielded a constant degree of dehalogenation over the duration of the analyte. This difference is probably due to the lack of accumulation of reduction products in the continuous flow mode[32]. It should be stressed that the observed extent of reduction can be relatively constant throughout the time of analysis under static conditions, suggesting a steady-state reduction process at the surface of the matrix as observed by Busch et al for the reduction of porphyrins[127]. A similar lack of time dependence was reported for the beam-induced dehalogenation of halonucleosides[30]. Hence, the presence of a time dependence is often interpreted as evidence for a beam-induced process but an absence of time dependence does not rule out the involvement of the beam in the artefact formation process.

2.5.2 Chemical parameters affecting reduction processes

2.5.2.1 Analyte structure

The fact that reduction processes occur in several classes of compounds hints at a relationship of beam-induced reduction and analyte structure[17,18,36,109,127]. Furthermore, for compounds in the same class there exists a different propensity to undergo reduction. The extensive studies carried out with organic dyes revealed a trend of increasing reduction with more positive half-wave reduction potential of the dyes[17,18]. The extent of reduction (in terms of $M+nH^+$) for a series of tetraphenyl metalloporphyrins was firmly correlated with the electrochemical reduction potential, yielding a linear relationship

with a high correlation coefficient[127]. The extent of reduction observed in the FAB spectra of pyridinium salts did not show a significant dependence on their respective reduction potentials[20].

A FAB study of the beam-induced reductive demetalation of metalloporphyrins showed that the incorporation of electron withdrawing groups in the porphyrin structure produced a significant decrease in reductive demetalation[109]. The decrease in demetalation (reduction) was explained in terms of slower electron transfer from the porphyrin moiety to the metal. A similar type of relationship was established for halogenated organic compounds[36].

Musselman and co-workers[128] reported that the extent of reduction observed in the glycerol FAB spectra of peptides varied from peptide to peptide. These results indicated that perhaps definite structural features were involved in the reduction process. There are three functional groups in peptides prone to reduction: disulfide bonds, aromatic rings, and carbonyl groups. The tendency of peptides to exhibit reduction was found to follow the above order[129]. A further analysis of the structural effects of peptides on the observed extent of reduction revealed a linear relationship between the extent of two-electron reductions with the number of unsaturated sites in the molecules[130]. However, this relationship is highly phenomenological since the exact site of reduction as well as the initiating agent are not known.

The relationship between reduction potentials and the extent of reduction observed in the FAB spectra of certain compounds should be treated with caution since the direction of the trend has been shown to depend on the process (reduction[127] vs reductive demetallation[109] in the case of porphyrins). The lack of mechanistic information as to the processes i.e. initiating agents is crippling for the clear formulation of a reduction mechanism. For example, organic dyes such as methylene blue can be reduced by more than one beam-generated reducing agents[48,131] (hydrogen atom, electrons and other reducing radicals) and one can reasonably speculate that the capacity of each matrix to scavenge those species will vary.

2.5.2.2 Surface activity

A further important point to be considered is the distribution of the analyte in the solution. It is logical to expect that analytes having a greater tendency to populate the surface of the matrix will be more likely to react with beam-generated reactive species and thus undergo reduction. The effect of analyte surface activity on beam-induced reduction processes has been alluded to[34, 25] though seldom probed[126] directly. Experiments using surfactant additives to 'artificially' increase the surface concentration of the analyte have shown that such an effect can indeed be observed[25]. Similar results were obtained by Heerma et al[132] though the increase in reduction was slight. The extent of reduction observed for analogs having different surface activity showed a distinct increase for the more surface active compound[126].

2.5.2.3 Matrix composition

Matrix selection has long been recognised as the single most important FAB/LSIMS experimental parameter. This is particularly true for reduction processes as the matrix can contribute to reduction in solution or upon bombardment. The occurrence of beam-induced reduction being much more common. The case of 'spontaneous' reduction or solution reduction is illustrated in the case of peptides with disulfide bonds in thioglycerol[28] and coordination compounds in glycerol[60].

In the case of beam-induced reductions, the multiplicity of reports of reduction phenomena pointed to the overwhelming importance of matrix selection as well as the propensity of glycerol to exhibit reduction in the most pronounced way. Unger et al[133] first reported differences in the extent of FAB-induced reductions which were associated with the use of different matrices. The introduction of matrices which were efficient reduction inhibitors occurred early in the history of FAB/LSIMS. In 1984, Seibl et al[134] suggested the use of the nitroaromatic compounds o-nitrophenyloctyl ether (NPOE) and m-nitrobenzyl alcohol (NBA) as alternatives to glycerol. The results obtained in the analysis of a dioxosecocorrin with NPOE exhibited total inhibition of the hydrogen addition products observed when glycerol was the matrix.

The matrices have been classified in terms of their ability to inhibit reduction and there appears to be a consensus on this issue. The matrices are generally arranged in terms of decreasing reducing power as follows; glycerol > sulfolane > thioglycerol > hydroxyethyl disulfide (HEDS) > NBA [21,22,31,34-5,73,130].

Despite the establishment of this rough reduction inhibiting capacity scale with a variety of compounds, the mechanistic aspects of reduction inhibition by the matrix have remained nebulous and relatively unexplored. In light of the mounting evidence indicating that matrix chemistry is the primary parameter which influences beam-induced reductions, there has been little effort to relate the physical properties of the matrix to the observed extent of reduction. The most recent and thourough reviews on liquid matrices barely address the subject[55,56]. In a study of the reduction of oximes[25], the 'proticity' of the matrix was invoked as an important parameter. However, this hypothesis ignores the lowest extent of reduction which was obtained with NBA, a protic compound whereas an aprotic matrix, NPOE, exhibited a similar extent of reduction. Also, given the energy supplied upon bombardment, it is difficult to imagine that there will be a dearth of hydrogen in the matrix, even when aprotic matrices are used. The role of beam-generated hydrogen atoms in FAB/LSIMS reductions has been suggested to be a dominant one[8,17].

It has been proposed that radicals, electrons, ions, and excited species are produced in the matrix under FAB/LSIMS conditions. Of these species, radicals[8] and/or electrons[110] are thought to be

involved in reduction processes. The reduction inhibiting capability of the matrix is thus referred to in terms of radical/electron scavenging capacity. Though convenient, this umbrella term only perpetuates the unclear mechanistic aspects of matrix reduction quenching. Williams[110] et al. has suggested a mechanism based on beam-generated secondary electrons to account for the occurrence of reduction processes in the FAB/LSIMS spectrum of organic compounds. In this model, the reducible compounds capture electron through unoccupied low energy orbitals. However, the production of secondary electrons upon keV particle bombardment has been questioned[8,104].

Laramée and Arbogast[134] calculated the electron affinities of common matrix compounds and correlated this parameter with the observed extent of reduction in derivatized oligonucleosides. The greater the electron affinity of the matrix, i.e. electron scavenging capacity, the greater the inhibition of reduction. Similar results were obtained by Kelley et al[31] for halonucleosides. Such an explanation is very limited since NBA is the only matrix with a positive electron affinity. The ability of NBA to inhibit reduction processes in FAB/LSIMS, is well documented.[21-2,31,34-5,135] In their work, Miller and co-workers[135] have suggested that this property of NBA is related to the fact that the matrix can act as an electron sink and thus mitigate chemical damage. Interestingly, a recent report[136] indicated that even for NBA, the reduction-inhibiting capability was limited.

Hence, although the correlation of matrix electron affinity versus the extent of reduction is instructive, it fails to explain the difference

observed amongst the other matrices which have no electron affinity. In fact, NBA is the only matrix currently in use with a positive electron affinity. All other compounds have a negative electron affinity which does not allow distinction of their electron scavenging capacity. The physical properties of matrices used in FAB/LSIMS have been collected[61]. However, the authors admit that the relative obscurity of some important matrix compounds have left important gaps in the tabulation. It is highly possible that the answer does not lie in the physical properties of the individual matrix molecules *per se* and is in fact much more complex given the dynamic nature of the FAB/LSIMS technique, involving various kinetic and thermodynamic factors that are highly system dependent. Indeed, it has been suggested that the more complex and less well characterized radical redox chemistry induced by the primary particle beam might be an important factor[61]. This aspect of FAB/LSIMS reduction processes will be extensively explored in the later chapters of this thesis.

Other matrix physical properties might come into play. The surface tension of the liquid matrix can affect the analyte surface concentration. Since it is widely held that most reduction processes occur at/or close to the surface of the droplet[25,31] a matrix of high surface tension could increase the analyte surface tension and exhibit a higher extent of reduction. This correlation has been demonstrated using glycerol and trihydroxyhexane as matrices[126].

The use of matrix additives to bolster the reduction inhibition capability of glycerol has been extensive. Additives such as

trifluoroacetic acid (TFA)[70] camphorsulfonic acid (CSA)[71] and copper (II)[72] have been experimented with because of their radical/electron scavenging capabilities.

To sum up, the mechanism of matrix reduction quenching has not been adequately explained. This stems largely from a lack of knowledge concerning (a) behaviour of various classes of analytes as well as matrix compounds towards the species purported to be responsible for reductions such as electrons and radicals, (b) the redox characteristics of the radicals produced by the respective matrix compounds under FAB/LSIMS conditions. Therefore, that matrix composition plays an overwhelmingly important role in FAB/LSIMS beam-induced reductions is undisputed. However, the mechanism of reduction quenching remains nebulous and relatively unexplored.

2.5.2.4 Analyte concentration

The effect of analyte concentration on the analyte signal intensity is well documented, particularly for surfactant analytes. In the case of reduction processes, it is generally held that reduction increases with decreasing analyte concentration. The work of Visentini[122-3] on the reduction of peptides indicated that the one- and two- electron processes were affected differently by variations in concentration. In fact, very few studies on beam-induced reduction have taken this experimental variable into consideration and fewer still have attempted to rationalize it.

Kazakoff[20] studied the effect of concentration on the reduction of pyridinium salts. The results indicated a increase in reduction with an increase in analyte concentration. Interestingly, results shown with methylene blue over a 76-fold concentration increase do indicate that for the concentration effect to be sizable, large differences in concentration must be used. In some cases, the extent of reduction increases with concentration, as is the case of the peptide pentaphenylalanine in glycerol[122].

Clearly, the effect of this experimental parameter are not easy to predict and appears to depend on the systems. The effect of analyte concentration may greatly depend on the surfactant behaviour of the compound since studies suggest that increased analyte surface concentration might lead to increased reduction. This can in turn be affected by whether the concentrations studied are above or below the critical micelle concentration (C.M.C.) or bracket it. This proposition is valid for analytes having surfactant properties.

2.6 Dehalogenation in mass spectrometry

2.6.1. Dehalogenation in chemical ionization

Given the tendency to compare the FAB/LSIMS ionization processes to those occurring in a chemical ionization plasma, a brief review of dehalogenation processes in chemical ionzation and other ionization techniques was thought to be *à propos*. A short survey of the possible

side reactions occurring in the plasma of a chemical ionization source has been published[137]. The reactions to which the analyte can be subjected to in the plasma include dehalogenation processes although their origin is not entirely clear.

2.6.1.1 Positive ion chemical ionization

The dehalogenation of haloaromatics in positive ion chemical ionization has been extensively studied by Harrison[138]. These were the first systematic studies of dehalogenation reactions in mass spectrometry. A thorough review of this work is not feasible within the constraints of this thesis. It is sufficient to point out that loss of the halogen, either as a radical or hydrogen halide, is significantly influenced by the nature of the reagent gas, the halogen type as well as the type and position of substituents. The effect of the above on the observed dehalogenation of simple haloaromatics are difficult to translate into a simple mechanism given the subtle interplay of a variety of structural and energetic effects.

Madsudanan et al.[139] investigated the dehalogenation of certain chalcones and phenylcinnamonitriles under positive chemical ionization conditions. The CI (NH_3) spectra of these compounds yielded ions of the type $[M-X+2H]^+$, reminiscent of those found in FAB/LSIMS. The genesis of the $[M-X+2H]^+$ ions was rationalized in terms of a radical mechanisms involving hydrogen radical addition to the analyte. The authors purported that the proposed radical mechanism was supported by the comparatively reduced abundances of the $[M-X+2H]^+$ ion when

tetracyanoquinidomethane (TCNQ) was added in the source. The compound TCNQ is proposed to act as a radical trap and hence the diminished occurrence of the dehalogenated ions is interpreted in terms of efficient hydrogen radical scavenging by TCNQ. Interestingly, this result could be interpreted in terms of an electron-initiated dehalogenation mechanism given that TCNQ could act as a very efficient electron scavenger since it possesses a very high electron affinity (2.82eV).

2.6.1.2 Electron capture mass spectrometry

The resurgence of interest in the formation of negative ion has largely resulted from the advent of electron capture mass spectrometry (ECMS). It was demonstrated that conditions favourable to negative ion formation could be implemented in a simple and convenient manner to instruments having chemical ionization capability[140]. A primary target of ECMS has been the environment-related electrophilic compounds of which haloorganics constitute an important group. Hence, the behaviour of haloorganic compounds under electron capture conditions is well documented though not completly understood.

Under electron capture conditions, enhanced negative ion formation results from the addition of a non-reactive (in terms of electron capture) reagent gas to elevate the ion source pressure (1 torr). Generally, a chemical ionization source is used to reduce gas conductance. A beam of electrons (50-200eV) is used to generate a plasma composed of electrons, ions, radicals and neutrals.

$$2CH_4 + 2e \longrightarrow CH_4^{+\cdot} + CH_3^+ + H + 2e\ (primary) + 2e\ (secondary) \qquad [5]$$

Under these conditions, the enhancement gas promotes negative ion formation by acting as a medium for electron thermalization and negative ion stabilization. It has been estimated that 50-60% of the electrons produced under conditions typical of ECNI have thermal energies (below 0.2 eV)[141]. Negative ions are formed by three processes involving interactions with electrons.

$$MX + e \longrightarrow MX^{-\cdot} \quad \text{(resonance electron capture)} \qquad [6]$$

$$MX + e \longrightarrow M^{\cdot} + X^- \quad \text{(dissociative electron capture)} \qquad [7]$$

$$MX + e \longrightarrow M^- + X^- \quad \text{(ion-pair formation)} \qquad [8]$$

The cleavage of the carbon-halogen bond is a characteristic degradation pathway for most halogenated compounds under electron capture conditions. The production of X^- ions is favored in the order $I^->Br^->Cl^->F^-$ for a series of analoguous compounds. For example, the ECMS spectra of the monohalogenated benzenes showed $I^->>Br^->Cl^-$ while F^- was not observed at all. When both M and X can accomodate an electron, both fragments will compete for the negative charge. The degree of fragmentation and the abundance of each fragment will be affected by the carbon-halogen bond strength, the electron affinity of the fragments and the energy of the captured electron.

However, in polyhalogenated aromatic compounds, ions due to straightforward loss of halogen such as $[M-nX]^-$ can be overshadowed by

ions of the type $[M+nH-nX]^-$. The latter species have attracted significant attention and a sizable effort has been aimed at elucidating their mechanism of formation[142,143]. These ions are thought to occur through surface assisted hydrogenation of the analyte on the source walls, followed by subsequent electron capture. However, research on this question is ongoing[144]. The origin of the $[M+nH-nX]^-$ ions is of interest in a broader context since substituton of a halogen by a hydrogen also occurs in FAB/LSIMS. In that case however, the wall-assisted dehalogenation mechanism proposed in ECMS does not appear to be applicable. It is worthy of note that chlorinated organics of moderate electron affinity such as 4-chloro-benzophenone (0.8eV) and chloronitrobenzene do not undergo dehalogenation under electron capture conditions[142].

2.6.2 Thermospray

The LC/MS thermospray characterization of the bromaromatic compound brimonidine was reported to yield the $[M-Br+H]^+$ ion. The intensity of this ion relative to the protonated molecule was not mentioned but was listed as being a 'characteristic ion' of the thermospray mass spectrum of brimonidine[145]. The thermospray ionisation mode (discharge on or discharge off) was not specified.

Volmer and Levsen[146] have observed aliphatic and aromatic dechlorination of pesticides analyzed by thermospray LC/MS. The dehalogenated ions were exclusively of the type $[M-Cl+2H]^+$. The amount of dechlorination was generally higher for compounds having aliphatic

chlorines as opposed to compounds having aromatic chlorines. These dehalogenated ions were observed only in the 'discharge assisted' thermospray mode. Thermospray in its original form affords no form of ionization other than the use of a volatile electrolyte. In the discharge mode, a discharge electrode ionizes the solvent vapour to create a plasma which in turn can give rise to CI-like reactions with the analyte. The authors postulated that the reductive dehalogenations probably take place via a radical reaction prior to ionization induced by radicals that are akin to those formed in the plasma generated in a CI source. Paradoxically, it is stated in the paper that FAB beam-induced dehalogenations proceed via a free radical mechanism. However, the referenced work cited by the authors clearly contradicts this statement.

2.6.3 Californium-252 plasma desorption

The only report of dehalogenation in ^{252}Cf plasma desorption concerns the halouracils (I, Br, Cl, F)[147]. The extent of dehalogenation was lower than that observed in FAB/LSIMS and followed the order I > Br > Cl > F. The loss of halogen was found to be less pronounced in the negative mode. No mechanism was proposed to account for the occurrence of the dehalogenated ions in the mass spectrum although the difference in matrix medium (solid aluminized Mylar film for ^{252}Cf and a glycerol liquid matrix for FAB/LSIMS) was invoked by the authors.

2.6.4 FAB/LSIMS

Dung et al.[29] obtained the LSIMS spectrum of chlorpromazine in glycerol before and after irradiation with an Hg lamp to monitor the photodegradation of the compound. However, the authors did not comment on the wider significance of the dehalogenated ion present in the test sample not irradiated by the Hg lamp i.e., that beam-induced dehalogenation was occurring. Sethi and McCloskey[30] investigated the FAB-induced dehalogenation of a series of halogenated nucleosides. Using C- and O-perdeuterioglycerol as the matrix, they demonstrated that the hydrogen replacing the halogen originated from the matrix. The extent of dehalogenation of 5-halouridines in glycerol was shown to be inversely proportional to the carbon-halogen bond strength (I>Br>Cl>F). The same phenomenon was observed for the fluoro, chloro, and bromo analogs of 4-halo-phenylalanines with glycerol as the liquid matrix[33]. It should be noted that the above investigations were limited to glycerol as the liquid matrix.

Using substituted nucleoside cyclophosphates, Schiebel[24] and co-workers showed that the beam-induced dehalogenated product could be detected in the glycerol matrix with post-bombardment HPLC analysis. A similar result was obtained in a later study using analogous compounds[31]. The fact that the dehalogenated product can be detected in the matrix after bombardment indicates that the reaction could possibly occur (at least partially) in the condensed phase.

Edom and McKay[32] have studied the dehalogenation of chlorpromazine showing that the dechlorinated ion arising during FAB analysis gave identical daughter ion MS/MS spectrum to that of the protonated unhalogenated analog, promazine. The dehalogenated ion also appeared in the continuous flow FAB mass spectrum of chlorpromazine in a water-methanol-glycerol matrix (90:5:5) at a relative intensity comparable to that obtained under static conditions though not subject to a time dependence. In a manner similar to Sethi et al.[30], the authors demonstrated that the hydrogen replacing the halogen originated from the matrix by using perdeuterated glycerol. The effect of matrix selection on the dehalogenation process was illustrated by the complete inhibition of the dechlorination of the peptide vancomycin when the matrix was NBA[148]. The result was explained by the electron scavenging properties of NBA.

In a further study using halogenated nucleosides as model compounds, the effect of the electron affinity of the matrix and analyte on the dehalogenation process was demonstrated[31]. The observed dehalogenation was linked to the calculated electron affinity of the matrix and analyte. The only matrix compound having positive electron affinity exhibited the strongest tendency to inhibit the extent of dehalogenation of halonucleosides in the FAB mass spectrum. In terms of the effect of analyte electron affinity, an increase in electron affinity resulted in decreased dehalogenation. These observations were rationalized on the basis of a dehalogenation mechanism involving electron capture. However, the analyte electron affinity range in that study was only 0.27 eV (7kcal). Also, the respective order of electron

affinities calculated for the halonucleosides did not correspond to that determined for the respective bases by Wentworth and co-workers using one electron reduction potentials[149]. Furthermore, the negative ion mass spectral evidence presented by the authors to validate the calculated electron affinities is highly susceptible to other interpretations.

2.7.1 Radiation chemistry and FAB/LSIMS

Radiation chemistry techniques

In light of the strong emphasis given in this work to radiation chemistry data and concepts, it is important to briefly summarize the two main techniques used to acquire information on the behaviour of chemical systems under radiolytic conditions. These techniques are pulse radiolysis and 'continuous' or steady-state radiolysis.

The steady state radiolysis technique is used mainly to study the behaviour of chemical systems under conditions of continuous irradiation. This allows the investigation of the breakdown of molecules submitted to irradiation. Generally, simple systems are irradiated for a given time and the radiation induced products subsequently analysed. The steady state technique has been used for dehalogenation studies since the end product of dehalogenation, the halide ion, can be selectively analysed with greater ease than a specific organic component in the complex mixture usually resulting from irradiation. The yield of product is usually defined in terms of

G values. The G value refers to the number of product molecules per 100eV of absorbed energy.

The pulse radiolysis technique is the radiation-chemical equivalent of flash photolysis. The difference is that the initiating flash illumination is replaced by a pulse of electrons or heavier charged particles of MeV energy. The time domain acessible to the technique ranges from micro to picoseconds. The transients generated in the solution irradiated by the energetic particle pulse can be detected by various means, mainly by optical absorption.

Pulse radiolysis experiments are generallly carried out either to detect transient species produced during radiolysis and to measure rate constants for the reaction such species undergo. This approach has been particularly successful for the transient species formed when water is irradiated. A substantial collection of rate constants with a wide variety of organic and inorganic substrates exist for the reactions of the hydrated electron, hydrogen atom, and hydroxyl radical[48]. The redox properties of some organic radicals have also been evaluated[47].

It is important to remember that alcohols are used as hydrogen atom scavengers in pulse radiolysis experiments. As a matter of fact, the most significant difference between radiolysis of water and alcohols (as long as they are not tertiary alcohols) is that the latter has a high capacity to scavenge hydrogen atoms. This capacity may cast a

new light on the role of hydrogen atoms in the beam-induced reduction processes when a matrix such as glycerol is used.

For example, isopropanol is used to ensure reducing conditions as it efficiently scavenges the hydrogen atom (K_H=9X10^7 M^{-1} s^{-1})[48] and the strongly oxidizing hydroxide radical, $^{\bullet}OH$ ($K^{\bullet}_{OH}$= 10^{10} M^{-1} s^{-1})[48].

$$H^{\bullet} + (CH_3)_2CHOH \longrightarrow (CH_3)_2C^{\bullet}OH + H_2 \quad [9]$$

$$^{\bullet}OH + (CH_3)_2CHOH \longrightarrow (CH_3)_2C^{\bullet}OH + H_2O \quad [10]$$

In some cases, t-butanol is used to scavenge hydroxy radicals. The resulting alkyl radical has a low reactivity with organic compounds and hence does not influence the chemistry observed on the pulse radiolysis time scale. The reactivity of H atoms with t-butanol is low.

Radiation chemistry and FAB/LSIMS

Almost from the outset, the proposition that FAB/LSIMS beam-induced processes could bear a resemblance to radiation chemistry was mentioned though not discussed. The suggestion that the beam-induced chemistry observed in FAB/LSIMS might bear similarities to known radiation chemistry was made early in the history of the technique[8]. This is hardly surprising given the physical similarities between the two techniques. In both cases, a sample is irradiated with energetic particles. The interaction of the energetic particles with the sample typically generates a track along which energy is deposited and the

production of radicals, ions, electrons and excited species is induced. The energy regimes (MeV for radiolysis and keV for FAB/LSIMS) of the two techniques may differ but the basic phenomena outlined above remain common although this contention was disputed[8].

In his study of the FAB behaviour of glycerol, Field[8] considered the possibility that beam-induced chemistry is similar to that generated with ionizing radiation i.e. production of secondary electrons. This idea was rejected on the basis of the Franck-Condon principle and the FAB-induced chemistry was likened instead to a kind of 'hot-atom' chemistry. Ligon[87] proposed the formation of the $(glycerol)^{+\cdot}$ radical cations (and hence the generation of secondary electrons) as one of the initial events of keV particle impacts. Clayton and Wakefield[112] suggested that the formation of 'unusual' ions such as $M^{+\cdot}$, $M^{-\cdot}$, $(M+H)^{-}$, and $(M-H)^{+}$ could be accounted for by the generation of ionization cascades upon bombardment. Such cascades would be similar to those proposed for radiation chemistry, the initial step involving ionization of an analyte or glycerol molecule by the ejection of an electron.

Sethi et al[30] pointed out that the beam-induced dehalogenation of halonucleosides had a direct analogy in both UV-photolysis and radiolysis. In their presentation of the 'gas phase collision' model elaborated to explain FAB/LSIMS ionization processes, Kebarle et al[92] contended that "the chemistry in FAB/LSIMS is, according to this model, expected to be similar to what is found in high energy radiation chemistry". Williams and co-workers[110] proposed that beam-

induced reductions are a common phenomenon in FAB/LSIMS and that these processes are frequently consistent with one-electron reductions. The premise of this proposed mechanism is that keV particle impacts cause the production of electrons (via ionization of the sample or matrix) and that these electrons can be effective reducing agents once they have reached thermal energies. Subsequent capture of these beam-generated electrons by the analyte ultimately causes reduction. The resemblance between some FAB/LSIMS reduction processes and those typical of pulse radiolysis was highlighted.

In an effort to further extend the work of Field[8], the stable end products formed in the FABMS and γ-irradiation of pure glycerol were analyzed by GC-MS and compared[104]. The results confirmed the hypothesis that keV particle bombardment produces free radicals which recombine to form new molecular species. On the basis of these experiments, the authors postulated that FAB/LSIMS and γ-irradiation (radiolysis) are mechanistically different. In accordance with the earlier suggestion of Field[8], the possibility of secondary electron generation upon keV particle bombardment was deemed to be negligible.

Field and Katz[44] observed the formation of numerous ions in the bombardment of rare gases by low keV rare gas atoms and ions. On the basis of these results, it was postulated that since gas phase FAB produced a fair amount of ionization, copious ionization should occur in the condensed phase. It is interesting to note that this consists in a complete change of position from the author's original work as cited above[8]. In a recent review of ionization in FAB/LSIMS, Sunner[83]

postulated that the chemistry fostered by the primary beam in FAB/LSIMS is similar to known radiation chemistry. This basic premise was used to explain the processes that determine the nature of ions in the FAB/LSIMS mass spectra. The distinction was made between 'prompt' beam-induced chemistry (that leading to the formation of ions) and 'delayed' chemistry (leading to formation of redox-derived products). In the former case, matrix molecular ion ($G^{+\bullet}$) and secondary electrons are formed upon particle impact. The resulting $G^{+\bullet}$ ions undergo proton transfer with the surrounding matrix molecules to form $(G+H)^{+}$ ions. The applications of radiation chemistry concepts to rationalize 'delayed' chemistry (such as beam-iduced redox processes) were not discussed.

The fact is that the literature reflects the *awareness* of the possible parallels between FAB/LSIMS processes and those common to radiation chemistry. The potential similarities between FAB/LSIMS conditions and radiolysis has been mentioned before[8,83,92,104] but there has been no attempt to systematically use radiation chemistry data and concepts to rationalize FAB/LSIMS beam-induced redox processes. This is somewhat surprising since in both cases a rich and diverse chemistry results from the subsequent reaction of the radiation-induced electrons and radicals with solutes. A distinctive facet of this thesis will be to draw extensively from the radiation chemistry literature in order to rationalize the behaviour of the haloaromatics under FAB/LSIMS conditions.

The radiation chemistry literature can provide useful information concerning beam-induced processes in FAB/LSIMS since the field is essentially about the chemical behaviour of irradiated material. Of particular usefulness is the ability of pulse radiolysis to provide information about the redox properties[47] (reduction potentials) of organic radical species as well as the kinetics[48] of reaction of such radicals with particular solutes. The reaction of organic radicals with organic solutes can consist of electron transfers (reduction, oxidation), and hydrogen abstraction. The radiation chemistry of some organic liquids have been investigated and the characteristics of their radiation-induced radicals tabulated. It is fortunate that alcohols have been particularly well studied[49-50], perhaps allowing insight into the beam-induced radical cascade of glycerol. This point is particularly important since glycerol is widely recognized as being the matrix where beam-induced reduction processes have the greatest tendency to occur. However, apart from from the alcohols, amides, hydrocarbons and carbon tetrachloride, the radiation chemistry literature of neat non-aqueous solvents is rather sparse[150].

Differences between FAB/LSIMS and radiation chemistry

Despite the proposed usefulness of radiation chemistry data and concepts to rationalize FAB/LSIMS beam-induced processes, it is essential to draw the attention to fundamental differences between the techniques. Therefore, it is useful to bear in mind the following limitations as well as the multiplicity of physico-chemical factors affecting FAB/LSIMS phenomena.

The overwhelming majority of pulse radiolysis experiments are carried out in aqueous media whereas FAB/LSIMS media are comprised of polar organic liquids. The principal features distinguishing water from organic liquids include the following:

1-Most organic liquids have a lower dielectric constant than that of water, which is about 80 at ambient temperature. There are few exceptions to this rule such as N-methyl acetamide (180) and formamide (110). The lower dielectric constant means that the coulombic field of the positive ions extends much further out than with water so that the reaction of isolated species plays a smaller part in the radiation chemistry.

2-Some organic molecules possess nondissociative excited states that have been characterized photochemically. For other other molecules, excited states have been characterized by radiation chemistry. Of course, all molecules produce excited states on irradiation, but those of water probably dissociate very rapidly to give free radicals, resembling those produced by ionization, or, alternatively, may simply dissipate their energy as heat. This is by no means the case for organic molecules.

3-The yield and type of radiation induced species are not necessarily well known for FAB/LSIMS matrices. For these, one must rely on pulse radiolysis data acquired in aqueous media for molecules having analogous structural features. The limitations of this approach is

obvious and compounded by the fact that the radiation chemistry of the neat liquid may be somewhat different. However, the radiation chemistry of neat alcohols is relatively well defined.

4-Organic molecules have more atoms than water. This and the presence of the carbon atom as well as others (sulfur for example) allow a much greater diversity of decomposition processes to take place than with water, resulting in a greater variety of reactions and products.

5-Organic liquids often have the capacity to scavenge the radicals originating from their own radiolysis. For example, the hydrogen atom and the hydroxyl radical produced by the radiolysis of aliphatic alcohols are quickly scavenged by the intact solvent molecules. This means that the contribition of such radicals to the radical cascade of aliphatic alcohols can be considered neglgible relative to that of water.

6-The different nature of the bombarding entities used in FAB/LSIMS and radiolysis gives rise to what radiation chemists call linear energy transfer (LET) effects. These effects are related to the rate at which energy is lost to the surrounding medium by the bombarding entity and are known to affect the radiation chemical yield.

Furthermore, FAB/LSIMS is basically a process of interfacial irradiation where transport processes, surface activity, and matrix evaporation can play important parts. Hence, physicochemical properties of the matrix which can affect the surface concentration of the analyte, such as surface tension, could have a significant effect

in the extent to which the analyte undergoes beam-induced reactions. Notwithstanding the differences between the experimental conditions prevalent in FAB/LSIMS and radiation chemistry, the data obtained and concepts developed in radiation chemistry can be fruitfully used to qualitatively rationalize the beam-induced redox processes observed in FAB/LSIMS.

Chapter 3

3. EXPERIMENTAL

3.1 Instrumentation

The instrument used in this study was a VG-AutoSpec-Q hybrid mass spectrometer (VG Analytical, Manchester, UK). This instrument consists of three sectors and two quadrupole analysers arranged in a EBEqQ configuration. This configuration is shown in Figure 2. The VG-AutoSpec uses the SIOS (spectrometer I/O System) interface (VG Analytical) for automated intrument control and the VG Opus data system (Version 3.0) on a VAX station (Digital Equipment Corporation, Maynard, Massachusetts) for data acquisition and treatment.

The instrument has a mass range of 3000 at an accelerating voltage of 8kV and is capable of mass resolution up to 60000 with an electron impact source. For the LSIMS experiments performed in this study, the resolution was kept at approximately 1000. Since the source and analyser regions are differentially pumped, the source can be operated at relatively high pressure while maintaining a low pressure in the analyzer section of the instrument. A 16 cm Diffstak pump (700 l/s) and two 10 cm diameter Diffstaks (280 l/s) are used to maintain the vacuum in the source and analyzer regions, respectively. The detection system consists of the VG photomultiplier dual detector which combines two non-switchable conversion dynodes with a long-life photomultiplier.

The LSIMS ionization source used in this study was standard on the VG-AutoSpec-Q instrument (VG Analytical, Manchester, UK). The primary ion

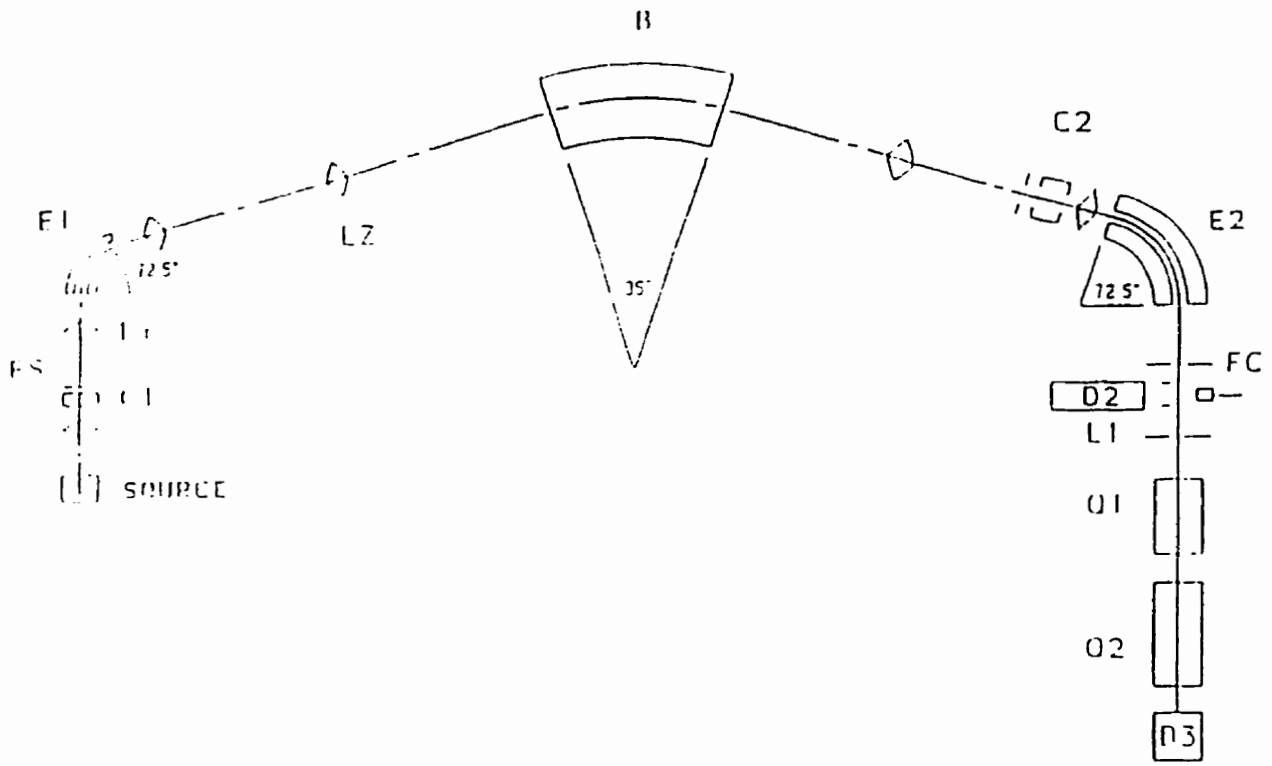

Figure 2. Diagram of the Autospec-Q hybrid mass spectrometer.

beam was generated using a variable energy (0-50keV) caesium ion gun (VG Analytical). The design consists of a caesium ion emitter (anode) based on the surface ionization principle. This type of emitter is prepared by embedding atomic caesium in a porous tungsten alloy. The embedded caesium, which has a 100% ionization efficiency on tungsten, will then be emitted as Cs^+ ions when the anode is heated to very high temperatures (>1000 ^oC) using an isolated 5V and 3A maximum winding on a transformer. The Cs^+ ions emitted from the anode are then focussed and accelerated towards the sample using two lens elements, Focus 1 and Focus 2. The ions are also further accelerated between the second lens element (Focus 2) on the gun and the final lens element mounted on the source. The final lens element contains a shield tube which screens the Cs^+ ions from the electric fields between the source electrodes and directs the primary beam to the sample on the target for bombardment. The ion gun is mechanically adjusted using headed screws to align the primary Cs^+ ion beam onto the sample.

3.2 Mass spectrometry conditions

The positive ion electrospray mass spectrometry data contained in this document are the courtesy of Dr G.J.C. Paul (U of M) and Dr R. Feng (Biotechnology Research Institute). Electrospray ionization (ESI) mass spectra were recorded using a API III triple quadrupole mass spectrometer (Sciex, Thornhill, Ontario, Canada) situated in the Montreal Biotechnology Research Institute. The instrument was operated with a cone voltage of 80 V. The solutions consisted of 10^{-4} M

analyte/water-methanol-HCl mixtures. Chlorpromazine and atrazine were the only compounds for which electrospray data was obtained.

All other mass spectral data were obtained using a VG AutoSpec-Q spectrometer (VG, Manchester, U.K.) equipped with a caesium ion gun. The accelerating voltage was 8kV and the mass resolution 1000. Magnet scans (5 sec/decade) were used over the mass range 50-1000. Standard analysis conditions consisted of a beam energy of 22 keV and a beam current of 2μA unless otherwise specified. All mass spectral data were treated with the VG Opus data system.

3.3 Sample preparation

Atrazine was a kind gift of CIBA-Geigy. All compounds were obtained from Aldrich Chemical Co. (Milwaukee, WI) and used without further purification. Compound **5** was prepared using the EDC (1-[3-dimethylaminopropyl]-3-ethylcarbodiimide hydrochloride) coupling of 2-bromo-3-nitrobenzoic acid and 2-aminoethylpiperidine to yield the amide. The product was purified using flash chromatography (ethyl acetate and 0.2% triethyl amine). Compound **4** was obtained by reacting 4'-bromo-4-chlorobutyrophenone with triethyl amine. The methyl ester of 4-bromo-phenylalanine was prepared from the zwitterionic form of the amino acid by reaction with thionyl chloride in methanol.

Compound **7** was synthesized using a modified literature procedure[151]. Sodium hydride (0.1g) was added to a solution of 2-chlorophenothiazine (0.5g or 0.15M) in 15 mL of dry tetrahydrofuran. The reaction mixture was stirred for 1 hour and subsequently added dropwise into a solution

of 1,12-dibromododecane (2.4g or 0.5M) in 15mL of dry tetrahydrofuran. The latter step was carried out slowly to avoid the formation of diphenothiazinylalkane. The crude mixture was filtered to remove solids and the solvent evaporated. The crude chloro-phenothiazine N-dodecyl bromide was purified using flash chromatography (hexane). This compound was then refluxed in acetonitrile with triethylamine to yield the quaternary ammonium salt **7**.

Solutions were prepared by dissolving the compound directly in the matrix. Mass spectral analysis was carried out immediately following mixing by applying 2 µL of the solution onto a square probe tip (7 mm^2) using a Wiretrol® II micropipette (Drummond Scientific Co. Broomall, PA).

The matrices used in this work are shown in Figure 3. The matrices are separated as aliphatic and aromatic compounds. The compounds 1,4-anhydroethrytol (AET), N-acetylethanolamine, 2-benzyloxy-1,3-propanediol (BOP), and 2-mercaptoethyl sulfide (MES) were investigated as potential new liquid matrices. Glycerol (Gly), thioglycerol (Thiogly), 3-nitrobenzyl alcohol (NBA), thiodiglycol (TDG), 3,4-dimethoxybenzyl alcohol (DMBA), 2-hydroxyethyl disulfide (HEDS), 2-hydroxyphenethyl alcohol (HPEA), 2-mercaptoethyl sulfide (MES), 1,4-anhydroerythritol (AET), 2-benzyloxy-1,3-propanediol (BOP), and 4-hydroxybenzene sulfonic acid (HBSA). HBSA is a 60% aqueous solution of that compound.

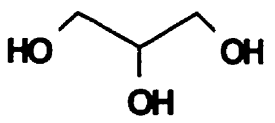

Glycerol (GLY)

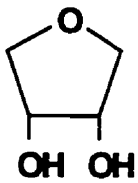

1,4-Anhydroerythrytol (AET)

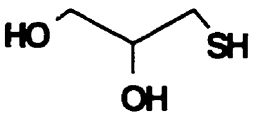

Thioglycerol (THIOGLY)

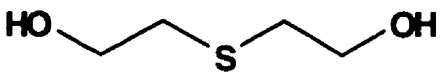

Thiodiglycol (TDG)

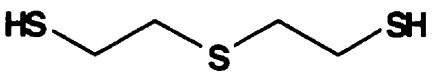

2-Mercaptoethyl sulfide (MES)

2-Hydroxyethyl disulfide (HEDS)

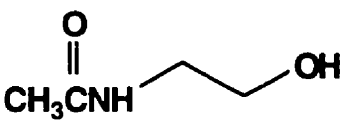

N-Acetylethanolamine

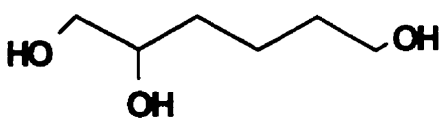

1,2,6-Trihydroxyhexane

Figure 3(a). Structure of the aliphatic matrices used in this study.

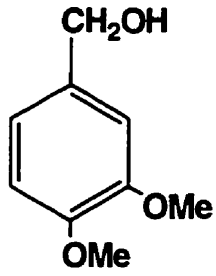

3,4-dimethoxybenzyl alcohol (DMBA)

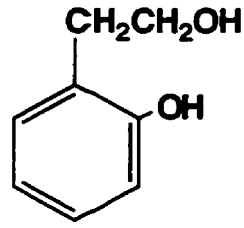

2-Hydroxyphenethyl alcohol (HPEA)

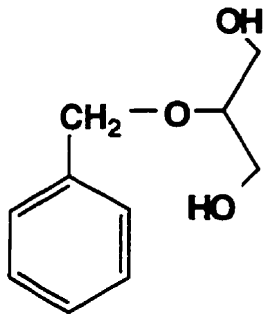

2-Benzyloxy-1,3-propanediol (BOP)

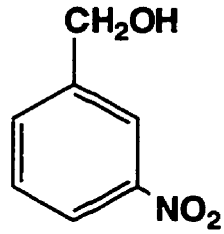

3-Nitrobenzyl alcohol (NBA)

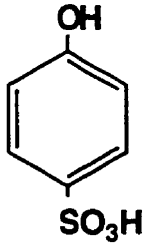

4-Hydroxybenzene sulfonic acid (HBSA)

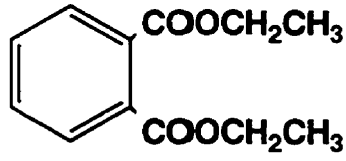

Diethyl phthalate (DEP)

Figure 3(b). Structure of the aromatic matrices used in this study.

Chapter 4

4. Effect of Experimental Parameters on Dehalogenation

The literature concerning the beam-induced dehalogenation of organic compounds in FAB/LSIMS clearly indicates an awareness that many experimental parameters can play a part in affecting the extent of artefact formation. The FAB/LSIMS experimental parameters can be separated into two distinct categories: physical and chemical. The *physical* parameters consist of time of sample irradiation and primary beam characteristics. The primary beam characteristics are the nature of the bombarding particle, the beam energy, and the beam flux (or density). The *chemical* aspects of the experimental parameters in FAB/LSIMS are generally englobed in matrix selection, matrix additives, and physico-chemical properties of the analyte pertaining to its structure.

Despite numerous reports of dehalogenation reactions occuring under FAB/LSIMS conditions[29-33], there has been little or no systematic study of the experimental factors that could potentially affect the extent of these reactions. The phenomenon is thus well known but poorly characterized. In order to systematically characterize the role of FAB/LSIMS experimental parameters, an LSIMS study was undertaken where the individual parameters were varied and the % dehalogenation observed for a model compound, chlorpromazine.

4.1 Effect of physical parameters on dehalogenation

The physical parameters involved in the LSIMS experiment which can potentially affect the observed beam-induced dehalogenation are as follows:

- Time of irradiation
- Primary ion beam characteristics: (a) beam flux
  (b) beam energy

In order to study the effect of these experimental parameters, a model compound was selected. The phenothiazine antipsychotic drug chlorpromazine hydrochloride was chosen for the following reasons:

(1) The compound is known to undergo pronounced dehalogenation under FAB/LSIMS conditions[32].

(2) Chlorpromazine is freely soluble in all the liquid matrices used in a broad range of concentrations.

(3) Since chlorpromazine is a salt and hence a classically defined pre-formed ion, the use of this molecule obviates the need to address ionization mechanism(s) pertaining to the technique. In addition, the compound exhibited good sensitivity in LSIMS.

(4) The ions due to the protonated 'intact' molecule $(M_XH)^+$ and dehalogenated molecule $(M_HH)^+$ appear at m/z values which are not isobaric with any ions originating from the matrices used.

(5) The extensive use of the compound as an anti-depressant means that the physico-chemical properties of chlorpromazine have been extensively studied.

(6) The 2-chlorophenothiazine moiety offers a useful and easily accessible synthetic template where the side chain length can be modified to change the surface active properties of the molecule. This feature of the compound will be exploited to investigate the effect of analyte surface activity on beam-induced dehalogenation which will be discussed in a subsequent chapter.

Factors (1) and (3) are important in that the need to take into account background signal is negated given the high signal to noise ratio of the $(M_XH)^+$ and $(M_HH)^+$ ions. In the experiments conducted in this study, the extent of dehalogenation in glycerol was pronounced and found to be in the range of 16%-60%. These values are the maximum and minimum values of % dehalogenation of chlorpromazine obtained when glycerol was the matrix under the different conditions used in this work. Additionally, the extent of dehalogenation exhibited in this study by chlorpromazine is in rough agreement with that observed by Edom et al[32]. Because the effect of physical parameters were the most pronounced in glycerol, the bulk of the data presented here will pertain to this matrix. The effect of matrices will be discussed in the next section which will present the effects of the chemical parameters of the LSIMS experiment.

In this section, the results pertaining to the effect(s) of physical parameters on the beam-induced dehalogenation of chlorpromazine will be presented. The results obtained will be compared with those obtained using 4-chloro-phenylalanine ethyl ester. Although analyte concentration is not really classified as a physical parameter, the effect of analyte concentration will be included in this section. This is due to the fact that concentration affects the extent of the effect of physical parameters such as time of sample irradiation, beam flux, and beam energy on dehalogenation.

4.1.1 Effect of concentration and time of irradiation

The positive ion LSIMS mass spectrum of chlorpromazine in glycerol is shown in Figure 4. The main peaks observed are the protonated molecular ion at m/z 319, characteristic fragments of the amino side chain at m/z 86 and 58, as well as an ion at m/z 285 that corresponds to dechlorinated chlorpromazine. This ion is a consequence of beam-induced replacement of chlorine by hydrogen[32] as shown in Scheme 1.

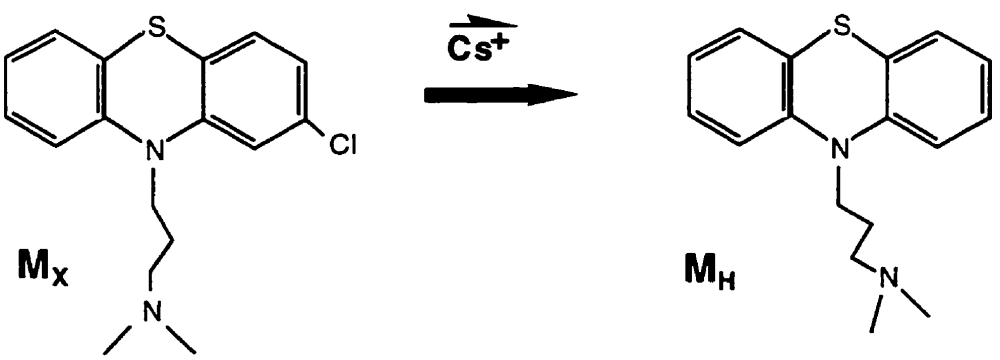

Scheme 1.

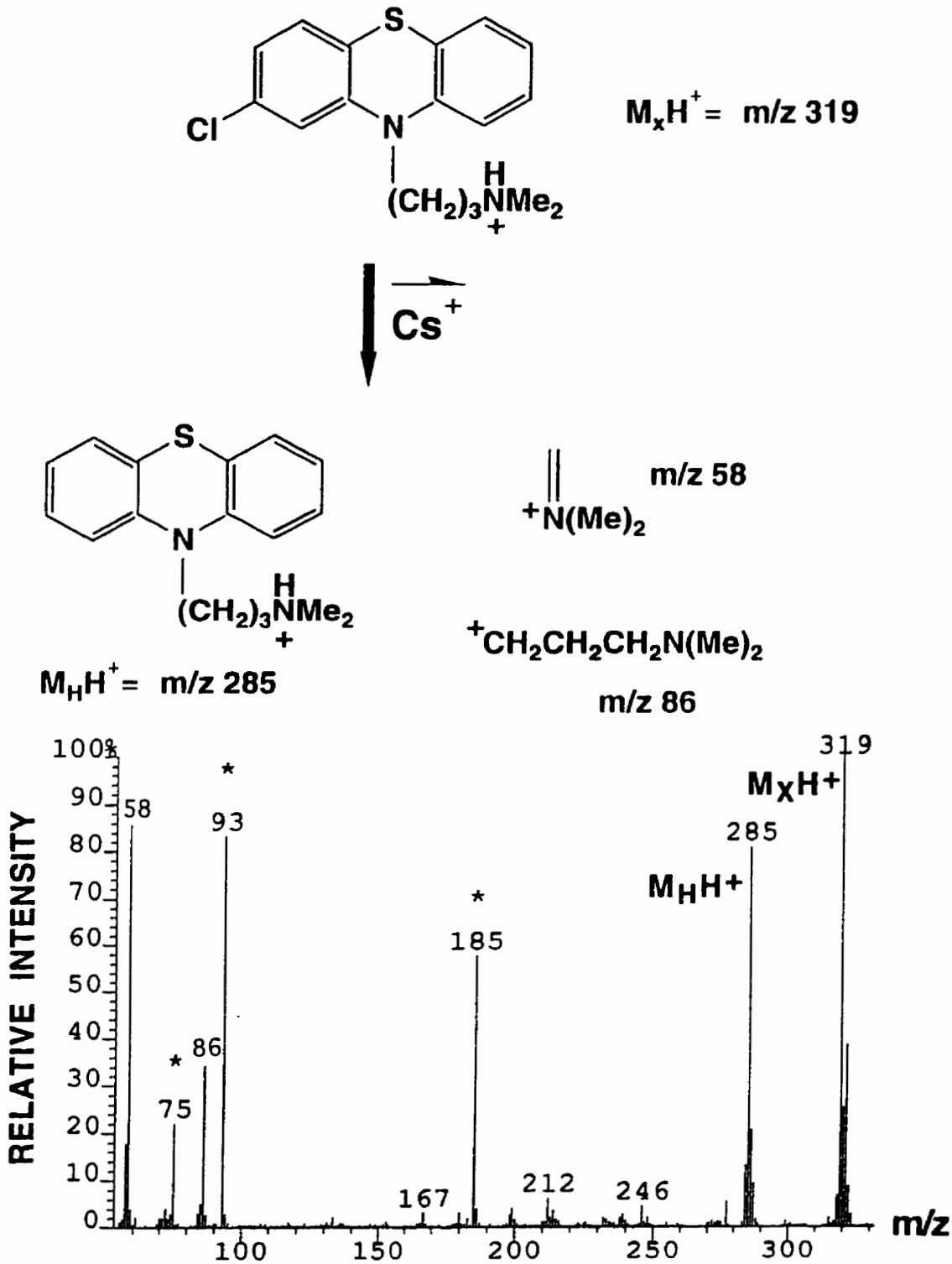

Figure 4. Positive LSIMS mass spectrum of chlorpromazine in glycerol (0.037M) and main ions found in the spectrum.
* Matrix peaks.

The extent of dehalogenation is expressed in percent as shown below.

$$\% \text{ Dehalogenation} = \frac{[M_H H]^+}{[M_H H]^\bullet + [M_X H]^+} \times 100 \qquad [11]$$

For chlorpromazine, $[M_H H]^+$ represents the relative intensity of m/z 285, the protonated dehalogenated molecule. The relative intensity of the protonated molecule at m/z 319 is represented by $[M_X H]^+$.

The dependence of the extent of dehalogenation on the time of irradiation can readily be seen in Figure 5 (a)-(d) on the next two pages. One can observe the 'growth' of the analyte ions with respect to the ions stemming from the matrix as the time of sample irradiation increases. Where the time dependent behaviour of the analyte ions is concerned, the relative abundance of the side chain fragment ion m/z 58 increases relative to the relative abundance of the chlorpromazine protonated molecule. The % dehalogenation of chlorpromazine was found to increase significantly with the duration of sample beam irradiation. The increase in dehalogenation with time of irradiation generally observed in this study is in agreement with a previous report on the beam-induced dehalogenation of chlorpromazine[32]. These spectra are representative of the time dependent behaviour of the chlorpromazine/glycerol system under bombardment conditions. It is interesting to note that in the continuous flow FAB analysis of chlorpromazine (90:5:5 solution of H_2O:CH_3OH:glycerol), the observed %

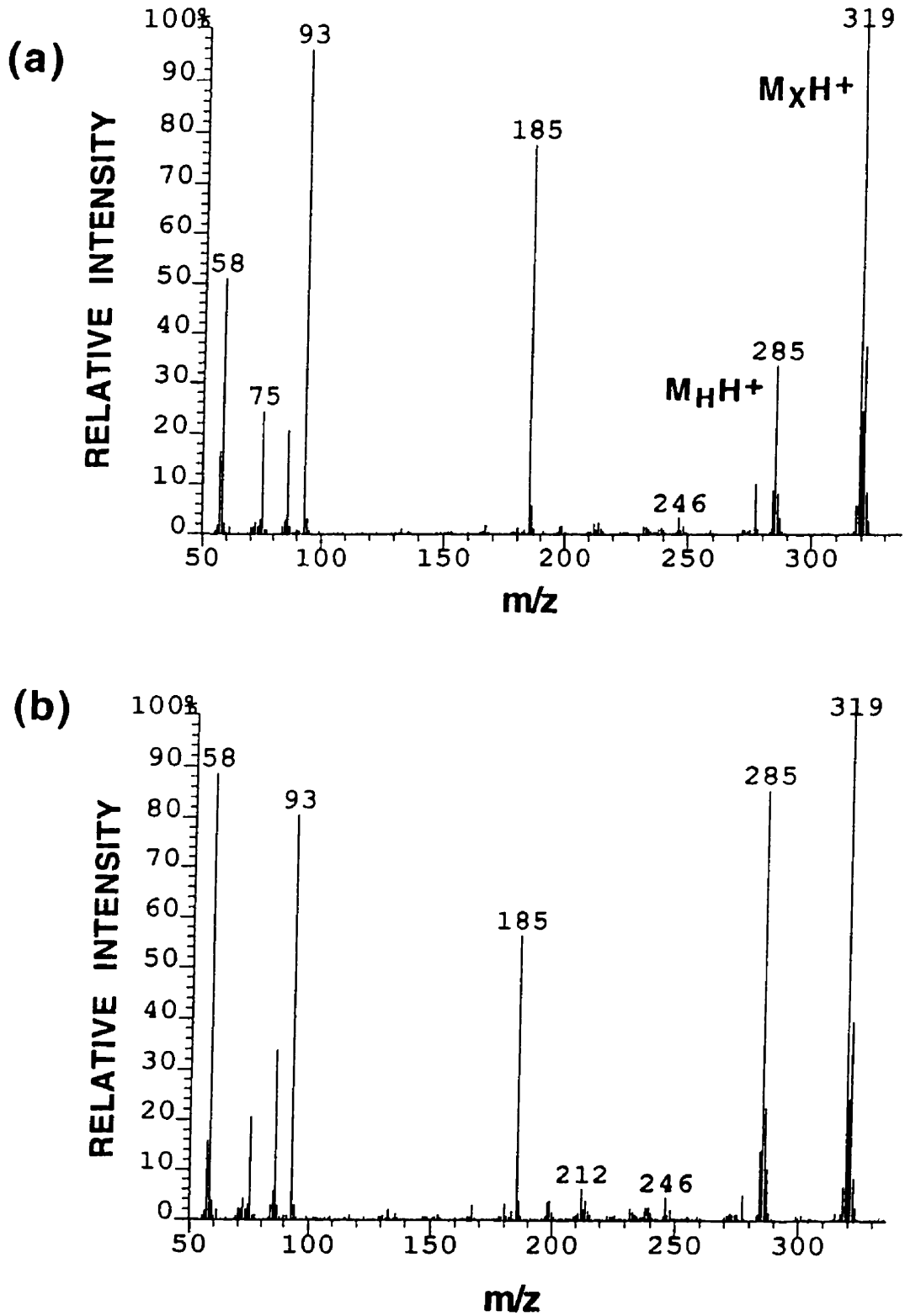

Figure 5. LSIMS spectrum of chlorpromazine in glycerol after the following irradiation times (a) 12 seconds, (b) 1 min, (c) 2 min, and (d) 4 min.

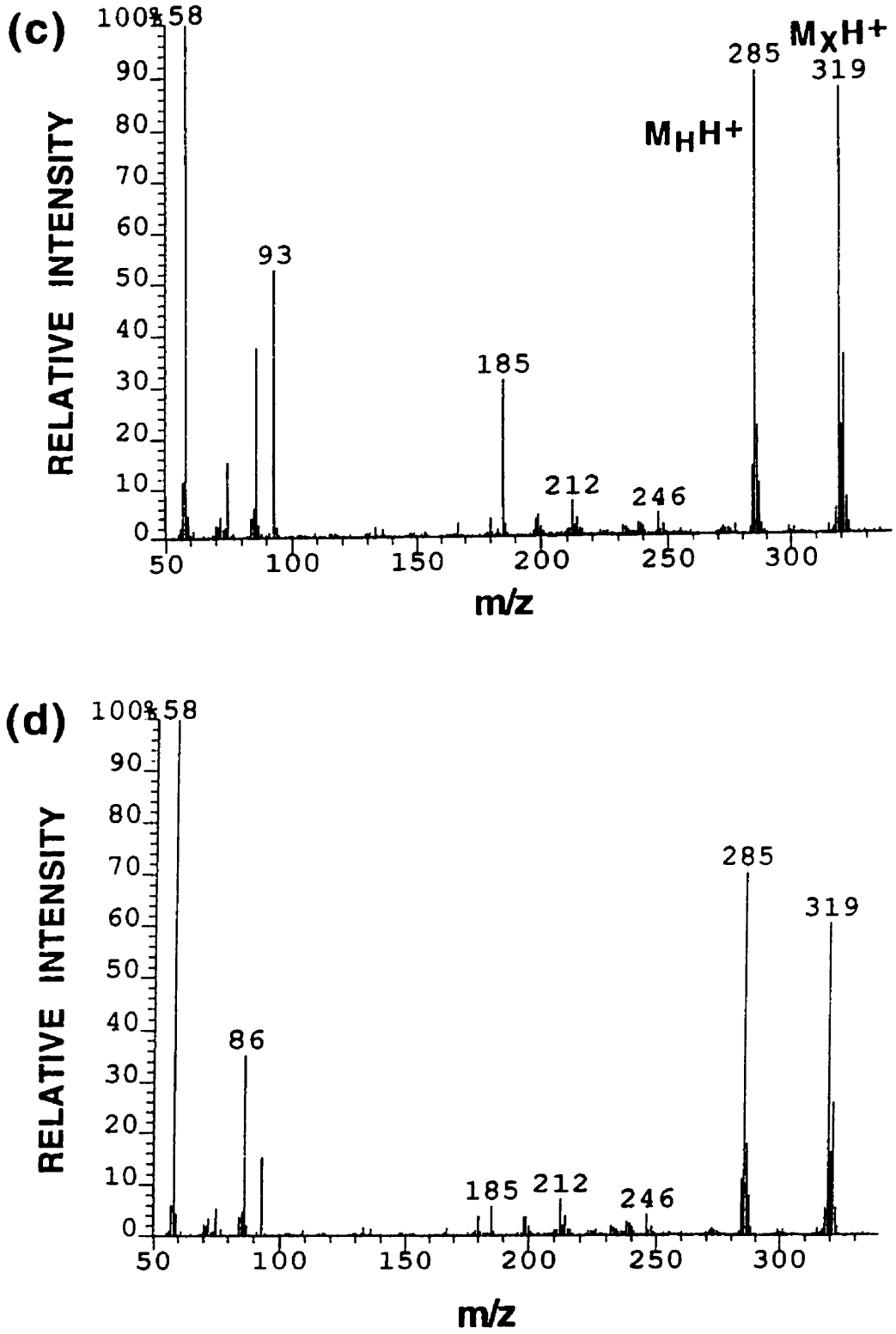

Figure 5. LSIMS spectrum of chlorpromazine in glycerol after the following irradiation times (a) 12 seconds, (b) 1 min, (c) 2 min, and (d) 4 min.

dehalogenation remained essentially constant during the time of analysis[32].

The % dehalogenation for chlorpromazine in glycerol at various concentrations with time of analysis is shown graphically in Figure 6. The effect of increased concentration appears to show a concomitant increase of the %dehalogenation except for the highest concentration. The plot for the highest chlorpromazine concentration (0.097M) seems anomalous as it appears below that of 0.037M. Furthermore, the plot for the 0.097M chlorpromazine/glycerol solution appears to indicate that the dechlorination maximizes after 3 minutes of beam irradiation and then decreases. These observations can be rationalized by considering the fragmentation behaviour of chlorpromazine with time and concentration. More specifically the m/z 58 fragment which is due to the cleavage of the C-C bond alpha to the amino side-chain nitrogen. The other amino side chain fragment ion at m/z 86 also increases with analyte concentration.

The increased fragmentation of the amino side chain at increasing chlorpromazine concentrations and time of irradiation can be seen in the LSIMS mass spectra where the relative intensities of m/z 285 and m/z 319 decrease while m/z 58 and m/z 86 increases with concentration and time of irradiation. This is substanstiated by plotting the ratio of the intensity of m/z 58 to that of m/z 319 with respect to time at different concentrations as shown in Figure 7. Therefore, the correction factor %R was introduced in the % dehalogenation expression

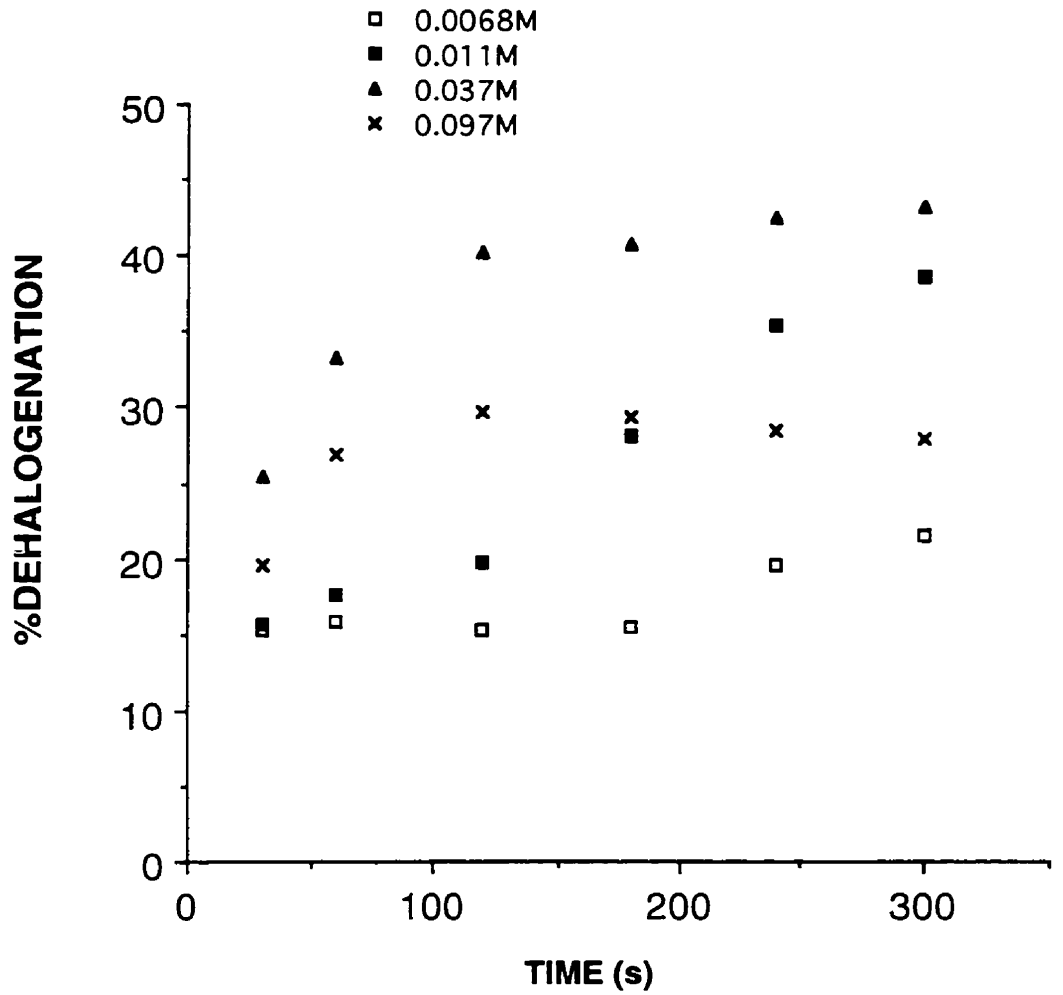

Figure 6. %dehalogenation of chlorpromazine at various concentrations in glycerol as a function of time of analysis. Concentrations: ❑ 0.0068M, ■ 0.011M, ▲ 0.037M, × 0.097M.

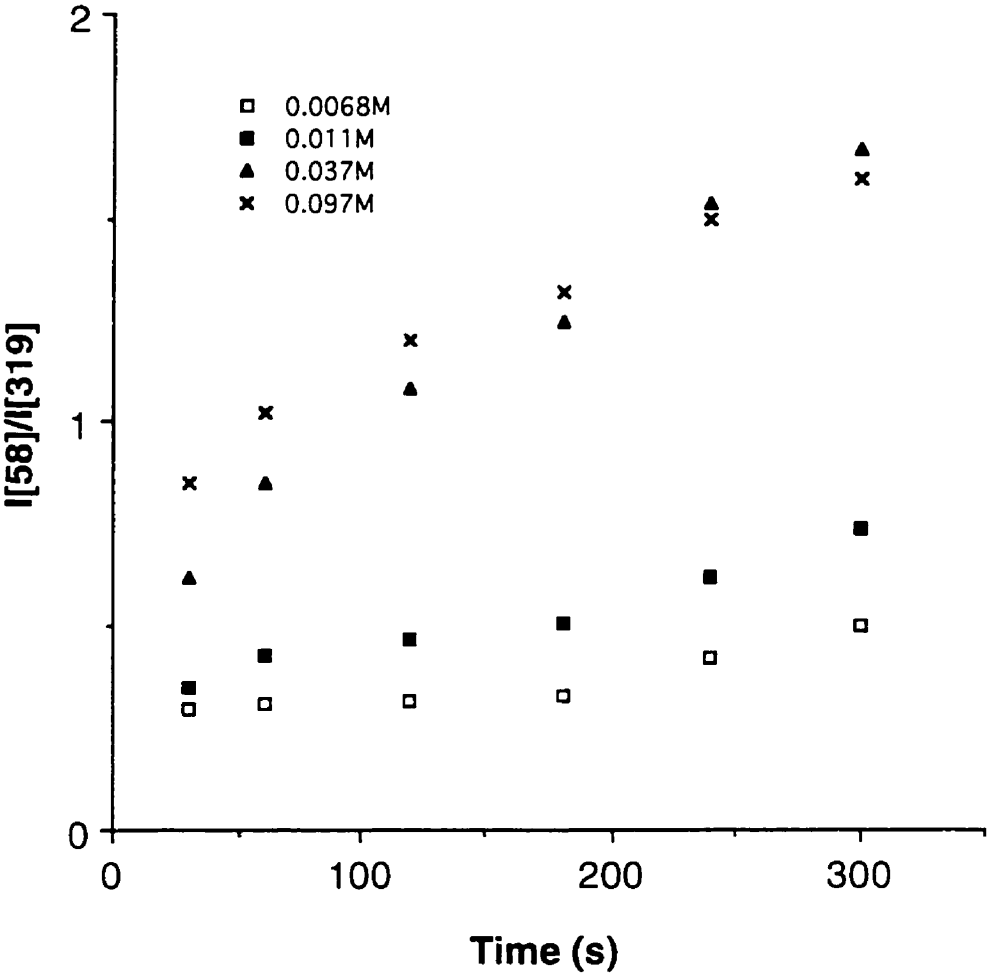

Figure 7. Ratio of relative intensity of the amino side chain fragment m/z 58 to the intensity of the protonated molecular ion m/z 319 as a function of time of analysis and concentration.
Concentrations: ❑ 0.0068M, ■ 0.011M, ▲ 0.037M, X 0.097M.

in order to take into account the increased fragmentation of m/z 285 and m/z 319 with time.

$$\%R = \frac{100\ (M_H + H)^+}{(M_H + H)^+ + (M_X + H)^+} \left[\frac{I_{58}}{I_R}\right] \qquad [12]$$

As can be seen %R represents the % dehalogenation corrected by the ratio of I_{58} (the actual intensity of m/z 58) to I_R (the average intensity of m/z 58 at the lowest concentration i.e. where the amine side chain fragmentation is lowest). As can be seen in Figure 7, the ratio of the intensity of the m/z 58 ion to that of the protonated molecule, m/z 319, is almost constant at the lowest concentration used throughout the time of analysis. The value of I_R was obtained from the averaged spectrum of a 0.0068M chlorpromazine/glycerol solution. The correction factor compensates for the increased fragmentation of the amino side chain which alters the calculated % dehalogenation by distorting the measured peak intensities of $(M_H+H)^+$ and $(M_X+H)^+$.

This distortion is due to the fact that M_H is most likely formed at the surface and thus more exposed to the beam causing more rapid decomposition than the parent molecule, M_X. It can be speculated that the internal energy of M_H is higher than that of M_X, thus increasing the likelihood of fragmentation of the molecule. The corrected data for %R is shown in Figure 8 and indicates that generally, dehalogenation increases with increasing time of irradiation and concentration. The fact that the plots representing the two higher concentrations coincide up to 3 minutes probably illustrates that the analyte is at, or close to its maximum surface concentration at 0.037M.

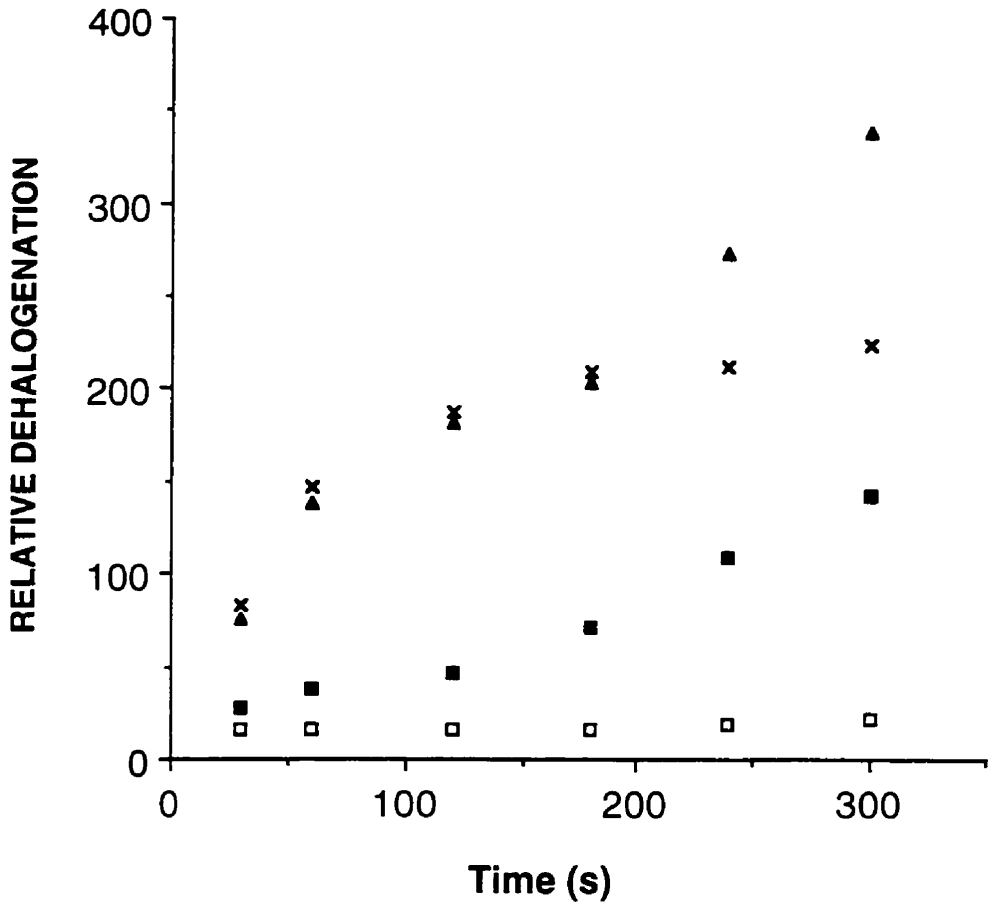

Figure 8. Relative dehalogenation of chlorpromazine at various concentrations in glycerol as a function of time of analysis. Concentrations: ❑ 0.0068M, ■ 0.011M, ▲ 0.037M, × 0.097M.

Of course, we are now dealing with *relative* values of dehalogenation which merely serve the purpose of illustrating the importance of the amino side chain fragmentation with respect to the dehalogenation process.

In order to compare the results obtained for chlorpromazine and allow perhaps more general conclusions to be drawn on the dehalogenation process, a second compound known to undergo dehalogenation was investigated. The time effect on % dehalogenation for varying concentrations of 4-chloro-phenylalanine ethyl ester in glycerol under standard conditions is shown in Figure 9. The most striking feature of Figure 9 is the similarity of the profiles for the different concentrations used. This is in marked contrast with the results obtained for chlorpromazine under similar conditions. The range of dechlorination values obtained was 15-50% for chlorpromazine and 12-18% for 4-chloro-phenylalanine ethyl ester respectively under standard conditions.

If one assumes that similar dehalogenation processes are involved for the two analytes, a tentative explanation of the differences observed on %dehalogenation with time of irradiation and concentrations can be suggested on the basis of their respective surface activity and/or solvation in glycerol. Since chlorpromazine can be assumed to be more hydrophobic and thus more surface active, it is expected to be more affected by concentration changes relative to 4-chloro-phenylalanine ethyl ester. Its propensity as compared to 4-chloro-phenylalanine ethyl ester will be to migrate to the surface of the droplet where

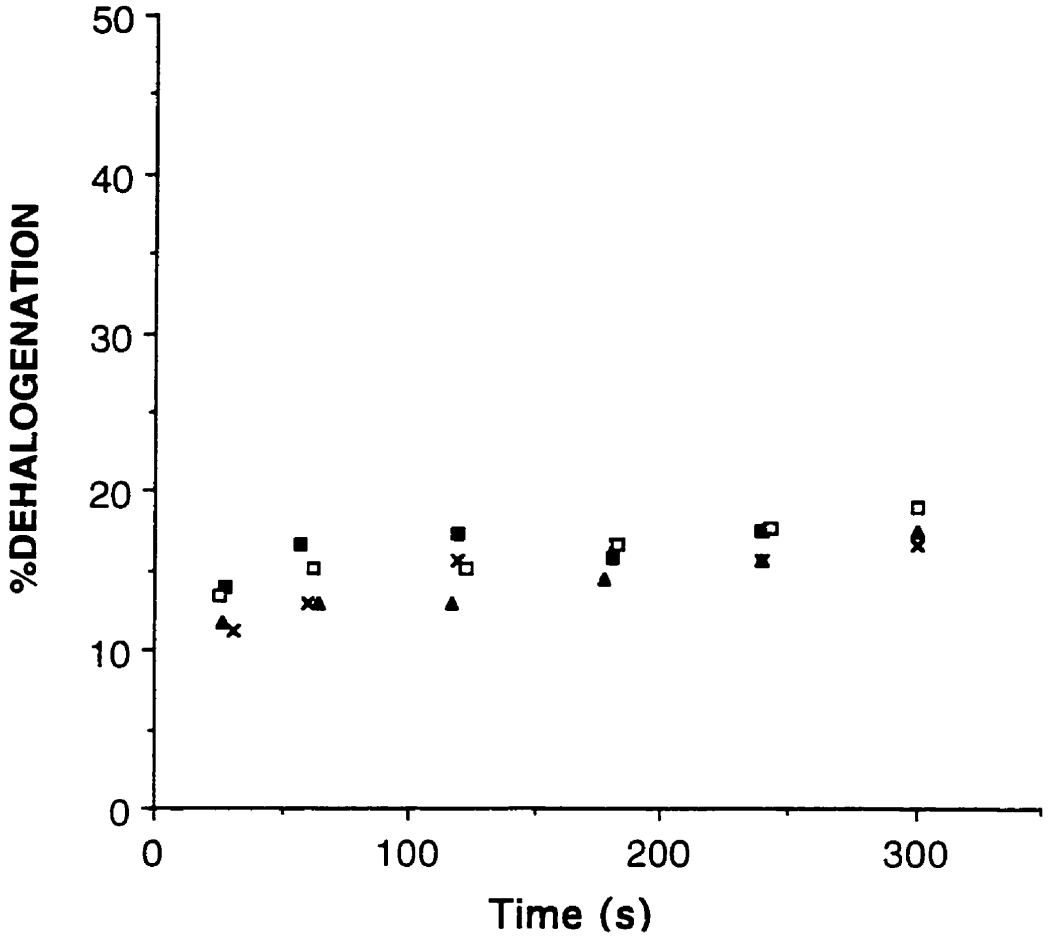

Figure 9. % dehalogenation of p-Cl-phenylalanine ethyl ester at various concentrations as a function of time of analysis. Concentrations: ❑ 0.0068M, ■ 0.011M, ▲ 0.037M, × 0.097M.

reactive species (radicals, ions, and thermal electrons) are locally being generated by the bombarding caesium ions, hence increasing the probability of the analyte undergoing reaction to form the beam-induced product. For opposite reasons, 4-chloro-phenylalanine ethyl ester does not exhibit marked time or concentration effects since it is less surface active and better solvated. This appears to be confirmed by the presence of glycerol adducts in the spectra of 4-chloro-phenylalanine ethyl ester which are absent in the chlorpromazine mass spectra at all studied concentrations. This rationalization of the differences observed between the two compounds is also in line with the trends observed in our experiments on the effect of beam flux on dehalogenation which is discussed in the next section. The effect of surface activity has been demonstrated in a study of the beam-induced reduction of oximes to the corresponding imines[25]. The authors found that an increased surface concentration of the analyte resulted in a greater abundance of the reduced species in the FAB mass spectrum. Surface activity was also invoked to rationalize the beam-induced generation of anomalous $(M-H)^+$ ions in the FAB mass spectra of cyclic acetals[81]. This aspect of beam-induced dehalogenation will be treated more extensively in section 5.4.

4.1.2 Beam density effect

An increase in beam density results in a corresponding increase in the % dehalogenation of chlorpromazine as illustrated by Figure 10. This phenomenon can be rationalized by the greater number of impacts per unit area per unit time thus creating an increase in the concentration

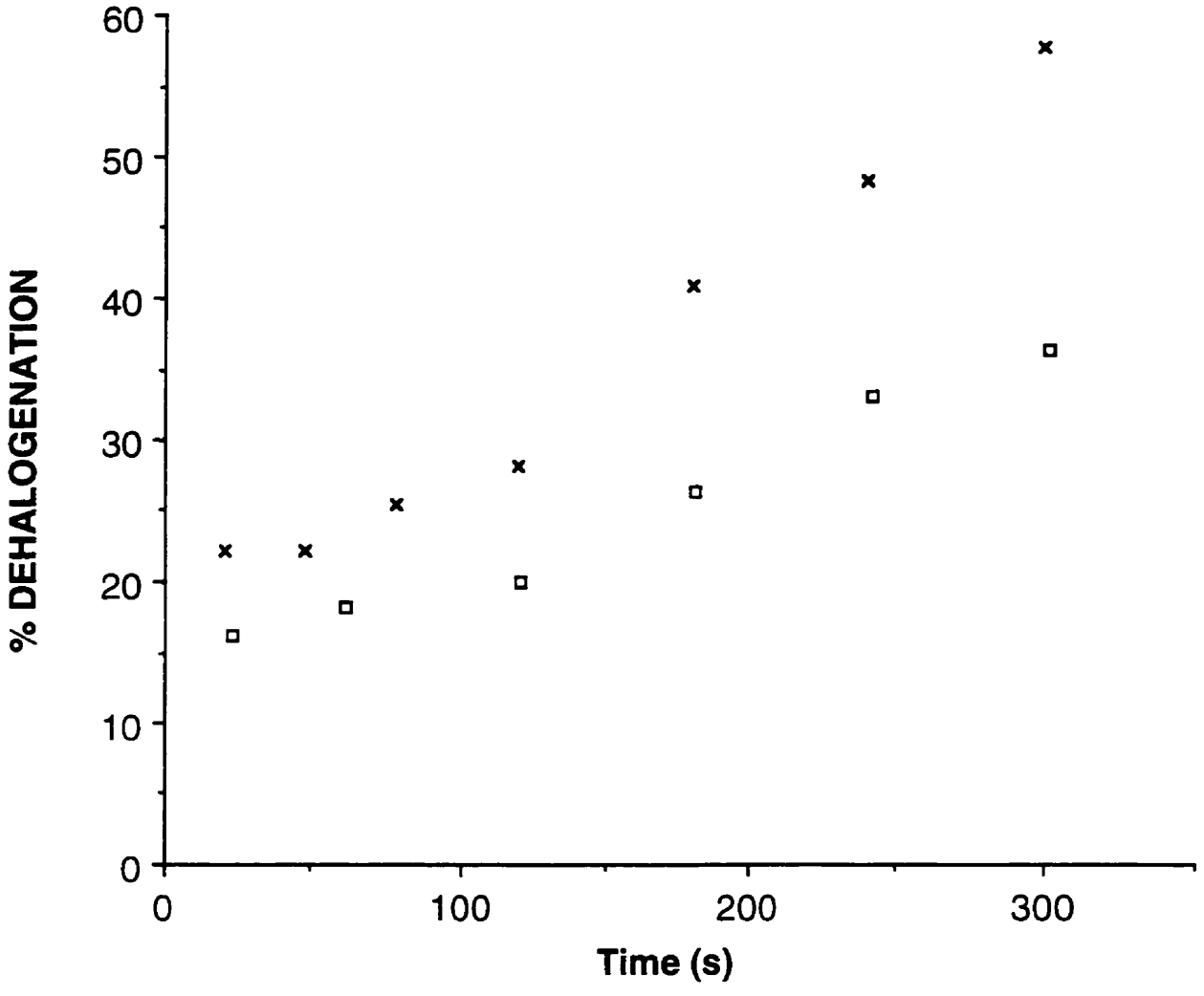

Figure 10. % dehalogenation of chlorpromazine (0.0068M in glycerol) at different beam densities as a function of time of analysis. Beam Densities: × 0.042μA/mm^2 ❑ 0.027μA/mm^2.

of reactive species such as ions, radicals, and electrons formed which may be ultimately responsible for beam-induced reactions. The effect of beam flux on the extent of reduction of organic dyes shows the same trend[22,121]. The data in Table I shows that the effect of flux levels out at the higher concentrations. This trend was observed earlier by Visentini et al in their study of the LSIMS redox behaviour of peptides[123].

Table I. % dehalogenation of chlorpromazine with varying concentration at beam fluxes of 0.027 and 0.042μA mm^{-2}. The % dehalogenation values are obtained from the average of the first 5 minutes of analysis.

Concentration (ML^{-1})	% Dehalogenation Beam Flux=0.027μA mm^{-2}	% Dehalogenation Beam Flux=0.042μA mm^{-2}
0.0068	16.8	26.7
0.016	27.3	37.4
0.037	38.4	39.1
0.097	28.3	27.8

For 4-chloro-phenylalanine ethyl ester the extent of the flux effect also seems to be significantly reduced compared to chlorpromazine as can be seen from Figure 11. This difference of the beam density effect on the dehalogenation behaviour of chlorpromazine and 4-chloro-phenylalanine ethyl ester can be rationalized along the lines of the surface activity/solvation argument suggested in the previous section. Thus, the surface concentration of the compounds appears to be an important factor affecting their dehalogenation behaviour since the more surface active compound, chlorpromazine, has a greater rate of

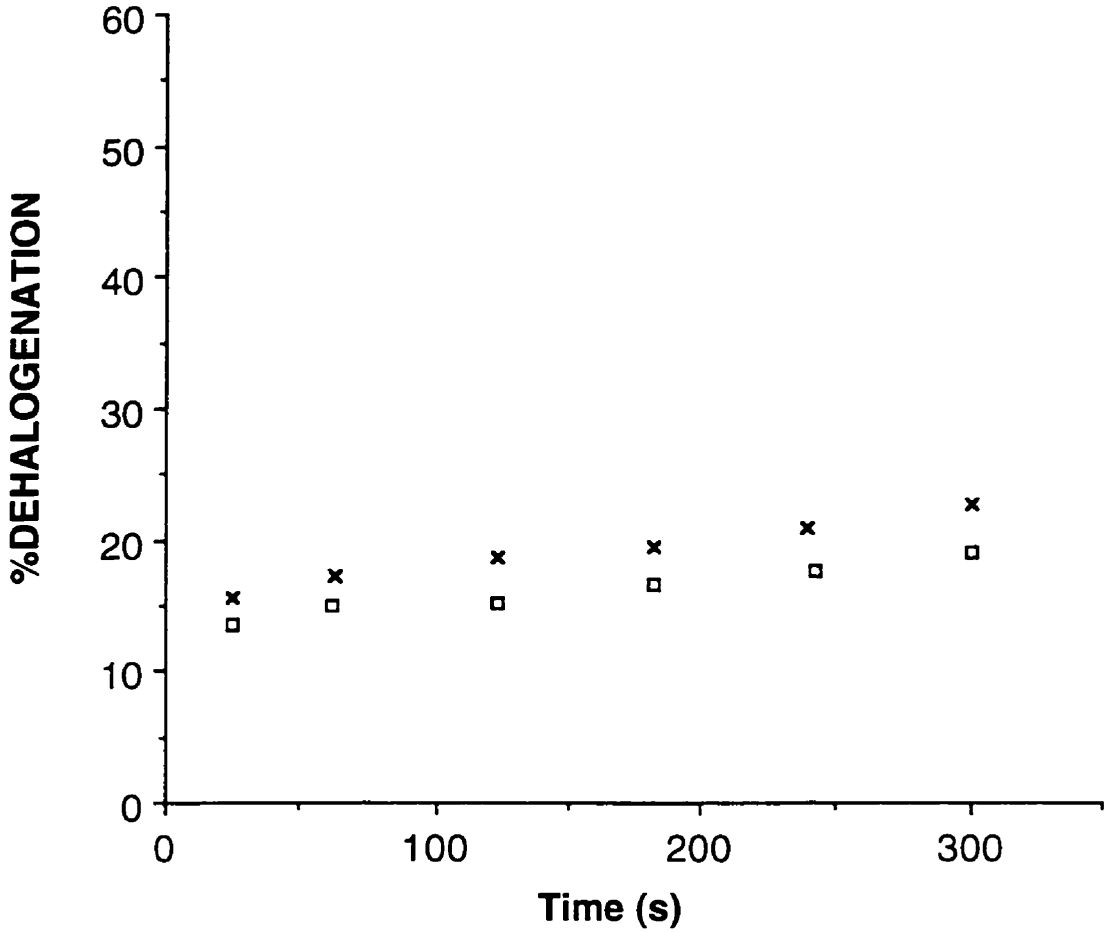

Figure 11. % dehalogenation of p-Cl-phenylalanine ethyl ester (0.0068M in glycerol) at different beam densities as a function of time of analysis. Beam Densities: × 0.027μA/mm^2 ❑ 0.042μA/mm^2.

dechlorination. This tentative rationalization will be further explored in section 5.4.

4.1.3 Beam energy effect

The study of the effect of beam energy on the beam-induced dehalogenation of chlorpromazine did not not yield recognizable trends. For example, the % dehalogenation at 16, 22, and 28 keV was 34, 38, and 37 at a concentration of 0.037M, respectively. Investigations concerning the effect of beam energy on reduction processes have always been performed under the caveat that a change in beam energy would likely bring a change in beam focussing[22]. The change in beam focussing inevitably causes a change in beam flux.

The interdependency of beam energy and beam flux obviates the possibility of carrying out a true investigation of beam energy effects on dehalogenation and other beam-induced reduction processes. This is particularly relevant for dehalogenation since this process is sensitive to beam flux. It is not surprising that the bulk of the literature concerning the effects of FAB/LSIMS experimental parameters on beam-induced reduction processes tend to concentrate on the chemical aspects of the problem since the effect of the physical parameters can often be masked by proper consideration of the chemical parameters. However, the effect of the chemical parameters on FAB/LSIMS data *cannot be significantly* mitigated by a variation of the physical parameters such as beam density and energy[22,34].

4.2-Effect of Chemical Parameters

4.2.1-Effect of matrix Selection

Given the wide variety of liquid matrices available for FAB/LSIMS and the importance of matrix chemistry in effecting or inhibiting beam-induced reactions, the LSIMS spectrum of chlorpromazine was obtained in 12 different matrices with standard beam conditions. The utilization of different matrices should give a greater insight into the dehalogenation process. The elaboration of a rough matrix structure-dehalogenation inhibiting tendency correlation might identify some important features of matrix chemistry. Three new matrix compounds not previously used in FAB/LSIMS studies were introduced in this work: AET, MES, and BOP.

The resulting % dehalogenation values obtained are shown in Table 2. From the data, it appears that the matrices can be grouped in three distinctive categories in terms of their ability to inhibit the dechlorination process. Glycerol and AET stand out as the least effective matrices of the eleven matrices used. Thioglycerol, TDG, MES, BOP, DMBA, and HPEA form another group where dehalogenation is substantially reduced with respect to glycerol and AET but is still present. The last group is comprised of NBA, HBSA, and HEDS. The LSIMS spectra obtained with these matrices show complete suppression of the dechlorination process. These results suggests that the

dehalogenation of chlorpromazine can be drastically reduced by matrix selection.

Table II. Effect of matrix selection on the dehalogenation of chlorpromazine at a concentration of 0.037M*.

Matrix	%Dehalogenation
Gly	34
AET	17
Thiogly	7
TDG	7
DMBA	5
BOP	4
HPEA	4
MES	2
HEDS	0
HBSA	0
NBA	0

*Average of the first 3 minutes of analysis.

In terms of the ability of the matrix to inhibit reductive processes, our results are generally in agreement with those of Vouros[21] and Cook[22] who found that for the reduction of organic dyes the order was NBA > HEDS > THIOGLY > GLY whereas we found that the dehalogenation inhibiting ability of the matrices to be:

NBA, HBSA, HEDS > DMBA, HPEA, BOP, MES > TDG, THIOGLY > AET, GLY

The two trends are essentially the same apart from HEDS. This can be rationalized by the suggestion that the propensity of organic dyes to be reduced in this matrix is greater than that of chlorpromazine to

undergo dehalogenation. Our results confirm the overwhelming importance of matrix chemistry with respect to physical parameters where a minimization of reductive processes and thus artefacts, is desired.

The importance of matrix selection having been established, it would be desirable to investigate the mechanism by which each matrix or group of matrices can inhibit dehalogenation. The interesting aspect of matrix dehalogenation inhibition is that the ability of matrices to inhibit dehalogenation appears to be related to certain specific matrix structural features. However, before investigating the mechanism behind matrix dehalogenation inhibition, further data are needed in order to identify the initiating agent(s) responsible for the onset of the dehalogenation process. Furthermore, the rough matrix dehalogenation inhibiting efficiency scale elaborated here should be validated by using a greater number of compounds. This work will be presented in subsequent sections, as the sole aim of what is presented here is to show the overwhelming importance of matrix selection as an experimental parameter in the inhibition of dehalogenation.

4.2.2 Effect matrix additives

In the event that glycerol must be used as the liquid matrix, dehalogenation can be reduced using doping agents such as TFA and NBA. This approach allows the analyst to use the versatile solvent properties of glycerol whilst diminishing or suppressing the extent of undesirable beam-induced dehalogenation. The effect of TFA doping on

the beam-induced dehalogenation of chlorpromazine is well illustrated in that the extent of dehalogenation is reduced more than three fold by the addition to the glycerol solution of a mere 1% TFA. The extent of dehalogenation observed from the FAB/LSIMS analysis of a 0.037M glycerol solution of chlorpromazine is 34% whilst that from the same solution containing 1% TFA is only 10%. The TFA and NBA doping results are shown in Table III and IV.

Table III. Effect of TFA doping on the extent of dehalogenation observed for chlorpromazine in glycerol (0.037M)*.

Matrix	% Dehalogenation
Glycerol	34
Glycerol/1% TFA	10
Glycerol/5% TFA	9
Glycerol/10% TFA	8
Glycerol/15% TFA	4
Glycerol/20% TFA	4

*Average of the first 2 minutes of analysis.

Table IV. Effect of NBA doping on the extent of dehalogenation observed for chlorpromazine in glycerol (0.037M).

Matrix	% Dehalogenation
Glycerol	34
Glycerol/1% NBA	9
Glycerol/3% NBA	2
Glycerol/10% NBA	1
Glycerol/15% NBA	0

*Average of the first 2 minutes of analysis.

However, the use of higher concentrations of TFA does not generate a very significant increase in the dehalogenation inhibition effect. As a matter of fact, no increase in the dehalogenation inhibition effect is observed when the amount of TFA doping is increased from 15 to 20%. This is not the case for NBA where dehalogenation is basically supressed when the glycerol solution is doped with 10% NBA. A further increase in the amount of NBA doping (15%) leads to total inhibition of chlorpromazine dehalogenation. This is well illustrated by Figure 12 (a) and (b) which compares the extent of dehalogenation observed even when the amount of NBA doping (3%) is lower than that used with TFA (5%), respectively. It should be mentioned that the inhibiting effect of the additives, particularly TFA, is somewhat transient and decreases significantly over time. If one studies the abundance of the dehalogenated chlorpromazine ion, m/z 285, over the time of analysis, it can be seen that the two additive yield different dehalogenation profiles as shown in Figure 13(a) and 13(b). In the case of TFA, the abundance of the dehalogenation product increases more or less linearly with time at all doping amounts. A higher amount of TFA doping generally results in a lower initial abundance of m/z 285. For NBA, The inhibition effect is relatively constant over the initial time of irradiation. A sharp and sudden increase in dehalogenation is then observed to take place followed by a more gentle increase. The onset of the progressive increase in dehalogenation is delayed with increasing amount of NBA doping Table V. The sudden increase in dehalogenation is probably the result of the complete evaporation of NBA and hence the removal of the dehalogenation inhibiting agent. The superior performance of NBA compared to TFA as a dehalogenation

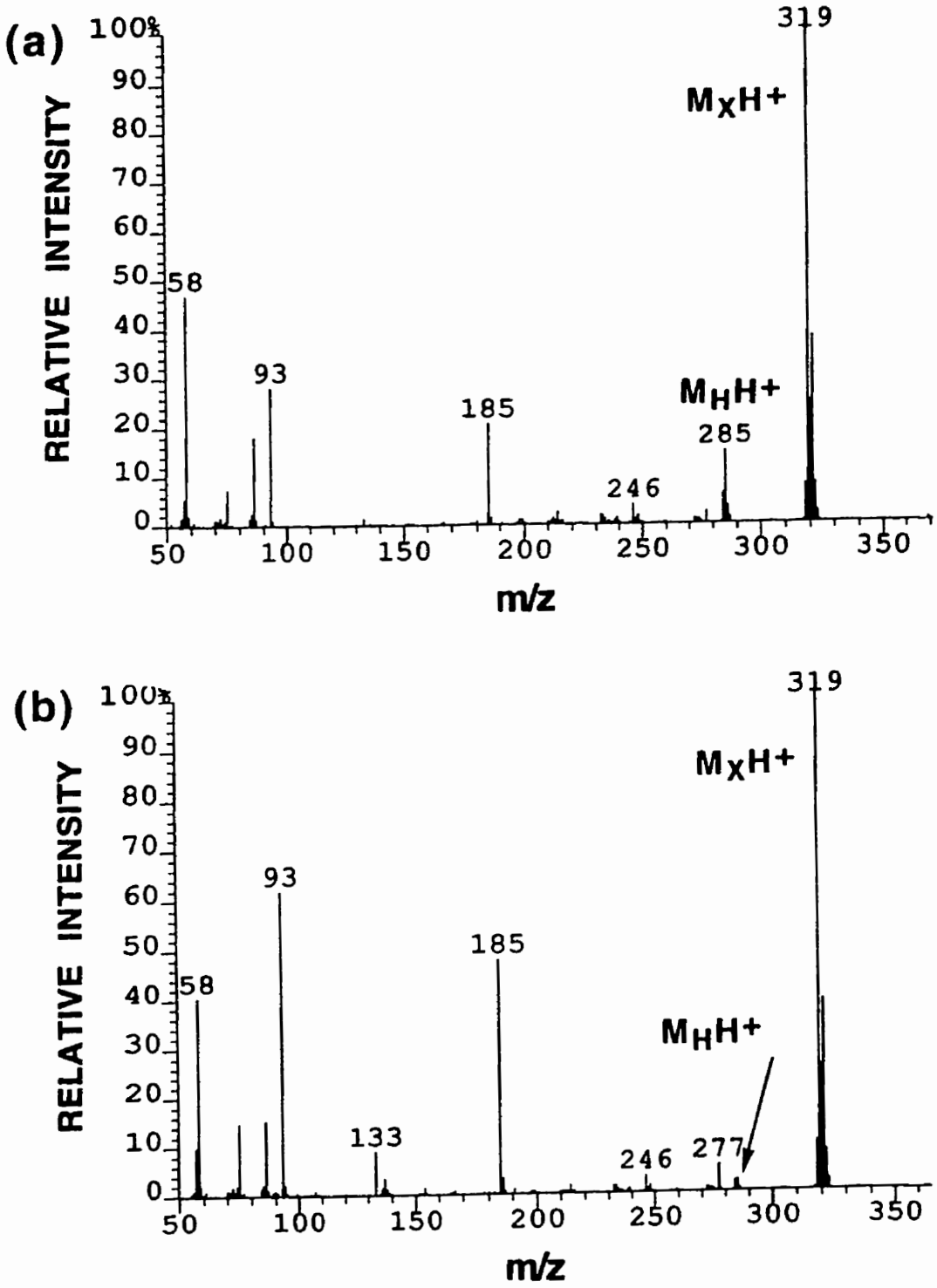

Figure 12. (a) Effect of 5% TFA doping on the positive LSIMS mass spectrum of chlorpromazine in glycerol.
(b) Effect of 3% NBA doping on the positive LSIMS mass spectrum of chlorpromazine in glycerol.

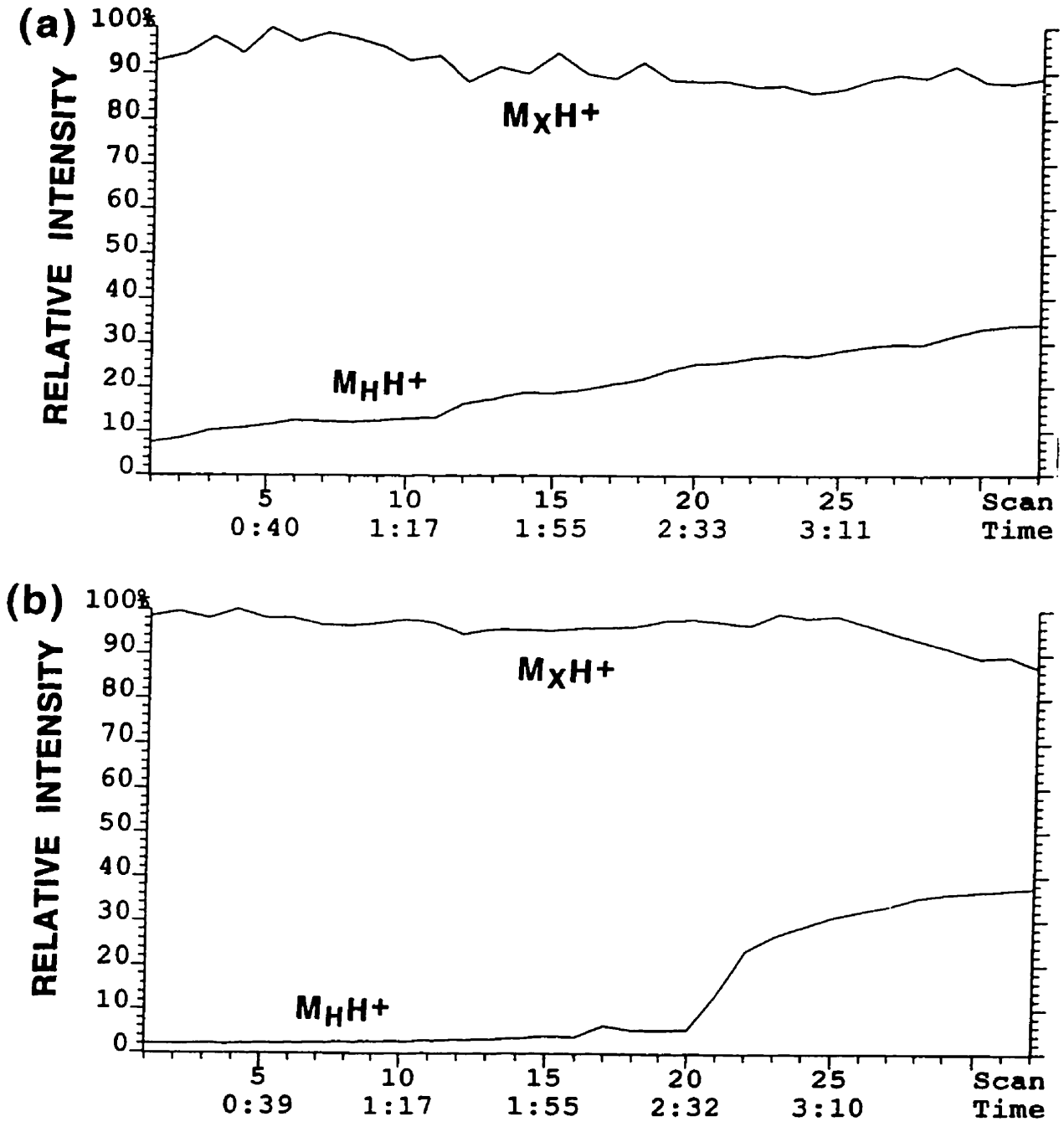

Figure 13 Effect of matrix additives on the ion intensities of M_XH^+ and M_HH^+ of chlorpromazine (a) 5% TFA doping (b) 3% NBA doping.

inhibiting doping agent can probably be attributed to its greater electron scavenging capacity and persistence in solution as indicated by its considerably higher boiling point (180°C/3mm vs 72°C).

Table V. Time of irradiation at which the onset of the dehalogenation is observed for chlorpromazine (0.037M) in various glycerol/NBA solutions.

Matrix	Time of onset of dehalogenation (Seconds)
Glycerol/1% NBA	90
Glycerol/3% NBA	160
Glycerol/10% NBA	270
Glycerol/15% NBA	300

An interesting feature of these additives is that they do not appear to cause the appearance of new ionic species in the LSIMS spectrum which could complicate the analysis process. In the case of NBA, this is consistent with the results of Kebarle et al[92] who showed that glycerol was preferably ionized to NBA under FAB/LSIMS conditions. Therefore, NBA and TFA doping of glycerol offer efficient inhibition of dehalogenation whilst such additives remain 'invisible' in the LSIMS spectrum.

The effect of TFA on FAB/LSIMS beam-induced reductions has focused on the inhibition of the reduction of peptide disulfide bridges[70]. It was observed that TFA essentially eliminates the reduction of disulfide bridges. This inhibition effect was rationalized invoking the electron/radical scavenging capacity of TFA. However, according to pulse radiolysis experiments[48], the trifluoracetate anion has very

poor electron scavenging capacity ($k<1X10^6\ M^{-1}\ s^{-1}$) in aqueous solution. Since the results presented here strongly implicate secondary electrons generated by the bombardment process as being the initiating agents of dehalogenation[36], the electron scavenging capacity of this compound is of interest.

Interestingly, addition of TFA to a glycerol/chlorpromazine solution caused the colour of the solution to change from clear to magenta. The oxidizing properties of TFA are well documented but not well understood[152,153]. It has been shown that TFA possesses light dependent oxidative electron transfer capabilities[152,153]. The work of Eberson et al[153] has shown that 1,2,3,4,5,6,7,8-octamethylanthracene (OMA) is oxidized to the radical cation when dissolved in a TFA/solvent mixture. This process was established to be light dependent. The oxidation was proposed to occur by excitation of OMA to $^1OMA^*$ followed by electron transfer to the dimer of trifluoroacetic acid.

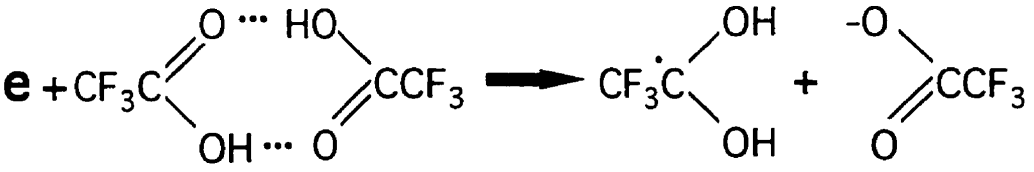

[13]

The involvement of the TFA dimer was supported by the detection of the $CF_3C^{\cdot}(OH)_2$ radical resulting from the photoreduction of TFA in methanol[154]. However, a clear mechanistic picture of the oxidizing processes involving TFA is yet to be formulated despite extensive research[155]. Quite apart from the peculiar redox properties of TFA,

the possibility of the contribution of a pH effect has to be considered. This is due to the observation of dimished dehalogenation upon addition of HCl to a chlorpromazine/glycerol solution. This inhibition effect is, however, much smaller than that observed with TFA and quite transient. The possibility of a pH effect appears to be warranted by the comparison of the electron scavenging capacity of acetic acid and the acetate anion. The acetate anion has an electron scavenging capacity similar to the trifluoroacetate anion as shown below.

$$CF_3COO^- + e \longrightarrow k<1.4X10^6\ M^{-1}\ s^{-1} \quad [14]$$

$$CH_3COO^- + e \longrightarrow k=1X10^6\ M^{-1}\ s^{-1} \quad [15]$$

Unfortunately, there is no existing data for trifluoroacetic acid. However, the rate of reaction of acetic acid with the solvated electron ($2X10^7\ M^{-1}\ s^{-1}$) is much higher than that of the acetate anion. This stronly suggests that trifluoroacetic acid would be a much better scavenger than its anion. As pointed out earlier, the redox chemistry of TFA remains unclear despite extensive study[155].

The effect of TFA doping on the oxidation of organic compounds in electrospray ionization mass spectrometry has been investigated[156]. The authors found that solvent systems containing TFA yielded the radical cation of polyaromatic hydrocarbons in the ESI mass spectrum. It thus appears that TFA has oxidative properties as a solvent or solvent additive. A similar effect has been observed for perfluorinated alcohols. These compounds have been reported to stabilize radical cations in solution[157].

Solution phase vs gas phase reaction: NBA Doping.

With a 50/50 glycerol/NBA solution, dehalogenation was not observed in the first 3 minutes of analysis. This fact allowed the following experiment to be performed. A 0.037 M solution of chlorpromazine in glycerol (1μL) was subjected to 2 minutes of beam irradiation. The sample was withdrawn from the mass spectrometer and 1μL of NBA was added. Upon re-analysis of this sample, a sizable peak corresponding to the dechlorinated ion of chlorpromazine was observed as shown in Figure 14. Since dechlorination of chlorpromazine was shown not to occur in 50/50 NBA/glycerol solutions under caesium ion bombardment, one is led to conclude that the observed m/z 285 can only be explained as a residue generated by the irradiation of the glycerol solution prior to NBA addition. The result of these experiments suggests that dechlorination could, at least in part, occur in the condensed phase. Similar conclusions were reached in experiments featuring post-bombardment HPLC analysis where the dehalogenated residue was detected in the matrix after bombardment. This is further substanstiated by the fact that no dechlorination of the type observed in FAB/LSIMS $(MH-Cl+H)^+$ is reported in the ammonia and methane CI mass spectra of chlorpromazine[158]. However, it is understood that the use of CI data to rule out gas phase mechanism in FAB/LSIMS rests on the assumption that the conditions are similar. The electrospray mass spectrum of chlorpromazine obtained in a water/methanol/HCl solution showed no significant amount of dehalogenation. The absence of dehalogenation in the ESI mass spectrum of chlorpromazine further implicates the beam-induced nature of the process.

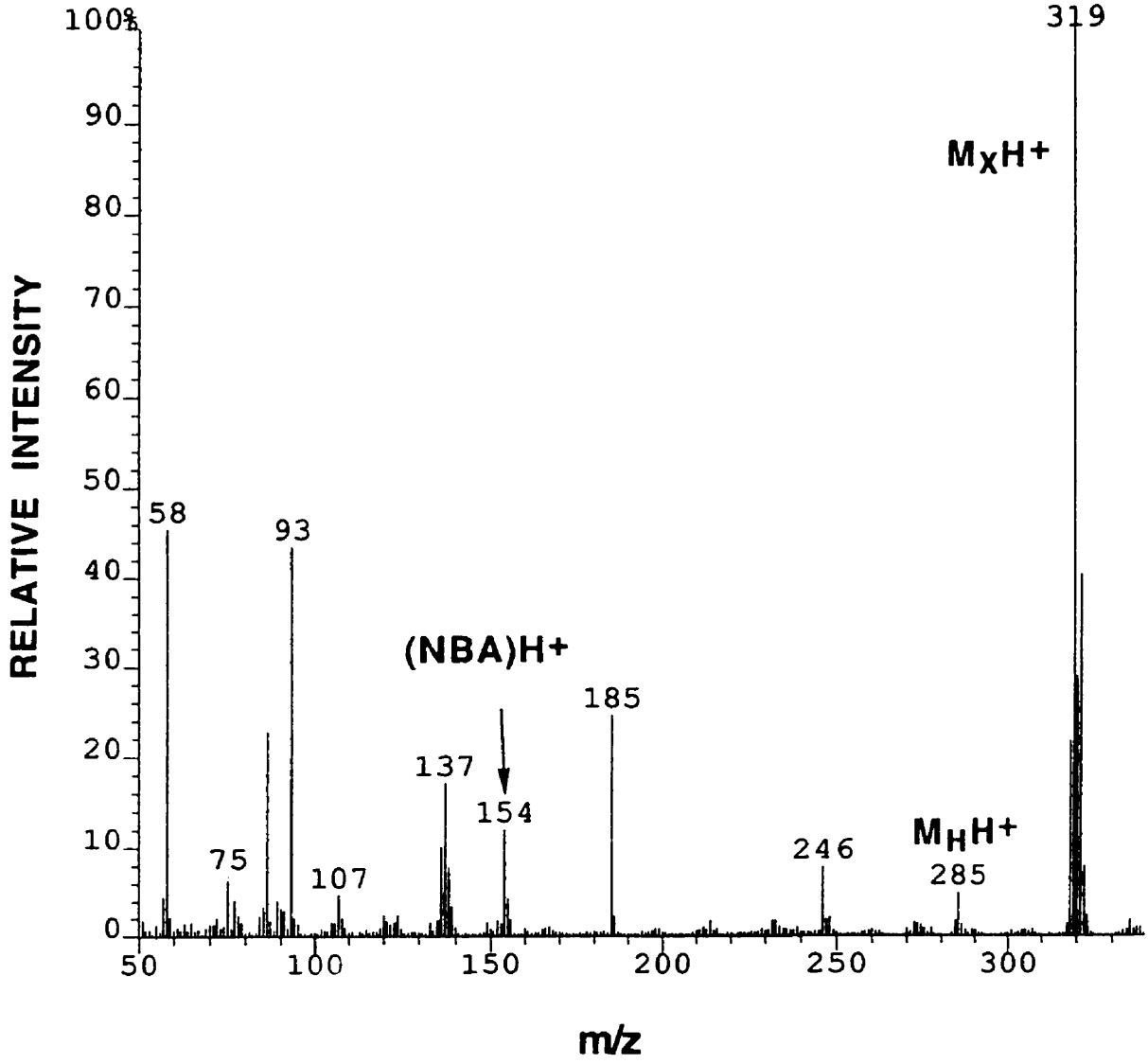

Figure 14. Positive LSIMS mass spectrum of the residue of a glycerol/chlorpromazine solution subjected to irradiationfor 2 minutes. An equal volume of NBA was added to the residue to prevent dehalogenation in the post-bombardment LSIMS analysis.

Chapter 5

5.1 Halogen type effect

The main goal behind the use of the para halogenated phenylalanine methyl esters was to extend as well as validate the observations pertaining to the matrix dehalogenation inhibiting capacity scale obtained with chlorpromazine. This is also the opportunity to gauge the effect of the halogen type for a series of structural analogs. The para halogenated phenylalanine methyl esters were chosen for the following reasons: (a) they are simple halogenated aromatic compounds in ionic form and (b) they can easily be synthesized in quantitative yield from the halogenated phenylalanines which can be commercially obtained in a high state of purity. The structural simplicity of the compounds allows meaningful, if indirect, comparison to the behaviour of simple halobenzenes under electrochemical and pulse radiolytic conditions.

The phenylalanines were used as methyl esters to afford increased solubility in all matrices save MES and DEP. The insolubility of the para halogenated phenylalanine methyl esters in MES and DEP rendered LSIMS analysis impossible in these matrices. The use of the methyl esters of the halogenated phenylalanines obviated the need for co-solvents which are necessary for the LSIMS analysis of the zwitterionic form of phenylalanine even in glycerol[33]. Given the fact that this study puts a heavy emphasis on the effect of matrix chemistry on beam-induced reduction processes, the use of co-solvents was generally avoided to keep the chemical systems as simple as possible. A further advantage of the methyl ester form was the ionic

form of the compounds which afforded pre-formed ions and hence higher sensitivity.

The positive ion LSIMS spectra of para halogenated phenylalanine methyl esters in glycerol are shown in Figure 15 (a)-(d). The main fragmention reaction consisted of the loss of 60 daltons (methyl formate) from the protonated molecule or the dehalogenated analog depending on the matrix. This fragmentation pattern is analogous to that found in chemical ionization of the methyl ester of amino acids[159]. The ion at m/z 120 stems from a similar loss of methyl formate but from the dehalogenated molecule. The glycerol-analyte adducts $(M+Gly+H)^+$, presumably hydrogen bonded, are also present. It is interesting to note that these adducts are absent in the chlorpromazine-glycerol LSIMS spectra. The para halogenated phenylalanine methyl esters undergo beam-induced dehalogenation as shown below in Scheme 2.

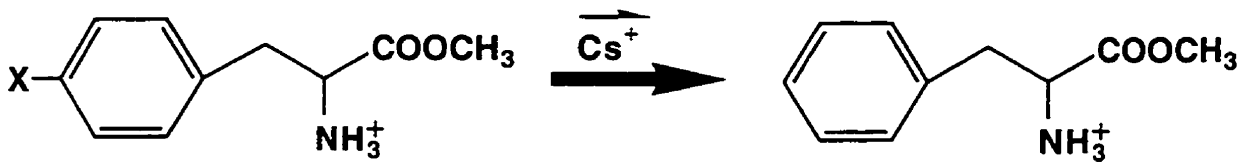

X = F, Cl, Br, I

M_XH^+ M_HH^+

Scheme 2

Where M_XH^+ and M_HH^+ are the intact protonated molecule and dehalogenated analog, respectively. The M_HH^+ ion appears at m/z 180 and represents the protonated phenylalanine methyl ester.

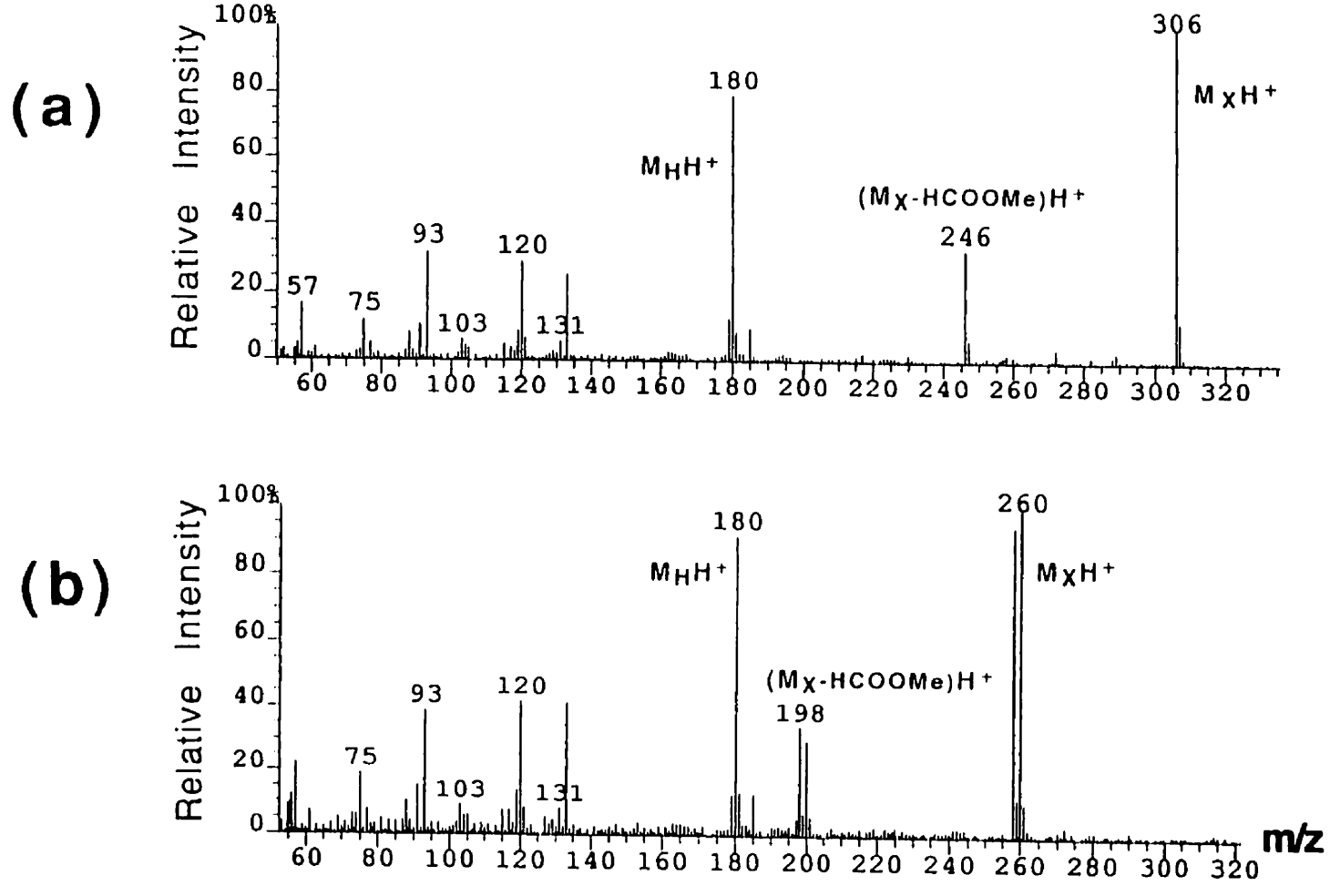

Figure 15. LSIMS mass spectra of the 4-halo-phenylalanine methyl ester in glycerol (0.05M), (a) iodo, (b) bromo, (c) chloro, (d) fluoro.

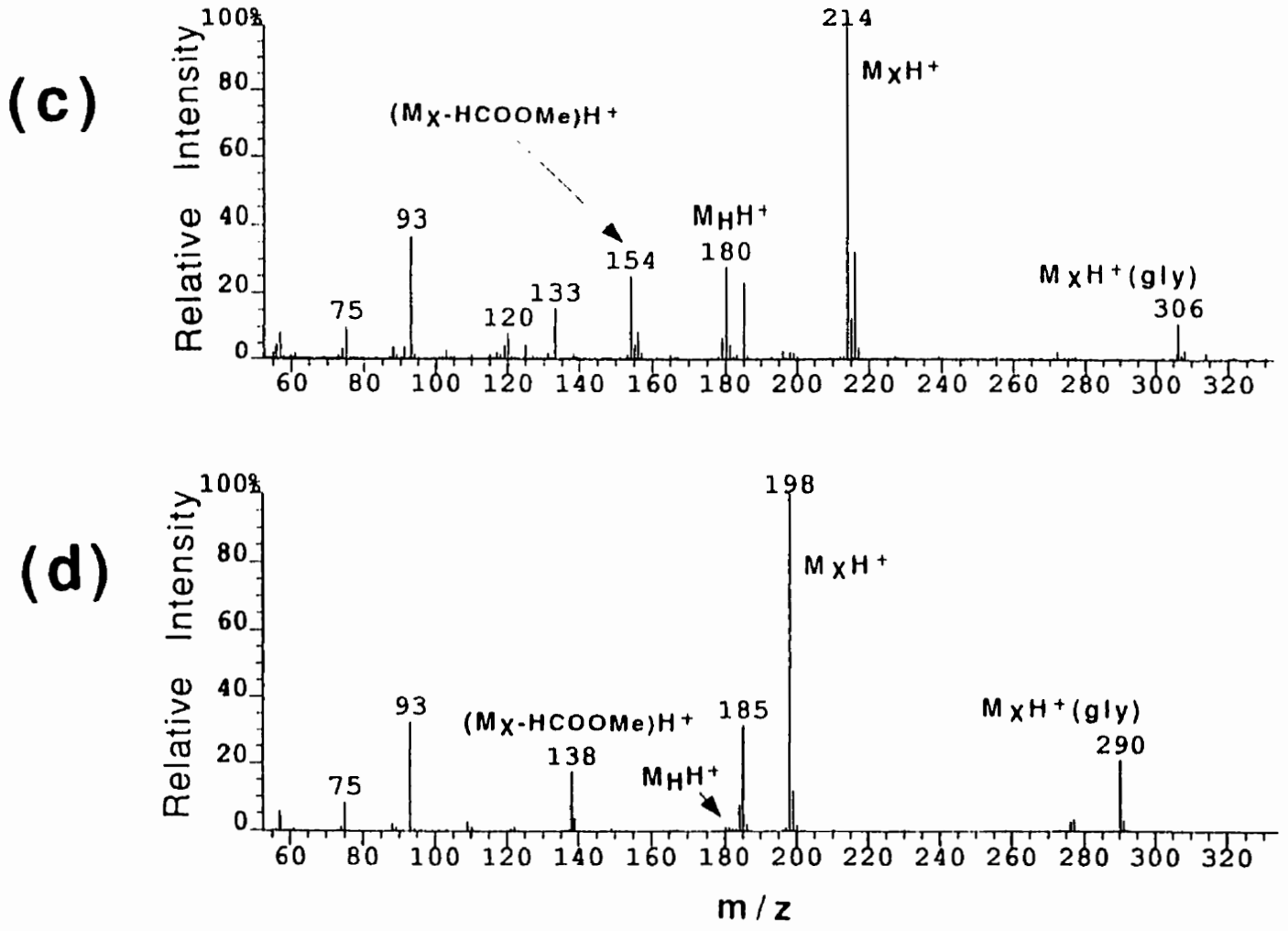

Figure 15. LSIMS mass spectra of the 4-halo-phenylalanine methyl ester in glycerol (0.05M), (a) iodo, (b) bromo, (c) chloro, (d) fluoro.

The % dehalogenation obtained in glycerol and other matrices are shown in Table **VI**. The results pertaining to atrazine will be discussed further on. As expected the effect of halogen type on the % dehalogenation observed in glycerol for the para halogenated phenylalanine methyl esters decreases in the order I > Br > Cl > F, reflecting the increasing C-X bond strength.

This observation is in agreement with previous FAB reports[30,33]. Nakamura[33] reported the beam-induced dehalogenation of bromo-, chloro-, and fluoro-phenylalanines and obtained dehalogenation values of 33, 19 and 3%, respectively. These numbers are surprisingly close to those exhibited in this study given the different conditions used. A similar trend was reported for the 5-halouridines where the % dehalogenation was 33, 21, 12, and 5.3 % from the iodo, bromo, chloro and fluoro analogs. Interestingly, a similar order of dehalogenation tendency was observed in electrochemical[40] and pulse radiolysis studies[37] where the solvated electron is the initiating reagent.

5.1.2 Matrices other than glycerol.

In the other matrices, the halogen effect observed in glycerol is also present. That is to say, the % dehalogenation obtained from the LSIMS spectra of the 4-halo-phenylalanine methyl esters reflects the dehalogenation inhibiting capacity of the matrix as previously defined with chlorpromazine. Of course, this is contingent on the dehalogenation inhibiting capacity of the matrix. For example, only

Table VI. Effect of matrix selection on the %Dehalogenation values for the 4-halo-phenylalanine methyl esters and atrazine.

Matrix	Atrazine	4-**X**-Phenylalanine methyl esters **X**=I	Br	Cl	F
Group 1 Hydroxy-aliphatic					
Gly	46	45	30	18	trace
AET	27	25	20	10	trace
Group 2a Sulfur containing aliphatic					
Thiogly	15	17	11	7	0
TDG	16	16	12	6	0
MES	4	NS	NS	NS	NS
HEDS	7	6	0	0	0
Group 2b Aromatics with electron donating groups					
HPEA	10	15	6	4	0
DMBA	MI	MI	MI	MI	MI
BOP	11	12	5	3	0
Group 3 Aromatics with electron withdrawing groups					
HBSA	0	0	0	0	0
NBA	0	0	0	0	0
DEP	0	0	0	0	0

NS=Not soluble MI=Matrix interference

iodo-phenylalanine methyl ester underwent dehalogenation in HEDS, a matrix with a high dehalogenation inhibiting capacity. As indicated in Table VI, the extent of dehalogenation could not be obtained for the 4-halo-phenylalanine methyl esters and atrazine in the liquid matrix DMBA. The ionic species resulting from the dehalogenation of the 4-halo-phenylalanines and atrazine, M_HH^+, appear at m/z 180 and

182, respectively. The LSIMS analysis of the pure matrix liquid generates a series of peaks in the mass range m/z 180-183. Though characteristically small (< 5% of the base peak of the matrix spectrum), the spectral interference produced by the matrix peaks prevented an accurate determination of the % dehalogenation of the 4-halo-phenylalanines and atrazine. Nevertheless, an estimation of the extent of dehalogenation of these compounds in DMBA indicates that there is qualitative agreement with the matrix dehalogenation inhibiting capacity established for aromatic matrices with electron donating groups.

However, it appears that the halogen effect is not overwhelming in determining the extent of dehalogenation in aromatic compounds. The %dehalogenation obtained with atrazine, a chloro- compound, was similar to that of iodo-phenylalanine methyl ester throughout the matrix series. This can be explained by the specific character of the C-Cl bond due to the π deficiency of the triazine ring. The diminished C-Cl bond strength is further substanstiated by the fact that the chlorine in the dimethoxy analog of atrazine can be nucleophilically displaced by the carboxylate anion (a weak nucleophile) in high yield under mild conditions[160]. A similar argument was invoked by Volmer and Levsen to explain the dehalogenated ions generated from analogous compounds under discharge-assisted thermospray conditions[146]. This results indicates that in some cases, the structure of the aromatic moiety can influence the extent of dehalogenation observed. Other effects due to the particulars of

the aromatic moiety structure, particularly the electron affinity[36], will be discussed in a further section.

The behaviour of atrazine under FAB/LSIMS conditions can provide useful data pertaining to the radical chemistry generated by the primary beam. The spectrum of atrazine in HEDS shown in Figure 16(a) reveals the presence of analyte matrix adduct which can be reasonably explained in terms of radical-radical recombination involving HO-$CH_2CH_2S^{\cdot}$. Similar results were obtained by Gross et al.[105] A possible mechanistic scheme is presented in Figure 17 to account for the formation of the dehalogenated atrazine-matrix adduct with a characteristic ion at m/z 258[105]. The presence of this adduct in the LSIMS spectrum of atrazine in HEDS can be interpreted as strong evidence for the beam-induced production of HO-$CH_2CH_2S^{\cdot}$ radicals. These sulfur-centered (thiyl) radicals have specific redox properties which can play an important role in beam-induced processes and will be further discussed in later sections. Interestingly, a similar adduct is observed in the LSIMS spectrum of atrazine in thioglycerol at m/z 288 as shown in Figure 16(b). This result offers strong evidence concerning the generation of thiyl radicals in the bombardment of sulfur-containing matrices. The halogen type effect confirms the matrix dehalogenation inhibiting efficiency scale established earlier with chlorpromazine and indicates the importance of the structure of the aromatic moiety of the analyte. Some aspects of the effect of the structure of the aromatic moiety on the dehalogenation process will be investigated in subsequent sections.

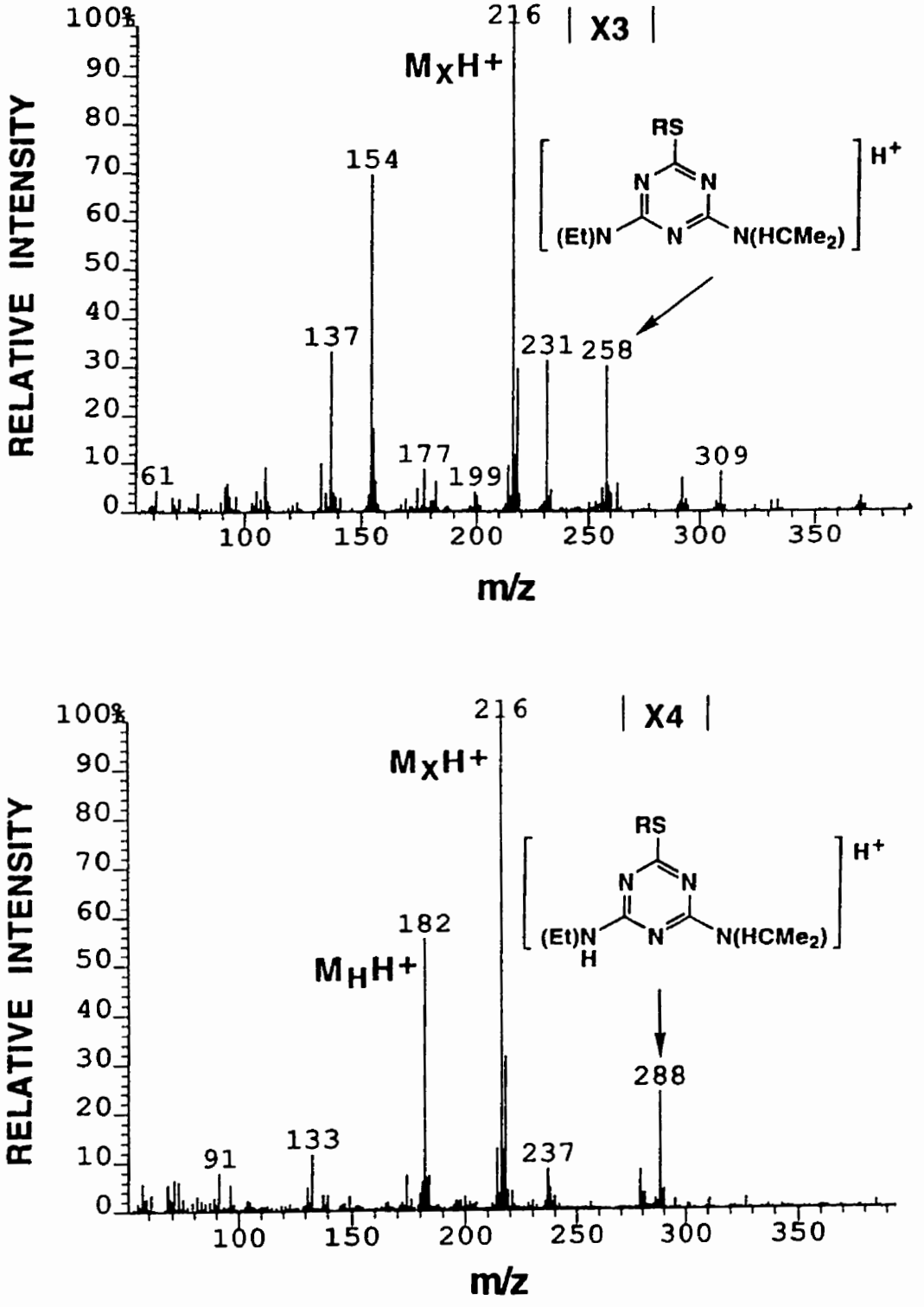

Figure 16 Positive ion mode LSIMS spectrum of (a) atrazine in HEDS matrix, (b) atrazine in thioglycerol matrix.

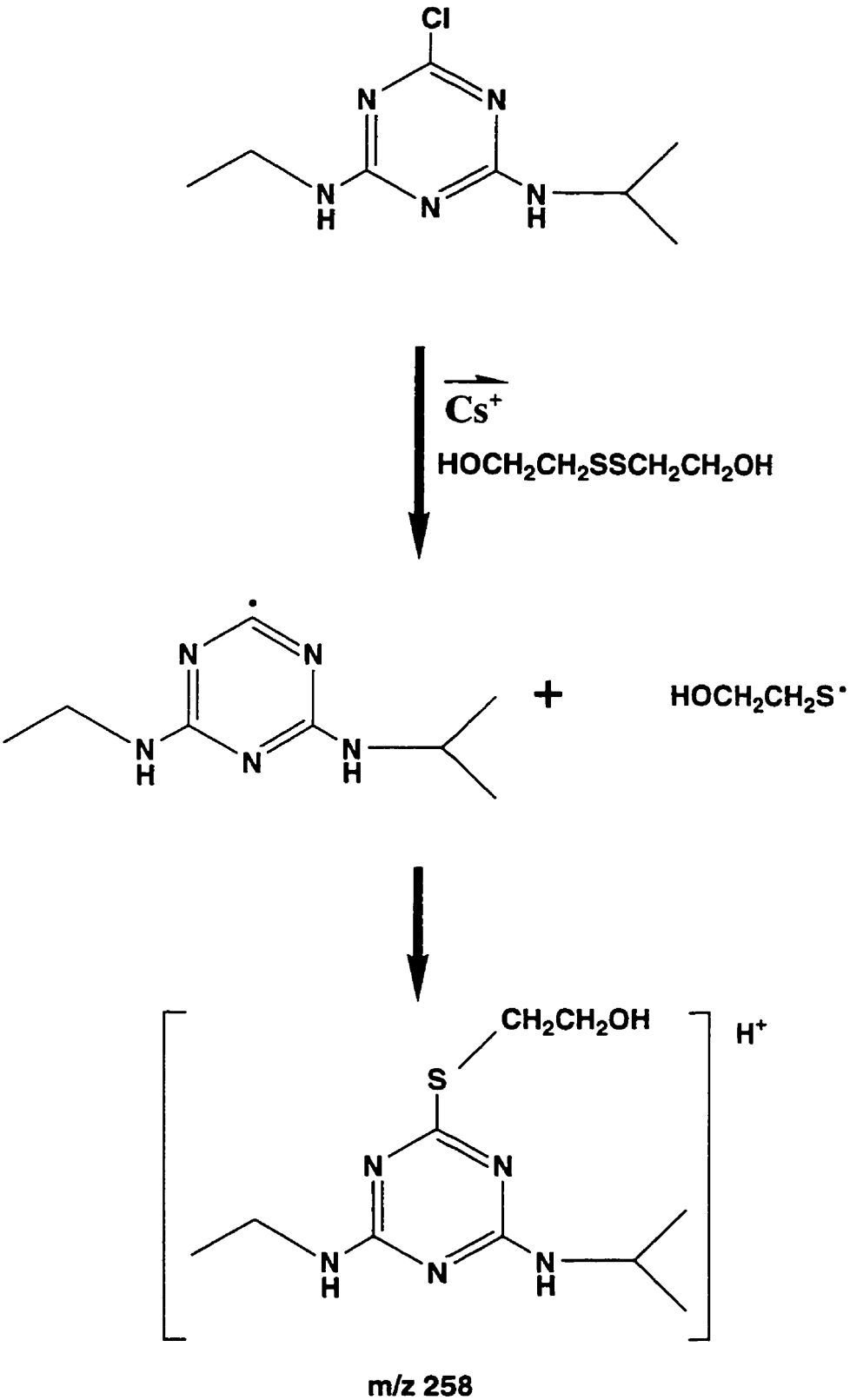

Figure 17. Scheme describing the possible source of m/z 258 in the LSIMS spectrum of atrazine in HEDS.

5.2 Effect of Analyte Electron Affinity on Dehalogenation.

5.2.1-Introduction

In order to further our understanding of the beam-induced dehalogenation of haloaromatics, we have studied the effect of analyte electron affinity on the extent of dehalogenation observed in the LSIMS spectra. This line of investigation is important in light of the oft-repeated suggestion[108,31] that FAB/LSIMS beam-induced reductions involve the availability of low-lying unoccupied molecular orbitals which can capture electrons produced by the interaction of the beam with the sample and initiate further reactions such as dehalogenation. The analyte electron affinity is a measure of the availability of such low-lying unoccupied orbitals as defined by the lowest unoccupied molecular orbital (LUMO).

This is also the opportunity to verify the observation of Kelley et al.[31], published in the course of this work. These authors investigated the effect of electron affinity on the beam-induced dehalogenation of halonucleosides in FABMS. Their observations indicate that the extent of dehalogenation decreased with increasing analyte electron affinity. However, several limitations are apparent in the aforementioned study. First, the range of electron affinities used in the study is only 0.27 eV (7kcal). It is important to note that in experimental electron affinity determinations, the error in measurement is normally $\pm$ 0.2eV. This implies that the analyte electron affinity range in the Kelley study is practically within experimental error. On such a small electron affinity range, it is

difficult to gauge with certainty the effect of that parameter on beam-induced dehalogenation.

Second, the respective order of electron affinities calculated for the halonucleosides did not correspond to that determined for the respective bases using one electron reduction potentials[161]. The respective order of the electron affinities of the bases from Wentworth[161] and Kelley[31] are presented below in Table VII. That the mere presence of a halogen on the bases should change the electron affinity order of these compounds appears unlikely. The electron affinities of the halonucleosides were calculated using semi-empirical methods since no experimental values were available.

Table VII. Comparison of the electron affinities obtained for bromo-nucleosides using semi-empirical calculations (MOPAC)[31] and nucleoside bases using reduction potentials[161].

Calculated electron affinities for halo-nucleosides using MOPAC	Electron affinities for bases derived from reduction potentials
6-Br-purine (0.4eV)	Guanine (1.6eV)
5-Br-cytidine (0.18eV)	Purine (1.0eV)
8-Br-adenosine (0.2eV)	Adenine (0.96eV)
8-Br-guanosine (0.2eV)	Cytosine (0.7eV).

The comparison between the electron affinities of nucleosides and bases is valid since the bases are the only electrophoric component of the nucleosides.

Third, the mass spectral evidence presented to validate the calculated electron affinities is highly susceptible to other interpretations. In this case, the negative ion FAB spectrum of two halonucleosides were compared in terms of their $M^{-\cdot}/(M-H)^-$ ratio. The argument presented by the authors being that the more electrophoric compound would exhibit a higher $M^{-\cdot}/(M-H)^-$ ratio. The respective $M^{-\cdot}/(M-H)^-$ ratios were found to correspond to the calculated electron affinities. However, this conclusion is quite possibly erroneous as the compound exhibiting the lower $M^{-\cdot}/(M-H)^-$ ratio possesses 5 functional groups containing acidic hydrogens (and thus capable of yielding abundant $(M-H)^-$) ions whereas the other halonucleoside has only one such group. Hence, these observations could simply be attributed to the greater tendency of compound **B** to yield $(M-H)^-$ on the basis of a higher number of acidic hydrogens rather than a relative measure of the respective electron affinities.

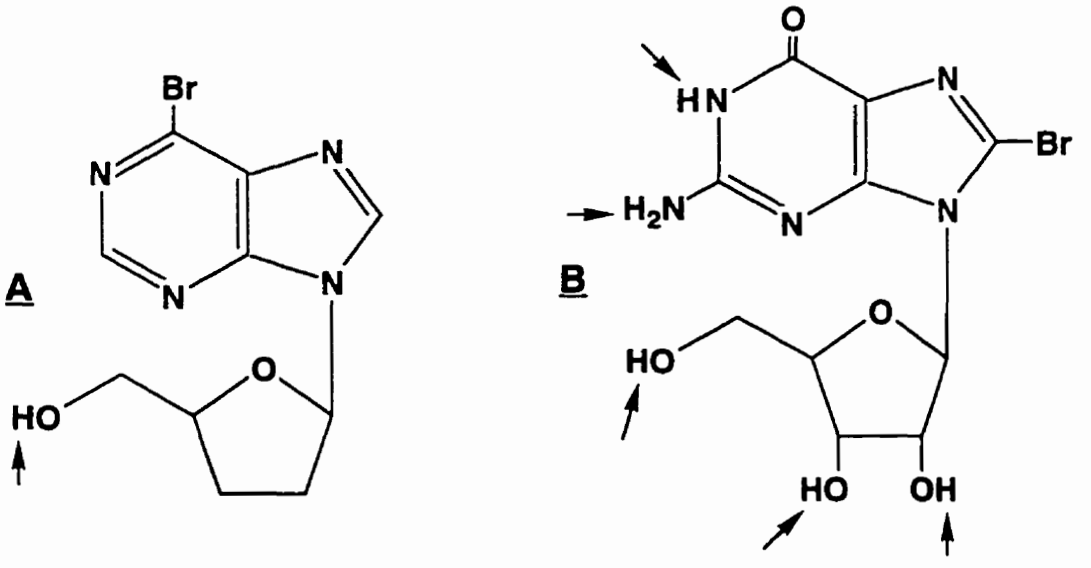

Figure 18. Halonucleosides used in the study[31] of beam-induced dehalogenation by Kelley and Musser. The arrows indicate the acidic hydrogens in each molecule.

On the basis of the aforementioned drawbacks, it was thought that the effect of analyte electron affinity on the extent of beam-induced dehalogenation remained to be more convincingly demonstrated. For this purpose, the compound selection is crucial. Bearing this in mind, simple substituted halobenzenes were used. The use of simple compounds ensures that the order of electron affinities can be intuitively established as well as easily rationalized using empirical considerations stemming from the effect of substituents on the electron affinity of simple halobenzenes.

The existence and direction of such an analyte electron affinity effect may allow for some mechanistic inferences to be made in order to implicate beam-generated electrons as initiating agents in the dehalogenation process. In turn, such mechanistic inferences may be substantiated using results obtained with pulse radiolysis[37-8] and electrochemical[39-40] techniques where the compounds studied are similar and electrons are the initiating reagents in the dehalogenation process.

5.2.2-Calculation of Electron Affinities Using a Semi-empirical Method.

The estimation of electron affinities from semi-empirical calculations rest on the assumption that electron affinities are directly related to the energy of the lowest unoccupied molecualr orbitals (LUMO). This is entirely reasonable since one would expect the anion radical to be formed by capture of an electron by the unoccupied molecular orbital of

lowest energy. The lower the LUMO energy of the molecule, the higher its electron affinity.

The semi-empirical method MNDO allows the calculation of the LUMO energy for a particular molecule. In order to obtain electron affinities from calculated LUMO energies, a calibration graph must be drawn up relating the LUMO energies of a series of 'standard' compounds whose electron affinities have been experimentally determined. The resulting calibration graph allows one to obtain the electron affinity of a molecule from its calculated LUMO energy. This method has already been used by Kelley et al[31] to determine the electron affinity of halonucleosides. A similar type of calculation has been performed for the bromoaromatic compounds used in this study to investigate the effect of electron affinity on the dehalogenation process.

The electron affinity of a molecule can also be estimated from its reduction potential[149]. In order to validate the electron affinities obtained from the MOPAC calculations, the values obtained were compared to those approximated from reduction potential values. It is therefore essential to define the relationship between electron affinities and reduction potentials.

5.2.3-Reduction potentials vs electron affinities

The properties defining the electron accepting capability of organic molecules in the gas and condensed phase are the electron affinity and the reduction potential. The relationship between electron affinities

and half-wave reduction potentials has long been recognized[149, 162-165] and is defined by equation 16.

$$E_{1/2} = -\Delta G^{o}_{gas}(A) - [\Delta G^{o}_{sol}(A^{-}) - \Delta G^{o}_{sol}(A)] + C \qquad [16]$$

Where $\Delta G^{o}_{gas}(A)$ is the gas phase free energy of electron attachment of species A. The free energy of electron attachment differs from electron affinities by approximately 1 kcal $mole^{-1}$. The entropy term is small and hence can be neglected. The terms $\Delta G^{o}_{sol}(A^{-})$ and $\Delta G^{o}_{sol}(A)$ represent the solution free energies of transfer of gas phase A and A^{-} to solution, respectively. The constant C depends on the nature of the reference electrode. The difference in free energies of solution is defined as follows.

$$\Delta\Delta G^{o}_{sol} = \Delta G^{o}_{sol}(A^{-}) - \Delta G^{o}_{sol}(A) \qquad [17]$$

The free energy of transfer of gaseous A to solution is small, therefore the term $\Delta\Delta G^{o}_{sol}$ is dominated by the free energy of solution of the anion, $\Delta G^{o}_{sol}(A^{-})$. Rewriting equation 18, we obtain the following expression.

$$E_{1/2} = E.A. - \Delta\Delta G^{o}_{sol} + C \qquad [18]$$

If the $\Delta\Delta G^{o}_{sol}$ is assumed to be constant for a particular series of compounds over a given electron affinity range, then plots of reduction potentials versus electron affinities will be linear with unity slope. In practice, such plots yield approximately linear relationships with

less than unity slope. This effect is due to the assumption that the $\Delta\Delta G^{\circ}_{sol}$ term is constant. The less than unity slope means that the $\Delta\Delta G^{\circ}_{sol}$ decreases with increasing electron affinity. This interpretation is easily rationalized considering that increased electron affinity is achieved by substitution with electron withdrawing groups. The result is greater charge delocalization in the anion. The increased charge delocalization leads to weaker solvation of the anion. The slope has been shown to be solvent dependent[166].

Wentworth et al[149]. have assumed that the difference in free energies of solvation $(\Delta\Delta G^{\circ}_{sol})$ is constant for a group of molecules so that equation **18** becomes

$$E_{1/2} = E.A. - C \qquad [19]$$

By adjusting the value of the constant to obtain agreement with known gas phase electron affinities, a large number of electron affinity values were predicted from reduction potentials obtained in non aqueous organic solvents such as dimethyl formamide and acetonitrile[149]. The constant C is directly related to the solvation energy difference betweeen the neutral molecule and the radical anion. The value of C is therefore related to the degree of delocalization of the negative charge in the radical anion. For example, the constant is 2.65 for aromatic hydrocarbons and other compounds where the degree of solvation is low. Where the degree of solvation is high (localized charge), such as with mononitrobenzenes, the constant is 2.19.

The ability to estimate electron affinities from reduction potentials is extremely useful since reduction potentials are more readily available. Furthermore, there are cases where empirical determinations of gas phase electron affinities can be troublesome for organic molecules having the following characteristics: (1) polar, thermally labile, involatile, and (2) possessing functional groups having labile hydrogens i.e. acidic hydrogens.

The above limitations are severe and explain the dearth of electron affinities as well as the need for alternate means of electron affinity determination. Indeed, it could be argued that the 2 provisos mentioned above aptly describe the properties of compounds amenable to FAB/LSIMS analysis. In other words, compounds having structural features favourable for FAB/LSIMS analysis are basically incompatible with direct experimental determination of electron affinities. The approximative determination of electron affinities from reduction potentials also serves a more concrete purpose, namely, a verification of the electron affinities calculated by semi-empirical methods.

5.2.4-Comparison of Electron Affinities Determined from Reduction Potentials and Semi-empirical Caculations

The electron affinities for the bromoaromatic compounds **1-5** (Figure 19) are not readily available. However, these may be expected to correlate with LUMO values, which can be readily calculated using the MOPAC program (version 6.0). To quantatively assess the correlation, LUMOs were calculated for the three compounds of known electron affinity listed in Table VIII below.

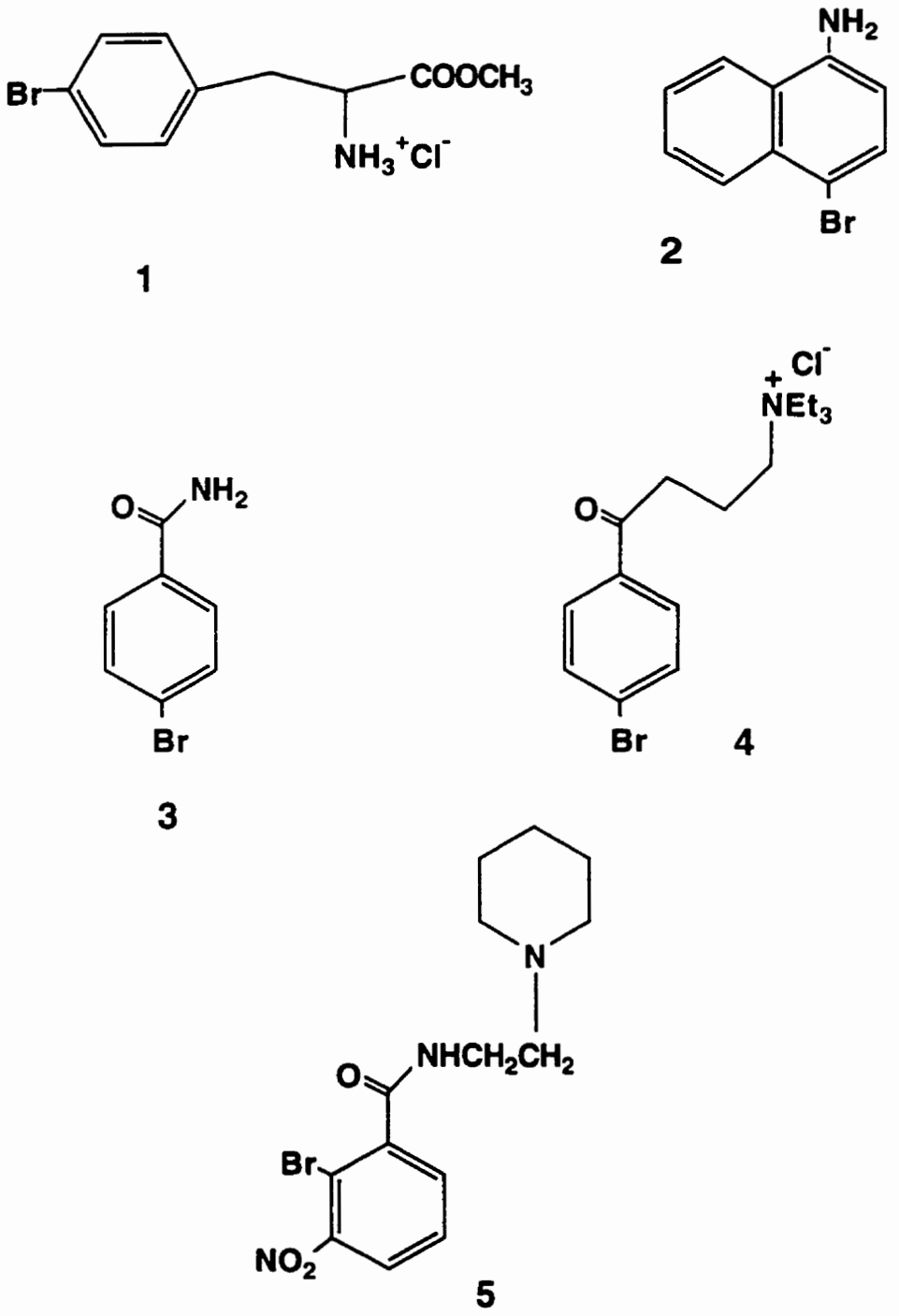

Figure 19. Structure of the bromoaromatic compounds used for the study of the effect of analyte electron affinity on dehalogenation.

Table VIII. Electron affinities[149] and calculated LUMO values (estimated using MOPAC) used for the elaboration of the calibration graph.

Compound	Electron Affinity (eV)	LUMO (eV)
1-Cl-naphthalene	0.28	-0.67
1-Cl-anthracene	0.75	-1.07
4-Br-nitrobenzene	1.30	-1.54

The linear regression of these electron affinity and LUMO values gives rise to equation **20**, which was used to estimate the electron affinities of the compounds of Figure 19.

$$E.A._X = -1.148(LUMO)_X - 0.478 \qquad [20]$$

The resulting trend in electron affinity values (Table IX) is consistent with known values of similar compounds. It should be stressed that the calculated electron affinity values obtained are used only to generate a *relative* order of electron affinities for compounds **1-5** and are not meant to reflect absolute values.

Table IX. Electron affinities obtained from equation **20** using the calculated LUMO values from MOPAC calculations.

Compound	LUMO (eV)	Electron Affinity (eV)
1	-0.198	-0.25
2	-0.329	0.10
3	-0.566	0.17
4	-0.852	0.50
5	-1.299	1.01

In order to verify the verisimilitude of the calculated electron affinities obtained from estimations of the lowest unoccupied molecualr orbital (LUMO) through MOPAC, the electron affinities of compounds **1-5** were approximately defined from empirical data. This can be done from reduction potentials and by using known gas phase electron affinity values in combination with substituent effects provided by Wentworth[149].

In the case of 4-bromo-phenylalanine methyl ester, compound **1**, it can be assumed that the electron affinity will be very similar to that of 4-bromotoluene since the the amino and carboxy functional groups are too remote from the aromatic ring to affect its electron accepting capability. The reduction potential of 4-bromotoluene is -2.67V[167]. Using the method outlined previously, the electron affinity can be estimated with equation **19**.

$$E_{1/2} = E.A. - C \qquad [19]$$

Since the constant is directly related to the solvation energy difference between the neutral molecule and the anion, the effect of the structure of the molecule on the charge delocalization in the anion must be taken into account. It has been proposed that 3 'averaged' constants could be used. Each constant is applicable to a broad family of organic compounds, each characterized by the extent of negative charge delocalization in the anion; small (2.19), average (2.42) and large (2.65). The anions formed by aromatic hydrocarbons upon electron capture are classified as having a large extent of charge

delocalization. Hence, the electron affinty of 4-bromo-phenylalanine estimated from the reduction potential of 4-bromotoluene is approximately -2.67 + 2.65 = -0.03eV.

For 1-amino-4-bromonaphthalene, compound **2**, a reduction potential value is not available. However, we can combine the electron affinity value obtained from the reduction potential of 1-bromonaphthalene and the substituent effect of the amino group. The electron affinity of bromonaphtalene can be estimated from its reduction potential as in the previous example giving, -2.19 + 2.65 = 0.47eV. The effect of alkyl, methoxy and amino groups on the electron affinity consistently cause a decrease of 0.1 to 0.2 eV[149]. For the present purpose, the effects of these electron donating substituents on the electron affinity will be arbitrarily set at -0.2eV. By adding this number to our estimate of the electron affinity of bromonaphthalene, a value of 0.37eV was obtained for the electron affinity of 1-amino-4-bromonaphthalene. This value does not appear to be unreasonable considering that the gas phase electron affinity of chloronaphthalene is 0.28eV[149].

Where 4-bromobenzamide, **3**, is concerned, the electron affinity can be estimated directly from its reduction potential[167] although the constant in equation **19** must be adjusted to take into account intermediate charge delocalization in the anion. Therefore, the electron affinity of 4-brombenzamide is -2.08 + 2.45 = 0.37eV. This result is in good agreement with the electron affinity values obtained through the semi-empirical method since the values for 4-brombenzamide

and 1-amino-4-bromonaphthalene are close in both methods used to evaluate the electron affinity.

For compound **4**, it is assumed that its electron affinity should correspond to that of 4-bromoacetophenone since it is reasonable to assume that the role of the propyltriethylammonium group will be negligible in the terms of the electron accepting capacity of the molecule. The electron affinity of 4-bromoacetophenone can be obtained in a manner similar to that of 4-bromobenzamide to give -1.84 + 2.45 = 0.62eV. The task of assigning an electron affinity value to compound **5** was not feasible given the absence of reduction potential data as well as the uncertainty pertaining to the substituent effect of a secondary amide group. All that can be said with any degree of certainty is that the electron affinity of compound **5** should be higher than that of ortho-bromonitrobenzene (1.3eV)[162].

In comparing the respective electron affinities obtained indirectly from empirical data and those obtained from semi-empirical calculations (Table X), it should be remembered that the main concern is the coherence of the trends obtained from the respective methods. In that regard, the two methods show good agreement. The fact that a sizable difference exist between the two methods is not a surprise considering the notoriously poor reputation of semi empirical methods in evaluating absolute electron affinities. However, if one compares the *differences* in electron affinity between each compound within their specific scales, the agreement is quite good. For example, the difference between compounds **1** and **2** in both methods is about 0.35 eV. The

values of compounds **2** and **3** are close in the two scales. The only significant drawback of the semi-empirical values is that they are not representative of the 'absolute' electron accepting capacity of the molecules.

Table X. The electron affinities of the bromoaromatic compounds **1-5** as obtained using semi-empirical calculation (MOPAC) and reduction potentials.

Compound	Electron Affinities (eV) (MOPAC)	Electron Affinities (eV) (Reduction Potentials)
1	-0.25	-0.02
2	0.1	0.36
3	0.17	0.37
4	0.5	0.61
5	1.0	>1.2

However, the determination of electron affinity values through semi-empirical calculations of LUMO energy is the only way tc obtain 'specific' numbers. For chloroaromatic compounds (Figure 20), electron affinities can be estimated through the use of reduction potentials and/or empirically defined substituent effects in the same manner as that shown above for bromoaromatic compounds. In any event, some of the chloroaromatic compounds used in the electron affinity effect study are analogs of the bromoaromatic compounds.The electron affinity of 4-chloro-phenylalanine methyl ester can be estimated from the reduction potential of 4-chloro-toluene[167] using equation **19** giving 2.65 - 2.765V = -0.12eV. For 4-chloro-benzamide[167], the reduction potential

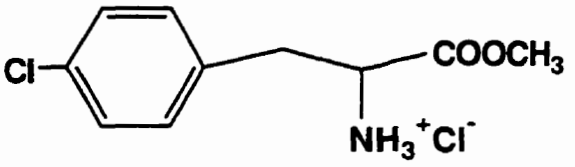

4-Cl-phenylalanine methyl ester

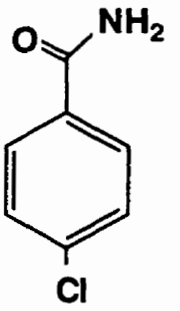

4-Cl-benzamide

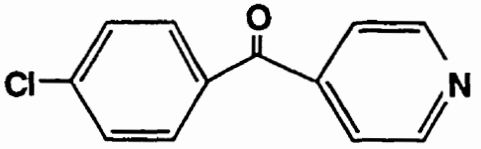

4-(4-Cl-benzoyl)pyridine

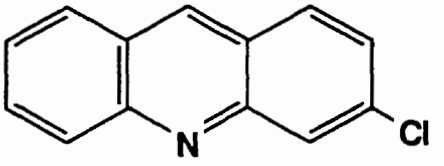

3-Cl-acridine

Figure 20. Structure of the chloroaromatic compounds used in the study of the electron affinity effect on dehalogenation.

is known and the electron affinity is calculated in the same manner as for 4-bromo-benzamide to give 2.45 + (-2.13V) = 0.33eV.

There is no experimental value for the electron affinity of 4-(4-chlorobenzoyl)pyridine. This compound is a structural analog of 4-chloro-benzophenone and its electron affinity could be similar (0.80eV). However, Dillow et al[168]. have shown that incorporation of a nitrogen atom into an aromatic system causes an electron affinity increase of 0.3-0.4 eV relative to the aromatic hydrocarbon analog. Since we do not have a reduction potential value for 4-(4-chlorobenzoyl)pyridine, the electron affinity of the compound must be evaluated in a more indirect fashion. The reduction potential of 4-benzoylpyridine is -1.51V. Its electron affinity can be estimated by assuming that the negative charge delocalization in 4-benzoylpyridine is similar to that of benzophenone, allowing the adjustement of the constant in equation **19** to give the expression 2.45 + (-1.51V) = 0.95eV. The effect of chloro substitution can be estimated by comparing the difference in the gas phase electron affinities of benzophenone (0.65eV) and 4-chloro-benzophenone (0.80eV). This comparison suggests that chloro substitution increases the electron affinity of benzophenone by 0.16 eV. It is reasonable to expect that the effect of chloro substitution will be approximately the same in 4-benzoylpyridine. Hence, the electron affinity of 4-(4-chlorobenzoyl)pyridine can be approximated to that of 4-benzoylpyridine plus the effect of chloro substitution giving the value 0.94 + 0.16 = 1.10eV.

For 3-chloro-acridine, no reduction potential value was found in the literature. The gas phase electron affinity of acridine is 0.89 eV[168]. If, as in the preceding case, the effect of chloro substitution is estimated from the non-aza analog, then the gas phase electron affinity data pertaining to anthracene (0.57eV) and 2-chloro-anthracene (0.75 eV) can be used to this effect. Thus, the effect of chloro substitution (+0.19eV) and the gas phase electron affinity of acridine combine to give the electron affinity value of 3-chloro-acridine as 1.08 eV. It should be stressed that the above electron affinity value rests on the assumption that the effect of chloro substitution on the electron affinities of aza and non-aza analogs are similar. The approximated electron affinities for the chloroaromatic compounds are shown in Table XI below

Table XI. Electron affinities of chloroaromatics otained from their respective reduction potentials using Wentworth's method[149].

Compound	Electron Affinity(eV)*
4-Cl-phenylalanine methyl ester	-0.11(18)
4-chlorobenzamide	0.32(3)
4-(4-chlorobenzoyl)pyridine	1.1(0)
3-chloroacridine	1.08(0)

* Estimated from reduction potentials using the method of Wentworth and Substituent effects.

The rough way in which the electron affinities of the compounds can be estimated using their respective reduction potentials is obviously subject to criticism given the lack of accuracy of the method. However, in the present context where a mere trend of electron affinities is desired, the use of reduction potentials is justified.

Furthermore, the trends obtained are substantiated by comparisons with analogous compounds and knowledge of the extent of substituent effects on the electron affinity of aromatic compounds.

There can be no doubt that electron affinities of organic compounds estimated in this way are not a definitive measure of the *absolute* electron affinity. However, one cannot stress the point sufficiently that what is desired here consist of well defined trends in order to identify the direction of the electron affinity effect on the dehalogenation process.

5.2.5-Positive Ion Mode Results

The results obtained in the positive ion mode for the dehalogenation of the bromoaromatic compounds **1-5** are shown in Table XII below. The compounds are listed in order of increasing electron affinity. The relationship is graphically illustrated in Figure 21.

Table XII. Calculated electron affinities and % dehalogenation in glycerol of the bromoaromatic compounds **1-5**.

Compound	Electron affinity (eV)	% Dehalogenation
1	-0.25	28
2	0.10	24
3	0.17	22
4	0.50	13
5	1.01	0

As can be seen in Figure 21, the extent of dehalogenation can be seen to decrease with increasing analyte electron affinity. This inverse

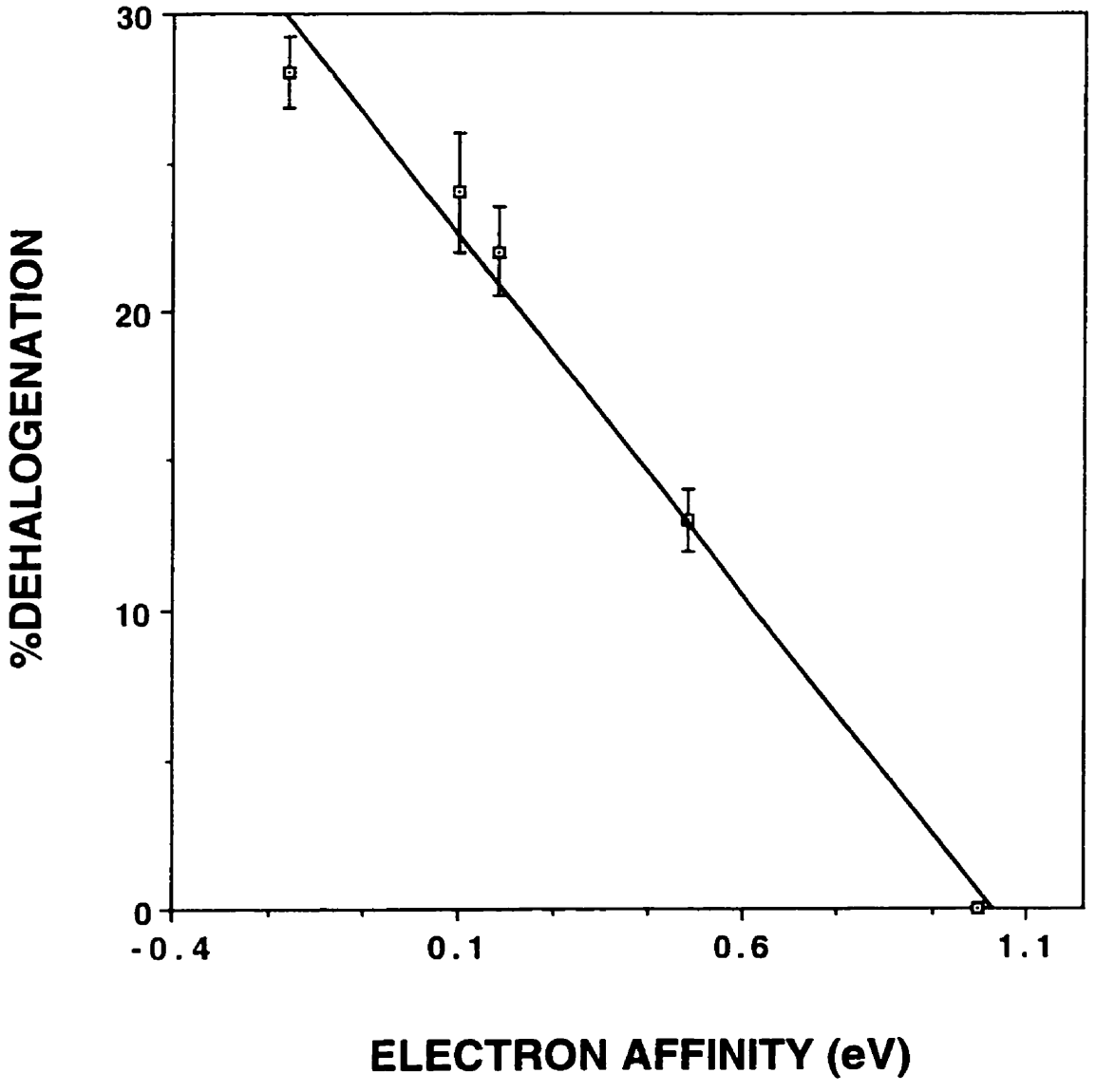

Figure 21. The effect of analyte electron affinity on the % dehalogenation of the bromoaromatic compounds 1-5.

relationship between haloaromatic electron affinity and the observed extent of dehalogenation in the glycerol LSIMS mass spectrum can be a useful guide in attempting to establish the likelihood of an electron initiated beam-induced dehalogenation mechanism. It has been proposed that radicals, electrons, ions, and excited species are produced in the matrix under FAB/LSIMS conditions. Of these species, radicals[8] and/or electrons[110] are thought to be involved in reduction processes. Sethi and co-workers[30] invoke the resemblance of beam-induced dehalogenation with that of radiolysis studies where reactions are initiated by the solvated electron. The similarity of FAB/LSIMS beam-induced processes with radiation chemistry has been reiterated in a recent review[169]. Williams et al[110] have suggested a mechanism to account for the occurrence of dehalogenation in the FAB/LSIMS spectra of organic compounds. The premise of this proposed mechanism is that keV particle impacts cause the production of electrons (via ionization of the sample or matrix) and that these electrons can be effective reducing agents once they have reached thermal energies. Subsequent capture of these beam-generated electrons by the analyte ultimately causes reductive dehalogenation (Scheme 3). In the first instance, the secondary electron is captured by Ar-X, a haloaromatic species, to form the radical anion (reaction **21**). This radical anion can decompose to expel the free halide (reaction **22**). The resulting aromatic radical, $Ar^{\cdot}$, then abstracts a hydrogen from a solvent molecule to yield the dehalogenated aromatic species, ArH (reaction **23**). This mechanism of reductive dehalogenation is in fact typical of the electrochemical[39-40] and pulse radiolysis[37-38] literature.

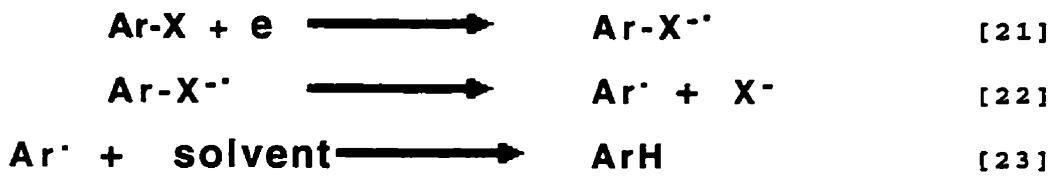

Scheme 3

On the basis of this mechanism, the inverse relationship of diminished dehalogenation with increasing analyte electron affinity appears to contradict the *a priori* notion that a molecule's propensity to dehalogenate should be commensurate with its ability to capture electrons. However, investigations carried out in pulse radiolysis[37] and electrochemistry[39-40] substantiate the trend observed in Figure 3. Using pulse radiolysis, Neta and Behar[37] have studied the behavior of a series of substituted haloaromatics reduced by the solvated electron in irradiated aqueous solution. The resulting anion radicals were found to undergo intramolecular electron transfer and subsequent dehalogenation to yield halide ions as in Scheme 3. For a series of substituted halobenzenes with a given halogen, rates of dehalogenation were found to decrease as the electron affinity of the molecule increased. Similarly, extensive electrochemical investigations of reductive dehalogenation have upheld the validity of this relationship[39-40]. In this case, a rough linear correlation between the cleavage rate of the anion radical and the standard potential of the $ArX/ArX^{-\cdot}$ couple was observed i.e. the more difficult ArX is to reduce, the faster the cleavage of the anion radical.

Thus, there appears to be an activation versus driving force relationship in the sense that the activation energy of the cleavage of the anion radical (reaction 4) seems to be related to the driving force of the electron transfer leading to the formation of the anion radical (reaction 3). The anion radical cleavage (reaction **22**) can be viewed as an intramolecular dissociative electron transfer[40,170-171].

Originally, electron capture occurs through the π^* (LUMO) orbital. For dissociation to occur, the unpaired electron must be transferred from the π^* (LUMO) orbital to the σ^* orbital of the C-X bond. Although this transition is forbidden, it can occur through vibronic coupling. The likelihood of this intramolecular electron transfer depends on the energy gap between the two orbitals. The energy of the σ^* orbital is not expected to be greatly affected by the nature of the aromatic moiety, whereas the π^* MO is very much dependent on the nature of the aromatic moiety. Calculations have shown that even for compounds of negative electron affinities, such as bromotoluenes, the σ^* orbital is always at higher energy than the π^* LUMO[167]. In a series of aromatic compounds with the same halogen, the difference in energy between the σ^* and the π^* LUMO should increase concomitantly with an increase in electron affinity (lowering of LUMO energy). Hence, the greater the electron affinity, the greater the energy gap between the LUMO and the σ^* orbital of the C-X bond, all of which results in a diminished propensity for the dissociative intramolecular electron transfer necessary for dehalogenation to occur. This holds for compounds capable of forming radical anions. However, given the negative electron affinity of compound **1**, dehalogenation in this case

is more likely to proceed through dissociative electron capture (reaction **24**).

[24]

Interestingly, the trend illustrated in Figure 21 is in agreement with an electrochemical scale determining haloarene radical anion stability. It should be pointed out that reduction potentials generally follow the same trend as electron affinities [149,162-165]. It has been suggested that the reduction potential limit above which the haloarene radical anions can be considered stable is defined for the respective halogens[172]. In the case of bromoaromatics, the reduction potential should be more positive than some value between -1.2 and -1.6V for the radical anions to be stable with respect to dehalogenation. The dehalogenation tendency of bromo aromatics should tend towards zero as the reduction potential of the compounds becomes more positive. For example, 4-bromoacetophenone and 4-bromonitrobenzene have reduction potentials of -1.8 and -1.0V, respecively[173]. Thus, the reduction potential of the bromonitroaromatic compound **5** should easily fall below the range of values (-1.2 to -1.6V) where the radical anion will be considered stable. In accord with this reasoning, no dehalogenation is detected in the glycerol LSIMS spectrum of compound **5**. In a pulse radiolysis study of the reactions of aryl bromides with the solvated electron, Von Sonntag and co-worker[174] did not observe a significant bromide ion yield upon irradiation of an aqueous solution of 4-bromonitrobenzene. The authors concluded that the radical anion of 4-bromonitrobenzene formed upon electron capture was stable with respect

to carbon-bromide bond scission. The reduction potential of **4** should be similar to that of 4-bromoacetophenone (-1.81V)[173]. Hence, on the basis of the reduction potential we would expect the radical anion of **4** to be deemed unstable and dehalogenation to occur. This is indeed what we observed. Of course, the criterion of anion radical stability is somewhat arbitrary but the rough agreement with our results is nonetheless interesting.

For chloroaromatics, the radical anions generated electrochemically will be stable if the reduction potential is more positive than -1.6V[172]. The reduction potential of 4-benzoylpyridine is -1.51V[175]. Hence, the reduction potential of 4-Cl-(4-benzoyl)pyridine should be even more positive. Thus, the radical anion formed by compound **6** is deemed to be stable according to the electrochemical scale determining haloarene radical anion stability since its reduction potential should be more positive than -1.6V . The same logic applies to 3-Cl-acridine as the reduction potential of acridine is -1.6V[168]. The reduction potential of 4-Cl-benzamide is -2.13V[167] and thus dehalogenation is observed in this case.

5.2.6-Negative ion studies

In order to ensure an element of thoroughness in our investigation, the negative ion LSIMS mass spectra of the haloaromatic compounds were obtained. A particular aspect of interest in the negative ion spectra consisted in establishing the existence of the radical anion of the haloaromatic compounds for mechanistic purposes. The observation of

the radical anion in the mass spectrum would lend weight to the proposed beam-induced dehalogenation mechanism in a twofold manner. First, the existence of the radical anion is postulated in the dehalogenation mechanism as a crucial, if short-lived, intermediate. Second, the formation of radical anions can only occur through electron capture and their observation in the LSIMS mass spectra would support the contention that electrons are produced under FAB/LSIMS conditions. Further, negative ion data has seldom been reported in the study of beam-induced processes.

We have obtained the negative ion data for compounds **2**, **3**, **5**, and **6**. The cationic compounds **1** and **4** do not give any useful signal in the negative ion mode since the counterions and their glycerol adducts dominate the mass spectrum. The spectrum obtained from **2** was too weak to be useful. The % dehalogenation for **3** was 7% in the negative ion mode compared to 22% in the positive ion mode. As stated earlier, compound **5** does not undergo dehalogenation. The negative ion data for **3** underline what is pointed out in the literature[30-31] where the negative ion mode was used to monitor the dehalogenation process, namely, that the extent of dehalogenation observed in the negative ion spectra is considerably lower (when not completely absent) than in the positive mode. Radical anions were observed for high electron affinity compounds such as **5** and **6**.

The negative LSIMS spectrum of 4-(4-chlorobenzoyl)pyridine in glycerol is shown in Figure 22. The molecular radical anion appears at m/z 217. At first glance, it would appear that determining the extent of

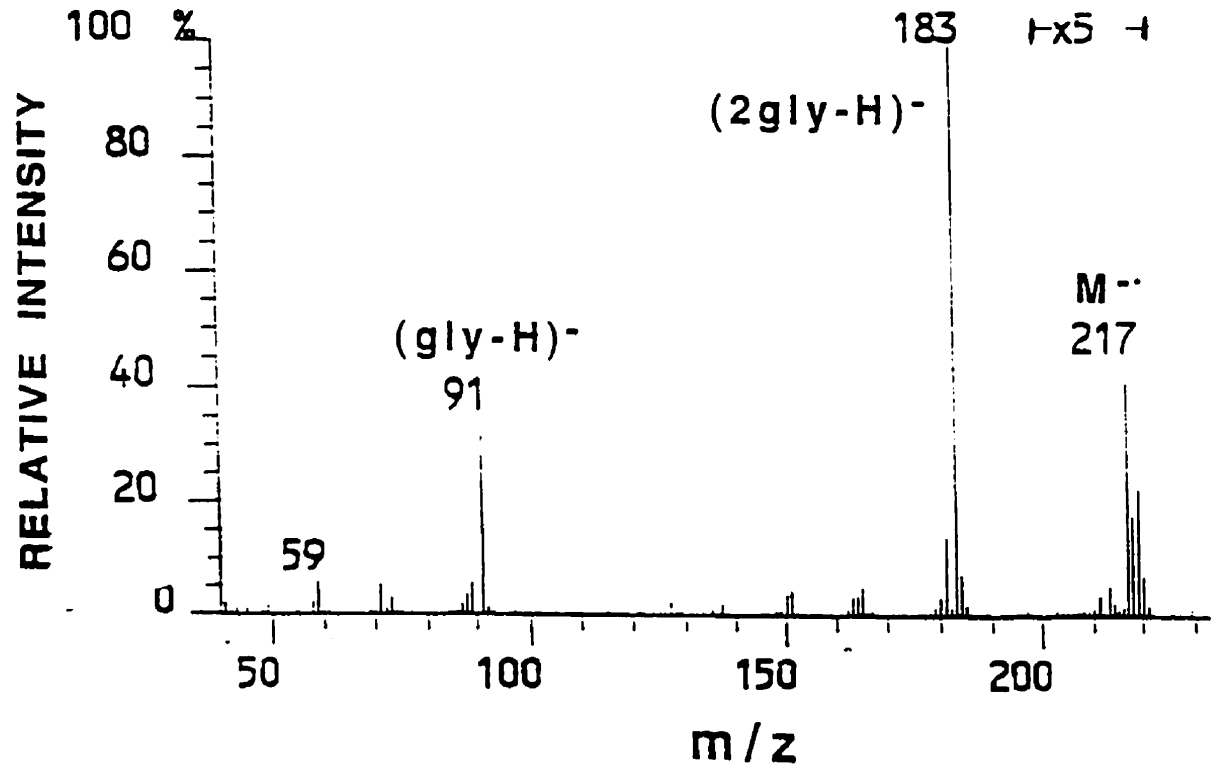

Figure 22. Negative ion LSIMS spectrum of 4-(4-Cl-benzoyl)pyridine (**6**) in glycerol(V95J1156FAz00).

dehalogenation from the spectrum would be problematic since the dehalogenated ion originating from 4-(4-chlorobenzoyl)pyridine is isobaric with the glycerol dimer, $(gly_2\text{-}H)^-$, at m/z 183. This is not the case since the Cl^- ion is conspicuously absent from the mass spectrum either as the 'naked' Cl^- ion (m/z 35) or as its glycerol adduct (m/z 127). Given the high sensitivity of inorganic anions in the negative LSIMS spectrum, the absence of any significant halide ion abundance in the mass spectrum can reasonably be assumed to be a reliable indicator of the lack of dehalogenation of the analyte investigated.

The usefulness of the negative ion mode to monitor the dehalogenation process is limited. This is due to the fact that the extent of dehalogenation is much lower in the negative ion mode and rapidly attains vanishingly small values even for compounds of moderate electron affinity. This phenomenon greatly reduces the range of compounds which can be studied for mechanistic purposes. For example, it is reported that dehalogenation is greatly diminished in the negative FAB spectrum of 5-bromouridine compared to the dehalogenation observed in the positive FAB spectrum (28% vs 9%)[30]. A similar trend was observed in a later report where the same compound was used under different primary beam energies (6 vs 8 keV)[31].

It is proposed that the diminished extent of dehalogenation observed in the negative ion mode with respect to the positive ion mode actually offers added evidence in favour of our reductive dehalogenation mechanism. The explanation for the diminished extent

of dehalogenation observed in the negative ion mode compared with the positive ion mode probably lies in the rapid extraction of all the negatively charged material including anion radicals and electrons. It is thus reasonable to suppose that electrons will be unavailable to trigger dehalogenation. In the positive mode, the beam-generated electrons are retained and may actually be forced to diffuse into the bulk of the solution under the influence of the positive voltage applied to the direct insertion probe. If the reaction was actually radical based, it would be reasonable to asssume that such neutral species should remain unaffected by the polarity of the ion extraction apparatus of the source. Hence, although the negative ion mode is not very useful in monitoring the effect of analyte electron affinity on the dehalogenation process, our negative ion data in conjunction with previous results[30-31] add weight to an electron based dehalogenation mechanism.

5.2.7 Radiation chemistry results implicating electrons as the initiating agents of dehalogenation.

As stated earlier, although the energy regimes of most radiation chemistry techniques and FAB/LSIMS are different (MeV vs. keV), a similarity lies in the way an energetic particle generates a track in the medium it penetrates, along which energy is deposited and radicals, ions, and electrons are formed. In radiolytic experiments, thermal electrons and hydrogen atoms are the main reducing agents generated by an energetic particle in an aqueous alcohol solution[176]. Electrons[108,110] and hydrogen atoms[8,17] are also thought to be involved in FAB/LSIMS reduction processes.

Where the contribution of hydrogen atoms to the dehalogenation process is concerned, pulse radiolysis experiments suggested that chloro- and bromobenzene do not react with hydrogen atoms to yield the free halide in aqueous solution[177]. Conversely, a pulse radiolysis study on the same compounds showed that electrons reacted with the above compounds to produce the free halide through reductive dehalogenation[178]. The results of a γ-radiolysis study of octachlorobiphenyl in pure isopropanol indicated that the solvated electron was the primary species responsible for dechlorination. By a judicious choice of experimental conditions and scavenger types, the authors established that the hydrogen atom was not significantly involved in the dehalogenation process[179]. Since the latter has been shown not to react with simple haloaromatics such as halobenzenes, this supports the contention that the role of secondary electrons in beam-induced reductive dehalogenation might be dominant[36].

The pulse radiolysis experiments ruling out the implication of hydrogen atoms in the dehalogenation process are supported by sonochemical results obtained with halophenols in aqueous solution[180]. When water is subjected to sonolysis (ultrasound), the hydrogen atom and hydroxyl radical are generated. The process has been shown not to produce electrons[181]. When aqueous solutions of halophenols were submitted to sonolysis, no reductive dehalogenation was observed[180].

5.3 On the formation of ketyl radicals

In the study of the effect of analyte electron affinity on the beam-induced dehalogenation process, a very interesting example of beam-induced reduction was unearthed which prompted a tangential investigation. In fact, the study further strengthened the concepts presented to rationalize the beam-induced dehalogenation process. Despite the absence of dehalogenation in the glycerol LSIMS mass spectrum of 4-(4-chlorobenzoyl)pyridine, evidence of beam-induced reduction is apparent upon inspection of the molecular ion region of the spectrum as shown in Figure 23. This reduction, in the form of hydrogen atom addition ($[M+nH]^+$, $n>1$), was indicated by the anomalous molecular ion region which did not match the calculated isotopic contribution from natural abundances (Figure 24).

The implication of a reduction process is further indicated by the results obtained using a reduction inhibiting matrix such as NBA. When NBA is the matrix, the isotopic pattern of the molecular ion region was much closer to that of the calculated contribution of the natural isotopes as shown in Figure 24. In hope of further understanding this reduction process, the LSIMS mass spectrum of 4-(4-chlorobenzoyl)pyridine was obtained in a variety of matrices to monitor the effect of matrix chemistry on the extent of reduction. The matrices selected for this purpose represent the main groups of matrix structural features associated with a specific capacity to inhibit reduction processes in increasing order; aliphatic alcohols (glycerol),

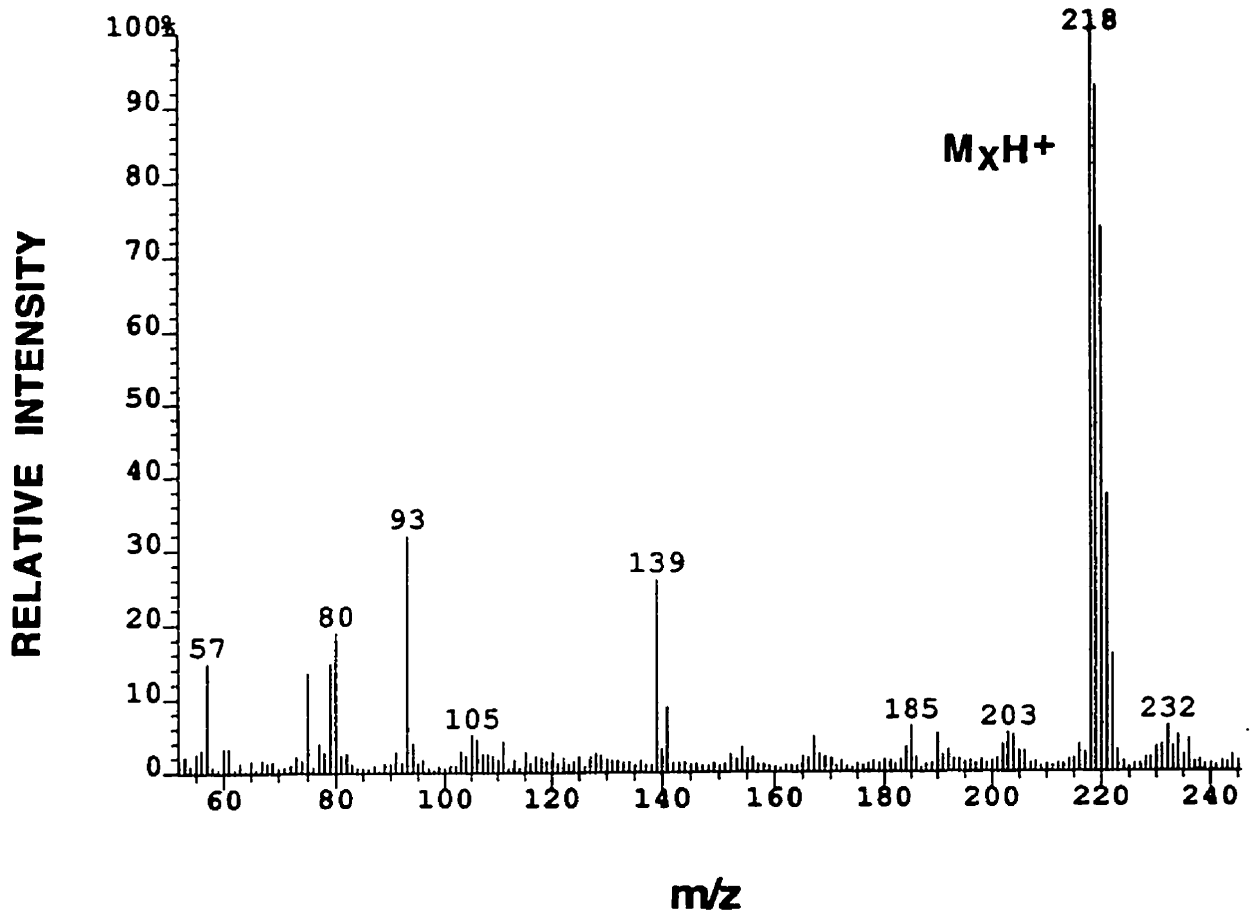

Figure 23. Positive LSIMS spectrum of 4-(4-Cl-benzoyl)pyridine (**6**) in glycerol.

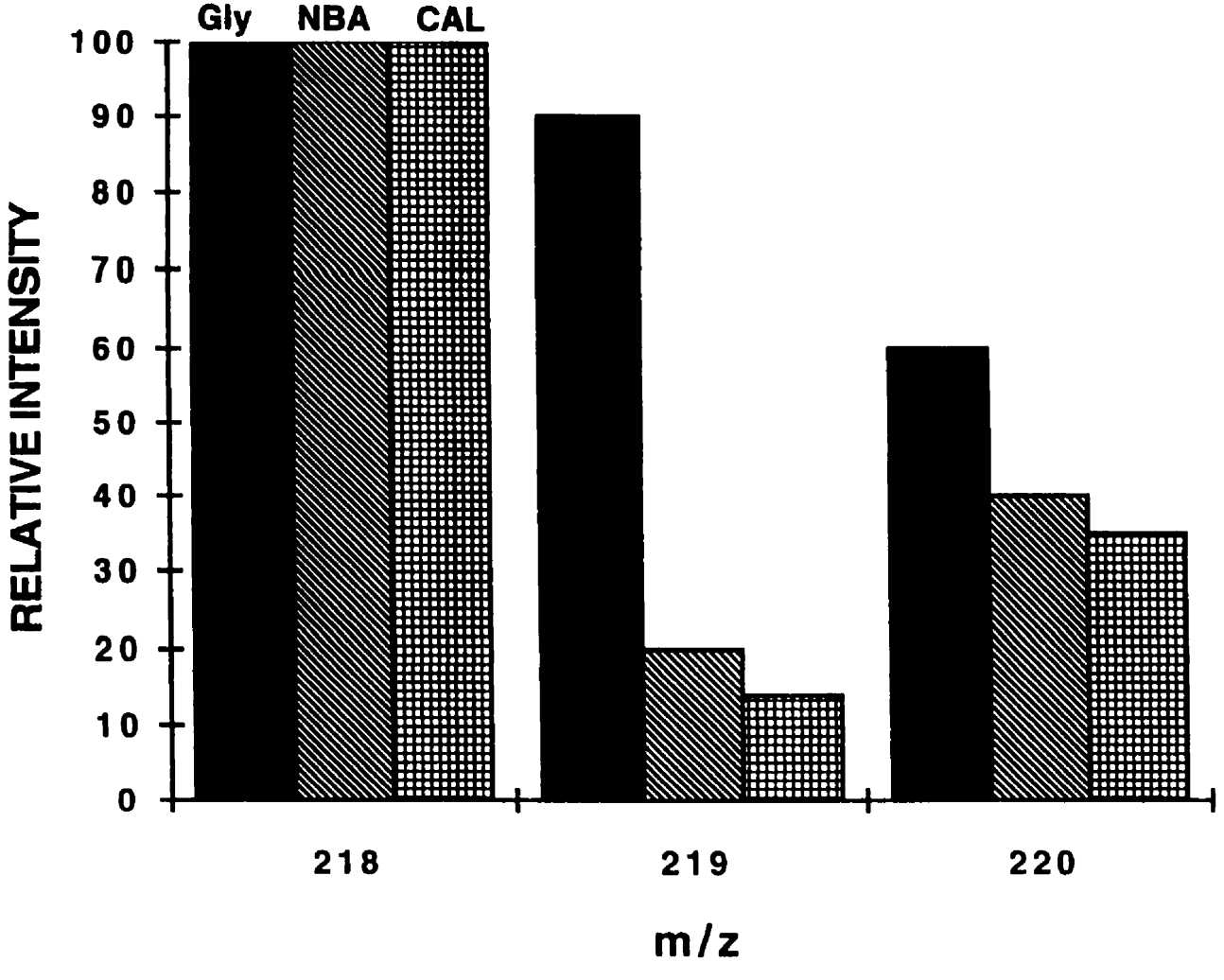

Figure 24. The molecular ion region of the LSIMS spectrum of 4-(4-Cl-benzoyl) pyridine (**6**) in glycerol (Gly) and nitrobenzyl alcohol (NBA). Also included is the natural isotopic distribution (CAL).

aliphatic compounds containing one sulphur (thioglycerol), aliphatic compounds containing two sulphurs (2-hydroxyethyl disulfide), aromatic compounds with electron donating substituents (3,4-dimethoxybenzyl alcohol), and aromatic compounds with electron withdrawing subtituents (3-nitrobenzyl alcohol).

The extent of reduction undergone by 4-(4-chlorobenzoyl)pyridine in each matrix was quantified by calculating the respective contribution of each molecular species to the sum of the relative intensities of the molecular species comprising the molecular ion region, from m/z 218 to m/z 222. The calculation was performed by manually deconvoluting the molecular ion region using the calculated isotopic contribution from natural abundances assuming that addition of a hydrogen did not significantly influence the isotopic pattern of the molecular formula $C_{12}H_9ONCl$ which represents the protonated molecule, $(M+H)^+$. Unfortunately, the SIMBROC program developed in our laboratory for the express purpose of assessing the 'true' extent of reduction could not be used since it is restricted to the elements carbon, hydrogen, oxygen, nitrogen and sulphur. This also prevented the calculation of the background contribution but such an effect can safely be neglected given the intensity of the signal of the analyte and its reduction products with respect to the background. The molecular species consisted of $[M+nH]^+$ ions, where n=1-3. These species represent the protonated molecule as well as one- and two-hydrogen additions, respectively. The addition of more than two hydrogens was not observed in any significant amount. No significant ionic species corresponding to oxidation of 4-(4-chlorobenzoyl)pyridine were observed.

The results are presented in Table XIII. As expected, the highest extent of reduction is exhibited by glycerol where the intact protonated molecule accounts for only 49% of the molecular species in the molecular ion region.

Table XIII. Relative distribution of the species present in the molecular ion region of the LSIMS mass spectrum of 4-(4-chlorobenzoyl)pyridine in various matrices. A=$(M+H)^+$, A+1=$(M+2H)^+$, A+2=$(M+3H)^+$.

Matrix	Species*	% of molecular ion region ion current
Glycerol	A	49
	A+1	38
	A+2	13
Thiogly	A	64
	A+1	30
	A+2	6
DMBA	A	74
	A+1	22
	A+2	4
HEDS	A	88
	A+1	11
	A+2	1
		92
NBA	A	
	A+1	8
	A+2	0

*The term species (A, A+1, A+2) refers to the *sum* of the ion abundances belonging to each molecular ion species $(M+H)^+$, $(M+2H)^+$ and $(M+3H)^+$.

The extent of one-hydrogen addition is greater than the two-hydrogen addition in all matrices and the latter is virtually absent in NBA. It is significant to note that the extent of reduction as defined by the % of intact protonated molecule parallels the dehalogenation-inhibiting capacity of the matrices defined earlier in sections 4.2.1 and 5.1. That is to say, the % of intact protonated molecule, $(M+H)^+$, with respect to one- and two-hydrogen addition products *increases* with the dehalogenation-inhibiting capacity of the matrices. This suggests that the causal aspects of the reduction of 4-(4-chlorobenzoyl)pyridine and dehalogenation might be similar.

As was outlined in section 5.2, the reducing species most often invoked in beam-induced reductions are the electron and the hydrogen atom. Thus, reduction of 4-(4-chlorobenzoyl)pyridine can possibly occur through two different pathways ; (a) from electron capture followed by subsequent protonation of the radical anion, or (b) direct attack of hydrogen atoms. In attempting to identify a particular bombardment-generated species which might be primarily responsible for the beam-induced reduction of 4-(4-chlorobenzoyl)pyridine, it is useful to consult the pulse radiolysis literature pertaining to benzoylpyridines[182]. Unfortunately, the only pulse radiolysis study addressing the behaviour of benzoylpyridines reveals little in that 4-benzoylpyridine reacts at fast rates with the solvated electron ($k(eaq+S)=2.8X10^{10}M^{-1}sec^{-1}$), the hydrogen atom ($k_{(H+S)}=2.4X10^{9}M^{-1}sec^{-1}$), and the α-hydroxyalkyl radical deriving from isopropanol ($k=2.4X10^{8}M^{-1}sec^{-1}$). The α-hydroxyalkyl radicals are reducing species

which react with electron affinic substrates such as benzoylpyridines through electron transfer. These radicals and their properties will be further discussed in section 6.2 pertaining to matrix chemistry.

Thus, although the rates of reaction of each of the reducing species differ from each other by an order of magnitude, it is difficult to rule conclusively on their possible contribution to the reduction process based on this data. This is particularly true where the hydrogen atom and the electron are concerned. A factor which may come into play is the scavenging capacity of glycerol for the solvated electron and the hydrogen atom. Alcohols are used as hydrogen atom scavengers in pulse radiolysis experiment. In contrast, it is noteworthy that the absorption spectrum of the solvated electron in glycerol shows a strong blue shift, reflecting the unusual stability of the solvated electron in glycerol[183]. Thus, alcohols scavenge hydrogen atoms whereas solvated electrons tend to have a relatively long half-life in such solvents. These opposite tendencies could probably exacerbate the importance of electron chemistry in the reduction observed for 4-(4-chlorobenzoyl)pyridine when glycerol is the matrix. A further argument can be made for the predominant role of secondary electrons in the reduction of 4-(4-chlorobenzoyl)pyridine if one considers the high extent of reduction observed when thioglycerol is the matrix (36%). The involvement of the hydrogen atom in the reduction process appears unlikely given the very high scavenging capacity of thiol compounds for the hydrogen atom. Thiol containing compounds react with the hydrogen atom at diffusion controlled rates[48].

However, the possible contributions of the hydrogen atom and the electron to the beam-induced reduction of 4-(4-chlorobenzoyl)pyridine can be further gauged by comparing the effect of various aromatic matrices on the extent reduction. This comparison can be attempted on the basis that aromatic compounds of widely different electron affinities have very similar rates of reaction with the hydrogen atom. The electron affinity of an aromatic compound normally defines its electron scavenging capacity in solution[184]. For example, benzene, benzyl alcohol, 1,3-dimethoxybenzene, and nitrobenzene react with the hydrogen atom at similar rates ($k \approx 1$ to $3X10^9 M^{-1}sec^{-1}$). In the above group of compounds, nitrobenzene is the only compound having a measurable electron affinity . This discrepancy in electron affinity translates into markedly different reaction rates with the solvated electron. The data shown in Table XIV highlights this discrepancy.

Table XIV. The rates of reaction of various simple aromatic compounds with the hydrogen atom (k_H) and the solvated electron (k_{es}) in aqueous solution from Buxton et al[48].

Compound	$k_{es}(M^{-1}s^{-1})$	$k_H(M^{-1}s^{-1})$	Electron Affinity (eV)
Benzene	$1.3X10^7$	$9.0X10^8$	0
Benzyl alcohol	$1.0X10^8$	$1.1X10^9$	0
Dimethoxybenzene	$<1.0X10^6$	$2.0X10^9$	0
Nitrobenzene	$3.7X10^{10}$	$1.0X10^9$	1.0

Hence, if the role of the hydrogen atom in the reduction of 4-(4-chlorobenzoyl)pyridine is dominant, there should exist little

difference in the observed extent of reduction when aromatic liquid matrices such as NBA and DMBA are used. In analogy to the compounds discussed in the previous paragraph, namely, nitrobenzene and 1,3-dimethoxybenzene, the matrix compounds NBA and DMBA can be assumed to have a similar reaction rate with the hydrogen atom but very different reaction rates with the solvated electron. A similar argument was presented by Mincher et al[179] to delineate the respective contributions of the hydrogen atom and solvated electron in the radiolytic dehalogenation of chlorinated aromatic hydrocarbons.

The results shown in Table XIV reveal a large difference between the extent of reduction exhibited by 4-(4-chlorobenzoyl)pyridine in NBA and DMBA. As expected if the reduction of 4-(4-chlorobenzoyl)pyridine is based on electron capture, the extent of reduction observed, as defined by the % intact protonated molecule in the molecular ion region, is much lower in NBA (92% intact $(M+H)^+$) compared to that in DMBA (74% intact $(M+H)^+$).

The greater extent of reduction observed in DMBA compared to NBA clearly indicates the importance of the electron affinity (and hence its electron scavenging capacity) of the matrix compound in inhibiting the reduction process. The results strongly suggest that the role of the hydrogen atom in the reduction process undergone by 4-(4-chlorobenzoyl)pyridine is minor whilst that of beam-generated secondary electrons is dominant. One can suspect that the inhibition of the reduction process by NBA was only partial because of the relatively high electron affinity of 4-(4-chlorobenzoyl)pyridine (E.A.=1.1eV)

which is estimated to be somewhat higher than that of the matrix ($E.A._{NBA}$=0.9eV). The electron affinity of 4-(4-chlorobenzoyl)pyridine was estimated from known electron affinities of analogs and electrochemical data using the method of Wentworth (see section 5.2). The electron accepting capability of 4-(4-chlorobenzoyl)pyridine is well illustrated in its glycerol LSIMS negative ion spectrum. The radical anion of the molecule, $M^{-\bullet}$, is present in high abundance at m/z 217 in Figure 22.

Interestingly, if the electrochemical behaviour of benzophenones and benzoylpyridines is assumed to be similar, parallels can be drawn between electrochemistry and FAB/LSIMS reduction of 4-(4-chlorobenzoyl)pyridine. The electrochemical reduction of 4-bromobenzophenone in a protic solvent (such as water) leads to the formation of the alcohol without any expulsion of the halide ion. This behaviour is akin to that observed in the LSIMS glycerol mass spectrum of 4-(4-chlorobenzoyl)pyridine, where expulsion of the halide is even less favoured given the stronger carbon-chlorine bond. The mechanism of reduction can be seen as electron capture by 4-(4-chlorobenzoyl)pyridine to form the radical anion (equation **25**) which is subsequently protonated to form a ketyl radical (equation **26**). This ketyl radical would most likely correspond to the A+1 ion observed in the molecular ion region of the LSIMS mass spectrum of 4-(4-chlorobenzoyl)pyridine.

[25]

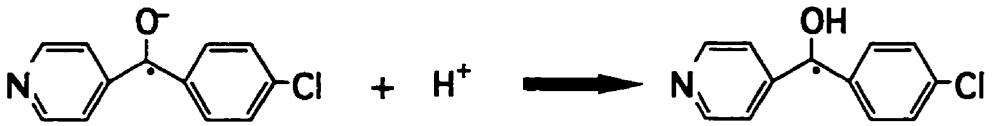

[26]

Extensive investigations have shown that electron capture by compounds such as benzophenones (compounds similar to the benzoylpyridines) is known to lead to the formation of ketyl radicals in protic solvents[185,186]. The unique structure of 4-(4-chlorobenzoyl)pyridine also contributes to the observation of $(M+nH)^+$ ions as reduction takes place remote from the presumed site of protonation at pyridine nitrogen.

The fact that 4-(4-chlorobenzoyl)pyridine is not overwhelmingly reduced to the alcohol could be due to the more negative reduction potential of the ketyl radical compared to the 'parent' ketone[186].

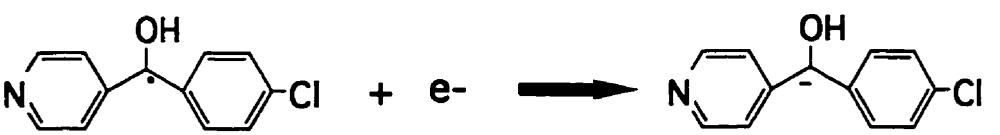

[27]

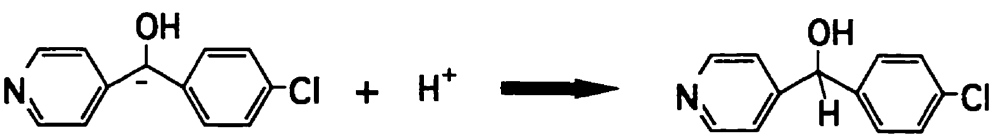

[28]

A similar type of behavior was observed for aromatic oximes[25]. The aromatic oximes are normally reduced to the amine with an imine as the intermediate. Under FAB/LSIMS conditions, the imine was the only reduction product observed. The almost complete absence of the reduction end product, the amine, was rationalised by invoking the slow

reduction of the imine to the amine compared to desorption. This is reasonable since most beam-induced products should be generated at/or close to the vacuum-liquid interface thus allowing their desorption.

The pKa (12) of the 4-benzoylpyridine radical anion implies that the radical anions of 4-(4-chlorobenzoyl)pyridine should be protonated very efficiently[182]. It should be pointed out that pulse radiolysis studies have shown that solvated electrons add to aromatic ketones to produce exclusively the ketyl radical and radical anion of the corresponding carbonyl compounds whereas hydrogen atoms are much less selective and add to the aromatic ring at more than one position[185].

The proposed reduction mechanism of (4-chlorobenzoyl)pyridine through electron capture and ketyl radical formation is consistent with the behaviour of an analogous compound under radiolytic conditions. This is a very interesting example where dehalogenation does not occur but another functionality, an aromatic ketone, is preferentially reduced. It could be argued that dehalogenation does not take place because of the high electron affinity of the compound rather than the preferential reduction of the ketone. Thus, beam-generated secondary electrons appear to play an important role in reduction processes other than dehalogenation.

5.4 Effect of analyte surface concentration

When any new mass spectrometry technique is introduced, the factors affecting its inherent sensitivity inevitably become the focal point of numerous investigations. Of similar concern to mass spectrometrists is the propensity of a technique to generate artefacts. Such concern is justified by the possibility of complicating spectrum interpretation and/or drawing erroneous conclusions as to the nature of the sample. In fast atom bombardment mass spectrometry, the pioneering investigations of Barber[187,62] and Ligon[188] convincingly demonstrated the often dramatic effects of analyte surface activity on sensitivity. The potential of the technique to produce artefacts fostered by the interaction of the primary beam with the sample was also recognized at an early stage of the technique by others[34,81]. However, despite a plethora of studies on beam-induced reactions[9], the correlation between extent of artefact formation and analyte surface activity has seldom been alluded to[34,81] and never systematically studied. Hence, a factor favoring increased sensitivity could also possibly enhance artefact formation. The goal of this section is to show the effect of analyte surface activity on beam-induced dehalogenation.

In a study of the effect of experimental parameters on the beam-induced dehalogenation of chlorpromazine, it was proposed that increased analyte surface concentration (activity) could lead to increased dehalogenation[34]. The increased dehalogenation would result

from the increased probability of the analyte undergoing reaction with bombardment-generated species (thought to be electrons) produced at and near the surface. This hypothesis appears to be correct given the following reports. The post-bombarment HPLC analysis of a glycerol/analyte solution revealed that the extent of dehalogenation was only one third of that observed in the positive ion FAB mass spectrum[24,31]. It was proposed that this discrepancy reflected the interfacial nature of the beam-induced dehalogenation process[31]. In this context, the term surface activity encompasses related phenomena such as surface tension modifications, hydrophobicity and surface enrichment of the analyte. In the following pages, the relationship between analyte surface activity and extent of dehalogenation was investigated using a three-pronged approach. First, the effect of doping a glycerol/analyte solution with an anionic surfactant was compared to the original solution for a variety of analytes. Second, the extent of dehalogenation observed for analogous compounds having markedly different surface activities was compared. Third, the effect of matrix surface tension on the dehalogenation process was probed using 1,2,6-trihydroxyhexane, a polyhydric matrix compound analogous to glycerol but having a significantly lower surface tension.

5.4.1 Effect of surfactant additive

The importance of analyte surface activity in FAB/LSIMS has long been recognized. Increased sensitivity[187] and the suppression[189] of hydrophilic components in peptide digest mixtures are well known consequences of surface activity effects. The addition of ionic

surfactants can increase sensitivity and diminish suppression effects[66]. Surfactant molecules have been used to 'bind' analyte ions to a position near the matrix surface where they can be efficiently desorbed[190,67-8]. For example, an anionic surfactant can form an ion pair with a cationic analyte which can then migrate to the surface because of the intrinsic surface activity of the surfactant. In order to further investigate the proposition[34] that increased surface concentration of the analyte could lead to increased dehalogenation due to the greater proximity of the analyte to the site of reactive species (secondary electrons) generation, we have studied the effect of an anionic surfactant, lithium dodecyl sulphate (LDS), on the extent of dehalogenation. It was hoped that doping an analyte/glycerol solution with LDS would 'artificially' increase analyte surface concentration. A simple comparison of the observed extent of dehalogenation obtained in the doped and undoped solution should allow one to draw inferences on the effect of analyte surface concentration.

With a cationic analyte such as chlorpromazine hydrochloride, a sizable and reproducible decrease in dehalogenation (30 to 20%) was observed with the LDS doped solution compared to the undoped solution as shown Figure 25. Also, the quality of the spectrum was visibly enhanced in the surfactant-doped spectrum. It can be seen that the intensities of the ions due to the matrix is greatly reduced with respect to those of the analyte. Furthermore, the mass spectrum exhibited no significant time dependence over a period of 5 minutes. This lack of time dependence is in contrast to that exhibited in the

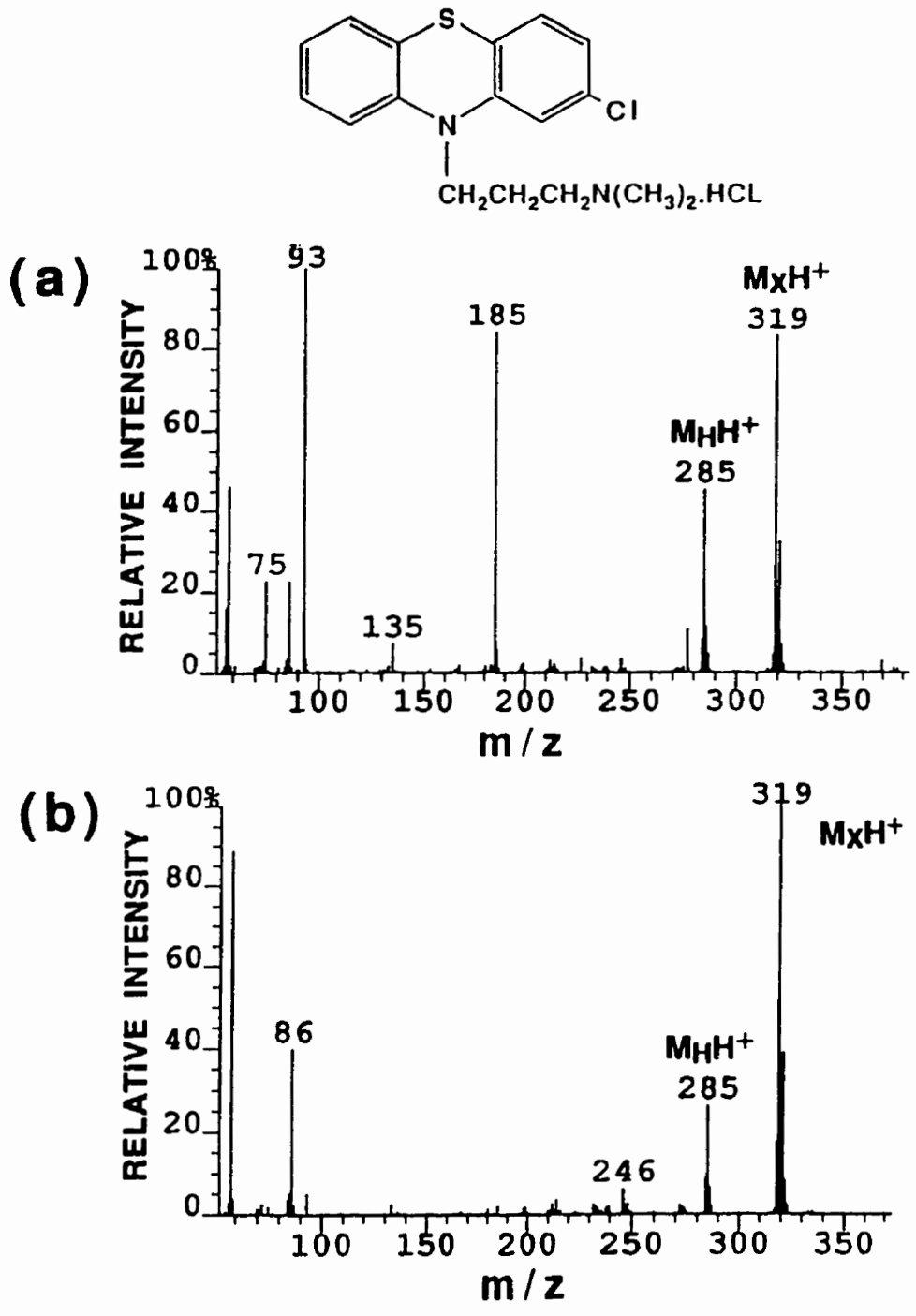

Figure 25. LSIMS spectrum of chlorpromazine in (a) glycerol, (b) glycerol/LDS.

undoped solution where one can observe the analyte ions increasing in abundance (relative to the matrix peaks) as well as a gradual increase in % dehalogenation with time (section 4.1.1). The lack of time dependence in the LDS doped solution could be due to the reduced rate of evaporation of the matrix. This phenomenon could be ascribed to the layer of surfactant covering the surface of the sample droplet thus slowing the rate of glycerol evaporation.

The unexpected decrease in extent of dehalogenation observed in the surfactant-doped case cannot be attributed to the electron capture capability of the surfactant as this compound reacts with the solvated electron 5 times less rapidly than threitol[48], a polyol compound analogous to glycerol. Aliphatic alcohols are considered to be unreactive towards the solvated electron[48]. However, when a neutral analyte such as 4-Cl-2,6-diaminopyrimidine was used, the extent of dehalogenation nearly doubled in the LDS doped spectrum (Figure 26(b)) relative to the undoped glycerol/analyte spectrum (Figure 26(a)). Similar trends were obtained for atrazine (neutral analyte) and 4-Cl-phenylalanine methyl ester hydrochloride (cationic analyte). Clearly, the initial charge state of the analyte appears to play an important role in determining the direction of the effect of surfactant doping on the extent of dehalogenation.

The surfactant effect could be attributed to the distribution of the analytes respective to the Stern layer. The Stern layer is formed by the anionic head groups of the surfactant molecules. If we assume that the surfactant molecules gather at the vacuum-liquid interface

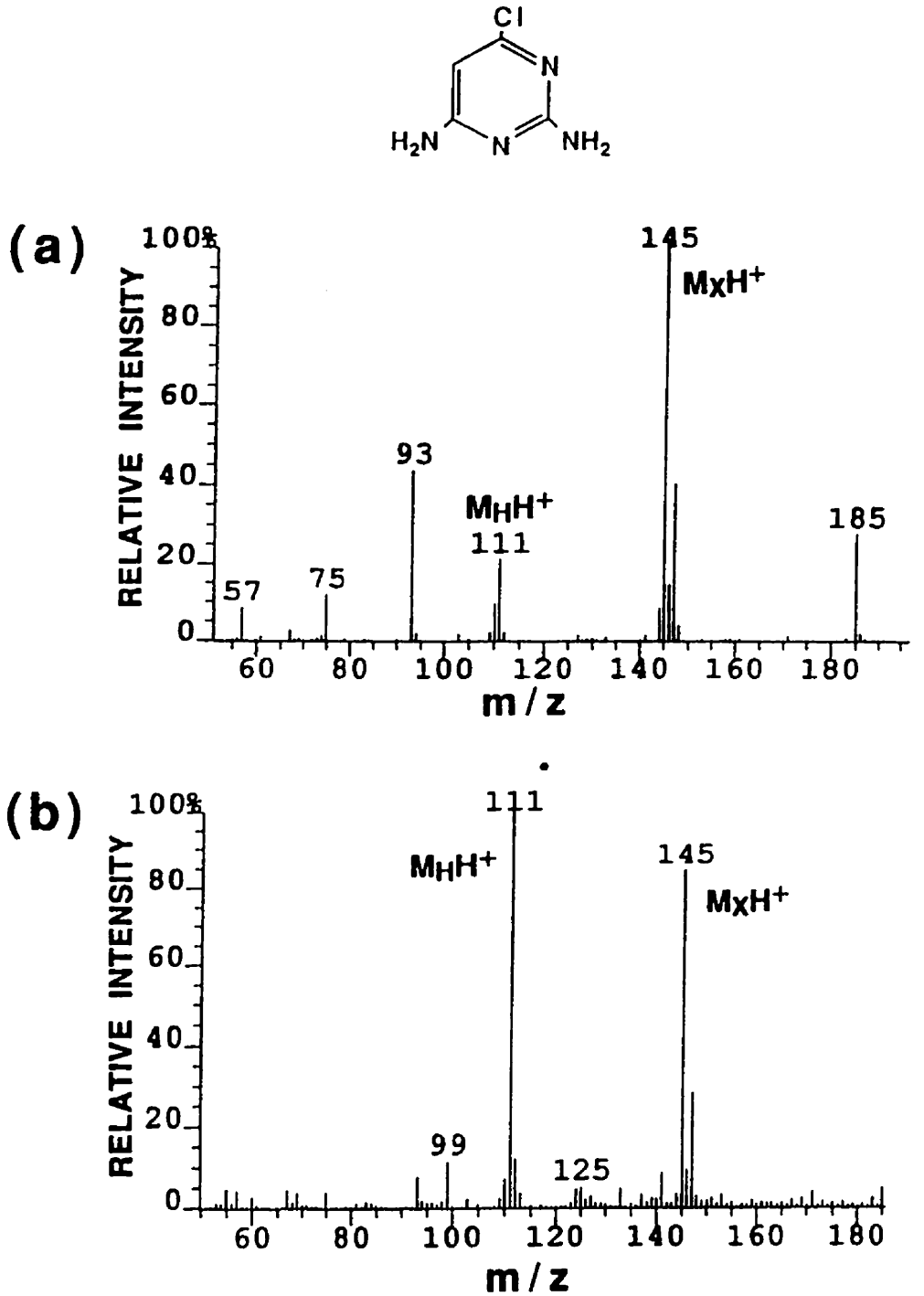

Figure 26. LSIMS spectrum of 4-Cl-2,6-diaminopyrimidine in, (a) glycerol, (b) glycerol/LDS.

and that the hydrophilic head groups are oriented towards the bulk, then we can picture a hydrophobic layer formed by the hydrocarbon tails at the surface. The hydrophobic layer is separated from the hydrophilic bulk by the Stern layer. This situation is described schematically in Figure 27.

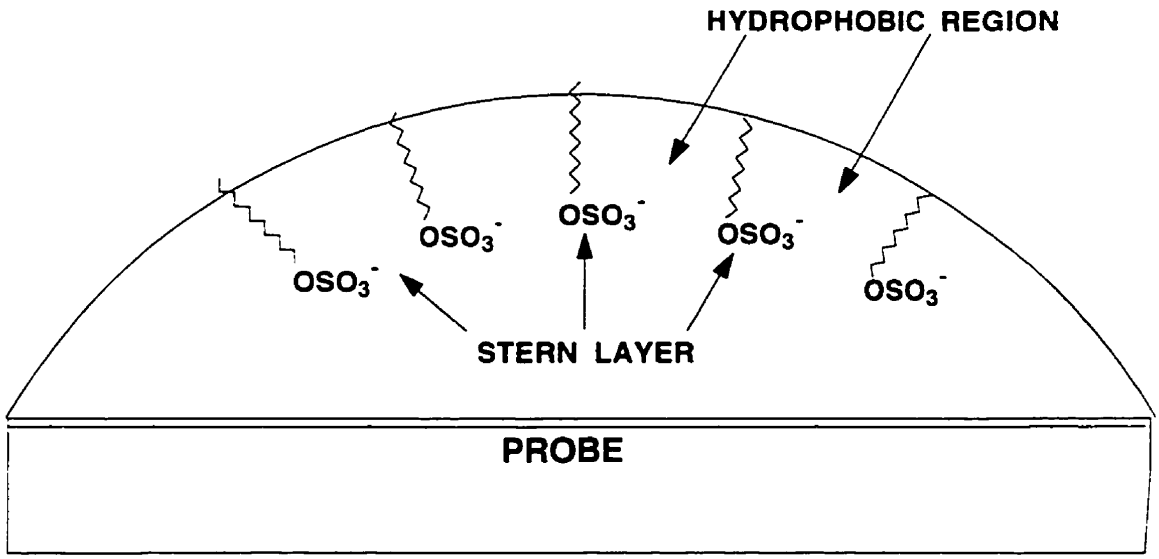

Figure 27. Schematic description of the distribution and orientation of molecules of the anionic surfactant lithium dodecyl sulfate in glycerol.

Cationic compounds will be below the Stern layer, where electrostatic repulsion of the electrons by the anionic head groups will reduce the interaction of analyte molecules with beam-generated electrons formed mostly near the surface. This type of surfactant effect has been observed in pulse radiolysis experiments with aqueous micellar media[191,192]. For example, the rate constant of the reaction of pyrene with the solvated electron is drastically diminished in anionic micelles compared with simple homogeneous media. Conversely, cationic micelles greatly accelerate the rate of reaction of the solvated electron with solutes located in its micelles based on the strong electrostatic attraction existing between the cationic head groups and

electrons. This effect further supports the contention that beam-induced dehalogenation is induced by secondary electrons.

For neutral analytes, increased surface concentration in the hydrophobic region (above the Stern layer) where the concentration of reducing species is highest, could explain the observed increase in dehalogenation. There exists a precedent where the addition of LDS to a glycerol/analyte solution increases the observed reduction. In his study of the FAB beam-induced reduction of the aromatic oximes, Gross and co-workers[25] observed the reduction of benzaldoxime dodecaphenone to the imine in glycerol solution. The extent of reduction increased when the solution was doped with LDS. Incidentally, the compounds used in that study were neutral organics, and the increased reduction observed upon surfactant addition is in agreement with the results of our study. Although the results obtained do not allow a generalization to be made regarding the effect of increased analyte surface concentration on the dehalogenation process, the effects observed above can be rationalized on that basis.

5.4.2 Effect of Analyte Surface Activity.

The effect of analyte hydrophobicity on beam-induced dehalogenation was probed using the analogous compounds chlorpromazine and **7**. Essentially, both compounds are comprised of a 2-chlorophenothiazine moiety and an alkyl ammonium side chain. The difference in alkyl side chain length accounts for the markedly different surface activities of chlorpromazine and **7**. Since the side chain is not involved in the

dehalogenation process, comparison of the respective mass spectra of each compound allows the unambiguous evaluation of the impact of analyte surface activity on the extent of dehalogenation. The compounds are shown below in Figure 28.

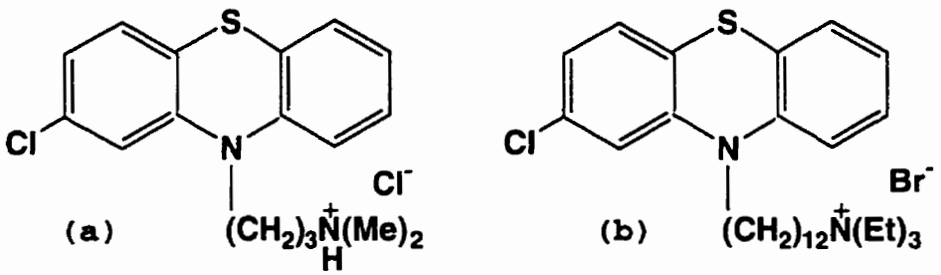

Figure 28. The structures of (a) chlorpromazine and (b) compound **7**, the analog possessing a dodecyl ammonium side chain.

For pre-formed ions, we can define the analyte surface activity in terms of the ratio of the intensity of the analyte ions (M_X^+ and M_H^+) to that of a glycerol oligomer. The ratio $[M_X]^+ + [M_H]^+ / [(gly)_3H]^+$ is 1 for chlorpromazine and 10 for compound **7**, respectively. As can be seen in Figures 29 and 30 from the intensity of the analyte ions with respect to the protonated glycerol trimer, $(gly)_3H^+$, the surface activity of compound **7** is much greater than that of chlorpromazine as expected.

The mass spectrum of compound **7** exhibits conspicuous charge remote fragmentation which is characteristic of surfactants[193]. This type of fragmentation is called charge remote because (a) bond cleavage takes place at a site in the ion that is removed from the charge site and (b) the mechanism of fragmentation does not involve any significant intervention of the charge site. The interest here is that charge remote fragmentation has traditionally been thought of occurring

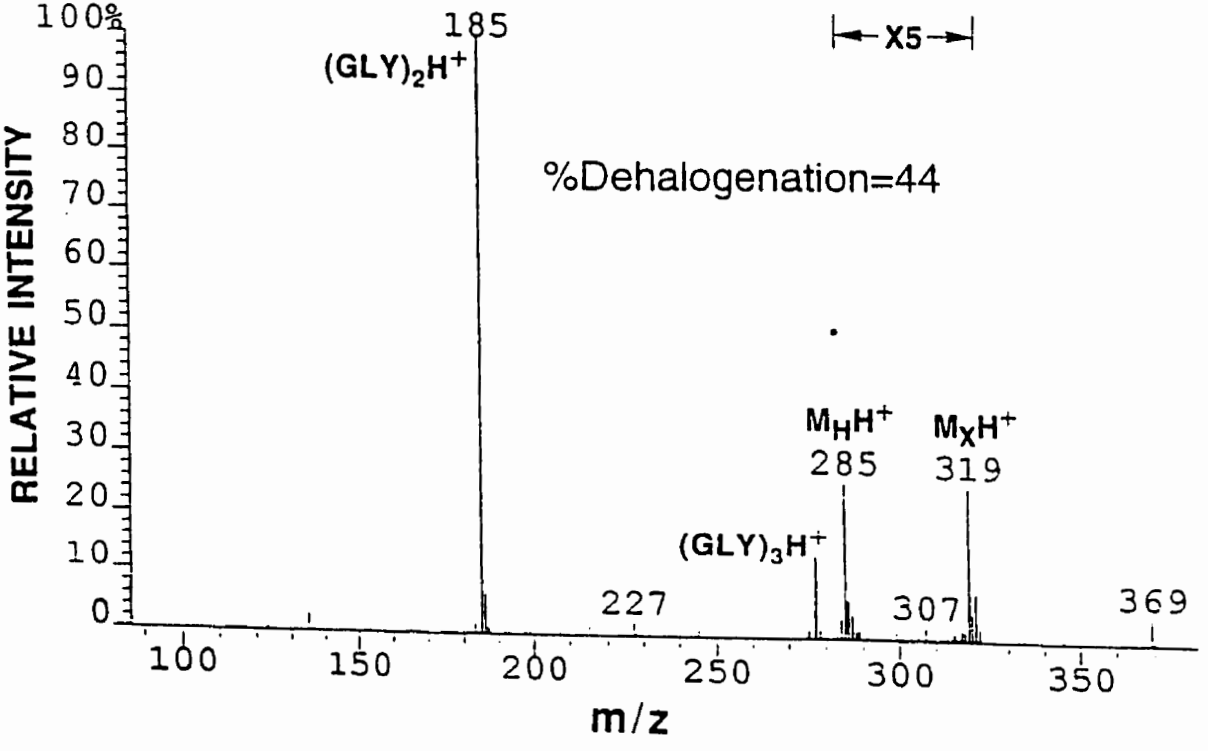

Figure 29. LSIMS spectrum of chlorpromazine in glycerol (0.0041M).

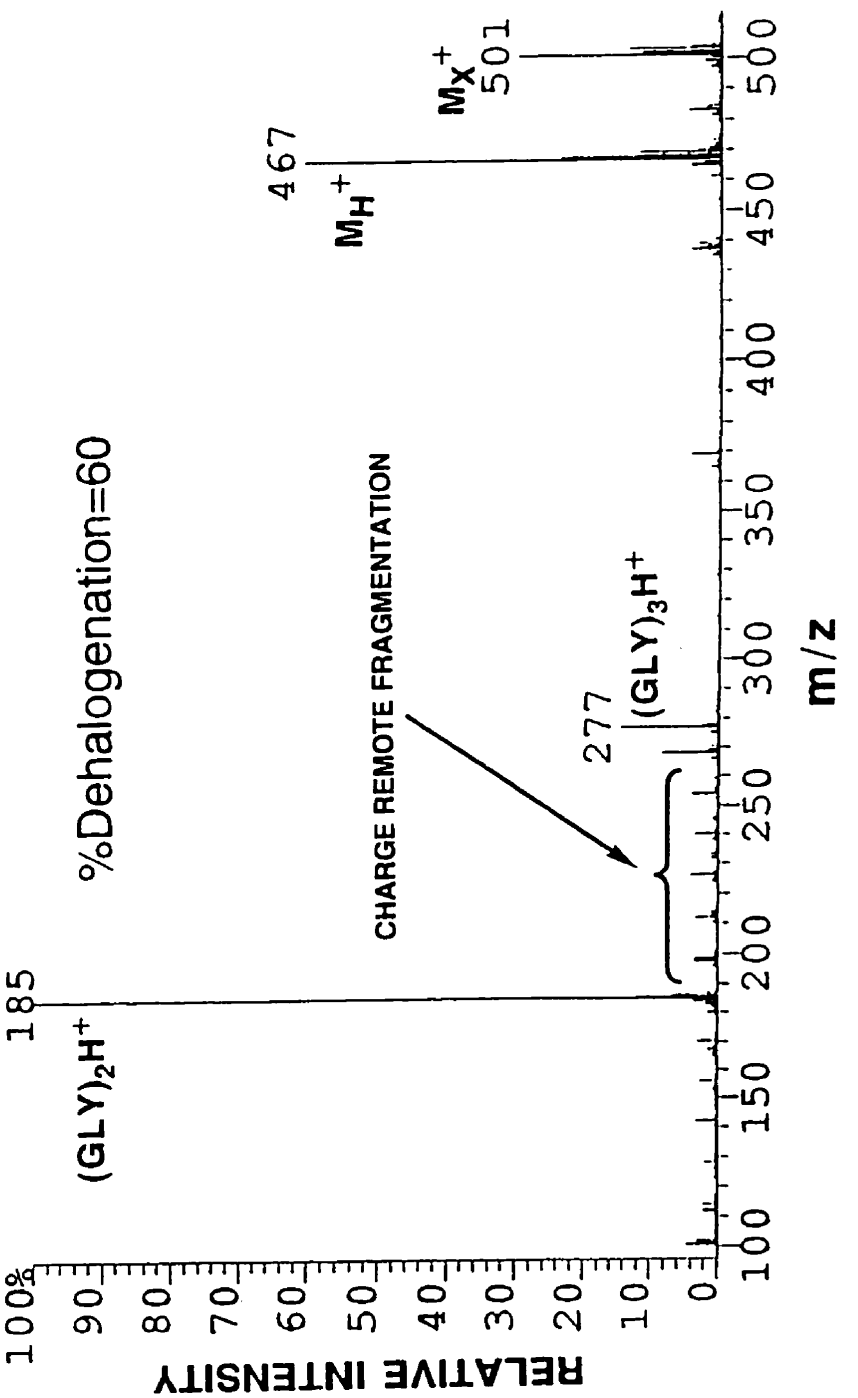

Figure 30. LSIMS spectrum of compound 7 in glycerol (0.0041M).

exclusively under conditions of collisional activation. However, recent reports indicate that this type of fragmentation can be observed without collisional activation[194,195]. In this context, it has been suggested that charge remote fragmentation occurs as a result of ion source reactions following desorption by FAB/LSIMS[194]. The aspects of charge remote fragmentation without collisional activation have not really been explored to any extent.

The establishment of a definite energy threshold for charge remote fragmentation could serve a very useful purpose in attempting to establish the internal energy acquired by the ions desorbed through keV particle bombardment in the FAB/LSIMS process. The energetics of the process have been extensively studied using tandem mass spectrometry in conjunction with desorption ionization techniques[194-196]. However, a variety of factors appear to lead to compound dependent energy requirements for the observation of charge remote fragmentations[197].

The ions arising from charge remote fragmentation span the range m/z 268 to m/z 114 and consist of the loss of neutral fragments of the type R-(C_nH_{2n-1}) where R is the chloro- or phenothiazine moiety as shown in Figure 31. These neutral losses are based on the chloro- and/or phenothiazine moiety with successive methylene units added to form higher mass fragments. This results in the regular picket fence pattern observed in the mass spectrum where each m/z is 14 mass units apart. The neutral fragment loss R-(C_nH_{2n-1}) is similar to the (C_nH_{2n}) loss observed in the charge remote fragmentation of alkyl

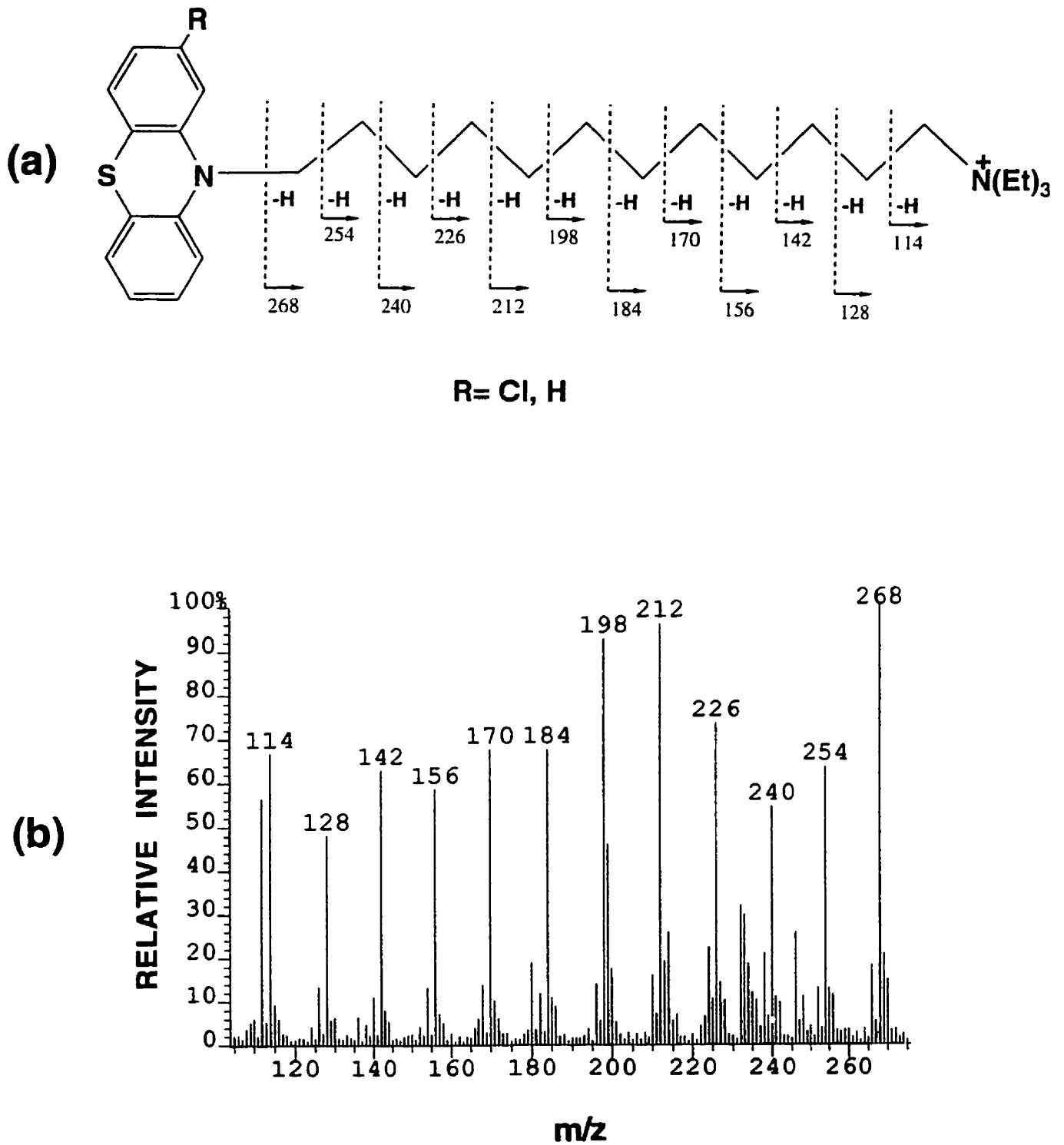

Figure 31. (a) Schematic representation of the CRF pattern of compound **7**. (b) CRF region of compound **7**.

trimethylammonium surfactants[194]. The proposed mechanism by which charge remote fragmentation is thought to occur is shown in Figure 32 and consists of 1,4-elimination of H_2 and C_nH_{2n}[193]. This mechanism can reasonably be used to explain the genesis of the ions observed between m/z 114 and 240.

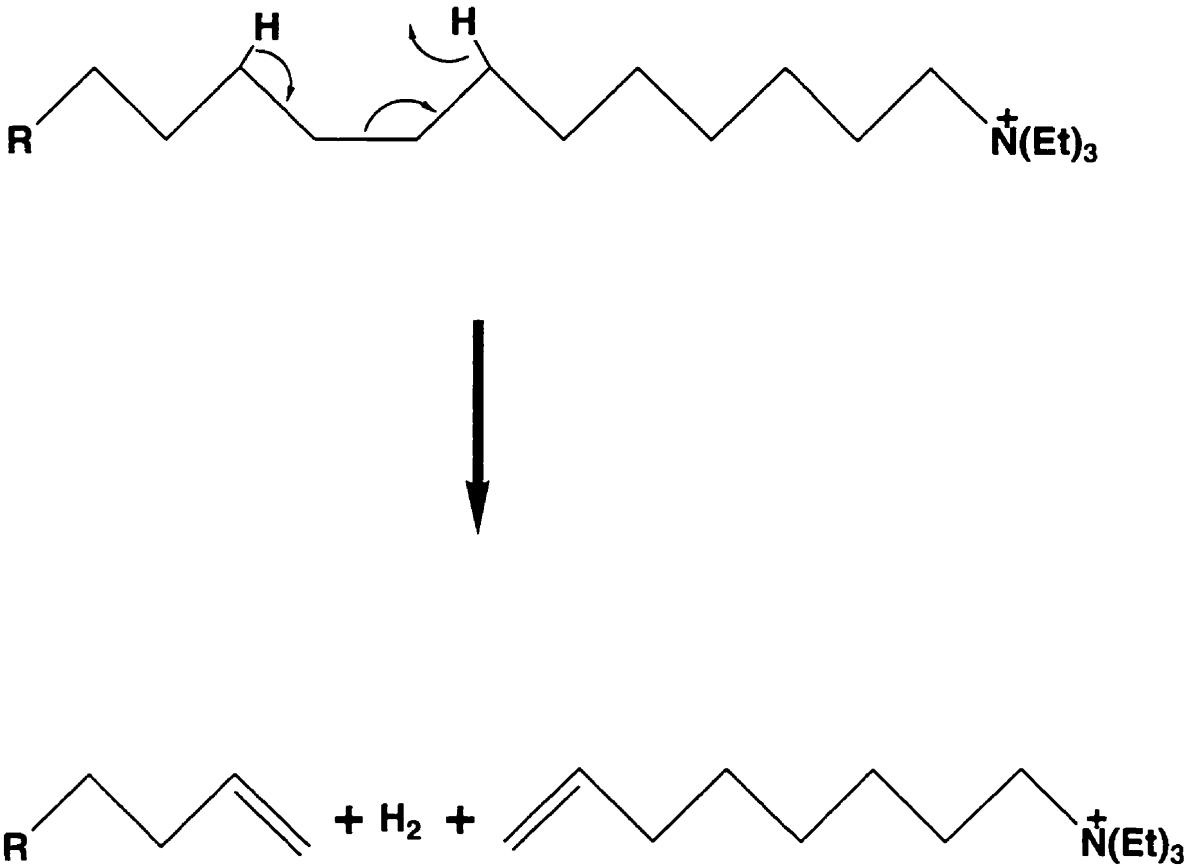

Figure 32. Proposed mechanism of 1,4-H_2-elimination for the generation of CRF ions in the LSIMS masss spectrum of compound 7.

The main feature of interest in comparing the LSIMS of 7 and chlorpromazine in glycerol is the significantly higher % dehalogenation exhibited by compound 7 (60%) with respect to the less surface active analyte, chlorpromazine (45%). These results *directly* support the contention that analyte surface activity can affect the observed extent of dehalogenation. This effect can be explained by the high concentration of beam-generated species (thought to be electrons) near the surface. Hence, higher analyte surface concentration should result in an increased probability of reaction with beam-generated electrons and result in greater % dehalogenation.

Interestingly, such an effect of analyte hydrophobicity also exists in sonolysis[198]. It has been found that hydrophobic solutes are more likely than hydrophilic solutes to undergo attack by sonolysis-generated radicals. The chemistry resulting from sonolysis is based on the production of radical species due to the effect of ultrasound. When an ultrasonic wave propagates through a liquid , the local pressure varies with time and space. If a gas bubble is present in the liquid it will expand and contract due to these pressure changes. The chemical effects of ultrasound are due to acoustic cavitation, referring to the formation, growth and collapse of bubbles in liquids. Cavities will expand to 2 or 3 times their resonance size before violently collapsing.

The temperature and pressure in the imploding cavity are very extreme. In water this leads to the formation of hydroxyl radicals and hydrogen atoms due to the thermal decomposition of water. The 'hot spot'

theory identifies three different regions of sonochemistry. The first is the interior of cavitation bubbles where extreme conditions of temperature and pressure exist. The second consists of the interfacial region between the collapsing gas bubbles and the bulk solvent. Hydrophobic solutes concentrate at this interface where the concentration of radicals is the highest. Therefore, solute hydrophobicity apparently leads to increased likelihood of radical attack. A further point to be made concerning sonolysis is its relationship to radiolysis. Many comparisons have been drawn between sonolysis and radiolysis. The motivation between such comparisons lies in the *radiomimetic* character of sonolysis

5.4.3 Effect of matrix surface tension

Apart from using a surfactant additive and synthetically modifying the analyte through inclusion of a hydrophobic side chain, analyte surface activity can be influenced in a predictable manner by changing the solvent and hence the surface tension. In a liquid such as glycerol where strong intermolecular interactions exist through hydrogen bonding, the surface tension is high. Since it is energetically favourable to lower the surface tension, a surfactant present in glycerol will tend to populate the surface to reduce the surface tension. If glycerol is substituted for a solvent of lower surface tension, the propensity of surfactant molecules to migrate to the surface is diminished. This results in a lower analyte surface concentration.

Selecting a liquid matrix compound possessing a surface tension inferior to that of glycerol is not problematic. However, since a correlation between analyte surface concentration and extent of dehalogenation is sought, care must be taken to select a matrix whose structural features are not inherently dehalogenation-inhibiting. Thus, the matrix compound 1,2,6-trihydroxyhexane (THH) was used to test the effect of matrix surface tension on dehalogenation. This compound is a structural analog of glycerol. The only difference is that 3 methylene carbons (a n-propyl unit) have been added to the glycerol structure between the 1 and 2 position. The presence of this hydrophobic moiety should result in a significant lowering of the surface tension. For example, the surface tensions of ethylene glycol and 1,2-propanediol are 48 dyn cm^{-2} and 39 dyn cm^{-2}, respectively[199]. Thinking along more qualitative lines, one can picture the hydrophobic moiety of THH aligning itself at the liquid-vacuum interface to lower the surface tension of the liquid. This interpretation stems from Langmuir[200,201] in what he termed the *principle of independent surface action*. This principle rests on the proposition that, qualitatively, one could suppose each part of a molecule to possess a local surface free energy. Taking methanol as an example, one can employ this principle to decide how molecules should be oriented at the surface according to the surface energy of the hydrophilic or hydrophobic portion of the molecule as shown in Figure 33 (a) and (b).

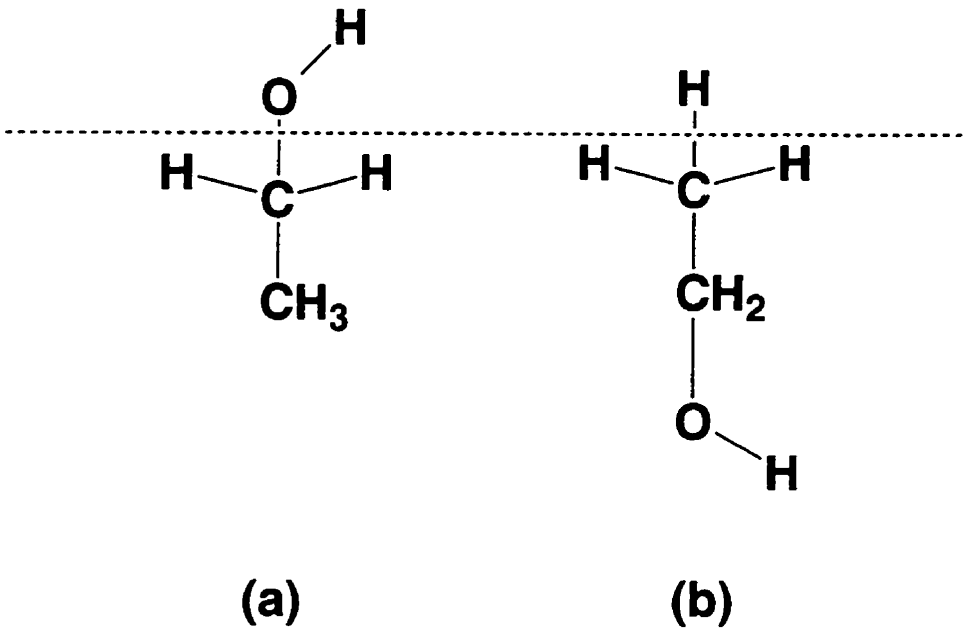

Figure 33. Schematic representation the principle of independent surface action defined by the orientations (a) and (b).

Calculations show that the molecular orientation shown in (b) results in a significantly smaller surface tension or surface energy. Hence, application of this principle to propose a lower surface tension for THH with respect to glycerol is reasonable.

With glycerol no such orientation is possible since the molecule can essentially be considered a hydrophilic ball. This idea is supported by the fact that the surface tension of glycerol is similar to that of water (63 vs 72 dyn cm^{-2})[199] thus illustrating the fact that this liquid has one of the highest surface tension known for an organic compound. In contrast, the surface tension of NBA (35 dyn cm^{-2})[202] and thioglycerol (53 dyn cm^{-2})[203] are significantly lower than that of glycerol.

The LSIMS mass spectrum of compound **7** in THH is shown in Figure 34. The most noticeable feature is the complete dominance of the matrix ions in the spectrum. The matrix spectrum is very similar to that of glycerol, consisting of ions stemming from a protonated molecule and protonated oligomers. The analyte ions necessitate an important magnification factor to be seen clearly. The % dehalogenation is 44. This value is much smaller than that obtained in glycerol (60%). These results are in agreement with a lower surface tension for THH.

A recent report highlighted the link between analyte signal intensity and matrix surface tension[203]. The authors carefully measured the surface tension of three matrix compounds and compared the intensity of the analyte signal in each. Their results clearly indicate that analyte signal diminishes with matrix surface tension. For example, a drop in matrix surface tension of 10 dyn cm^{-2} resulted in a very significant decrease of the analyte signal intensity. However, these results were obtained with a hydrophilic analyte, EDTA. In addition, the mass spectral data presented was limited as the absolute intensity of the protonated molecule due to the analyte was not available. Furthermore, the solutions used for mass spectral purposes consisted of matrices acidified with aqueous hydrochloric acid. The changing composition (and thus surface tension) of such aqueous type matrices under high vacuum conditions greatly obscures the validity of conclusions that can be drawn from such experiments.

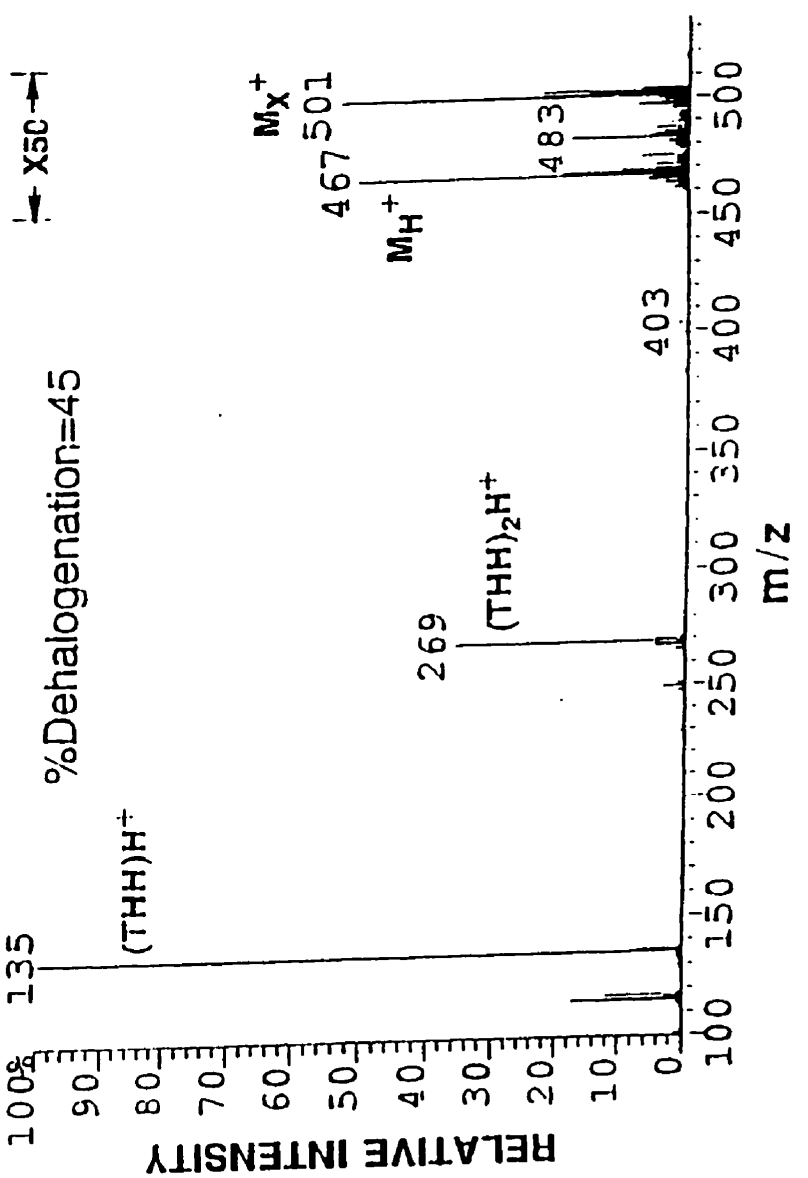

Figure 34. LSIMS spectrum of compound 7 in 1,2,6-trihydroxyhexane (0.0041M).

Chapter 6

6.1 $M^{+\cdot}$ Formation and dehalogenation inhibiting tendencies of Matrices

In the LSIMS study of the effect of the experimental parameters on the dehalogenation of chlorpromazine[34], it was observed that the analyte radical cation, $M^{+\cdot}$, was present in the spectrum. Interestingly, the abundance of $M^{+\cdot}$ relative to the $[M+H]^+$ appeared to increase with the dehalogenation inhibiting tendency of the matrix as evident in Figure 35. This trend is well illustrated in Table XV. Consequently, we decided to investigate the link between $M^{+\cdot}$ formation and the dehalogenation inhibiting capacity of the matrix. By monitoring the presence or absence of the $M^{+\cdot}$ of various compounds of known oxidation potentials in a series of matrices, it was hoped to roughly bracket the reduction potentials of the various matrices under bombardment conditions.

Table XV. The effect of matrix selection on the $M^{+\cdot}/(M+H)^+$ ratio for chlorpromazine.

Matrix	$M^{+\cdot}/(M+H)^+$
NBA	0.26
DEP	0.30
HEDS	0.28
MES	0.30
HPEA	0.15
DMBA	0.13
BOP	0.13
THIOGLY	0.10
TDG	0.12
Gly	0.06

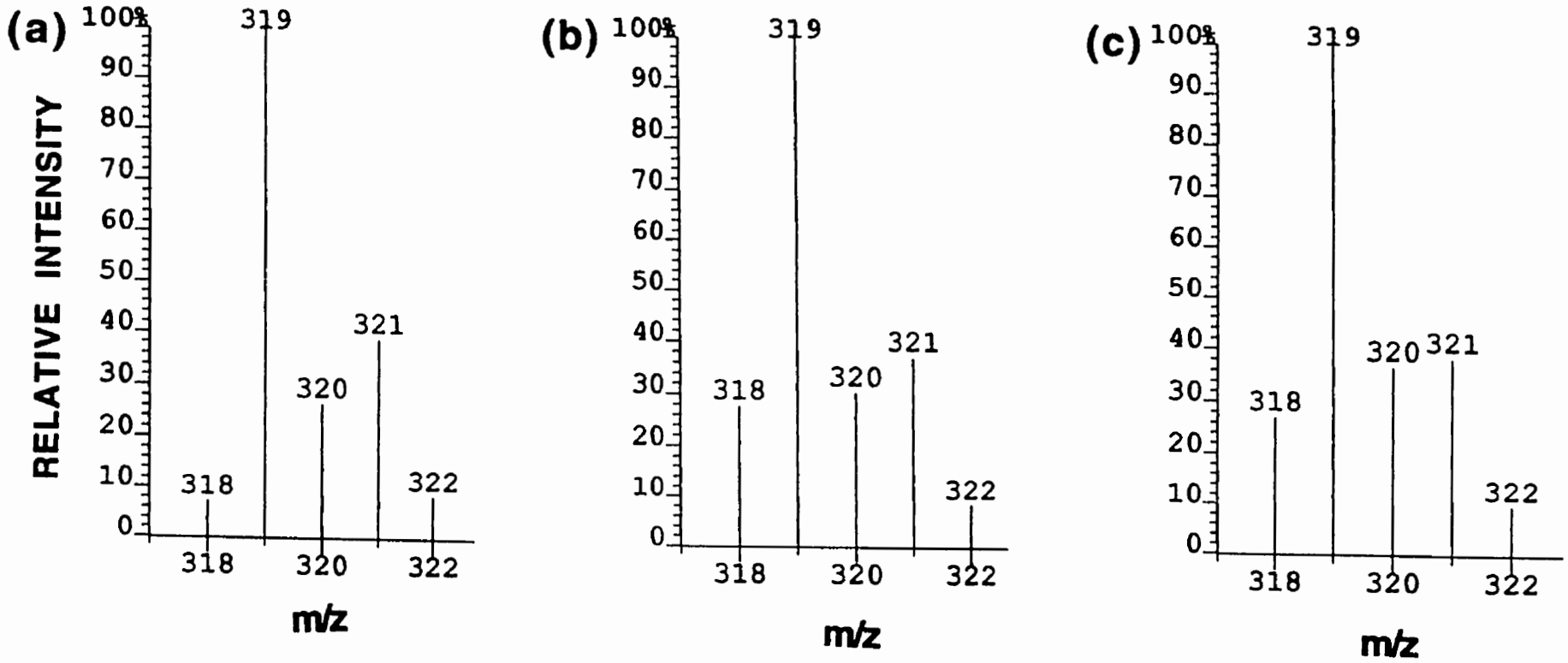

Figure 35. Molecular ion region of chlorpromazine in (a) glycerol, (b) HEDS and (c) NBA.

Although there are numerous reports in the literature of $M^{+\cdot}$ ion formation under FAB/LSIMS conditions[115-6,118-9], the mechanistic aspects of $M^{+\cdot}$ ion formation remain nebulous. It has been suggested that $M^{+\cdot}$ ion formation occurs by a mechanism in which neutral analytes are sputtered and subsequently ionized through collisions with the high energy bombarding particles of the primary beam (Reaction(#)).

$$M_{gas} + Xe_{fast} \text{ or } Cs^{+}_{fast} \longrightarrow M^{+\cdot} + e + Xe_{fast} \text{ or } Cs^{+}_{fast} \qquad [29]$$

This process is normally referred to as gas-phase FAB. Bojesen[204] showed that $M^{+\cdot}$ ions could be generated under FAB conditions when vaporized organic samples were introduced in the source of the mass spectrometer. This study is widely quoted in support of gas phase formation of $M^{+\cdot}$. However, the fact that spectra showed variations similar to those obtained under charge transfer ionization implies that the $M^{+\cdot}$ ion formation process is more akin to charge exchange.

$$M + Xe^{+\cdot} \longrightarrow M^{+\cdot} + Xe \qquad [30]$$

The possibility of Penning ionization is also present where FAB is concerned. The possibility of charge transfer and Penning ionization as described above does not exist in LSIMS, where the bombarding entities, cesium ions, *cannot partake in the aforementioned processes*. Recently, it has been suggested that the formation of $M^{+\cdot}$ ions under FAB/LSIMS conditions is not due to direct collisions between analytes and bombarding particles but rather to collision interactions between the analyte and recoiling matrix molecules (B) or matrix ions

($B^{+\cdot}$)[205]. The latter process being a charge transfer interaction (Reaction (31)) arising from beam-induced ionization of the matrix.

$$M + B^{+\cdot} \longrightarrow M^{+\cdot} + B \qquad [31]$$

The formation of $M^{+\cdot}$ due to direct collisions between gas phase analytes and bombarding particles was not retained as a significant mechanism. This is rationalized by the difference observed in the FAB spectra when the analytes are introduced in the source in a gaseous form and when the spectrum is obtained with the assistance of a liquid matrix. The gas phase results show the formation of $M^{+\cdot}$, M^{2+}, and M^{3+} from the polyaromatic analytes. In the matrix-assisted FAB spectra, only $M^{+\cdot}$ was observed.

The effect of liquid matrix selection on $M^{+\cdot}$ formation has been observed[206-208,109]. Naylor et al[109] reported the increased proportion of the radical cation of porphyrins with respect to $[M+H]^+$ in NBA compared with TDG. This was attributed to the electron accepting capacity of NBA. A series of alkaloid indoles also gave significant $M^{+\cdot}$ formation in FAB with several liquid matrices. The most intense $M^{+\cdot}$ ions were observed in NBA and HEDS, matrices recognised as strong inhibitors of reduction processes[207]. Takayama[208] has reported the effect of matrix selection on the $M^{+\cdot}/[M+H]^+$ ratio of various analytes. The $M^{+\cdot}/[M+H]^+$ ratio increased gradually on going from 'alcoholic' to nitroaromatic matrices. Intermediate values were obtained with thiol containing matrices. This order of 'alcoholic'< thiol-containing < nitroaromatic matrices

is similar to the electron scavenging capacity of the compounds estimated on the basis of the dehalogenation inhibiting capacity. It appears that the formation of $M^{+\cdot}$ ions is favored in matrices with a significant electron scavenging capacity. If $M^{+\cdot}$ formation is increased in electron scavenging matrices, this observation would be consistent with a previous study on the ionization processes occurring in the LSIMS of derivatized oligosaccharides[206]. It should be stressed that electron scavenging matrices are not a prerequisite for $M^{+\cdot}$ formation in FAB/LSIMS. However, there are strong indications that such matrices favour $M^{+\cdot}$ formation. In order to rationalize the relationship between the electron scavenging capacity of the matrix and increased $M^{+\cdot}$ formation, the following mechanistic scheme is proposed (*vide infra*).

$M^{+\cdot}$ formation can occur in the condensed phase upon interaction of the analyte with the fast ion beam (reaction **32**) or with a beam generated oxidizing transient species. Furthermore, with an electron scavenging matrix (reaction **33**), ion-electron recombination in solution (reaction **34**) would be diminished. Hence, beam-induced $M^{+\cdot}$ ions formed in the condensed phase as a result of the net process (reaction **35**) could be ejected and detected.

$$M \xrightarrow{\overrightarrow{Cs^+}} M^{+\cdot} + e \qquad [32]$$

$$Matrix + e \longrightarrow Matrix^{-\cdot} \qquad [33]$$

$$M^{+\cdot} + e \longrightarrow M \qquad [34]$$

$$M + Matrix \longrightarrow Matrix^{-\cdot} + M^{+\cdot} \quad [35]$$

This is a beam-induced oxidation process where the redox properties of the matrix or that of its beam-induced transients could play a dominant role.

By monitoring the presence or absence of the $M^{+\cdot}$ of various compounds of known oxidation potentials in a series of matrices, it was hoped to roughly bracket the reduction potentials of the various matrices under bombardment conditions. The structure of the compounds are shown in Figure 36. The results of the redox potential bracketing experiment are shown below in Table XVI. Unfortunatly, data could not be obtained in glycerol due to the insolubility of the compounds used. However, this is not a major drawback as glycerol is widely recognized as being the most 'reducing' matrix available.

Table XVI. Matrices showing $M^{+\cdot}$ for various compounds of known oxidation potential.

COMPOUNDS	Eox (Volts)	MATRICES with $M^{+\cdot}$
Tetramethylphenylene diamine (TMPD)	0.16	Thiogly, TDG, HPEA,
Benzidine	0.32	DMBA, MES, HEDS,DEP,
Phenothiazine	0.70	and NBA
Tris(4-bromophenyl)amine (TBA)	1.00	MES, HEDS, NBA
Anthracene	1.20	NBA

As can be seen from the data presented in Table XVI, there appears to be a correlation between the ability of the matrix to induce $M^{+\cdot}$ ion

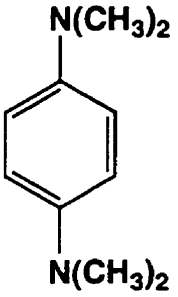

Tetramethyl phenylene diamine (TMPD)

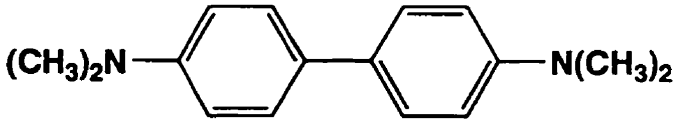

N,N,N',N'-Tetramethylbenzidine

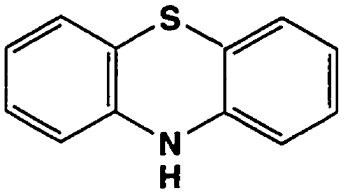

Phenothiazine

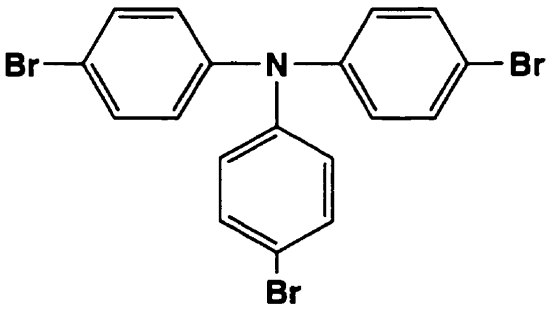

Tris(4-bromophenyl)amine (TBA)

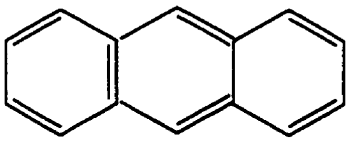

Anthracene

Figure 36. The structure of the compounds used for the matrix redox potential bracketing study

formation from the analyte and to inhibit a reduction process such as dehalogenation. Thus, as the oxidation potential of the analyte increases, fewer matrices appear capable of generating a significant $M^{+\cdot}$. These matrices are invariably the compounds possessing the highest dehalogenation inhibiting efficiency. The implication of high dehalogenation inhibition efficiency matrices in oxidation processes involving the analyte is substantiated by a study of the factors affecting the extent of reduction observed in the FAB/LSIMS spectra of peptides[130]. In this study, the extent of analyte oxidation observed in HEDS, NBA, and HBSA were generally found to be higher than for other matrices. These results are in agreement with the arguments presented here.

The matrix most apt at inhibiting dehalogenation, NBA, can generate the radical cation from all the compounds used in this study including anthracene, the molecule with the highest oxidation potential in the series. The capacity of NBA to induce $M^{+\cdot}$ formation from aromatic molecules under FAB/LSIMS conditions has been previously reported[206-210,109]. The one electron reduction potential of NBA *under bombardment conditions* was estimated to be around 1.2V[136] The reduction potential value was later confirmed by Kuruno et al[210] in their LSIMS study of π-electron donors. This value is much greater than that obtained by cyclic voltametry (-1.15V in acetonitrile)[210]. The great difference in the one electron reduction potential between the electrochemical value and that obtained using the FAB/LSIMS bracketing technique was rationalized by invoking the involvement of excited matrix species generated by the bombardment process. This

argument originates from the work of Kemp et al. who demonstrated through pulse radiolysis that excited nitroaromatics were powerful oxidative quenchers[211]. For example, the difference in reduction potential of the nitroaromatic compound N-(n-butyl)-5-nitro-2-furamide ($BNFA/BNFA^{-\cdot}$ = -0.23V vs NHE) and its triplet excited state ($^3BNFA/BNFA^{-\cdot} \approx 2.23$V vs NHE) is approximately 2 volts. This value is similar to the difference between that obtained for the reduction potential of NBA determined electrochemically and that estimated under LSIMS bombardment conditions[210]. The possible involvement of the triplet excited state of NBA is feasible since triplet states tend to be longer lived than others.

In the case of the analyte with the second highest oxidation potential, TBA, significant $M^{+\cdot}$ can be generated when the matrix is NBA, MES, or HEDS. Significant $M^{+\cdot}$ generation in HEDS could be the result of its electron scavenging properties. The role of the $(HEDS)^{+\cdot}$ species may be determining as the reduction potential of the $(R\text{-}SS\text{-}R)^{+\cdot}$ species (1.13V)[212] may allow the oxidation of TBA. There does not appear to be a ready explanation for the ability of MES to foster $M^{+\cdot}$ formation in this instance. We can only note the parallel between the propensity of the matrix to yield $M^{+\cdot}$ ions and its dehalogenation inhibiting tendency.

TMPD, benzidine, and phenothiazine yield a significant $M^{+\cdot}$ ion in all the matrices used. Thus, most matrices except those with high dehalogenation inhibiting efficiency will have difficulty fostering

$M^{+\cdot}$ formation for compounds having oxidation potentials higher than 0.7-0.9V.

For aromatic matrices with electron donating groups, another possible mechanism of $M^{+\cdot}$ ion formation would consist of charge transfer. In a manner analogous to that of HEDS, the radical cations of DMBA and HPEA are dominant in the molecular ion of the LSIMS spectra of these matrices. The formation of the matrix radical cations are anticipated to occur through beam-induced processes in the condensed phase (Reaction **36**).

$$\text{Matrix} \xrightarrow{\overrightarrow{Cs^+}} \text{Matrix}^{+\cdot} \qquad [36]$$

The beam-induced matrix radical cations could possibly contribute to the $M^{+\cdot}$ intensities observed in DMBA and HPEA through charge exchange with the analyte (Reaction **37**).

$$M + \text{Matrix}^{+\cdot} \longrightarrow \text{Matrix} + M^{+\cdot} \qquad [37]$$

For phenothiazine, the interest lies in monitoring the $M^{+\cdot}/[M+H]^+$ ratio in the different matrices in order to compare the trend obtained with chlorpromazine. These results, shown in Table XVII, confirm the trend initially observed for chlorpromazine. Namely, that $M^{+\cdot}$ formation is more favored in matrices of higher dehalogenation inhibiting efficiency or electron scavenging capacity. Takayama[208]

has reported the effect of matrix selection on the $M^{+\cdot}/[M+H]^+$ ratio of various analytes. Although the number of matrices used was smaller and did not include aromatic matrices with electron donating substituents, the trend observed is similar to the one observed in this study. As a matter of fact, some of the $M^{+\cdot}/[M+H]^+$ ratios obtained in that study can be interpreted on the basis of analyte oxidation potential. When NBA is the matrix, the $M^{+\cdot}/[M+H]^+$ ratio exhibited by trolox (E_{ox}=0.48V)[47] was 5.2 compared to that of antipyrine, 0.33, with an E_{ox} greater than 1.2V[213]. When the thiol containing matrix dithiothreitol/thioglycerol was used, the $M^{+\cdot}/[M+H]^+$ ratio was 1.6 and 0.13, respectively.

Table XVII. The effect of matrix selection on the $M^{+\cdot}/(M+H)^+$ ratio for phenothiazine.

Matrix	$M^{+\cdot}/(M+H)^+$
NBA	3.6
DEP	3.2
HEDS	3.1
MES	2.9
HPEA	2.4
DMBA	2.3
THIOGLY	1.7
TDG	2.1

The observation that matrices such as thioglycerol can generate $M^{+\cdot}$ under LSIMS conditions for compound of oxidation potential lower than 1.0V is in agreement with the hypothesis that the bombardment process produces thiyl radicals ($RS^{\cdot}$). Using pulse radiolysis techniques, it has been shown that thiyl radicals oxidize phenothiazine drugs (Eox $\leq$

0.8V)[214,216]. The reduction potential of thiyl radicals has been estimated to be 0.84V[212].

The fact that $M^{+\cdot}$ formation is increased in electron scavenging matrices is consistent with our previous study on the ionization processes occurring in the LSIMS of derivatized monosaccharides[206]. $M^{+\cdot}$ formation can occur in the condensed phase upon interaction of the analyte with the fast ion beam or interaction with beam-generated oxidizing transient species, such as thiyl radicals. With an electron scavenging matrix, ion-electron recombination in solution would be prevented. Hence, $M^{+\cdot}$ ions could be ejected and detected.

The role of solution charge transfer reactions has been suggested previously to account for important $M^{+\cdot}$ formation[116]. The possible role of charge transfer complex formation is illustrated by the colour change observed when benzidine and phenothiazine were dissolved in NBA prior to analysis. The resulting mass spectra showed almost complete matrix suppression, perhaps indicating the significant presence of pre-formed ions in solution. The mass spectrum of phenothiazine and benzidine in NBA are shown in Figures 37(a)-(b), respectively.

The importance of the radical cascade generated by the FAB/LSIMS bombardment process in the reduction-oxidation behaviour of the respective matrices is underlined by the following observations pertaining to the methylene blue system[117]. Prior to bombardment, the colour of a methylene blue/glycerol solution is a brilliant royal blue. After exposure to the primary beam for a given time, the

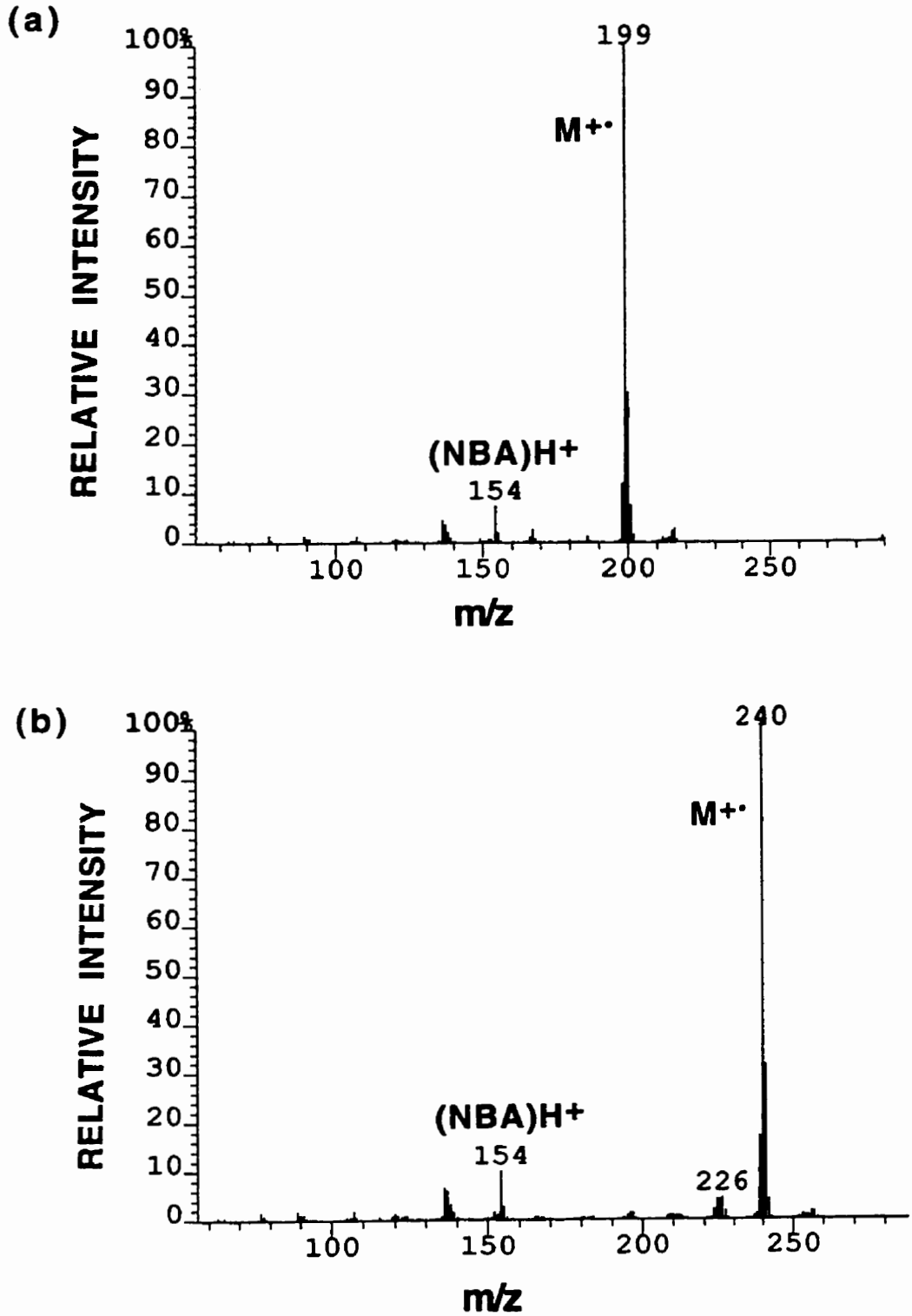

Figure 37. LSIMS mass spectrum of (a) phenothiazine in NBA, (b) benzidine in NBA.

solution has become clear. The clear colour indicates the presence of the completely reduced form of the analyte, called leucomethylene blue. Conversely, when methylene blue is dissolved in thioglycerol, the solution eventually turns clear. This is a well known though complicated chemical reduction reaction of the dye by thiols[215]. When this clear solution is submitted to bombardment, the colour of the solution partly reverts to the original blue colour.

An interpretation of these observation could easily be linked to the nature of the radical cascades initiated by the bombarment process in the respective matrices, glycerol and thioglycerol. In the case of glycerol, the bombardment of the solution is accompanied by a colour change indicative of a reduction process. This implies that the bombardment-generated radical cascade is of a reducing nature. This interpretation is in accord with pulse radiolysis literature. In the case of the thioglycerol/methylene blue system, the solution is chemically reduced prior to the bombardment process which, in turn, apparently oxydizes the analyte or part of it to its original state (blue colour). It is likely that oxidizing thiyl radicals are generated in the bombardment process, thus leading ultimately to the initial state of the analyte. This behaviour is schematically described in Figure 38.

It should be noted that the leuco (reduced) form of methylene blue is a phenothiazine ring system with electron donating substituents. The ease of oxidation of leucomethylene blue should therefore be comparable, if not lower, than phenothiazine itself. This last point

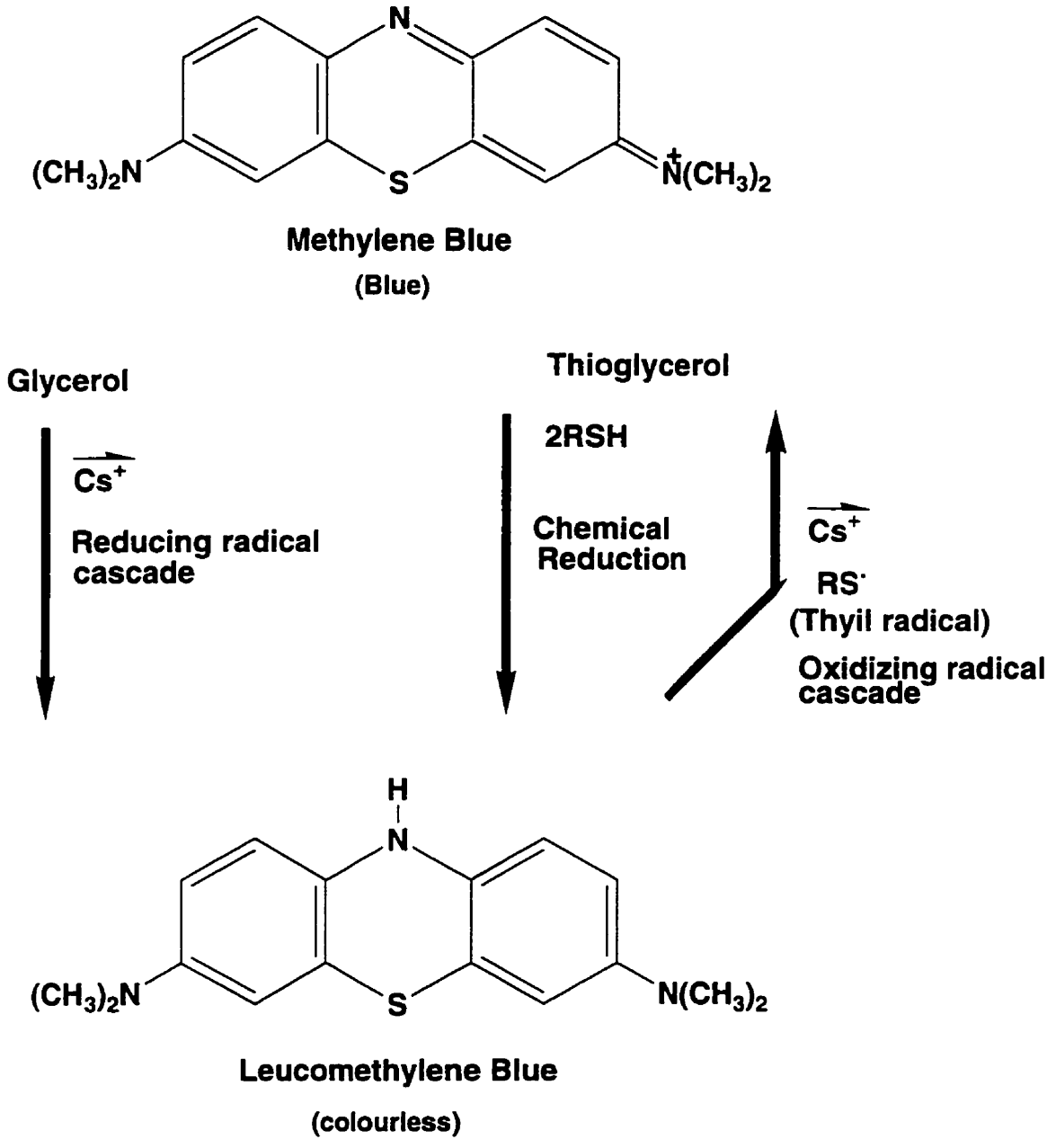

Figure 38. Scheme illustrating the redox processes proposed to occur in the methylene blue/thioglycerol system.

is important since it would be consistent with the beam-induced generation of thiyl radicals in thioglycerol. A pulse radiolysis study have shown that thiyl radicals generated from mercaptoethanol can oxidize phenothiazine at a fast rate[216].

It cannot be overemphasized that the extent of the role of the matrix in favouring or even fostering $M^{+\cdot}$ formation in FAB/LSIMS remains largely unknown. A multiplicity of processes may contribute to $M^{+\cdot}$ formation. The correlation between $M^{+\cdot}$ formation and the matrix can only be acknowledged and rationalized along lines similar to those used to explain the dehalogenation inhibition efficiency scale. Essentially, the matrix may contribute to the appearance of $M^{+\cdot}$ ions in the FAB/LSIMS spectrum by two pathways. The first one would involve the inhibition of ion-electron recombinations (reaction **33**). In the second case, the analyte molecule may be oxidized to $M^{+\cdot}$ by a beam-induced matrix species such as the thiyl radical.

6.2 Beam-induced matrix chemistry and radiation chemistry

6.2.1 Introduction

This section of the thesis is meant to offer an in depth discussion of the application of radiolytic data and concepts to the rationalization of the redox behaviour of matrices under FAB/LSIMS conditions. This will allow a qualitative description of the medium created by the matrix under conditions of bombardment.

Matrix selection has been shown to be the overwhelmingly dominant FAB/LSIMS experimental factor affecting dehalogenation as well as other beam-induced processes[9,21,22,31,34-36]. Although many studies have been devoted to the effect of matrix selection on beam-induced processes, few have sought to explain the mechanistic trappings of reduction quenching by the matrix. The problems underlying an attempt to establish such a mechanistic framework are two-fold:

(a) The identification of the agents responsible for the reduction process.

(b) The emphasis on the properties of the 'intact' matrix molecule and neglect of the role of the nature of the radical cascade generated under FAB/LSIMS conditions which has never been addressed in a systematic fashion and remains a relatively unexplored area. The electron/radical scavenging capacity of the intact matrix molecule is a very limited approach.

The rationalization of matrix electron scavenging capacity on the basis of the properties of the intact matrix molecule such as electron

affinity is of limited usefulness to rationalize the reduction inhibiting capacity obtained with the aliphatic matrices since little is known on their electron affinities or the correlation between their structural features and that physical property. Furthermore, semi-empirical MNDO calculations for the electron affinities of glycerol and thioglycerol give large negative values which appears to imply rather convincingly that these molecules are unlikely to scavenge electrons[31,35]. This reasoning also applies to the aromatic matrices possessing electron-donating groups. Hence, on the basis of the most advanced reasoning presented in the literature, the matrix electron scavenging capacity of only two matrices (DEP and NBA) out of the 12 used in this study can be explained on solid empirical grounds.

In the case of dehalogenation, evidence has been presented in section 5.2 strongly supporting the dominant role of beam-generated secondary electrons as initiating agents of this reduction process. The above interpretation is supported by results obtained with other techniques, since a similar trend exists in pulse radiolysis[37-38] and electrochemistry[39-40], where reductive dehalogenation is initiated by the electron. Similar findings pointing to the role of secondary electrons were presented concerning the reduction of 4-(4-chlorobenzoyl)pyridine (see section 5.3). These findings allow the matrix effects on the dehalogenation process to be examined in terms of the electron scavenging capacity of the matrix.

The LSIMS spectra obtained for various haloaromatics in the wide variety of matrices used in this study has yielded a relationship

between specific matrix structural features and the observed extent of dehalogenation. This relationship is well illustrated by the data obtained from chlorpromazine and the 4-halophenylalanine methyl esters and is shown in Tables II and VI. From this data, it appears that the matrices can be grouped in three distinctive categories in terms of their ability to inhibit the dehalogenation process. Glycerol and AET stand out as the least effective matrices of the twelve matrices used. Thioglycerol, TDG, MES, HEDS, BOP, DMBA, and HPEA form another group where dehalogenation is substantially reduced with respect to hydroxy-only aliphatic matrices but is still present. Matrices in which dehalogenation is absent form the last group including NBA, DEP, and HBSA. In fact, the aromatic and sulfur-containing matrices can be further split into 2 sub-groups to give a total of five matrix structural features which qualitatively match the observed extent of dehalogenation in the compounds studied.

A closer look at the data reveals that grouping the matrices in terms of structural features qualitatively corresponds to the extend of dehalogenation observed for the compounds exhibiting the greatest propensity to dehalogenate, atrazine and 4-iodophenylalanine methyl ester. The relationship between matrix structural feature and dehalogenation inhibiting capacity is as follows:

AROMATIC e-withdrawing groups	> ALIPHATIC >1 sulfur RSSR	> AROMATIC e-donating groups	> ALIPHATIC 1 sulfur RSH	> ALIPHATIC alcohol groups

NBA, HBSA, DEP > HEDS, MES > HPEA, DMBA, BOP > TDG, THIOGLY > AET, GLY

In terms of the ability of the matrix to inhibit reduction processes, our results are generally in agreement with those of Vouros[21] who found that for the reduction of organic dyes the order was NBA > HEDS > THIOGLY > GLY. Similar results were obtained by Cook et al.[22] for methylene blue namely, NBA> THIOGLY> GLY. Our scale of dehalogenation inhibiting efficiency is consistent with that of Kelley[31] save for DMBA. In that study, the authors rank DMBA on the same level as glycerol. However, they used only one model compound and six liquid matrices whereas our trends are built upon 6 analytes and 12 liquid matrices. The chlorpromazine[34] results rank DMBA above glycerol and thioglycerol in terms of dehalogenation inhibiting efficiency. This is consistent with the ranking of the two other aromatic matrices having electron donating groups, HPEA and BOP. Unfortunately, it is not possible to use the results obtained for the halo-phenylalanine methyl esters and atrazine to further substantiate our ranking of DMBA since that matrix generates spectral interferences with the dehalogenated products of these analytes (section 5.1). The reduced species resulting from the dehalogenation of the halo-phenylalanine methyl esters and atrazine appear at m/z 180 and 182, respectively. The matrix generates a series of peaks in the mass range m/z 180-183.

In the following pages, the dehalogenation inhibition capacity of the matrices will be rationalised on the basis of the physico-chemical properties of the intact matrix molecules such as electron affinity or reduction potential. Furthermore, the possible contribution of the radical cascades originating from matrix molecules under FAB/LSIMS conditions will be taken into account to explain the extent of

dehalogenation characteristic of each matrix structural feature. In order to investigate radical cascades, a close analogy will be made between the FAB/LSIMS behaviour of matrices and the radiolysis of analogous organic liquids. The analogy is appropriate since both FAB/LSIMS and radiolysis impart energy to a sample indiscriminately which generates radicals, ions, electrons and excited species. The analogy is further justified since electrons and radicals generally tend to react with functional groups present in an organic molecule rather than with the molecule as a whole[217]. Given the evidence presented in previous sections concerning the role of beam-generated secondary electrons as initiating agents of dehalogenation, the emphasis will clearly be on electron scavenging. The radiation chemistry of many organic liquids have been investigated and the characteristics of their radiation-induced transients elucidated[47-48]. This body of literature will be extensively drawn upon.

It is hoped that this systematic overview of beam-induced matrix chemistry based on radiolytic data and concepts will help define the features which determine the redox chemistry observed in FAB/LSIMS of haloaromatics. It should be stressed that what is desired here is the identification of the *salient features* of beam-induced matrix redox chemistry. The complete elucidation of such processes is not the goal sought. Rather, it is the ability to systematically rationalize the matrix redox chemistry observed in FAB/LSIMS on the basis of sound concepts and data that is of interest as well as being of more realistic intent.

6.2.1 Glycerol and the radiation chemistry of alcohols

The extensive body of literature concerned with reduction phenomena under FAB/LSIMS conditions has invariably focused on secondary electrons and 'radicals' as the bombardment-generated reducing agents. However, there appears to have been little effort to describe more accurately the radicals which may take part in beam-induced reduction processes. Given the fact that glycerol is usually the matrix of choice as well as being the matrix where beam-induced reduction processes have the greatest propensity to occur[21,22,31,34-36], a careful study of the literature concerning the radiolytic behaviour of alcohols might yield useful information. It is fortunate that the radiation chemistry of alcohols has been extensively studied. This is probably due to the fact that alcohols are the organic liquids which resemble water the most. In order to gain an insight on the basic radiation chemistry of alcohols and circumvent complexities, it is instructive to look at the simplest alcohol, methanol. Upon irradiation of methanol by ionizing radiation, a complicated mixture of radicals are formed[218]:

$$CH_3OH \rightsquigarrow e^-,\ {}^{\cdot}CH_2OH,\ CH_3O^{\cdot},\ H^{\cdot},\ {}^{\cdot}OH,\ {}^{\cdot}CH_3 \qquad [38]$$

Many of these radicals react very rapidly with the intact alcohol itself to yield more $^{\cdot}CH_2OH$. Therefore, the generation of oxidizing radicals such as $CH_3O^{\cdot}$ and $^{\cdot}OH$ upon irradiation is very quickly neutralized by their fast reaction with an alcohol molecule. The hydroxyl radical reacts with alcohol molecules at diffusion controlled

rates[48]. The fast rate of reaction of the $CH_3O^{\cdot}$ radical with other methanol molecules means that its contribution to the radiation chemistry of methanol is virtually eliminated[219,220]. The reaction of hydrogen atoms with methanol in neat methanol proceeds at a very fast rate ($2.8X10^8$ $M^{-1}s^{-1}$)[221].

$$CH_3O^{\cdot} + CH_3OH \longrightarrow CH_3OH + {}^{\cdot}CH_2OH \quad [39]$$

$$H^{\cdot} + CH_3OH \longrightarrow H_2 + {}^{\cdot}CH_2OH \quad [40]$$

$$^{\cdot}OH + CH_3OH \longrightarrow H_2O + {}^{\cdot}CH_2OH \quad [41]$$

It is noteworthy that most radicals in the radical cascade of aliphatic alcohols react selectively and quickly with intact alcohol molecules to abstract hydrogen from carbons alpha to the hydroxy group thus yielding the reducing α-hydroxyalkyl radical, $^{\cdot}CH_2OH$[218].

$$CH_3OH \xrightarrow{\gamma\text{-Radiolysis}} {}^{\cdot}CH_3 + {}^{\cdot}OH + H^{\cdot} + CH_3O^{\cdot} + {}^{\cdot}CH_2OH + e \quad [42]$$

(CH_3OH under the bracketed $^{\cdot}CH_3 + {}^{\cdot}OH + H^{\cdot} + CH_3O^{\cdot}$)

In short, all the radicals (save e^-) generated upon irradiation are potential precursors to the α-hydroxyalkyl radical. These reactions, coupled with the notoriously slow reaction of electrons with alcohols (or inherent stability of e_{solv} in alcohols) reduce the primary act of irradiation to:

$$CH_3OH \sim\!\!\sim\!\!\longrightarrow e^-, {}^{\cdot}CH_2OH \quad [43]$$

Both e- and $^{\cdot}CH_2OH$ are reducing species. The $^{\cdot}CH_2OH$ is an α-hydroxyalkyl radical ($R_1R_2C^{\cdot}OH$) and these radicals are capable of undergoing one-electron transfer with electron affinic organic compounds[222]. This simple scheme, based on extensive radiolytic investigations[218], offers a very good explanation of the reducing capabilities of alcohols under irradiation. It is noteworthy that electrons and α-hydroxyalkyl radicals are 'stable' i.e. not quickly scavenged in alcohols[222] as other transient species.

The reducing power of α-hydroxyalkyl radicals depends on the degree of substitution and type of substituent[223]. In general, alkyl substitution on the carbon bearing the unpaired electron increases the reducing power of the radical. The reduction potential values for some simple α-hydroxyalkyl radicals are tabulated below (Table XVIII). These values were obtained at pH 7 and converted to the normal hydrogen electrode (NHE). The reducing power of α-hydroxyalkyl radicals greatly increases at high pH and can generate chain reactions. The one-electron reduction potentials for some of the alcohol-derived α-hydroxyalkyl radicals have been reported for methanol, ethanol and isopropanol. The reduction potential values of the solvated electron, hydrogen atom and hydroxyl radical are included below to give a relative idea of the reducing power of α-hydroxyalkyl radicals.The reduction potential of the α-hydroxyalkyl radicals originating from isopropanol, ethanol, and methanol have been measured by many researchers and the values listed above reflect the most recent experimental values determined by Schoneich et al.[224]. These numbers are in agreement with the most often cited values of Lilie[225]. The

question of the *relative* reducing power of the α-hydroxyalkyl radicals is clear but not the absolute reducing power[224].

Table XVIII. Redox potentials of α-hydroxyalkyl radicals compared with the hydrated electron, hydrogen atom and hydroxyl radical[176].

Species	Reduction potential (volts)
e^-	-2.9
$H^\cdot$	-2.4
$(CH_3)_2C^\cdot OH$	-1.32
$(CH_3)HC^\cdot OH$	-1.14
$^\cdot CH_2OH$	-1.05
$^\cdot OH$	1.9

The $(CH_3)_2C^\cdot OH$ radical can be generated from isopropanol under pulse radiolysis conditions. Isopropanol is frequently used in pulse radiolysis as an $H^\cdot$ and $^\cdot OH$ scavenger to ensure reducing conditions where reactions of the solvated electron are being studied[16e]. Consequently, its reactions with a large number of molecules have been investigated[222]. This is obviously essential given the possibility that these radicals have the capability of engaging in reducing electron transfer reactions and these must be differentiated from those of solvated electrons. Given its redox potential, it is not surprising that this species can react by electron transfer with molecules that are sufficiently electrophoric such as acridine, quinoxaline, and 4-amino-nitrobenzene[222]. The ability of α-hydroxyalkyl radicals to reduce porphyrins[226], metalloporphyrins[227], aromatic ketones[228], quinones[229], quaternary pyridinium salts[230], metal ions[231] and cationic dyes[232] is also well documented. All the evidence presented

above clearly illustrates that the reducing power of α-hydroxyalkyl radicals has been amply demonstrated by pulse radiolysis. Furthermore, this type of radical has been shown to be a dominant species resulting from the radiolysis of alcohols. Therefore, the radiation chemistry of aliphatic alcohols is generally characterized by the following 'net' process:

$$R\text{-}CH_2OH \rightsquigarrow R\text{-}^{\bullet}CHOH + e \qquad [44]$$

where the radical cascade is rapidly reduced to 'solvated' electrons and α-hydroxyalkyl radicals both of which are highly reducing species. Hence, the radiolytic radical cascade of aliphatic alcohols is highly reducing in nature. It should be stressed that there are no efficient mechanism to quench these reducing species. The stability of electrons in liquid alcohols is well known[101]. Furthermore, secondary alcohols are used as hydrogen atom and hydroxyl radical scavengers in the study of the reaction of electrons in aqueous pulse radiolysis to ensure that only reducing reactions due to the hydrated electron (and possibly α-hydroxyalkyl radicals) are observed[176]. If the analogy between the radiolytic behaviour of alcohols and that of glycerol under FAB/LSIMS conditions can be demonstrated to be valid, the high propensity of glycerol to favour reduction processes under FAB/LSIMS conditions could be rationalised on solid empirical grounds. In order to establish the analogy between the radiolytic and FAB/LSIMS behaviour of alcohols, it is important to demonstrate the existence of evidence supporting the generation of secondary electrons and α-hydroxyalkyl radicals in glycerol under keV particle bombardment.

The production of α-hydroxyalkyl radicals upon keV particle bombardment of glycerol has been firmly established[8,102,104-5]. Field[8] suggested that new compounds produced upon bombardment of glycerol originated from the recombination of C-centered (α-hydroxyalkyl) radicals. In an effort to further extend the work of Field, the stable end products formed by the FAB irradiation of pure glycerol were analyzed by GC-MS[104]. The results confirmed the hypothesis that keV particle bombardment of glycerol produces α-hydroxyalkyl radicals which recombine to form new molecular species. The identity of these molecular products was further confirmed by Gross et al[105] using tandem mass spectrometry and high resolution measurements. The FAB/LSIMS analysis of cationic surfactant in glycerol has been shown to yield molecular products corresponding to the ion series $(M+30)^+$, $(M+60)^+$, and $(M+90)^+$. These surfactant-matrix adduct ions presumably arise from the recombinations of beam-induced α-hydroxyalkyl radicals with surfactant radicals arising from the hydrogen abstraction on the saturated carbon chain[102,103]. The α-hydroxyalkyl radicals that can be formed from glycerol are shown below in Figure 39.

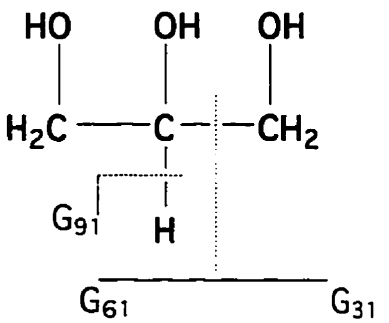

Figure 39. Diagram depicting the α-hydroxyalkyl radicals formed from glycerol in the FAB/LSIMS process.

The beam-induced homolytic cleavage of C-C and C-H bonds lead to the formation $^{\cdot}G_{31}$, $^{\cdot}G_{61}$, and $^{\cdot}G_{91}$ α-hydroxyalkyl radicals. The $^{\cdot}G_{91}$ α-hydroxyalkyl radical could also arise from beam-induced radical attack on a glycerol molecule. The implication of the above exposé in the context of FAB/LSIMS is that having firmly established the notion that generation of α-hydroxyalkyl radicals is an intrinsic part of the bombardment process, their possible contribution as reducing agents (through electron transfer) has been completely overlooked. For example, numerous FAB/LSIMS studies have been devoted to the reduction of organic dyes[17-22], particularly methylene blue. A pulse radiolysis study has demonstrated that this compound reacts at fast rates with the $(CH_3)_2C^{\cdot}OH$ and $^{\cdot}CH_2OH$ radicals by electron transfer[232].

The α-hydroxyalkyl radicals could also be involved in the formation of molecular radical anions observed in the negative ion FAB/LSIMS mass spectra of electron affinic compounds (nitro compounds). The α-hydroxyalkyl radicals are also known to reduce porphyrins[226] and metalloporphyrins[227]. These radicals could be involved in the beam-induced reductive demetallation of metalloporphyrins in FAB[109].

It is reasonable to postulate that the electron transfer reactions of the $(CH_3)_2C^{\cdot}OH$ radical with molecules of known reduction potential can be used to estimate the likelihood of such reactions in FAB/LSIMS when glycerol is the matrix. The analysis of beam-induced radical-radical coupling products originating from neat glycerol indicate that one of the precursors to many such products is $HOCH_2C^{\cdot}(OH)CH_2OH$[8,102-5] ($^{\cdot}G_{91}$).

This radical bears a structural resemblance to the α-hydroxyisopropyl radical and one can reasonably assume its reducing power to be similar. The range of the reducing power of the α-hydroxyalkyl radicals produced by the keV particle impact of glycerol can be roughly estimated using pulse radiolysis data.

The reducing power of $^{\cdot}G_{91}$ and the α-hydroxyisopropyl radical appear to be similar as the rate of reaction of these radicals with the metalloporphyrin hemin III c are comparable. The rate constants for electron transfer of the $^{\cdot}G_{91}$ and α-hydroxyisopropyl radicals with hemin III c are 1.3×10^9 and 2.8×10^9 $M^{-1}s^{-1}$, respectively[233]. The only other comparison of the reducing power of the α-hydroxyalkyl radicals generated from isopropanol and glycerol concern electron transfer to the radiosensitizer (and thus electron affinic) anti-5-nitro-furaldoxime[234]. For the $^{\cdot}G_{91}$ and α-hydroxyisopropyl radicals the rate constants for electron transfer are 1.3×10^9 and 3.3×10^9 $M^{-1}s^{-1}$ The difference in rate constants is strikingly similar to the metalloporphyrin study. In fact, the reducing power of $^{\cdot}G_{91}$ was more similar to the α-hydroxyethyl radical as demonstrated by the similarity in the rates of electron transfer with anti-5-nitro-furaldoxime.

For $^{\cdot}G_{61}$, which is essentially the α-hydroxyalkyl radical stemming from ethylene glycol, the situation is clearer as polarographic and pulse radiolysis experiments have shown that its reducing power is somewhat less than that of the structurally analogous α-hydroxyethyl radical[235]. The $^{\cdot}G_{31}$ radical is the α-hydroxymethyl radical which can

be generated from methanol and hence represents the lower end of the reducing power of the α-hydroxyalkyl radicals generated from the irradiation of glycerol.

Admitedly, the above data is limited and comparison of the reducing power of the α-hydroxyalkyl radicals generated from glycerol to those originating from structurally analogous alcohols is based on few examples. However, one can place the range of the reducing power of the α-hydroxyalkyl radicals generated from glycerol as falling between that of the the α-hydroxymethyl and α-hydroxyethyl radical. In terms of reduction potentials, this implies a range of -1.14 to -1.05V if one relies on the most recent determination of these properties[234].

Similarly, species such as $^{\cdot}CH(OH)CH_2OH$ ($^{\cdot}G_{61}$) and $^{\cdot}CH_2OH$ ($^{\cdot}G_{31}$) have been proposed as precursors of radical-radical coupling in FAB/LSIMS. The yield of such radicals and their contribution to reduction processes under FAB/LSIMS conditions are difficult to evaluate but should certainly not be entirely ignored. For example, the reduction of the methyl viologen dication to $M^{+\cdot}$ in the glycerol FAB spectrum[112] could be due in part to electron transfer from secondary α-hydroxyalkyl radical formed during the bombardment process. This is in fact confirmed by a pulse radiolysis study where it was established that methyl viologen was quickly reduced to the radical ion $M^{+\cdot}$ by the $^{\cdot}CH_2OH$ radical ($k=3X10^8\ M^{-1}s^{-1}$)[236]. Other FAB/LSIMS examples involving compounds for which α-hydroxyalkyl radicals have been demonstrated to be efficient reducing agents involve quinones[112], aromatic ketones[36],

metal ions[17] and pyridinium salts[112], organic dyes[17-22] and porhyrins[109,127].

In a pulse radiolysis study of reductive dehalogenation, the authors concluded that α-hydroxyalkyl radicals did not react with chlorotoluene[237]. This is not surprising since α-hydroxyalkyl radicals transfer electrons to compounds having an electron affinity greater than about 0.5eV. The results presented in section 5.2 indicate that dehalogenation does not occur when the electron affinity of the haloaromatic compound is high. Hence, when electron transfer occurs from a α-hydroxyalkyl radical, dehalogenation is not likely to occur. The point is further made by considering the work of Mincher et al[179] where the radiolytic degradation of octachlorobiphenyl was investigated in pure isopropanol. Scavenging experiments suggested that dehalogenation was almost totally initiated by the solvated electron and marginally by α–hydroxyalkyl radicals. Hence, it is reasonable to propose that α-hydroxyalkyl radicals do not significantly contribute to the beam-induced dehalogenation process.

As stated earlier, there exists ample experimental evidence supporting the generation of α–hydroxyalkyl radicals under FAB/LSIMS conditions. The situation is not as clear where secondary electrons are concerned. The proposition[36,83,87,92,105,110,112] concerning the initial processes occurring upon keV particle impact where glycerol molecules are ionized through ejection of secondary electrons has generally been accepted. The results presented in this thesis (section 5.2 and 5.3)

and elsewhere[36] strongly support the contention that beam-induced generation of secondary electrons occurs in FAB/LSIMS.

Clayton and Wakefield[112] suggested that the formation of 'unusual' ions such as $M^{+\cdot}$, $M^{-\cdot}$, $(M+H)^-$, and $(M-H)^+$ could be accounted for by the generation of ionization cascades upon bombardment. Such cascades would be similar to those proposed for radiation chemistry. The initial step would involve ionization of an analyte or glycerol molecule by the ejection of an electron. Kebarle et al.[92] contended that "the chemistry in FAB/LSIMS is, according to our model, expected to be similar to what is found in high energy radiation chemistry" where the production of secondary electrons is characteristic. Williams and co-workers[110] proposed that keV particle impacts cause the production of electrons (via ionization of the sample or matrix) and that these electrons can be effective reducing agents once they have reached thermal energies.

Field and Katz[44] observed the formation of numerous ions in the bombardment of gaseous rare gases by low keV rare gas atoms and ions. On the basis of these results, it was postulated that since gas phase FAB produced a fair amount of ionization, copious ionization should occur in the condensed phase. It is interesting to note that this consists in a complete change of position from the author's original work on the FAB/LSIMS behaviour of glycerol. In a recent review of ionization in FAB/LSIMS, Sunner[83] postulated that the chemistry fostered by the primary beam in FAB/LSIMS is similar to known

radiation chemistry where matrix molecular ions ($G^{+\cdot}$) and secondary electrons are initially formed upon particle impact.

The idea of secondary electron production under FAB/LSIMS conditions was initially rejected[8] and this proposition was later substantiated by comparison of the stable end products formed in the FABMS and γ-irradiation of pure glycerol. On the basis of these experiments, important mechanistic differences between FAB and γ-irradiation were proposed to exist. The authors concluded that FAB generated products were mostly formed by recombination of carbon-centered radicals whilst γ-radiolysis products resulted primarily from the recombination of O-centered radicals. This result seems odd as the net reaction for alcohol radiolysis (as pointed out earlier) results in the formation α-hydroxyalkyl radicals. Furthermore, the formation of molecular products based on the recombination of α-hydroxyalkyl radicals is a basic radiolysis mechanism also operative for polyhydric alcohols[101]. This result may be due to improper degassing of the alcohol prior to γ-radiolysis since the presence of trace oxygen is known to quench all α-hydroxyalkyl radicals thus preventing the formation of the products typical of recombination reactions involving α-hydroxyalkyl radicals[101].

The resemblance of the stable end product distribution in the FAB of neat glycerol and a γ-irradiated aqueous glycerol solution saturated with N_2O was interpreted as additional evidence of this hypothesis. The γ-irradiation aqueous alcohols solutions saturated with N_2O is known to favour the formation of C-centered radicals. The main flaw

behind the comparison of the stable end products in FAB and γ-irradiation of glycerol is that the radical products observed in FAB are those that accumulate in the matrix. Thus the radical precursors had to be retained in the liquid. The evaporation and sputtering of at least part of the newly formed molecular products could affect the stable end product distrinution. Hence, the products that accumulate in the matrix are not necessarily representative of the original radicals generated by the bombardment process.

In highlighting the mechanistic differences between FAB and γ-irradiation, the authors completely ignore the different nature of the irradiating particles. The different nature of the irradiating particles gives rise to what radiation chemists call linear energy transfer (LET) effects. The concept of linear energy transfer (LET) refers to the rate at which the radiation (bombarding particle) loses energy to the surrounding medium. In the case of γ-radiation, which consists of high energy photons, the linear energy transfer is low. The consequences of this fact is that the energy is deposited in small isolated clusters of ions and excited molecules and that the radiation penetrates the medium to a great depth. In the case of irradiation with heavy ions, the LET is high. The energy is deposited in columnar tracks which results in a greater density of radiation-induced radicals and ionization. Hence, one product may predominate with low LET radiation and another with high LET radiation though both products should be formed to some extent by both types of radiation[238]. Furthermore, the use of higher LET particles in the radiolysis of

alcohols is known to affect the yield of glycols, which arise from the recombination of α-hydroxyalkyl radicals[238].

Furthermore, there is no knowledge of the similarity of experimental conditions between FAB and γ-irradiation. More specifically, the dose (time of irradiation) and dose rate (beam density) for the two techniques are probably not comparable and these experimental variables are certainly not taken into account in the paper. The lack of dosimetric systems on the FAB/LSIMS side of the experiment renders the possibility of comparison tenuous. The difference in the stable end products generated by FAB and γ-irradiation prompted the authors to conclude that no ionization of glycerol (secondary electron production) occurred under FAB conditions. Discounting the possibility that electrons may be produced in the bombardment process on the basis of stable end product distribution (as above) appears to be unjustified given the notoriously unreactive nature of electrons with alcohols relative to free radical processes triggered by γ-irradiation or keV particles. The production or absence of secondary electrons is unlikely to be gauged by the incomplete stable end product distribution observed in FAB.

The aim of this study is not to elucidate mechanistic details but rather to present a general scheme of beam-induced matrix redox chemistry through the radiation chemistry of analogous organic liquids. On the basis of the above discussion, it is reasonable to postulate that the processes induced in glycerol by keV particle impact bear a general similarity to the basic radiation chemistry of alcohols. The

yields of secondary electrons and α-hydroxyalkyl radicals will undoubtedly be different. The LET effect introduced by the use of a different energy regime and bombarding species undoubtedly will have an effect. However, this does not take away from the fact that this resemblance offers an excellent qualitative rationalisation of the high propensity of glycerol to foster reduction processes under FAB/LSIMS conditions. Hence, the FAB/LSIMS redox chemistry of glycerol can be summed up in the following scheme.

[45]

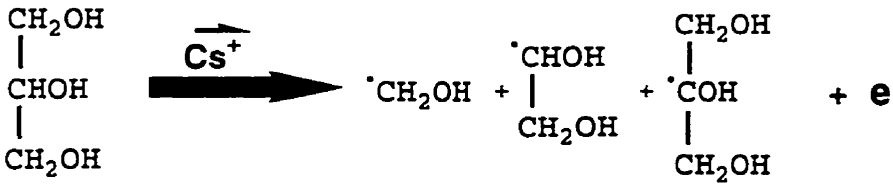

[46]

This scheme is also applicable to beam-induced reduction processes other than dehalogenation. As stated earlier, α-hydroxyalkyl radicals could be involved in the FAB/LSIMS reduction of quinones[112], aromatic ketones[36], metal ions[17] and pyridinium salts[112], organic dyes[17-22] and porhyrins[109,127].

6.2.3 Sulfur containing matrices

The radiation chemistry of thiols and disulfides is dominated by the sulfur containing functionalities. The role of thiols (RSH) and disulfides (RSSR) in radiation protection has been known for many years[239]. The observation that sulphydryl compounds can to some

extent prevent radiation damage *in vivo* has stimulated considerable interest in the radiation chemistry of these compounds[240,212]. The redox properties of organic sulfur and sufur-centered radicals are of particular interest for the understanding of many processes in biological and related systems. In the following section, the matrix redox chemistry of sulfur containing molecules will be examined in light of the known radiation chemistry of thiols and disulfides. Given the complexity of the subject, only the main processes pertaining to the radiation chemistry of sulfur-containing molecules will be dealt with. Some aspects of the redox chemistry of sulfur-containing matrices have already been introduced in section 6.1 and will be mentioned here to ensure a thorough treatment of the subject.

6.2.2.1 Thiols

The electron scavenging capacity of thiol containing matrix molecule has often been mentioned but seldom defined with respect to the other matrices. This is largely due to the fact that electron affinity is not an applicable concept to rationalize the electron scavenging of aliphatic sulfur-containing matrices. A measure of the electron scavenging capacity of thiols can be elaborated by consulting the pulse radiolysis literature. The most recent determination of the rate constant for the reaction of sulphydryl species with the hydrated electron in aqueous solution was performed by Mezyk[241].

$$\mathbf{RSH + e \longrightarrow Products} \qquad [47]$$

A value of $6X10^9$ M^{-1} s^{-1} was obtained for the reaction of mercaptoethanol with the hydrated electron. This result is in general agreement with the data tabulated by Buxton[48] and substantiates the commmonly held view in radiation chemistry as to the good electron scavenging capacity of thiols[240]. The reaction is highly pH dependent and is still under study[241]. This last point is important since the value obtained by Mecyk is lower than the previously accepted numbers.

Given the weakness of the S-H bond, the sulphydryl hydrogen is easily abstracted by most radicals (Reaction **48**) and this results in the thiyl radical ($RS^{\bullet}$) being the most frequent radical species in irradiated thiols. In the case of thioglycerol, if α-hydroxyalkyl radicals are formed, these will also react with the thiol group to abstract a hydrogen and form the thiyl radical. This is the so-called 'repair' reaction which has prompted a great deal of investigative effort given its relevance to DNA radiation damage. The $RS^{\bullet}$ radical could also be formed directly from the interaction of the matrix with the primary beam.

$$RSH + {}^{\bullet}OH,\ H^{\bullet},\ R^{\bullet},\ R\text{-}{}^{\bullet}CHOH \longrightarrow RS^{\bullet} \qquad [48]$$

The generation of thiyl radicals under FAB/LSIMS conditions is supported by experiments performed with methylene blue (see section 6.1) as well as the observation of covalent adducts of dehalogenated atrazine with thioglycerol (see section 5.1). The redox properties of the thiyl radical are those of a good oxidizing agent[212,214,216] (section 6.1). This radical is capable of oxidizing phenothiazine

drugs[214,216] and the redox potential of the thiyl radical generated from the irradiation of mercaptoethanol under pulse radiolysis conditions has been estimated to be 0.8 V[212]. Although the contribution of thiyl radicals to the electron scavenging capacity of thiol-containing matrices is difficult to evaluate, there is no doubt as to the electron scavenging properties of such species.

The implications of the above is that a brief overview of the radiation chemistry of thiols has shown that (a) intact thiol containing molecules have good electron scavenging capacity and (b) the radical cascade is of an oxidative nature as embodied by the thiyl radical and can presumably contribute to the electron scavenging capacity of thiol-containing matrices under FAB/LSIMS conditions. This is a diametrically opposed situation to that found in the radiation chemistry of alcohols (and hence presumably glycerol) where the molecules have essentially no electron scavenging capacity and the radical cascade is reducing. The respective electron scavenging capacities of thiol-containing matrices and alcohols are reflected in the extent of dehalogenation observed in each type of matrix.

An interesting feature of thiyl radicals is that their disproportionation/combination ratios tend to be small. This leads to disulfide formation which have excellent electron scavenging capacity (see next section). The beam-induced formation of disulfides, the extent of which is difficult to gauge, could probably bolster the electron scavenging capacity of the thiol-containing matrices.

6.2.2.2 Disulfides

The electron scavenging capacity of disulfides is excellent as reflected by the diffusion-controlled rate of reaction of these compounds with the hydrated electron ($1\text{-}2X10^{10}$ M^{-1} s^{-1})[240-242] to give a radical anion. The electron scavenging capacity of the intact HEDS molecule is confirmed by the observation of significant $M^{-\cdot}$ ion in the molecular ion region of the negative mode LSIMS spectrum of the matrix which is shown in Figure 40(b).

$$RSSR + e \longrightarrow RSSR^{-\cdot} \qquad k=1\text{-}2X10^{10}\ M^{-1}s^{-1} \qquad [49]$$

The most interesting aspect of electron scavenging by disulfides is that the disulfide radical anion formed through electron capture quickly dissociates to form the thiyl radical and the thiolate anion[242].

$$RSSR + e \longrightarrow RSSR^{-\cdot} \longrightarrow RS^{-} + RS^{\cdot} \qquad [50]$$

The implications of this reaction are important since electron scavenging by the disulfide molecule rapidly leads to the generation of an oxidizing radical, $RS^{\cdot}$. The generation of thiyl radicals from HEDS under FAB/LSIMS conditions is supported by the following observations. In the negative ion spectrum of HEDS, the main peaks consist of HO-CH_2CH_2-S^- and the (HEDS+HO-CH_2CH_2-S)$^-$ adduct. Furthermore, the spectrum of atrazine in HEDS reveals the presence of analyte matrix adduct which can be reasonably explained in terms of radical-radical

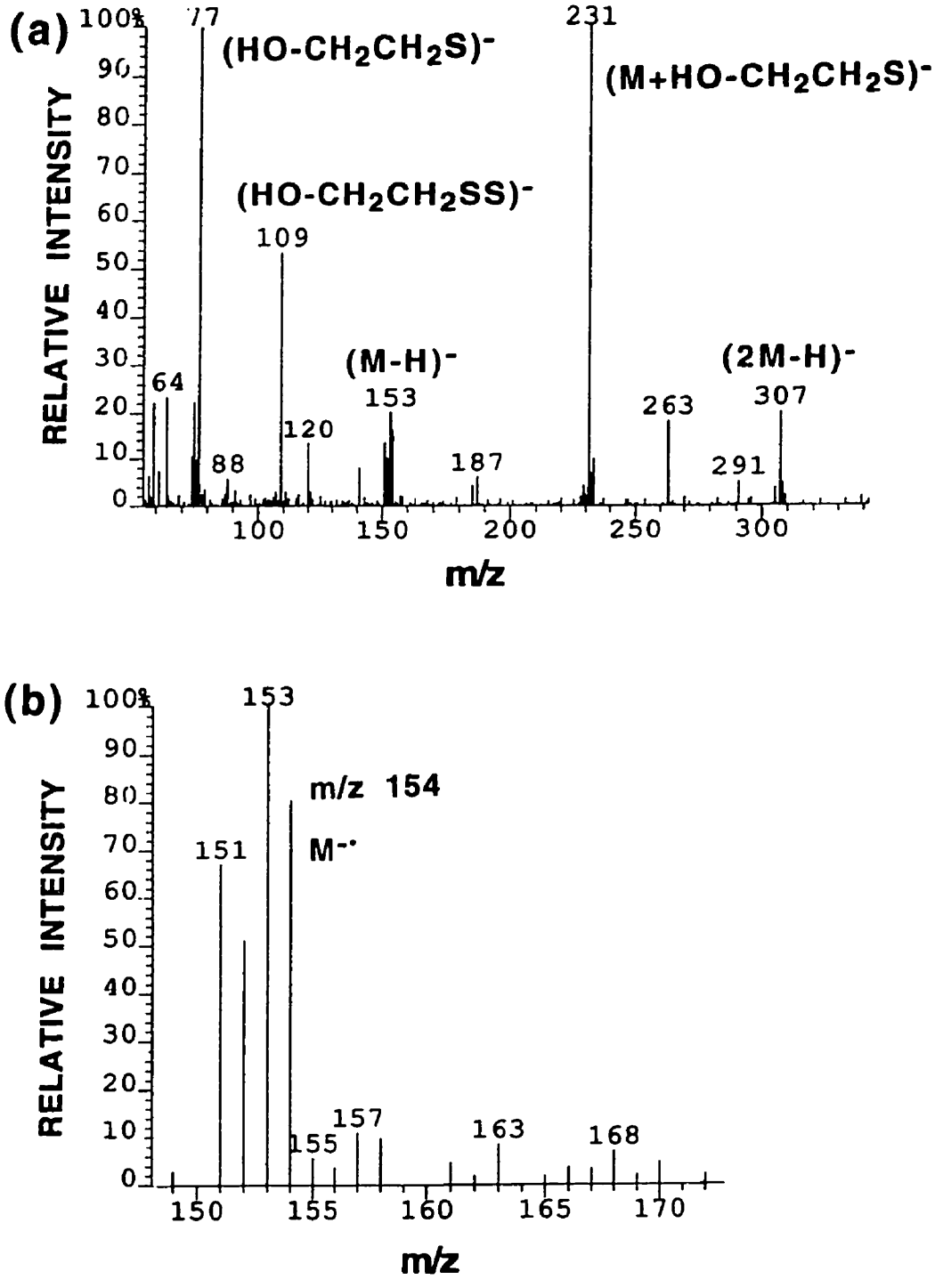

Figure 40. Negative ion mode LSIMS mass spectrum of (a) HEDS, (b) the molecular ion region of HEDS.

recombination involving $HO\text{-}CH_2CH_2S^{\bullet}$ (see section 5.1). It is worthy of note that hydrogen atom scavenging by disulfides is also a very efficient process which also leads to the formation of thiyl radicals[48,240].

Of further interest is the positive LSIMS spectrum of HEDS, where the base peak is the radical cation , $M^{+\bullet}$. This species, undoubtedly the result of beam irradiation, is known to be strongly oxidizing[243-244]. The redox potential of $(CH_3SSCH_3)^{+\bullet}$ has been estimated to be 1.1V by pulse radiolysis experiments. The easy formation and relatively long lifetimes of radical cations is a common feature of the radiation chemistry of disulfides[240]. Thus, in the case of HEDS the quenching of beam-generated secondary electrons occurs through the intact disulfide as well as the thiyl radical and possibly the radical cation $(HEDS)^{+\bullet}$. In this case, the electron scavenging takes place through the matrix molecule and the beam-induced oxidative radical cascade.

$$RSSR \xrightarrow{\overrightarrow{Cs^+}} RSSR^{+\bullet} + e \qquad [51]$$

$$e \xrightarrow{RSSR} RSSR^{-\bullet} \longrightarrow RS^{\bullet} + RS^{\bullet}$$

The interesting aspect of the beam-induced redox chemistry of sulfur containing matrices is that the generation of beam-induced transient species derived from the matrix may bolster the reduction inhibiting capability of a matrix. This is contrary to the view generally

presented in the FAB/LSIMS literature where radicals are invariably involved in fostering reduction, not quenching it. In essence, the salient feature of sulfur-containing matrices is that sulfur functionalities such as thiols and disulfides are highly susceptible to radical attack to yield the oxidizing thiyl radical. Additionally, the matrix molecules possess a measure of electron scavenging capacity which ranges from good (thiols) to excellent (HEDS). In essence, this a behaviour opposite to that of the aliphatic alcohols which have no electron scavenging capacity and which are highly susceptible to radical attack to form reducing species (α-hydroxyalkyl radicals).

6.2.4 Summary for aliphatic molecules

From the previous discussion, it is possible to paint a broad mechanistic scheme describing the beam-induced redox processes pertaining to aliphatic matrices. However, it is important to stress the very complex nature of the radiation chemistry of organic liquids. Therefore, one should remember that what is presented involves a significant amount of simplification. Nevertheless, the qualitative correlation between the main features of the radiation chemistry of specific matrix structural features with the extent of dehalogenation observed in the LSIMS spectrum validates such an exercise.

Essentially, the bombardment process initiates the formation of ions, electrons, excited species, and numerous radical species. The crucial point in the radiation chemistry of the aliphatic matrices is that the numerous radical species initially produced quickly react with the

intact molecule to yield a specific type of radical. Thus, there appears to be a convergence of the radical cascade to a specific radical product. In this way, the radical cascade can be reduced to a few species of specific properties. In the case of alcohols, the convergence of the radical cascade leads to the reducing α-hydroxyalkyl radicals. For sulfur-containing matrices, the thiyl radical is the ubiquitous species resulting from the convergence process. The other factor to consider is the electron scavenging capacity of the intact molecule. The alcohols have virtually no electron scavenging capacity whereas the sulfur containing matrices exhibit good to excellent electron scavenging capacity. As a matter of fact, the stability of electrons in alcohols are well known. The combination of these factors offers good qualitative agreement with the dehalogenation and reduction inhibiting capacity of aliphatic matrices.

6.2.5 Aromatic molecules

The aromatic matrices will be treated in one section. Initially, the contrast in electron scavenging capacity between aromatic compounds with electron withdrawing groups and those with electron donating groups will be explained. Subsequently, a scheme will be drawn up to account for the intermediate ability of aromatic matrices with electron donating groups to mitigate the dehalogenation process.

Since there is a wealth of data on the electron affinity behaviour of aromatic compounds, the electron scavenging capacity of aromatic

matrices can be rationalized on that basis as a starting point. Dehalogenation is present in mass spectra obtained with BOP, DMBA and HPEA. These molecules are comprised of aromatic rings with electron donating groups which should reduce the electron scavenging capability of the molecule. The dehalogenation process is completly inhibited in NBA, DEP, and HBSA. These molecules are comprised of aromatic rings substituted with electron withdrawing groups which should increase the electron scavenging capabilities of the molecule. The above interpretation is, of course, limited, but in the absence of electron affinity data (or other) for all compounds, it is not possible to offer a rationalization of a higher order. The electron affinity of DMBA has been calculated by Kelley[31] and a negative value was obtained. Kebarle et al[162] have shown that the electron affinity of an aromatic compound substituted with an electron withdrawing substituent will be greater than that which is substituted with an electron donating substituent. It is important to note that electron affinities (a gas phase property) appear to follow the same general trend as polarographic half-wave reduction potentials (a condensed phase property).[39,40] The electron affinity of DEP has been experimentally determined to be 0.5eV[149]. The electron scavenging capacity of the phthalate moiety is further demonstrated by the negative ion FAB mass spectrum of the ß-glucoside of mono(2-ethyl-5-hydroxy hexyl) phthalate where an abundant $M^{-\cdot}$ was observed[245]. This ion undoubtedly arises from electron capture by the phthalate moiety which is the only electron affinic component of the molecule.

The electron affinity of NBA could be approximated from the experimental value obtained for an analogous compound, methyl nitrobenzene, which has an electron affinity of about 0.9 eV[2e]. This value is also in accord with the calculated value of 0.92 eV for NBA[31]. The capacity of NBA to scavenge electrons is exemplified by the presence of a proeminent $M^{-\cdot}$ ion in the FAB spectrum of NBA[120]. No electron affinity data exist for HBSA but the structural analog, benzene sulfonic acid, reacts with the hydrated electron at a fast rate in aqueous solution ($4X10^9$ M^{-1} s^{-1})[48].

The ability of NBA to inhibit reduction processes in FAB/LSIMS, including dehalogenation, is well documented[21-2,31,34-5,135]. In their work, Miller and co-workers[135] have suggested that this property of NBA is related to the fact that the matrix can act as an electron sink and thus mitigate chemical damage. Interestingly, a recent report[136] indicated that even for NBA, the reduction-inhibiting capability was limited, though it should be stressed that these results were obtained with organometallic compounds. The reduction inhibiting efficiency of HBSA (the matrix itself is a 60% HBSA/water solution) has been previously compared and found similar to that of NBA in a study of the reduction of disulfide-bridge containing peptides[246].

Hence, the ability of aromatic matrices with electron withdrawing groups to inhibit reduction processes such as dehalogenation is directly linked to their high electron affinity which is a measure of their electron scavenging capacity. However, the electron affinity

framework cannot explain the intermediate dehalogenation inhibiting capacity of aromatic matrices with electron donating groups since these compounds by definition have no electron affinity. The problem can alternatively be defined in terms of differentiating between the behaviour of aromatic and aliphatic structures under conditions of irradiation.

Also neglected is the *yield* of reactive species generated upon particle bombardment as opposed to quenching mechanisms whether it originates from the radical cascade or from the properties of the intact molecule. However, the radiation chemistry classification of aromatic compounds as antirads offers a possible explanation to this state of affairs. Aromatic compounds are much more resistant to radiation than the corresponding alkanes (benzene vs hexane). The truth of this assertion can be verified from the yield of molecular hydrogen and molecular compounds of the respective irradiated liquids. This yield is sixfold higher in hexane compared to benzene.

This can be explained by the electronic structure of aromatic compounds which allows a large fraction of the energy of excited molecules to be channeled to relatively low energy excited states that have a low probability of dissociation[247]. Aromatic groups can also act as energy sinks for energy absorbed by other part of the molecule, and yields of hydrogen and low molecular weight products from substituted benzenes in the condensed phase are generally no greater than those from benzene itself. Furthermore, aromatic hydrocarbons readily form negative ions by electron capture in solution, so that

ion recombination will be between two organic ions rather than between an organic cation and an electron.

$$Ar \xrightarrow{\overrightarrow{Cs^+}} Ar^{+\cdot} + e \qquad [52]$$

$$Ar + e \longrightarrow Ar^{-\cdot} \qquad [53]$$

$$Ar^{+\cdot} + Ar^{-\cdot} \longrightarrow Ar^* + Ar \qquad [54]$$

Negative ions release less energy than electrons in neutralizing reactions, and the probability that the products of the reaction will dissociate is therefore lower than with electron neutralization. The only pulse radiolysis study of an aromatic liquid having electron donating groups is that concerning benzyl alcohol[248]. This study revealed that solvated electrons were not observed using nanosecond pulse radiolysis. This must be due to the electron scavenging capacity of the liquid. This point was further demonstrated by using biphenyl and t-stilbene as solutes. These compounds react very rapidly with the solvated electron in alcohols or water to form the radical anion, $M^{-\cdot}$[48]. However, the radical anions of the solutes were not observed in benzyl alcohol. This was attributed to the electron scavenging capacity of benzyl alcohol. This investigation shows that despite not having a positive electron affinity, aromatic liquids with electron donating groups are capable of scavenging electrons in solution.

A good illustration of the effect of aromatic structure (without the benefit of e-withdrawing groups) on dehalogenation is the matrix BOP. This compound is essentially a glycerol molecule with a benzene

substituted for a hydrogen. BOP has a much higher dehalogenation inhibiting efficiency than glycerol. This obviously can only be due to the presence of the benzene ring. The effect of the phenyl substituent on the aliphatic structure can be rationalized in terms mentioned previously.

Figure 41 summarizes the basic redox properties of the matrices representative of the salient matrix structure features with the extent of dehalogenation observed with 4-I-phenylalanine methyl ester. Although the use of the radiolytic behaviour of salient matrix structural features can only qualitatively describe the general redox behaviour of matrices, this approach nevertheless constitutes an advance relative to the existing views on this complex topic.

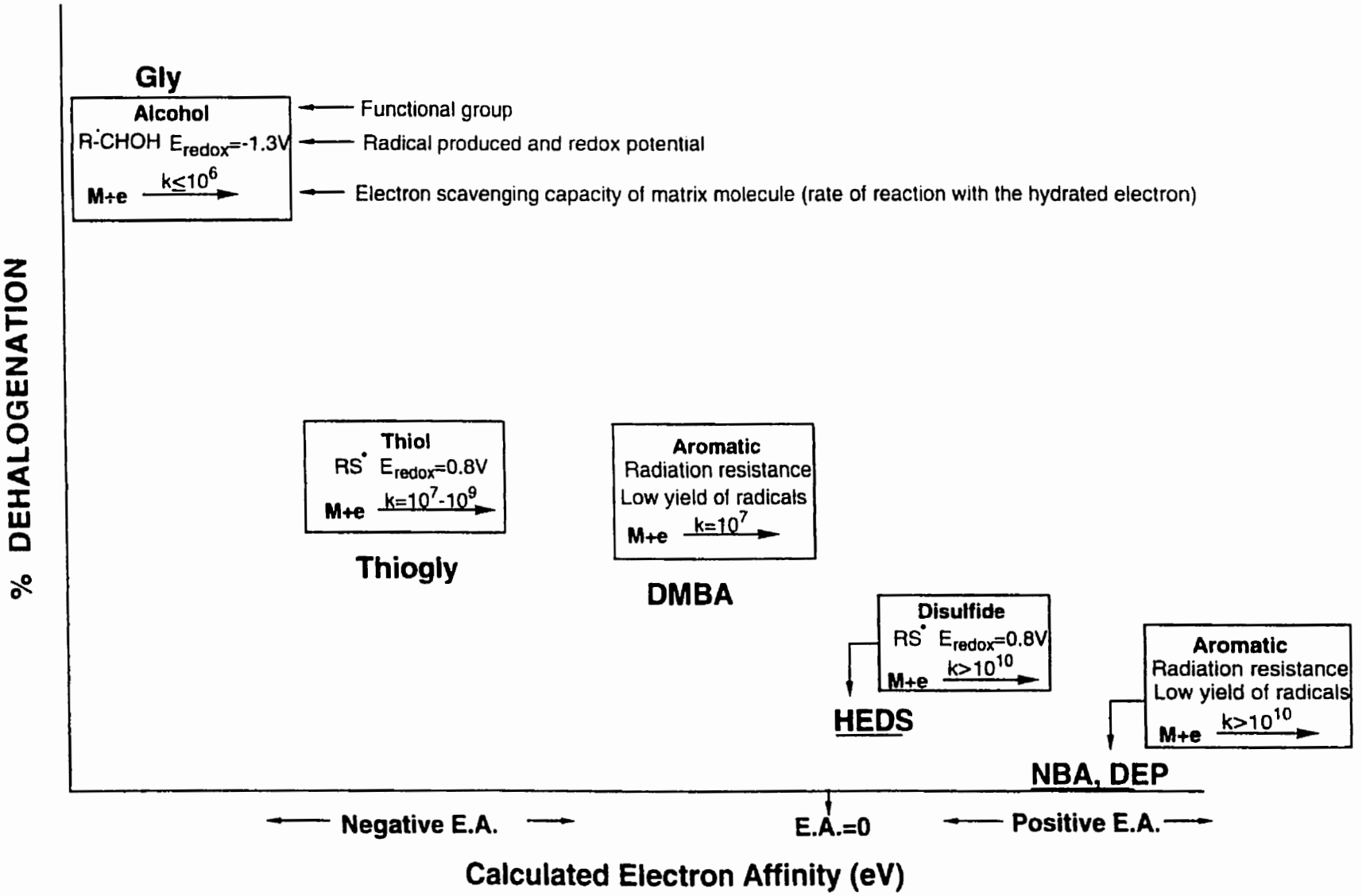

Figure 41. Correlation of the basic redox properties of matrices representative of matrix structural features with the extent of dehalogenation of 4-I-phenylalanine methyl ester.

Chapter 7

Conclusion

The motivation behind the investigation of the LSIMS beam-induced dehalogenation of haloaromatic compounds lies primarily in a desire to dissipate the typically nebulous discourse surrounding most attempts to rationalise beam-induced reduction processes observed in FAB/LSIMS. Of particular interest was the endeavour consisting in fostering a more systematic mechanistic understanding of beam-induced matrix redox processes involved in the inhibition of dehalogenation and perhaps other beam-induced processes. The commonly used umbrella term matrix 'electron/radical scavenging' capacity, though useful, perpetuates the conception that the identity of the agents responsible for beam-induced reductions cannot be pinpointed.

In order to strive towards a clearer understanding of reduction processes through dehalogenation, the effect of experimental parameters on the dehalogenation of the model compound chlorpromazine was investigated. The overwhelming importance of chemical parameters, such as matrix selection, was clearly demonstrated. A rough matrix dehalogenation inhibiting efficiency scale was drawn up and further validated using the complete series of para-halogenated phenylalnine methyl esters. The matrix dehalogenation inhibiting efficiency scale is consistent with the matrix reduction inhibiting capabilities mentioned in the literature. Grouping the matrices in terms of structural features qualitatively corresponds to the extend of dehalogenation observed. Hence, particular matrix structural features (functional groups) qualitatively correspond to a relatively narrow range of % dehalogenation for a specific compound. The relationship

between matrix structural feature and dehalogenation inhibiting capacity is as follows:

AROMATIC e-withdrawing groups	>	ALIPHATIC RSSR	>	AROMATIC e-donating groups	>	ALIPHATIC RSH	>	ALIPHATIC alcohol groups

NBA, HBSA, DEP > HEDS, MES > HPEA, DMBA, BOP > TDG, THIOGLY > AET, GLY

In the LSIMS study of the dehalogenation of chlorpromazine,[34] it was observed that the the analyte radical cation, $M^{+\cdot}$, was present in the spectrum. It was speculated that this species could arise in large part due to matrix-dependent redox processes under LSIMS conditions. Consequently, it was attempted to bracket matrix reduction potentials under bombardment conditions by monitoring $M^{+\cdot}$ formation in different matrices using compounds of known oxidation potentials. This has yielded a link between matrix dehalogenation inhibiting efficiency and $M^{+\cdot}$ formation. The ability of matrices to induce $M^{+\cdot}$ formation parallels their dehalogenation and reduction inhibiting efficiencies. The ability of a matrix to foster a significant $M^{+\cdot}$ ion in the mass spectrum was related to the electron scavenging capacity of the matrix molecule or the generation of oxidizing transient species under bombardment conditions.

In order to elucidate the mechanistic trappings of dehalogenation quenching, the agents responsible for the dehalogenation of haloaromatics had to be identified. This was done through the effects of analyte structure, more specifically those of the aromatic moiety such as electron affinity. The observed trend of decreased dehalogenation with the increasing electron affinity of bromo- and

chloroaromatic compounds was interpreted as being mechanistically consistent with beam-generated secondary electrons being the initiating agents of dehalogenation. The above interpretation is supported by results obtained with other techniques, since a similar trend exists in pulse radiolysis[37] and electrochemistry[39-40] where reductive dehalogenation is initiated by the electron. Pulse radiolysis experiments have also demonstrated that haloaromatics in alcohol solution are exclusively dehalogenated by the solvated electron. These results substantiate the proposition that secondary electrons production is an intrinsic part of the bombardment process in FAB/LSIMS.

Further evidence pointing to the involvement of electrons in the dehalogenation process consists in the respective scavenging affinities of aromatic matrices for hydrogen atoms and electrons. The hydrogen atom has often been invoked as a major contributor to beam-induced reduction processes. In the course of this work, a study of the pulse radiolysis literature revealed that aromatic analogs of the aromatic matrices used in this work had a very similar affinity for the hydrogen atom. Therefore, the involvement of hydrogen atoms in dehalogenation or even some of the other reduction processes could not be rationalised given the very different reduction inhibition efficiency of aromatic matrices with electron withdrawing groups compared to aromatic matrices with electron donating groups. This distinction led to the conclusion that the reduction of 4-(4-chlorobenzoyl)pyridine occured through electron capture followed by protonation and not through direct hydrogen atom addition to the molecule.

This strong evidence implicating beam-generated secondary electrons as the agents responsible for the dehalogenation allowed matrix dehalogenation inhibiting efficiency to be rationalised according to the electron scavenging capacity of the matrix. However, the rationalisation of matrix electron scavenging capacity on the basis of the properties of the intact matrix molecule such as electron affinity is of limited usefulness to rationalize the reduction inhibiting capacity obtained except for aromatic matrices with electon withdrawing groups such as NBA, DEP and HBSA. This concept of electron scavenging by the 'intact' matrix molecule has little meaning for aliphatic matrices since these compounds have essentially no electron affinity. Given the limitations of this approach, an analogy was drawn between the dehalogenation inhibiting properties of the aliphatic matrices and the behaviour of analogous organic liquids under radiolytic conditions. The analogy is appropriate since both FAB/LSIMS and radiolysis impart energy to a sample indiscriminately, which generates radicals, ions, electrons and excited species. In this case, the emphasis is shifted from the redox properties of the intact molecule to those of the transient species produced under the influence of energetic particle bombardment, the so-called radical cascade.

In the case of alcohols, electrons and a number of radicals are produced by particle bombardment. Most of the radicals react very quickly with intact alcohol molecules to give rise to α-alkylhydroxy radicals through hydrogen abstraction. In other words, there is a 'convergence' of the radical cascade towards α-alkylhydroxy radicals.

The free electrons are relatively stable in alcohols. Hence, after a very short time, the alcohol radical cascade can be resumed by the following scheme.

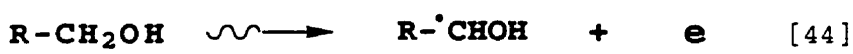

[44]

The α-alkylhydroxy radicals are highly reducing radicals capable of undergoing electron transfer with a variety of organic compounds. Therefore, the behaviour of alcohols under energetic particle bombardment is characterised by (a) the generation of a highly reducing radical cascade and (b) lack of quenching mechanism for the free electrons produced by the bombardment process i.e. alcohols have no electron scavenging capacity. The radiolytic behaviour of aliphatic alcohols offers an excellent qualitative rationalisation of the high propensity of glycerol to foster reduction processes under FAB/LSIMS conditions. Hence, the FAB/LSIMS redox chemistry of glycerol can be summed up in the following scheme.

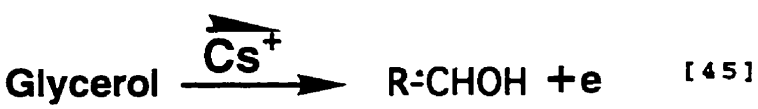

[45]

The generation of α-alkylhydroxy radicals under FAB/LSIMS conditions has been extensively demonstrated. However, the potential contribution of these radicals to beam-induced reduction processes has been hitherto completly overlooked. For example, the reduction of the methyl viologen dication to $M^{+\cdot}$ in the glycerol FAB spectrum[112] could be due in part to electron transfer from secondary α-hydroxyalkyl

radical formed during the bombardment process. Other FAB/LSIMS examples involving compounds which α-hydroxyalkyl radicals have been demonstrated to be efficient reducing agents involve quinones[112], aromatic ketones[36], metal ions[17] and pyridinium salts[20]. These radicals could be involved in the beam-induced reduction of porphyrins[109,127]. However, as demonstrated in section 5.2 these reducing radicals do not contribute to dehalogenation.

The thiol containing matrices such as thioglycerol offer a diametrically opposed case to that of the alcohols. In this case, the oxidizing thiyl radical ($RS^{\bullet}$) is the ubiquitous transient species emerging from the convergence of the radical cascade of thiol-containing molecules. The beam-induced formation of $RS^{\bullet}$ radicals is supported by the observation of certain analyte-matrix adducts in the mass spectrum which can be reasonably explained in terms of radical-radical recombination. Conversely, 'intact' thiol-containing molecules offer a good electron scavenging capacity as demonstrated by pulse radiolysis experiments. This electron scavenging capacity can be bolstered by the oxidizing radical cascade embodied by the thiyl radical.

The case of HEDS (-SS- containing molecule) is a little different in that the electron scavenging properties of the intact molecule are excellent as exemplified by the presence of a significant $M^{-\bullet}$ ion in the negative ion mode of the LSIMS spectrum of the matrix. The excellent electron scavenging capacity of disulfide containing molecules is also supported by pulse radiolysis experiments. As a

matter of fact, electron scavenging by the disulfide group leads to the formation of the oxidizing thiyl radical.

From the previous discussion, it is possible to paint a broad mechanistic scheme describing the beam-induced redox processes pertaining to aliphatic matrices. However, it is important to stress the very complex nature of the radiation chemistry of organic liquids. Therefore, one should remember that what is presented involves a significant amount of simplification. Nevertheless, the qualitative correlation between the main features of the radiation chemistry of specific matrix structural features (functional group) with the extent of dehalogenation observed in the LSIMS spectrum validates such an exercise.

The aromatic matrices having electron donating groups represent a special case since they have no electron affinity to speak of and aromatic structures do not generate a significant radical cascade given their resistance to radiation. Nevertheless, these compounds have a moderate electron scavenging capacity as shown by pulse radiolysis experiments. The above factors alone are probably sufficient to justify the intermediate dehalogenation inhibiting capacity of aromatic matrices with electron donating substituents. The fact that dehalogenation is an electron-initited process and that the matrix dehalogenation inhibition efficiency scale parallels the reduction efficiency observed with dyes[22], oximes[25], and peptides[130] argues that electrons could be the dominant reduction agents in other beam-induced reduction processes. A further case against the hydrogen

atom is the fact that secondary alcohols are used as hydrogen atom scavengers in pulse radiolysis experiments carried out in aqueous media.

In the study of the effect of experimental parameters on the beam-induced dehalogenation of the model compound chlorpromazine, it was proposed that increased analyte surface concentration could lead to increased dehalogenation. The increased dehalogenation would result from the increased probability of the analyte undergoing reaction with bombardment-generated species (thought to be electrons) produced at/or near the surface. The relationship between analyte surface activity and extent of dehalogenation was investigated using a three-pronged approach. First, the effect of doping a glycerol/analyte solution with an anionic surfactant was compared to the undoped solution for a variety of analytes. An anionic surfactant was used to 'artificially' increase the analyte surface concentration. The results show that the effect of the anionic surfactant on the extent of dehalogenation depended in large part, if not wholly, on the charge state of the analyte. This effect could be rationalized on the basis of the preferred distribution of the analyte with respect to the layer formed by the hydrophilic head groups of the surfactant molecules (Stern layer) and hence the surface. Similarities can be drawn from pulse radiolysis experiments involving micellar media to support the above interpretation.

Second, the extent of dehalogenation observed for chlorpromazine and an analogous compound having a higher surface activities was compared.

The analog of higher surface activity (and hence higher surface concentration) exhibited the higher %dehalogenation. These results *directly* support the contention that analyte surface activity can affect the observed extent of dehalogenation. This effect can be explained by the high concentration of beam-generated reductive species (thought to be electrons) near the surface. Hence, higher analyte surface concentration should result in an increased probability of reaction with beam-generated electrons and result in a greater % dehalogenation.

Third, the effect of matrix surface tension on the dehalogenation process was probed using 1,2,6-trihydroxyhexane, a polyhydric matrix compound analogous to glycerol but having a significantly lower surface tension. The lower matrix surface tension supposedly leads to lower analyte surface concentration. The significantly lower %dehalogenation obtained in THH with respect to glycerol is in agreement with a reduced analyte surface concentration in the matrix having the lower surface tension. In this context, it is interesting to note that of the matrices of known surface tension, the matrix surface tension decreases as the dehalogenation inhibiting capacity increases:

NBA (35 dyn cm^{-2}) > thiogly (53 dyn cm^{-2}) > Gly (62 dyn cm^{-2})

This relationship may be purely fortuitous but it is nonetheless interesting. However, the matrix beam-induced chemistry would certainly be an overwhelmingly more important factor compared to analyte surface concentration if one were to asssume that this

variable played a role in non-alcohol matrices. In this instance, it is safe to say that in a matrix where the radical cascade is essentially reducing and quenching mechanisms are essentially non-existent, the high surface tension of the matrix is bound to increase the likelihood of beam-induced reduction for analytes with significant surface active properties. It is proposed that the findings relating to the effect of analyte surface concentration on beam-induced dehalogenation could be applicable in a broad and general fashion to some of the other beam-induced reduction processes.

Although the ideas presented above do not provide a complete and unified explanation of FAB/LSIMS beam-induced processes, they undoubtedly constitute a systematic approach to a complex problem. It should be stressed that the aim of this thesis was primarily the identification of the *salient features* of beam-induced matrix redox chemistry. The complete elucidation of such processes was not the goal sought The distinctive facet of the investigation to draw on the analogy between FAB/LSIMS and radiolysis has been reasonably successful in rationalising the dehalogenation inhibiting efficiency of liquid matrices. This approach has been particularly helpful in describing the beam-induced chemistry of glycerol and rationalising the propensity of this matrix to exhibit the highest extent of reduction of all matrices. It is hoped that the approach presented here will encourage scientists in general not to hesitate to consult outside their field of expertise to tackle problems peculiar to their own.

References

REFERENCES

(1) *Rays of positive electricity and their application to chemical analysis*, J.J. Thomson, Longmans Green and Co. London, 1913.

(2) S.A. Borman, *Anal Chem.* **56**, 1273A (1984).

(3) A. Nier, *Z. Elektrochem.* **58**, 559 (1954).

(4) R.D. MacFarlane and D.F. Torgerson, *Science* **191**, 920 (1976).

(5) A. Benninghoven, *Surf. Sci.* **35**, 427 (1973).

(6) M. Barber, R.S. Bordoli, R.D. Sedgwick and A.N.J. Tyler, *J.Chem. Soc. Chem. Commun.* 325 (1981).

(7) F.M. Devienne and J.C. Roustand, *Org. Mass Spectrom.* **17**, 173 (1983).

(8) F.H. Field, *J. Phys. Chem.* **86**, 5115 (1982).

(9) D.D. Detter, O.W. Hand, R.G. Cooks and R.A. Walton, *Mass Spectrom. Rev.* **7**, 465 (1988).

(10) O.W. Hand, B.H. Hsu and R.G. Cooks, *Org. Mass Spectrom.* **23**, 16 (1983).

(11) K. Vekey, *Rapid Commun. Mass Spectrom.* **5**, 1 (1991).

(12) W.D. Lehman, M. Kessler and W.A. Konig *Biomed. Mass Spectrom.* **11**, 217 (1984).

(13) C. Dass and D.M. Desiderio, *Anal. Chem.* **60**, 2723 (1988).

(14) E. De Pauw and A. Agnello, *J. Am. Soc. Mass Spectrom.* **4**, 312 (1993).

(15) K. Vekey, *Int. J. Mass Spectrom. Ion Proc.* **97**, 265 (1990).

(16) M.J. Bertrand, J. Visentini, G.J.C. Paul and D. Zidarov, *Rapid Commun. Mass Spectrom.* **6**, 485 (1992).

(17) G. Pelzer, E. De Pauw, D.V. Dung and J. Marien, *J. Phys. Chem.* **88**, 5604 (1984).

(18) P.J. Gale, B.L. Bentz, B.T. Chait, F.H. Field and R.J. Cotter, *Anal. Chem.* **58**, 1070 (1986).

(19) D.J. Burinski, R. L. Diliplane, G.C. Didonato and K.L. Busch, *Org. Mass Spectrom.* **23**, 231 (1988).

(20) C.W. Kazakoff, R.T.B. Rye and O.S. Tee, *Can J. Chem.* **67**, 183 (1989).

(21) J.N. Kyranos and P. Vouros, *Biol. Mass Spectrom.* **19**, 628 (1990).

(22) K.D. Cook and J.D. Reynolds, *J. Am. Soc. Mass Spectrom.* **1**, 149 (1990).

(23) F. De Angelis, G. Doddi and G. Ercolani, *J. Chem. Soc. Perkin II* 633 (1987).

(24) H.M. Schiebel, W.D. Stohrer, D. Leibfritz, B. Jastorff, P. Schulze and K.H. Maurer, *Biomed. Mass Spectrom.* **12**, 170 (1985).

(25) M.G.O. Santana-Marques, A.J.V. Ferrer-Correia and M.L. Gross, *Anal. Chem.* **61**, 1442 (1989).

(26) J.L. Aubagnac, S. Doulut, M. Rodriguez and J. Martinez, *Org. Mass Spectrom.* **27**, 645 (1992).

(27) J.L. Aubagnac, R.M. Claramunt and D. Sanz, *Org. Mass Spectrom.* **19**, 628 (1990).

(28) R. Yazdanparast, P. Andrews, D.L. Smith and J.E. Dixon, *Anal. Biochem.* **153**, 348 (1986).

(29) D.V. Dung, J. Marien, E. De Pauw and J. Decuypr, *Org. Mass Spectrom.* **19**, 276 (1984).

(30) J.A. McCloskey, C.C. Nelson and S.K. Sehti, *Anal. Chem.* **56**, 1975 (1984).

(31) S.M. Musser and J.A. Kelley, *Org. Mass Spectrom.* **28**, 672 (1992).

(32) R.W. Edom, G. McKay, J.W. Hubbard and K.K. Midha, *Biol. Mass Spectrom.* **20**, 585 (1991).

(33) T. Nakaruma, H. Nagaki and T. Kinoshita, *Bull. Chem. Soc. Jpn.* **58**, 2798 (1985).

(34) R. Théberge, G. Paul and M.J. Bertrand, *Org. Mass Spectrom.* **29**, 18 (1994).

(35) R. Théberge and M.J. Bertrand, *J. Mass Spectrom.* **1**, 163 (1995).

(36) R. Théberge and M.J. Bertrand, *J. Am. Soc. Mass Spectrom.* in Press.

(37) P. Neta and D. Behar, *J. Am. Chem. Soc.* **103**, 2280 (1981).

(38) A. Horowitz, in *Supplement D: The Chemistry of halides, Pseudo-halides and Azides*, Edited by S. Patai, p. 369, Wiley and Sons, London, (1983).

(39) C.P. Andrieux, J.M. Savéant and D. Zann, *Nouv. J. Chim.* **8**, 107 (1984).

(40) J.M. Savéant, *Adv. Phys. Org. Chem.* **26**, 1 (1990).

(41) E. Clayton, A.J.C. Wakefield, *J. Chem. Soc. Chem. Commun.* 969 (1984).

(42) W.V. Ligon, *Int. J. Mass Spectrom. Ion Proc.* **52**, 189 (1983).

(43) J. Sunner, *Org. Mass Spectrom.* **28**, 805 (1993).

(44) Katz, R.N.; Field, F.H. *proceedings of the 11th international Mass Spectrometry Conference,* Bordeaux, **1988**, 1022-1023.

(45) D.H. Williams, A.F. Findeis, S. Naylor and B.W. Gibson, *J. Am. Chem. Soc.* **109**, 1980 (1987).

(46) J.H. Baxendale and R.D. Sedgwick, *Trans. Faraday Soc.* **60**, 685 (1964).

(47) P. Wardman, *J. Phys. Chem. Ref. Data* **18**, 1637 (1989).

(48) C.V. Buxton, C.V. Greenstock, W.P. Helman and A.B. Ross, *J. Phys. Chem. Ref. Data* **17**, 513 (1988).

(49) R.A. Basson, in *The Chemistry of the Hydroxyl Group part 2*, Edited by S. Patai, p. 937, Wiley and Sons, (1971).

(50) C.V. Von Sonntag and H.P. Schuchmann, in *Supplement E: The Chemistry of Ethers, Crown Ethers, Hydroxyl Groups and their Sulfur Analogs Part 2*, Edited by S. Patai, p. 935, Wiley and Sons, (1980).

(51) J. Perel, in *Desorption Mass Spectrometry, Are FAB and SIMS the Same?*, Edited by P.A. Lyon, A.C.S. Symposium Series, No. 291, Am. Chem Soc. Washington, (1985).

(52) M. Barber, R.J. Bordoli and R.D. Sedgwick, in *Soft Ionization Mass Spectrometry* Edited by H.R. Morris, p. 137, Heyden, London, (1981).

(53) W. Aberth, K.M. Straub and A.L. Burlingame, *Anal. Chem.* **54**, 2029 (1982).

(54) J.L. Gower, *Biomed. Mass Spectrom.* **12**, 191 (1985).

(55) E. De Pauw, *Mass Spectrom. Rev.* **5**, 191 (1986).

(56) E. De Pauw, *Adv. Mass Spectrom.* **11**, 383 (1989).

(57) E. De Pauw, A. Agnello and F. Derwa, *Mass Spectrom. Rev.* **10**, 283 (1991).

(58) C. Dass, *J. Mass Spectrom.* **31**, 77 (1996).

(59) M.S. Kriger, K.D. Cook, R.T. Short and P.J. Todd, *Anal. Chem.* **64**, 3052 (1992).

(60) J.H. Calahan, K. Hool, J.D. Reynolds and K.D. Cook, *Anal. Chem.* **60**, 714 (1988).

(61) K.D. Cook, P.J. Todd and D.H. Friar, *Biomed. Environ. Mass Spectrom.* **18**, 492 (1989).

(62) M. Barber, R.S. Bordoli, R.D. Sedgwick, G.J. Elliott and A.N.J. Tyler, *J. Chem. Soc. Faraday Trans. I* **79**, 1249 (1983).

(63) K.I. Karada, M. Suzuki and H. Kambara, *Org. Mass Spectrom.* **17**, 386 (1982).

(64) W.V. Ligon and S.B. Dorn, *J. Am. Chem. Soc.* **110**, 6684 (1988).

(65) J. Shiea and J. Sunner, *Org. Mass Spectrom.* **26**, 38 (1991).

(66) W.V. Ligon and S.B. Dorn, *Int. J. Mass Spectrom. Ion Proc.* **61**, 113 (1984).

(67) W.V. Ligon, *Anal. Chem.* **58**, 487 (1986).

(68) B.D. Bennett and R.A. Day, *Anal. Lett.* **25**, 763 (1992).

(69) J. Rossenski and P.H. Herdewijn, *Rapid Commun. Mass Spectrom.* **9**, 1499 (1995).

(70) J. Visentini, P. Gauthier and M.J. Bertrand, *Rapid Commun. Mass Spectrom.* **3**, 390 (1989).

(71) A. Agnello and E. De Pauw, *Org. Mass Spectrom.* **26**, 175 (1991).

(72) V.S. Murthy and J.M. Miller, *Rapid Commun. Mass Spectrom.* **7**, 874 (1993).

(73) P. Vouros and J. Cunnif, *J. Am. Soc. Mass Spectrom.* **5**, 638 (1994).

(74) A. Benninghoven, in *Ion Formation from Organic Solids*, vol. **25**, Edited by A. Benninghoven, p. 64, Springer-Verlag, Berlin, (1983).

(75) S.S. Wong and F.W. Rollgen, *Nucl. Instrum. Methods Phys. Res.* **B14**, 436 (1986).

(76) M.L. Vestal, in *Ion Formation from Organic Solids* vol. **25**, Edited by A. Benninghoven, p. 246, Springer-Verlag, Berlin (1983).

(77) P.J. Todd, *Org. Mass Spectrom.* **23**, 419 (1988).

(78) P.J. Todd, *J. Am. Soc. Mass Spectrom.* **2**, 33 (1991).

(79)J. Sunner, A. Morales and P. Kebarle, *Anal. Chem.* **59**, 1378 (1987).

(80) G.J.C. Paul, S. Bourg and M.J. Bertrand, *Rapid Commun. Mass Spectrom.* **6**, 85 (1992).

(81) G.J.C. Paul, S. Bourg and M.J. Bertrand, *J. Am. Soc. Mass Spectrom.* **4**, 493 (1993).

(82) N. Dookeran and A.G. Harrison, *J. Am. Soc. Mass Spectrom.* **6**, 19 (1995).

(83) J. Sunner, *Org. Mass Spectrom.* **28**, 805 (1993).

(84) F. Honda, G.M. Lancaster, Y. Fukuda and J.W. Rabalais *J. Chem. Phys.* **69**, 4931 (1978).

(85) R.G. Cooks and K.L. Busch, *Int. J. Mass Spectrom. Ion Proc.* **53**, 11 (1983).

(86) S.J. Pachuta and R.G. Cooks, *Chem. Rev.* **87**, 647 (1987).

(87) W.V. Ligon, *Int. J. Mass Spectrom. Ion Phys.* **52**, 189 (1983).

(88) S.J. Pachuta and R.G. Cooks, in *Desorption Mass Spectrometry, Are FAB and SIMS the Same?*, Edited P.A. Lyon, p. 1, Am. Chem. Soc. Symposium Series, No. 291, Washington, (1985).

(89) D.H. Williams, C. Bradley, G. Bojeson, S. Santikarn and L.C. Taylor, *J. Am. Chem. Soc.* **103**, 5700 (1981).

(90) E. Schroeder, H. Munster and H. Budzikiewicz, *Org. Mass Spectrom.* **21**, 707 (1986).

(91) J. Michl, *Int. J. Mass Spectrom. Ion Phys.* **53**, 255 (1983).

(92) J. Sunner, R. Kulatunga and P. Kebarle, *Anal Chem.* **58**, 1312 (1986).

(93) J. Sunner, A. Morales and P. Kebarle, *Anal Chem.* **59**, 1378 (1987).

(94) M. Barber, R.S. Bordoli, R.D. Sedgwick and L.W. Tetler, *Org. Mass Spectrom.* **16**, 256 (1981).

(95) B.T. Chait and F.H. Field, *Int. J. Mass Spectrom. Ion Phys.* **41**, 17 (1981).

(96) C. Fenselau and R.J. Cotter, *Chem. Rev.* **87**, 501 (1987).

(97) J.R. Chapman, *Practical Organic mass Spectrometry* 2nd ed. Wiley & Sons, p. 154 (1993).

(98) L.R. Shronk and R.J. Cotter, *Biomed. Environ. Mass Spectrom.* **13**, 395 (1986).

(99) A. Dell and C.E. Ballou, *Biomed. Mass Spectrom.* **10**, 50 (1983).

(100) S.A. Martin, C.E.Costello and K. Biemann, *Anal. Chem.* **54**, 2362 (1982).

(101) R.A. Basson, in *The Chemistry of the Hydroxyl Group part 2*, Edited by S Patai, Wiley and Sons, N.Y. (1971).

(102) T. Keough, *Int. J. Mass Spectrom. Ion Proc.* **86**, 155 (1988).

(103) A.A. Tuinman, K.D.Cook and L. Magid, *J. Am. Soc. Mass Spectrom.* **3**, 318 (1992).

(104) T. Keough, F.S. Ezra, A.F. Russell and J.D. Pryne, *Org. Mass Spectrom.* **22**, 241 (1987).

(105) K.A. Caldwell and M.L. Gross, *J. Am. Soc. Mass Spectrom.* **5**, 72 (1994).

(106) A.A. Tuinman and K.D. Cook, *J. Am. Soc. Mass Spectrom.* **5**, 92 (1994).

(107) M. Barber, D.J. Bell, M. Morris, L.W. Tetler, M.D. Woods, J.J. Monaghan and W.E. Morden, *Rapid Commun. Mass Spectrom.* **2**, 181 (1988).

(108) R.L. Cerny and M.L. Gross, *Anal. Chem.* **57**, 1160 (1985).

(109) S. Naylor, C.A. Hunter, J.A. Cowan, J.H. Lamb and J.K.M. Sanders, *J. Am. Chem. Soc.* **112**, 6507 (1990).

(110) D.H. Williams, A.F. Findeis, S. Naylor and B.W. Gibson, *J. Am. Chem. Soc.* **109**, 1980 (1987).

(111) C.W. Kazakoff, P.H. Bird and R.T.B. Rye,*Org. Mass Spectrom.* **24**, 703 (1989).

(112) E. Clayton and A.J.C. Wakefield, *J. Chem. Soc. Chem. Commun.* 969 (1984).

(113) B. Bogess and K.D. Cook, *J. Am. Soc. Mass Spectrom.* **5**, 100 (1994).

(114) C.W. Kazakoff and R.T.B. Rye,*Org. Mass Spectrom.* **26**, 154 (1991).

(115) M. Takayama, *Org. Mass Spectrom.* **26**, 1123 (1991).

(116) E. De Pauw, *Anal Chem.* **55**, 2195 (1983).

(117) M. Allard and M.J. Bertrand, Proceedings of the 44th ASMS Conference on Mass Spectrometry and Allied Topics, Portland, ORE, (1996).

(118) R.T. Rosen, T.G. Harman, J.D. Rosen and C.T. Ho, *Rapid Commun. Mass Spectrom.* **2**, 21 (1989).

(119) M. Takayama, T. Fukai, T. Nomura and K. Nojima, *Rapid Commun. Mass Spectrom.* **3**, 4 (1989).

(120) K. Balasanmugam and J.M. Miller, *Org. Mass Spectrom.* **23**, 267 (1988).

(121) S.M. Brown and K.L. Busch, *Rapid Commun. Mass Spectrom.* **2**, 256 (1988).

(122) M.J. Bertrand, G.J.C. Paul, J. Visentini and D. Zidarov, *Rapid Commun. Mass Spectrom.* **6**, 485 (1992).

(123) J. Visentini, D. Zidarov, M. Allard and M.J. Bertrand, *J. Am. Soc. Mass Spectrom.* **4**, 483 (1993).

(124) B.E. Winger, O.W. Hand and R.G. Cooks, *Int. J. Mass Spectrom. Ion Proc.* **84**, 89 (1988).

(125) K.P. Wirth, E. Junker, F.W. Rollgen, P. Fonrobert and M. Przybylski, *J. Chem. Soc. Chem. Commun.* 1387 (1987).

(126) R. Théberge and M.J. Bertrand Proceedings of the 43rd ASMS Conference on Mass Spectrometry and Allied Topics, p. 1064, Atlanta, GA, (1995).

(127) H.H. Schurz and K.L. Busch, *Energy and Fuels* **4**, 730 (1990).

(128) B.D. Musselman and J.T. Watson, *Biomed Environ. Mass Spectrom.* **14**, 247 (1987).

(129) J. Visentini, P.Thibeault and M.J. Bertrand, Proceedings of the 37th ASMS Conference on Mass Spectrometry and Allied Topics, p. 887, Miami, FLA, (1989).

(130) J. Visentini, PhD thesis, Univ. de Montréal, (1993).

(131) P.S. Rao and E. Hayon, *J. Phys. Chem.* **77**, 2753 (1973).

(132) M.H. Florencio and W. Heerma, *Org. Mass Spectrom.* **26**, 657 (1993).

(133) R. Cooper and S. Unger, *J. Antibiotics* **38**, 24 (1985).

(134) J.A. Laramée, B. Arbogast and M.L. Deinzer, *Anal. Chem.* **61**, 171 (1989).

(135) J.M. Miller, K. Balasunmugam, J. Nye, G.B. Deacon and N.C. Thomas, *Inorg. Chem.* **26**, 560 (1987).

(136) K.D. Cook, J.D. Reynolds, J.L.E. Burns and C. Woods, *J. Am. Soc. Mass Spectrom.* **3**, 113 (1992).

(137) H. Budziekiewich, *Org. Mass Spectrom.* **23**, 561(1988).

(138) A.G. Harrison and P.H. Lin, *Can. J. Chem.* **53**, 1314 (1975).

(139) K.P. Madhusudanan, V.S. Murthy and D. Fraise, *J. Chem. Soc. Perkin Trans II* 1255 (1989).

(140) D.F. Hunt, G.C. Stafford, F.W. Crow and J.W. Russell, *Anal Chem.* **48** 2098 (1976).

(141) V.S. Ong and R.A. Hites, *J. Am. Soc. Mass Spectrom.* **4**, 270 (1994).

(142) E.A. Stemmler and R.A. Hites, *Biomed. Environ. Mass Spectrom.* 17, 311 (1988).

(143) W.T. Naff, R.N. Compton and C.D. Cooper, *J. Chem. Phys.* **54**, 212 (1971).

(144) R. O'Brien, R. Guevremont, K.W.M. Siu and B.R. Hollebone, Proceedings of the 42nd ASMS Conference on Mass Spectrometry and Allied Topics, p. 742, Chicago, Il., (1994).

(145) A. Acheampong, H. Nguyen, D. Harcourt, D. Tang-Liu, M. Garst Proceedings of the 41st Annual ASMS Conference on Mass Spectrometry and Allied Topics, Washington, D.C., p 48a, (1993).

(146) D. Volmer and K. Levsen, *J. Am. Soc. Mass Spectrom.* **5**, 655 (1994).

(147) Y.M. Yang, H.M. Fales and L. Pannell, *Anal. Chem.* **57**, 1771 (1985).

(148) A.N.R. Nedderman and D.H. Williams, *Biol. Mass Spectrom.* **20**, 289 (1991).

(149) W.E. Wentworth and E.C.M. Chen, *Mol. Cryst. Liq. Cryst.* **171**, 270 (1989).

(150) K. Madden, Radiation Chemistry Data Center, Notre Dame University, personal communication.

(151) Y.S. Kang, H.G.D. McManus and L. Kevan, *J. Phys. Chem.* **97**, 2027 (1993).

(152) L. Eberson and F. Radner, *Acta Chem. Scand.* **45**, 1093 (1991).

(153) L. Eberson and F. Radner, *Acta Chem. Scand.* **46**, 630 (1992).

(154) T. Kaiser, L. Grossi and H. Fischer, *Helv. Chim. Acta* **61**, 223 (1978).

(155) L. Eberson, personal communication.

(156) G.J. Van Berkel, S.A. McLuckey and G. Glish, *Anal. Chem.* **64**, 1586 (1992).

(157) L. Eberson, *J. Chem. Soc. Perkin Trans. II* 141 (1996).

(158) R.A. Flurer and K.L. Busch, *Org. Mass Spectrom.* **23**, 118 (1988).

(159) P.A. Leclerq and D.M. Desiderio, *Org. Mass Spectrom.* **7**, 515 (1973).

(160) Z.J. Kaminski, *Synthesis* 917 (1987).

(161) J.R. Wiley, J.M. Robinson, S. Ehdaie, E.C.M. Chen, E.S.D. Chen and W.E. Wentworth, *Biochem. Biophys. Res Commun.* **180**, 841 (1991).

(162) P. Kebarle and S. Chowdhury, *Chem. Rev.* **87**, 513 (1987).

(163) G. Paul and P. Kebarle, *J. Am. Chem. Soc.* **111**, 464 (1989).

(164) D.D. Tanner, N. Deonarian and A. Kharrat, *Can. J. Chem.*. **67**, 171 (1989).

(165) H. Shalev and D.H. Evans, *J. Am. Chem. Soc.* **111**, 2667 (1989).

(166) P. Kebarle, *J. Am. Chem. Soc.* **107**, 4627 (1985).

(167) G.B. Gavioli, M. Borsari and C. Fontanesi, *J. Chem. Soc. Faraday Trans.* **89**, 3931 (1993).

(168) G.W. Dillow and P. Kebarle, *Can. J. Chem.* **67**, 1628 (1989).

(169) T.J. Kemp, *Coord. Chem. Rev.* **125**, 333 (1993).

(170) R.A. Rossi, *Acc. Chem. Res.* **15**, 164 (1982).

(171) J.M. Savéant, *Bull. Soc. Chim. Fran.* 225 (1988).

(172) K. Alwair and J. Grimshaw, *J. Chem. Soc. Perkin Trans. 2* 1811 (1973).

(173) C.P. Andrieux, J.M. Savéant and D. Zann, *Nouv. J. Chim.* **8**, 107 (1984).

(174) C. Von Sonntag, X. Fang and R. Mertens, *J. Chem. Soc. Perkins Trans 2* 1033 (1995).

(175) Ching-Fong Shu and Wrighton, *Inorg. Chem.* **27**, 4326 (1988).

(176) C. Von Sonntag, *The Chemical Basis of Radiation Biology.*, Taylor and Francis, New York, (1987).

(177) J. Lichtscheidl and N. Getoff, *Monasch Chem.* **110**, 1377 (1979).

(178) J. Lichtscheidl and N. Getoff, *Monasch Chem.* **110**, 1367 (1979).

(179) B.J. Mincher, R.E. Arbon, W.B. Knighton and D.H. Meikrantz, *Applied Radiat. Isot.* **45**, 879 (1994).

(180) N. Serpone, R. Terzian, H. Hidaka and E. Pelizetti, *J. Phys. Chem.* **98**, 2634 (1994).

(181) M. Gutierrz, A. Henglein and J.K.H. Dohrman, *J. Phys. Chem.* **91**, 6687 (1987).

(182) D.A. Nelson and E. Hayon, *J. Phys. Chem.* **76**, 3200 (1972).

(183) R.A. Holroy, in *Fundamental Processes in Radiation Chemistry*, Edited by P. Ausloos, p. 413, Wiley Interscience, N.Y. (1968).

(184) E.J. Hart and M. Anbar, in *The Hydrated Electron*, p.149, Wiley-interscience, N.Y. (1970).

(185) E. Hayon, T. Ibata, N.N. Lichtin and M. Simic, J. *Phys. Chem.* **76**, 2072 (1972).

(186) C.P. Andrieux, M. Robert and J.M. Savéant, *J. Am. Chem. Soc.* **117**, 9340 (1995).

(187) M. Barber, R.S. Bordoli, G.J. Elliott, R.D Sedgwick and A.N.J. Tyler, *Anal. Chem.* **54**, 645A (1982).

(188) W.V. Ligon and S.B. Dorn, *Int. J. Mass Spectrom. Ion Proc.* **57**, 75 (1984).

(189) S. Naylor, A.F. Findeis, B.W. Gibson and D.H. William, *J. Am. Chem. Soc.* **108**, 6359 (1986).

(190) W.V. Ligon, in *Biological Mass Spectrometry,* Edited by A.L. Burlingame and J.A. McCloskey, Elsevier, (1990).

(191) J.K. Thomas, Radiation chemistry of colloidal aggregates, in *Radiation Chemistry: Applications and Principles*, Edited by R. Farhatiz, VCH publishers, (1986).

(192) A. Bernas, D. Grand and S. Hautecloque, Excess electrons in microheterogeneous systems, in *Excess Electrons in Dielectric Media*, Edited by C. Ferradini and J.P. Jay-Gerin, p. 367, CRC Press, Boca Raton, (1991).

(193) M.L. Gross, N.J. Jensen and K.B. Tomer, *J. Am. Chem. Soc.* **107**, 1863 (1985).

(194) J. Adams, *Mass Spectrom. Rev.* **9**, 141 (1990).

(195) R.E. Carlson and K.L. Busch, *Org. Mass Spectrom.* **29**, 632 (1994).

(196) M.L. Gross, *Int. J. Mass Spectrom. Ion Proc.* **118/119**, 137 (1992).

(197) W.H. Wysocki, M.E. Bier and R.G. Cooks, *Org. Mass Spectrom.* **23**, 627 (1988).

(198) P. Riesz and T. Kondo, *Free Rad. Biol. Med.* **13**, 247 (1992).

(199) J.N. Israelachvili, *Intermolecular and Surface Forces*, Academic Press, N. Y., (1992).

(200) A.W. Adamson, *Physical Chemistry of Surfaces*, 4th edition, Wiley N.Y, (1982).

(201) I. Langmuir, *Colloid Symposium Monograph*, p. 48, the Chemical Catalog Company, N.Y., (1925).

(202) A.N. Tyler, L.K. Romo, M.H. Frey, B.D. Musselman, J. Tamura and R.B. Cody, J. Am. Soc. Mass Spectrom. 3, 367 (1992).

(203) A. Santos, B. Saramago, F. Duarte and H.M. Florencio, *J. Chem. Soc. Faraday Trans.* **91**, 1203 (1995).

(204) G. Bojeson and M. Moller, *Int. J. Mass Spectrom. Ion Proc.* **68**, 239 (1986).

(205) M. Takayama *J. Am. Soc. Mass Spectrom.* **6**, 114 (1995).

(206) G. Paul, R. Théberge, M.J. Bertrand, R. Feng, M.D. Bailey, *Org. Mass Spectrom.* **28**, 1329 (1993).

(207) F.M. Rubino and L. Zecca, *Org. Mass Spectrom.* **26**, 961 (1991).

(208) M. Takayama, Y. Tanaka and T. Nomura, *Org. Mass Spectrom.* **28**, 1529 (1993).

(209) W.Vetter and W. Meister, *Org. Mass Spectrom.* **20**, 266 (1985).

(210) S. Kurono, T. Tani, T. Hirano, K. Tsujimoto and M. Ohashi, *Org. Mass Spectrom.* **27**, 1365 (1992).

(211) L.J.A. Martins and T.K. Kemp, *J. Chem. Soc. Faraday Trans 1* **80**, 2509 (1984).

(212) D.A. Armstrong, *Sulfur-Centered Reactive Intermediates in Chemistry and Biology*, NATO ASI Series, Series A, Edited by C. Chatgilialoglu and K.D. Asmus, p. 341, Plenum Press, New York, (1990).

(213) L.G. Forni, V.O. Mora-Arellano, J.E. Packer and R.L. Willson, *J. Chem. Soc. Perkin Trans. II* 1579 (1988).

(214) M. Tamba and P. O'Neil, *J. Chem. Soc. Perkin Trans. 2*, 1681 (1991).

(215) E.S. Huyser and H.N. Tang, A.C.S. Symp. Ser. **69**, 258 (1978).

(216) M. Lal and H.S. Mahal, *Can. J. Chem.* **68**, 1376 (1990).

(217) J.W.T. Spinks and R.J. Woods, *Introduction to Radiation Chemistry*, 2nd edition, Wiley Interscience, N.Y., 1976.

(218) R.V. Bensasson, E.J. Land and T.G. Truscott, *Flash Photolysis and Pulse Radiolysis: Contributions to the Chemistry and Biology of Medicine*, p. 8, Pergamon Press, N.Y., (1983).

(219) D.H. Ellison, G.A. Salmon and F. Wilkinson, *Proc. Royal Soc.* A **328**, 23 (1972).

(220) D.W. Johnson and G.A. Salmon, *J. Chem. Soc. Faraday Trans. 1* 446 (1979).

(221) G. Zhang and J.K. Thomas, *J. Phys. Chem.* **98**, 11714 (1994).

(222) A.G. Swallow, *Prog. React. Kinet.* **9**, 195 (1978).

(223) Z.B. Alfassi, in *Chemical Kinetics of Small Organic Molecules*, **4**, p.165, CRC Press, Boca Raton, (1988).

(224) C. Schoneich, K.D. Asmus and M. Bonifacic, *J. Chem. Soc. Faraday Trans. 2* **91**, 1923 (1995).

(225) V.J. Lillie, G. Beck and A. Henglein, *Ber Bunsenges Phys Chem.* **75**, 458 (1971).

(226) P. Neta, *J. Phys. Chem.* **85**, 3678 (1981).

(227) Y. Harel and D. Meyerstein, *J. Am. Chem. Soc.* **96**, 2720 (1974).

(228) G.E. Adams and R.L. Willson, *J. Chem. Soc. Faraday Trans.1* **69**, 719 (1973).

(229) R.L. Willson, *Trans. Faraday Soc.* **67**, 3020 (1971).

(230) P. Neta and L.K. Patterson, *J. Phys. Chem.* **78**, 2211 (1974).

(231) H. Cohen and D. Meyerstein, *J. Am. Chem. Soc.* **94**, 6944 (1972).

(232) P.S. Rao and E. Hayon, *J. Phys. Chem.* **77**, 2753 (1973).

(233) H. Goff and M.G. Simic, *Biochim. Biophys. Acta* **392**, 201 (1975).

(234) C.L. Greenstock and I. Dunlop, *Radiat. Res.* **56**, 428 (1973).

(235) K. Bansal, M. Gratzel, A. Henglein and E. Janata, *J. Phys. Chem.* **77**, 16 (1973).

(236) L.K.Patterson, R.D. Small and J.C. Scaiano, *Radiat. Res.* **72**, 218 (1977).

(237) H. Mohan, M. Mudaliar, B.S.M. Rao, J.P. Mittal, *Radiat. Phys. Chem.* **40**, 513 (1992).

(238) R.J. Woods and A.K. Pikaev, *Applied Radiation Chemistry: Radiation Processing*, p. 59, Wiley, N.Y., (1994).

(239) Z.M. Bacq, in *Chemical Protection against Ionizing Radiation*, Edited by C.C Thomas, Springfield IL., (1965).

(240) C.V. Von Sonntag and H.P. Schuchmann, in *Supplement E: The Chemistry of Ethers, Crown Ethers, Hydroxyl Groups and their Sulfur Analogs Part 2*, Edited by S. Patai, p. 935, Wiley and Sons, (1980).

(241) S. Mezyk, *J. Phys. Chem.* **99**, 13970 (1995).

(242) M.Z. Hoffman and E. Hayon, *J. Am. Chem. Soc.* **94**, 7950 (1972).

(243) M. Bonfacic and K.D. Asmus, *J. Chem. Soc. Perkin Trans. 2* 1805 (1986).

(244) D. Brahneman, K.D. Asmus and R.S. Wilson, *J. Chem. Soc. Perkin Trans.* 1661 (1983).

(245) B. Egestad and P. Sjoberg, *Rapid Commun. Mass Spectrom.* **7**, 812 (1993).

(246) J. Visentini, P.M. Nguyen and M.J. Bertrand, *Rapid Commun. Mass Spectrom.* **5**, 586 (1991).

(247) V.E. Zubarev and A. Halpern, *J. Chem. Soc. Faraday Trans.* **90**, 721 (1994).

(248) A. Kira and J.K. Thomas, *J. Chem. Phys.* **60**, 766 (1974).

IMAGE EVALUATION TEST TARGET (QA-3)

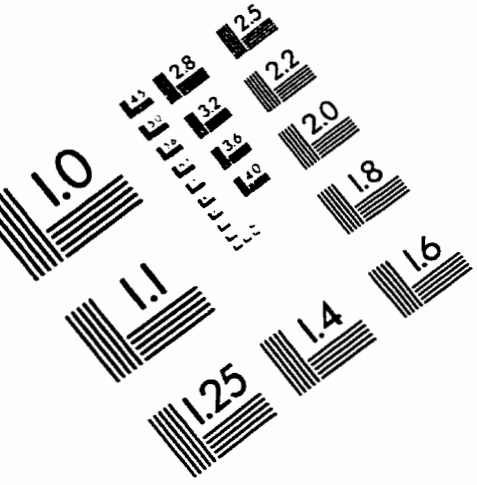

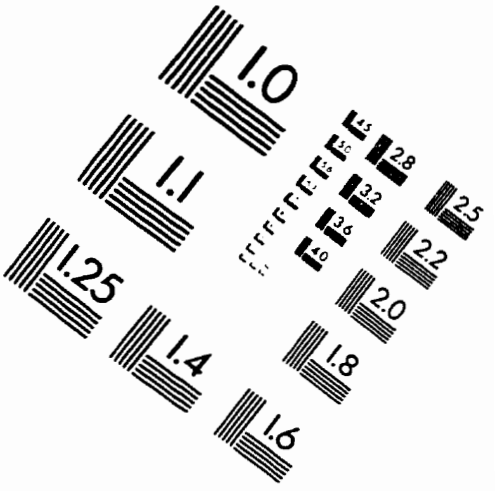

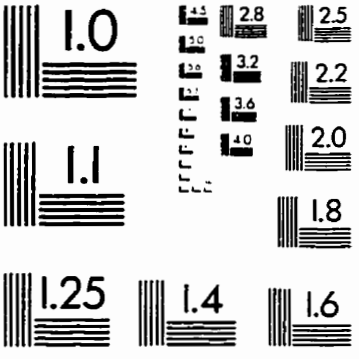

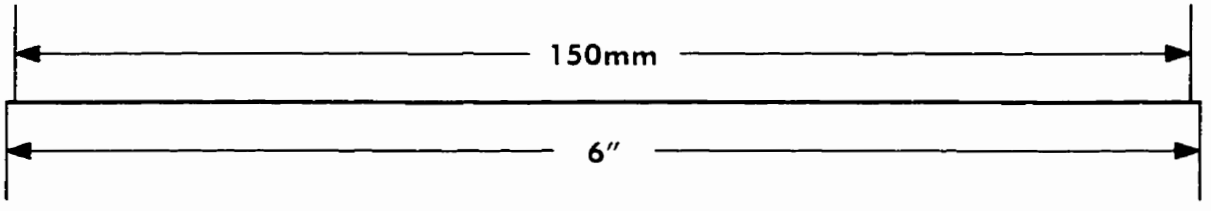

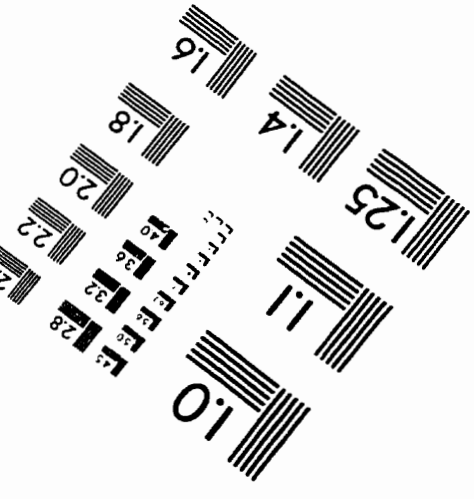

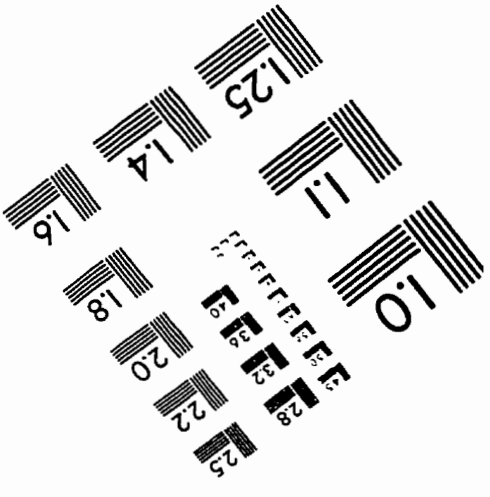

APPLIED IMAGE, Inc
1653 East Main Street
Rochester, NY 14609 USA
Phone: 716/482-0300
Fax: 716/288-5989